



**Application to Food Standards Australia New Zealand
for the Inclusion of Soybean MON 94313
in *Standard 1.5.2 - Food Derived from Gene Technology***

Submitted by:

Bayer CropScience Proprietary Limited

[Redacted]
[Redacted]

[Redacted]

© 2023 Bayer Group. All Rights Reserved.

This document is protected under national and international copyright law and intellectual property right treaties. This document and any accompanying materials are for use only by the regulatory authority to which it has been submitted by the Bayer Group, including all subsidiaries and affiliated companies, and only in support of actions requested by the Bayer Group. Any other use, copying, or transmission, including internet posting, of this document and the materials described in or accompanying this document, without prior consent of Bayer Group, is strictly prohibited; except that Bayer Group hereby grants such consent to the regulatory authority where required under applicable law or regulation. The intellectual property, information and materials described in or accompanying this document are owned by Bayer Group, who has filed for or been granted patents on those materials. By submitting this document and any accompanying materials, Bayer Group does not grant any party or entity any right or license to the information, materials or intellectual property described or contained in this submission.

TABLE OF CONTENTS

TABLE OF CONTENTS.....	ii
LIST OF FIGURES	v
LIST OF TABLES.....	viii
UNPUBLISHED REPORTS BEING SUBMITTED	xi
CHECKLIST.....	xiii
ABBREVIATIONS AND DEFINITIONS.....	xv
PART 1 GENERAL INFORMATION.....	1
1.1 Applicant Details	1
1.2 Purpose of the Application.....	1
1.3 Justification for the Application.....	2
1.3(a) The need for the proposed change.....	2
1.3(b) The advantages of the proposed change over the status quo, taking into account any disadvantages.....	2
1.4 Regulatory Impact Information.....	2
1.5 Impact of International Trade	3
1.6 Assessment Procedure	3
1.7 Exclusive Capturable Commercial Benefit.....	4
1.8 International and Other National Standards.....	4
1.8(a) International standards	4
1.8(b) Other national standards or regulations.....	4
PART 2 SPECIFIC DATA REQUIREMENTS FOR SAFETY ASSESSMENT	5
A. TECHNICAL INFORMATION ON THE GM FOOD.....	5
A.1 Nature and Identity of the Genetically Modified Food.....	5
A.1(a) A description of the new GM organism from which the new GM food is derived	5
A.1(b) Name, line number and OECD Unique Identifier of each of the new lines or strains of GM organism from which the food is derived.....	5
A.1(c) The name the food will be marketed under (if known)	5
A.2 History of Use of the Host and Donor Organisms.....	6
A.2(a) For the donor organism(s) from which the genetic elements are derived:	6
A.2(a)(i) Any known pathogenicity, toxicity or allergenicity relevance to the food	6
A.2(a)(ii) History of use of the organism in food supply or history of human exposure to the organism through other than intended food use (e.g. as a normal contaminant).....	8
A.2(b) For the host organism into which the genes were transferred:	9
A.2(b)(i) Its history of safe use for food.....	9
A.2(b)(ii) The part of the organism typically used as food.....	9
A.2(b)(iii) The types of products likely to include the food or food ingredient.....	9
A.2(b)(iv) Whether special processing is required to render food safe to eat	9
A.3 The Nature of the Genetic Modification.....	10
A.3(a) A description of the method used to transform the host organism.....	12
A.3(b) A description of the construct and the transformation vectors used, including:	14
A.3(b)(i) The size, source and function of all the genetic components including marker genes, regulatory and other elements	14
A.3(b)(ii) A detailed map of the location and orientation of all genetic elements contained within the construct and vector, including the location of relevant restriction sites.....	24

A.3(c)	A full molecular characterisation of the genetic modification in the new organism, including:	25
A.3(c)(i)	Identification of all transferred genetic material and whether it has undergone any rearrangements.....	25
A.3(c)(ii)	A determination of number of insertion sites, and the number of copies at each insertion site	28
A.3(c)(iii)	Full DNA sequence of each insertion site, including junction regions with the host DNA.....	38
A.3(c)(iv)	A map depicting the organisation of the inserted genetic material at each insertion site.....	42
A.3(c)(v)	Details of an analysis of the insert and junction regions for the occurrence of any open reading frames (ORFs)	42
A.3(d)	A description of how the line or strain from which food is derived was obtained from the original transformant (i.e. provide a family tree or describe the breeding process) including which generations have been used for each study.....	44
A.3(e)	Evidence of the stability of the genetic changes, including:	45
A.3(e)(i)	The pattern of inheritance of the transferred gene(s) and the number of generations over which this has been monitored.....	45
A.3(e)(ii)	The pattern of inheritance and expression of the phenotype over several generations and, where appropriate, across different environments	46
A.3(f)	An analysis of the expressed RNA transcripts, where RNA interference has been used	56
B.	CHARACTERISATION AND SAFETY ASSESSMENT OF NEW SUBSTANCES.....	57
B.1	Characterisation and Safety Assessment of New Substances.....	57
B.1(a)	Full description of the biochemical and phenotypic effects of all new substances (e.g. a protein or an untranslated RNA) that are expressed in the new GM organism, including their levels and site of accumulation, particularly in edible portions.....	57
B.1(a)(i)	Description, mode-of-action, and specificity of DMO, PAT, FT_T.1 and TDO proteins expressed in MON 94313.....	57
B.1(a)(ii)	Characterisation of the DMO, PAT, FT_T.1 and TDO Proteins	70
B.1(a)(iii)	Expression levels of DMO, PAT, FT_T.1 and TDO proteins in MON 94313.....	131
B.1(b)	Information about prior history of human consumption of the new substances, if any, or their similarity to substances previously consumed in food.....	137
B.1(c)	Information on whether any new protein has undergone any unexpected post-translational modification in the new host.....	137
B.1(d)	Where any ORFs have been identified, bioinformatics analysis to indicate the potential for allergenicity and toxicity of the ORFs	137
B.2	New Proteins.....	138
B.2(a)	Information on the potential toxicity of any new proteins, including:	138
B.2(a)(i)	A bioinformatic comparison of the amino acid sequence of each of the new proteins to known protein toxins and anti-nutrients (e.g. protease inhibitors, lectins)	138
B.2(a)(ii)	Information on the stability of the proteins to proteolysis in appropriate gastrointestinal model systems	139

B.2(a)(iii)	An animal toxicity study if the bioinformatic comparison and biochemical studies indicate either a relationship with known protein toxins/anti-nutrients or resistance to proteolysis	167
B.2(b)	Information on the potential allergenicity of any new proteins, including:	167
B.2(b)(i)	Source of the new proteins	167
B.2(b)(ii)	A bioinformatics comparison of the amino acid sequence to known allergens.....	169
B.2(b)(iii)	The new protein's structural properties, including, but not limited to, its susceptibility to enzymatic degradation (e.g. proteolysis), heat and/or acid stability	170
B.2(b)(iv)	Specific serum screening where a new protein is derived from a source known to be allergenic or has sequence homology with a know allergen... ..	188
B.2(b)(v)	Information on whether the new protein(s) have a role in the elicitation of gluten-sensitive enteropathy, in cases where the introduced genetic material is obtained from wheat, rye, barley, oats, or related cereal grains.. ..	188
B.3	Other (non-protein) New Substances.....	188
B.4	Novel Herbicide Metabolites in GM Herbicide-Tolerant Plants	188
B.5	Compositional Assessment	194
B.5(a)	Levels of key nutrients, toxicants and anti-nutrients in the food produced using gene technology compared with the levels in an appropriate comparator	195
B.5(b)	Information on the range of natural variation for each constituent measure to allow for assessment of biological significance	211
C.	INFORMATION RELATED TO THE NUTRITIONAL IMPACT OF THE FOOD PRODUCED USING GENE TECHNOLOGY	213
D.	OTHER INFORMATION	213
PART 3	STATUTORY DECLARATION – AUSTRALIA	214
PART 4	REFERENCES	215

LIST OF FIGURES

Figure 1. Schematic of the Development of MON 94313	13
Figure 2. Circular Map of PV- GMHT529103	24
Figure 3. Molecular Characterisation using Sequencing and Bioinformatics	25
Figure 4. Five Types of NGS Reads	27
Figure 5. Schematic Representation of the Insert and Flanking Sequences in MON 94313..	32
Figure 6. Breeding History of MON 94313	33
Figure 7. Read Mapping of Conventional Soybean A3555 Versus PV-GMHT529103.....	36
Figure 8. Read Mapping of MON 94313 (R3) Versus PV-GMHT529103	37
Figure 9. Analysis of Overlapping PCR Analysis Across the Insert in MON 94313.....	39
Figure 10. PCR Amplification of the MON 94313 Insertion Site	41
Figure 11. Schematic Summary of MON 94313 Bioinformatic Analyses	44
Figure 12. Breeding Path for Generating Segregation Data for MON 94313	47
Figure 13. Presence of DMO Protein in Multiple Generations of MON 94313.....	52
Figure 14. Presence of PAT Protein in Multiple Generations of MON 94313.....	53
Figure 15. Presence of FT_T.1 Protein in Multiple Generations of MON 94313	54
Figure 16. Presence of TDO Protein in Multiple Generations of MON 94313	55
Figure 17. Three Components of the DMO Oxygenase System	58
Figure 18. Dicamba and Potential Endogenous Substrates Tested through Previous <i>In Vitro</i> Experiments with DMO	60
Figure 19. Amino Acid Sequence Comparison between FT_T.1, FT_T and RdpA	62
Figure 20. Substrate and Metabolites of FT_T.1 Protein Reaction with 2,4-D	63
Figure 21. Alignment of MON 94313 TDO and <i>Oryza sativa</i> HIS1.....	65
Figure 22. MON 94313 TDO Biochemical Mode of Action.....	66
Figure 23. <i>In silico</i> and <i>In vitro</i> Protocol for TDO Endogenous Substrate Specificity Screen	67
Figure 24. N-terminal Sequence of the MON 94313-Produced DMO Protein	71
Figure 25. Peptide Map of the MON 94313-Produced DMO and <i>E. coli</i> -Produced DMO ...	77
Figure 26. Western Blot Analysis of MON 94313-Produced and <i>E. coli</i> -Produced DMO Proteins.....	79
Figure 27. Purity and Apparent Molecular Weight Analysis of the MON 94313-Produced DMO Protein.....	81
Figure 28. Glycosylation Analysis of the MON 94313-Produced DMO Protein and <i>E. coli</i> - Produced DMO Protein.....	83
Figure 29. N-terminal Sequence of the MON 94313-Produced PAT Protein	86

Figure 30. Peptide Maps of the MON 94313-Produced PAT and <i>E. coli</i> -Produced PAT Proteins.....	90
Figure 31. Western Blot Analysis of MON 94313-Produced and <i>E. coli</i> -Produced PAT	92
Figure 32. Purity and Apparent Molecular Weight Analysis of the MON 94313-Produced and <i>E. coli</i> -Produced PAT Proteins	94
Figure 33. Glycosylation Analysis of the MON 94313-Produced PAT Protein.....	96
Figure 34. N-Terminal Sequence of the MON 94313-Produced FT_T.1 Protein	100
Figure 35. Peptide Map of the MON 94313-Produced FT_T.1 and <i>E. coli</i> -Produced FT_T.1 Proteins.....	106
Figure 36. Western Blot Analysis of MON 94313-Produced and <i>E. coli</i> -Produced FT_T.1 Proteins.....	108
Figure 37. Purity and Apparent Molecular Weight Analysis of the MON 94313-Produced FT_T.1 Protein	110
Figure 38. Glycosylation Analysis of the MON 94313-Produced and <i>E. coli</i> -Produced FT_T.1 Proteins	112
Figure 39. N-terminal Sequence of the MON 94313-Produced TDO Protein	117
Figure 40. Peptide Map of the MON 94313-Produced TDO and <i>E. coli</i> -Produced TDO....	123
Figure 41. Western Blot Analysis of MON 94313-Produced and <i>E. coli</i> -Produced TDO....	125
Figure 42. Purity and Apparent Molecular Weight Analysis of the MON 94313-Produced and <i>E. coli</i> -Produced TDO Proteins.....	127
Figure 43. Glycosylation Analysis of the MON 94313-Produced TDO Protein.....	129
Figure 44. SDS-PAGE Analysis of the Degradation of DMO Protein by Pepsin.....	141
Figure 45. Western Blot Analysis of the Degradation of DMO Protein by Pepsin.....	143
Figure 46. Western Blot Analysis of the Degradation of DMO Protein by Pancreatin.....	145
Figure 47. SDS-PAGE Analysis of the Degradation of FT_T.1 Protein by Pepsin	154
Figure 48. Western Blot Analysis of the Degradation of FT_T.1 Protein by Pepsin	156
Figure 49. Western Blot Analysis of the Degradation of FT_T.1 Protein by Pancreatin.....	158
Figure 50. SDS-PAGE and Western Blot Analysis of the Degradation of FT_T.1 Protein by Sequential Digestion	160
Figure 51. SDS-PAGE Analysis of the Degradation of PAT Protein by Pepsin.....	148
Figure 52. Western Blot Analysis of the Degradation of PAT Protein by Pepsin.....	150
Figure 53. Western Blot Analysis of the Degradation of PAT Protein by Pancreatin.....	152
Figure 54. SDS-PAGE Analysis of the Degradation of TDO Protein by Pepsin	162
Figure 55. Western Blot Analysis of the Degradation of the Produced TDO Protein by Pepsin	164
Figure 56. Western Blot Analysis of the TDO Protein Degradation in Pancreatin	166
Figure 57. SDS-PAGE of <i>E. coli</i> -Produced DMO Protein Demonstrating the Effect After 15 Minutes at Elevated Temperatures on Protein Structural Stability.....	174

Figure 58. SDS-PAGE of <i>E. coli</i> -Produced DMO Protein Demonstrating the Effect After 30 Minutes at Elevated Temperatures on Protein Structural Stability.....	175
Figure 59. SDS-PAGE of <i>E. coli</i> -Produced PAT Protein Following Heat Treatment for 15 Minutes.....	178
Figure 60. SDS-PAGE of <i>E. coli</i> -Produced PAT Protein Following Heat Treatment for 30 Minutes.....	179
Figure 61. SDS-PAGE of <i>E. coli</i> -Produced FT_T.1 Protein Demonstrating the Effect After 15 Minutes at Elevated Temperatures on Protein Structural Stability.....	182
Figure 62. SDS-PAGE of <i>E. coli</i> -Produced FT_T.1 Protein Demonstrating the Effect After 30 Minutes at Elevated Temperatures on Protein Structural Stability.....	183
Figure 63. SDS-PAGE of <i>E. coli</i> -Produced TDO Protein Following Heat Treatment for 15 Minutes.....	186
Figure 64. SDS-PAGE of <i>E. coli</i> -Produced TDO Protein Following Heat Treatment for 30 Minutes.....	187

LIST OF TABLES

Table 1. Summary of Genetic Elements in PV-GMHT529103	19
Table 2. Summary of Genetic Elements in MON 94313	29
Table 3. Unique Junction Sequence Results	35
Table 4. Junction Sequence Detected	45
Table 5. Segregation of the T-DNA I During the Development of MON 94313	49
Table 6. Comparison of RdpA, FT_T, and FT_T.1 Activity on Different Herbicide Substrates	64
Table 7. Results of <i>in vitro</i> TDO Assays with Available Plant Metabolites Identified in the <i>in silico</i> Screen	68
Table 8. Summary of MON 94313 DMO Protein Identity and Equivalence	70
Table 9. Summary of the Tryptic Masses Identified for the MON 94313-Produced DMO Using Nano LC-MS/MS ¹	73
Table 10. Summary of the Tryptic Masses Identified for <i>E. coli</i> -Produced DMO Protein Using Nano LC-MS/MS ¹	75
Table 11. Immunoreactivity of the MON 94313-Produced DMO Protein and <i>E. coli</i> -Produced DMO Protein	80
Table 12. Apparent Molecular Weight and Purity Analysis of the MON 94313-Produced DMO Protein	82
Table 13. Apparent Molecular Weight Comparison Between the MON 94313-Produced DMO and <i>E. coli</i> -Produced DMO Proteins	82
Table 14. Functional Activity Comparison of MON 94313-Produced DMO and <i>E. coli</i> - Produced DMO Proteins	84
Table 15. Summary of MON 94313 PAT Protein Identity and Equivalence	85
Table 16. Summary of the Tryptic Masses Identified for the MON 94313-Produced PAT Using Nano LC-MS/MS ¹	88
Table 17. Summary of the Tryptic Masses Identified for the <i>E. coli</i> -Produced PAT Using MALDI-TOF MS ¹	89
Table 18. Immunoreactivity of the MON 94313-Produced and <i>E. coli</i> -Produced PAT Proteins	93
Table 19. Apparent Molecular Weight and Purity Analysis of the MON 94313-Produced PAT Protein	95
Table 20. Apparent Molecular Weight Comparison Between the MON 94313-Produced PAT and <i>E. coli</i> -Produced PAT Proteins	95
Table 21. Functional Activity of MON 94313-Produced and <i>E. coli</i> -Produced PAT Proteins	97
Table 22. Summary of MON 94313 FT_T.1 Protein Identity and Equivalence.....	99

Table 23. Summary of the Tryptic and Asp-N Masses Identified for the MON 94313-Produced FT_T.1 Using Nano LC-MS/MS	102
Table 24. Summary of the Tryptic Masses Identified for <i>E. coli</i> -produced FT_T.1 using Nano LC-MS/MS ¹	104
Table 25. Immunoreactivity of the MON 94313-Produced and <i>E. coli</i> -Produced FT_T.1 Proteins.....	109
Table 26. Apparent Molecular Weight and Purity Analysis of the MON 94313-Produced FT_T.1 Protein	111
Table 27. Apparent Molecular Weight Comparison Between the MON 94313-Produced FT_T.1 and <i>E. coli</i> -Produced FT_T.1 Proteins.....	111
Table 28. Functional Activity of MON 94313-Produced and <i>E. coli</i> -Produced FT_T.1 Proteins.....	113
Table 29. Summary of MON 94313 TDO Protein Identity and Equivalence	116
Table 30. Summary of the Tryptic Masses Identified for the MON 94313-Produced TDO Using Nano LC-MS/MS	118
Table 31. Summary of the Tryptic Masses Identified for the <i>E. coli</i> -Produced TDO Using Nano LC-MS/MS	120
Table 32. Immunoreactivity of the MON 94313-Produced and <i>E. coli</i> -Produced TDO Proteins.....	126
Table 33. Apparent Molecular Weight and Purity Analysis of the MON 94313-Produced TDO Protein	128
Table 34. Apparent Molecular Weight Comparison Between the MON 94313-Produced TDO and <i>E. coli</i> -Produced TDO Proteins.....	128
Table 35. Functional Activity of MON 94313-Produced and <i>E. coli</i> -Produced TDO Proteins	130
Table 36. Summary of DMO Protein Levels in Tissues Collected from MON 94313 Soybean Produced in United States Field Trials During 2020	132
Table 37. Summary of PAT Protein Levels in Tissues Collected from MON 94313 Soybean Produced in United States Field Trials During 2020	133
Table 38. Summary of FT_T.1 Protein Levels in Tissues Collected from MON 94313 Soybean Produced in United States Field Trials During 2020	135
Table 39. Summary of TDO Protein Levels in Tissues Collected from MON 94313 Soybean Produced in United States Field Trials During 2020	137
Table 40. Dicamba Monooxygenase Activity of Heat-Treated <i>E. coli</i> -Produced DMO Protein after 15 Minutes	171
Table 41. Dicamba Monooxygenase Activity of Heat-Treated <i>E. coli</i> -Produced DMO Protein After 30 Minutes	173
Table 42. Functional Activity of PAT Protein after 15 Minutes at Elevated Temperatures .	177
Table 43. Functional Activity of PAT Protein after 30 Minutes at Elevated Temperatures .	177
Table 44. Functional Activity of Heat Treated FT_T.1 Protein After 15 Minutes at Elevated Temperatures.....	181

Table 45. Functional Activity of Heat Treated FT_T.1 Protein After 30 Minutes at Elevated Temperatures.....	181
Table 46. TDO Activity After 15 Minutes at Elevated Temperatures.....	185
Table 47. TDO Activity After 30 Minutes at Elevated Temperatures.....	185
Table 48. Summary of Soybean Grain Protein and Amino Acids for MON 94313 and the Conventional Control.....	199
Table 49. Summary of Soybean Grain Total Fat and Fatty Acids for MON 94313 and the Conventional Control.....	202
Table 50. Summary of Soybean Grain Carbohydrates by Calculation and Fiber for MON 94313 and the Conventional Control.....	205
Table 51. Summary of Soybean Grain Ash and Minerals for MON 94313 and the Conventional Control.....	206
Table 52. Summary of Soybean Grain Vitamins for MON 94313 and the Conventional Control	207
Table 53. Summary of Soybean Grain Anti-Nutrients and Isoflavones for MON 94313 and the Conventional Control	208
Table 54. Summary of Soybean Forage Proximates, Carbohydrates by Calculation, Fiber and Minerals for MON 94313 and the Conventional Control.....	210
Table 55. Literature and AFSI Database Ranges for Components in Soybean Grain and Forage.....	211

UNPUBLISHED REPORTS BEING SUBMITTED

- Appendix 1. M-815764-02-1. Amended from TRR0001418: Molecular Characterization of Herbicide Tolerant Soybean MON 94313.
- Appendix 2. M-825482-01-1 Updated Bioinformatics Evaluation of the T-DNA in MON 94313 Utilizing the AD_2022, TOX_2022, and PRT_2022 Databases
- Appendix 3. M-826095-01-1 Updated Bioinformatics Evaluation of Putative Flank-Junction Peptides in MON 94313 Utilizing the AD_2022, TOX_2022, and PRT_2022 Databases
- Appendix 4. M-816874-02-1. Segregation Analysis of the T-DNA Insert in Herbicide Tolerant Soybean MON 94313 Across Three Generations.
- Appendix 5. M-820306-01-1. Demonstration of the Presence of DMO, FT_T.1, PAT, and TDO Proteins in Soybean Seed Samples Across Multiple Generations of MON 94313.
- Appendix 6. M-822040-02-1 Characterization of the Dicamba mono-oxygenase protein purified from the seed of MON 94313 soybean and comparison of the physicochemical and functional properties of the plant produced and *Escherichia coli* (*E. coli*) produced Dicamba a mono-oxygenase proteins - Amendment no 1 to final study report M-822040-01-1.
- Appendix 7. M-821946-02-1 Characterization of the PAT protein purified from seed of MON 94313 soybean and comparison of the physicochemical and functional properties of the plant-produced and *Escherichia coli* (*E. coli*)-produced PAT proteins - Amendment no 1 to final study report M-821946-01-1.
- Appendix 8. M-820215-02-1 Characterization of the FT_T.1 protein purified from the soybean seed of MON 94313 and comparison of the physicochemical and functional properties of the plant produced and *Escherichia coli* (*E. coli*) produced FT_T.1 proteins - Amendment no 1 to final study report M-820215-01-
- Appendix 9. M-822523-02-1 Characterization of the TDO protein purified from seed of MON 94313 soybean and comparison of the physicochemical and functional properties of the plant-produced and *Escherichia coli* (*E. coli*)-produced TDO proteins - Amendment no 1 to final study report M-822523-01-1.
- Appendix 10. TRR0001494. Assessment of DMO, PAT, FT_T.1, and TDO Protein Levels in Herbicide Treated Soybean Forage, Grain, Leaf, and Root Tissues Collected from MON 94313 Produced in United States Field Trials During 2020.
- Appendix 11. M-826109-01-1 Updated Bioinformatics Evaluation of DMO, FT_T.1, and TDO in MON 94313 utilizing the AD_2022, TOX_2022, and PRT_2022 databases.
- Appendix 12. M-816143-01-1 Updated Bioinformatics Evaluation of PAT Utilizing the AD_2022, TOX_2022, and PRT_2022 Database.s
- Appendix 13. TRR0001533. Assessment of the *in vitro* Digestibility of *Escherichia coli* (*E. coli*)-produced MON 94313 DMO Protein by Pepsin and Pancreatin.
- Appendix 14. MSL0030948. Amended Summary for Assessment of the *in vitro* Digestibility of Phosphinothricin N-Acetyltransferase Protein by Pepsin and Pancreatin.

- Appendix 15. TRR0000874. *In vitro* Digestibility of *E.coli*-produced FT_T.1 Protein by Pepsin and Pancreatin.
- Appendix 16. TRR0001573. Amended Report for TRR0001315: *In vitro* Digestibility of *E.coli*-produced TDO Protein by Pepsin and Pancreatin.
- Appendix 17. TRR0001399. The Effect of Heat Treatment on the Functional Activity of *Escherichia coli* (*E. coli*)-produced MON 94313 DMO Protein.
- Appendix 18. SCR-2019-0110. Effect of Heat Treatment on the Functional Activity of *Escherichia coli*-Produced Phosphinothricin N-acetyltransferase Protein.
- Appendix 19. TRR0001512. The Effect of Heat Treatment on the Functional Activity of *Escherichia coli*-produced MON 94313 FT_T.1 Protein.
- Appendix 20. TRR0001400. The Effect of Heat Treatment on the Functional Activity of *Escherichia coli* (*E. coli*)-produced MON 94313 TDO Protein.
- Appendix 21. M-829221-02-1 Summary of the Magnitude of Residues in Herbicide-Tolerant Soybean MON 94313 Raw Agricultural Commodities Following Applications of a Mesotrione-Based Formulation – 2020 U.S. Trials
- Appendix 22. M-829222-01-1 Summary of the Magnitude of Residues in Herbicide-Tolerant Soybean MON 94313 Raw Agricultural Commodities Following Applications of a 2,4-D-Based Formulation – 2021 U.S. Trials
- Appendix 23. TRR0001412. Amended Report of TRR0001366: Compositional Analyses of Soybean Grain and Forage Harvested from MON 94313 Grown in United States During the 2020 Season.

CHECKLIST

General Requirements (3.1.1)	Reference
A Form of application	
<input checked="" type="checkbox"/> <i>Application in English</i>	<i>Available</i>
<input checked="" type="checkbox"/> <i>Executive Summary (separated from main application electronically)</i>	<i>Separate document prepared</i>
<input checked="" type="checkbox"/> <i>Relevant sections of Part 3 clearly identified</i>	<i>Completed</i>
<input checked="" type="checkbox"/> <i>Pages sequentially numbered</i>	<i>Completed</i>
<input checked="" type="checkbox"/> <i>Electronic copy (searchable)</i>	<i>Prepared</i>
<input checked="" type="checkbox"/> <i>All references provided</i>	<i>Prepared</i>
B Applicant details	<i>Page 1</i>
C Purpose of the application	<i>Page 1</i>
D Justification for the application	
<input checked="" type="checkbox"/> <i>Regulatory impact information</i>	<i>Page 2</i>
<input checked="" type="checkbox"/> <i>Impact of international trade</i>	<i>Page 3</i>
E Information to support the application	
<input checked="" type="checkbox"/> <i>Data requirement</i>	<i>14</i>
F Assessment procedure	
<input checked="" type="checkbox"/> <i>General</i>	<i>Page 3</i>
<input type="checkbox"/> <i>Major</i>	
<input type="checkbox"/> <i>Minor</i>	
<input type="checkbox"/> <i>High level health claim variation</i>	
G Confidential Commercial Information	
<input checked="" type="checkbox"/> <i>CCI material separated from other application material</i>	<i>Completed</i>
<input type="checkbox"/> <i>Formal request including reasons</i>	
<input type="checkbox"/> <i>Non-confidential summary provided</i>	
H Other confidential information	
<input checked="" type="checkbox"/> <i>Confidential material separated from other application material</i>	<i>Completed</i>
<input type="checkbox"/> <i>Formal request including reasons</i>	
I Exclusive Capturable Commercial Benefit	

<input checked="" type="checkbox"/> <i>Justification provided</i>	<i>Page 4</i>
J International and Other National Standards	
<input checked="" type="checkbox"/> <i>International standards</i>	<i>Page 4</i>
<input checked="" type="checkbox"/> <i>Other national standards</i>	<i>Page 4</i>
K Statutory Declaration	<i>Page 214</i>
L Checklist/s provided with Application	
<input checked="" type="checkbox"/> <i>3.1.1 Checklist</i>	<i>Page xiii</i>
<input checked="" type="checkbox"/> <i>All page number references from application included</i>	<i>Completed</i>
<input checked="" type="checkbox"/> <i>Any other relevant checklists for Sections 3.2 – 3.7</i>	<i>Checklist 3.5.1</i>
Foods Produced using Gene Technology (3.5.1)	
<input checked="" type="checkbox"/> <i>A.1 Nature and identity of the GM food</i>	<i>Page 5</i>
<input checked="" type="checkbox"/> <i>A.2 History of use of host and donor organisms</i>	<i>Page 6</i>
<input checked="" type="checkbox"/> <i>A.3 Nature of genetic modification</i>	<i>Page 10</i>
<input checked="" type="checkbox"/> <i>B.1 Characterisation and safety assessment of new substances</i>	<i>Page 57</i>
<input checked="" type="checkbox"/> <i>B.2 New proteins</i>	<i>Page 133</i>
<input checked="" type="checkbox"/> <i>B.3 Other (non-protein) new substances</i>	<i>Page 188</i>
<input checked="" type="checkbox"/> <i>B.4 Novel herbicide metabolites in GM herbicide-tolerant plants</i>	<i>Page 188</i>
<input checked="" type="checkbox"/> <i>B.5 Compositional assessment</i>	<i>Page 194</i>
<input checked="" type="checkbox"/> <i>C Information related to the nutritional impact of the food produced using gene technology</i>	<i>Page 213</i>
<input checked="" type="checkbox"/> <i>D Other information</i>	<i>Page 213</i>

ABBREVIATIONS AND DEFINITIONS

AA	Amino Acid
ADF	Acid Detergent Fiber
AEX	Anion Exchange Chromatography
APHIS	Animal and Plant Health Inspection Service
BSA	Bovine Serum Albumin
CFR	Code of Federal Regulations
CID	Collision Induced Dissociation
COMPARE	COMprehensive Protein Allergen REsource
CTP	Chloroplast Transit Peptide
DAP	Days After Planting
DCSA	3,6-Dichlorosalicylic Acid
DMO	Dicamba Mono-Oxygenase
DNA	Deoxyribonucleic Acid
dw	Dry Weight
DWCF	Dry Weight Conversion Factor
E. coli	Escherichia coli
EFSA	European Food Safety Authority
ECL	Enhanced Chemiluminescence
ELISA	Enzyme-Linked Immunosorbent Assay
ELN	Electronic Lab Notebook
E-score	Expectation score
ETS	Excellence Through Stewardship
FA	Fatty Acid
FASTER	Food Allergy Safety, Treatment, Education and Research
FDA	Food and Drug Administration (U.S.)
FFDCA	Federal Food, Drug and Cosmetic Act
FOIA	Freedom of Information Act
FSANZ	Food Standards Australia New Zealand
FT T.1	Modified fops and 2,4-D dioxygenase protein
fw	Fresh Weight
g	Gram
GLP	Good Laboratory Practice
GRAS	Generally Recognized as Safe
HRP	Horseradish Peroxidase
IAC	Immunoaffinity Chromatography
ICP-OES	Inductively Coupled Plasma Optical Emission Spectroscopy
ILSI	International Life Science Institute
IUPAC-IUB	Union of Pure and Applied Chemistry - International Union of Biochemistry
kb	Kilobase
KTI	Kunitz Trypsin Inhibitor
LOD	Limit of Detection
LOQ	Limit of Quantitation
M	Methionine
MW	Molecular Weight

NDF	Neutral Detergent Fiber
NGS	Next Generation Sequencing
NOAEL	No Observed Adverse Effect Level
OECD	Organization for Economic Co-operation and Development
ORF	Open Reading Frame
OSL	Over-Season Leaf
PAT	Phosphinothricin N-Acetyltransferase
PCR	Polymerase Chain Reaction
RO	Reverse Osmosis
ROP	Repressor of Primer
RSR	Regulatory Status Review
SE	Standard Error
SEC	Size Exclusion Chromatography
T	Treated
TCA	Trichloroacetic Acid
TDO	Triketone Dioxygenase
U.S.	United States
USDA	United States Department of Agriculture
UTR	Untranslated Region
µg	Microgram

PART 1 GENERAL INFORMATION

1.1 Applicant Details

- (a) Applicant's name/s [REDACTED]
- (b) Company/organisation name [REDACTED]
- (c) Address (street and postal) [REDACTED]
- (d) Telephone number [REDACTED]
- (e) Email address [REDACTED]
- (f) Nature of applicant's business Technology Provider to the Agricultural and Food Industries
- (g) Details of other individuals, companies or organisations associated with the application

1.2 Purpose of the Application

This application is submitted to Food Standards Australia New Zealand by Bayer CropScience Proprietary Limited on behalf of Bayer Group.

The purpose of this submission is to make an application to vary **Standard 1.5.2 – Food Produced Using Gene Technology** of the *Australia New Zealand Food Standards Code* to seek the addition of MON 94313 soybean and products containing MON 94313 soybean (hereafter referred to as MON 94313) to the Table to Clause 2 (see below).

Food derived from gene technology	Special requirements
Food derived from MON 94313 soybean	None

1.3 Justification for the Application

1.3(a) The need for the proposed change

Bayer has developed herbicide tolerant MON 94313 soybean, which is tolerant to the herbicides glufosinate (2-amino-4-(hydroxymethylphosphinyl) butanoic acid), dicamba (3,6-dichloro-2-methoxybenzoic acid), 2,4-D (2,4-dichlorophenoxyacetate), and mesotrione (2-[4-(methylsulfonyl)-2-nitrobenzoyl]-1,3-cyclohexanedione). MON 94313 contains the phosphinothricin N-acetyltransferase (*pat*) gene from *Streptomyces viridochromogenes* that expresses the PAT protein to confer tolerance to glufosinate herbicide, a demethylase gene from *Stenotrophomonas maltophilia* that expresses a dicamba mono-oxygenase (DMO) protein to confer tolerance to dicamba herbicide, the *ft_t.1* gene, a modified version of the R-2,4-dichlorophenoxypropionate dioxygenase (*RdpA*) gene from *Sphingobium herbicidovorans* that expresses a FOPs and 2,4-D dioxygenase protein (FT_T.1) to confer tolerance to 2,4-D herbicide, and the *TDO* gene from *Oryza sativa* that expresses the triketone dioxygenase (TDO) protein to confer tolerance to mesotrione herbicide.

1.3(b) The advantages of the proposed change over the status quo, taking into account any disadvantages

MON 94313 soybean will offer growers multiple choices for effective weed management including tough-to-control and herbicide-resistant broadleaf and grass weeds. The flexibility to use combinations of any of these four herbicides representing multiple modes-of-action provides an effective and durable weed management system for soybean production. The best management practices for minimizing the development of herbicide resistant weeds are built on the concept of implementing diversified weed management programs, which includes using multiple herbicides with different modes of action either in mixtures, sequences or in rotation, and other recommended integrated weed management principles.

MON 94313 soybean will be combined, through traditional breeding methods, with other deregulated events (e.g., glyphosate-tolerant trait). MON 94313 soybean combined with glyphosate-tolerant soybean systems through traditional breeding will provide: 1) an opportunity for an efficient, effective weed management system for hard-to-control and herbicide-resistant weeds; 2) a flexible system with multiple herbicide modes-of-action for in-crop application in current soybean production systems; 3) an opportunity to delay selection for further resistance to glyphosate and other herbicides that are important in crop production; 4) excellent crop tolerance to dicamba, glufosinate, 2,4-D, mesotrione and glyphosate; and 5) additional tools to enhance weed management systems necessary to maintain or improve soybean yield and quality to meet the growing needs of the food, feed, and industrial markets.

1.4 Regulatory Impact Information

Costs and benefits

If the draft variation to permit the sale and use of food derived from MON 94313 is approved, possible affected parties may include consumers, industry sectors and government. The consumers who may be affected are those that consume food containing ingredients derived from soybean. Industry sectors affected may be food importers and exporters, distributors, processors and manufacturers. Lastly, government enforcement agencies may be affected.

A cost/benefit analysis quantified in monetary terms is difficult to determine. In fact, most of the impacts that need to be considered cannot be assigned a dollar value. Criteria would need

to be deliberately limited to those involving broad areas such as trade, consumer information and compliance. If the draft variation is approved:

Consumers:

- There would be benefits in the broader availability of soybean products.
- There is unlikely to be any significant increase in the prices of foods if manufacturers are able to use comingled soybean products.
- Consumers wishing to do so will be able to avoid GM soybean products as a result of labeling requirements and marketing activities.

Government:

- Benefit that if soybean MON 94313 was detected in food products, approval would ensure compliance of those products with the Code. This would ensure no potential for trade disruption on regulatory grounds.
- Approval of soybean MON 94313 would ensure no potential conflict with WTO responsibilities.
- In the case of approved GM foods, monitoring is required to ensure compliance with the labeling requirements, and in the case of GM foods that have not been approved, monitoring is required to ensure they are not illegally entering the food supply. The costs of monitoring are thus expected to be comparable, whether a GM food is approved or not.

Industry:

- Sellers of processed foods containing soybean derivatives would benefit as foods derived from soybean MON 94313 would be compliant with the Code, allowing broader market access and increased choice in raw materials. Retailers may be able to offer a broader range of soybean products or imported foods manufactured using soybean derivatives.
- Possible cost to food industry as some food ingredients derived from soybean MON 94313 would be required to be labelled

1.5 Impact of International Trade

If the draft variation to permit the sale and use of food derived from MON 94313 was rejected it would result in the requirement for segregation of any soybean derived products containing MON 94313 from those containing approved soybean, which would be likely to increase the costs of imported soybean derived foods.

It is important to note that if the draft variation is approved, soybean MON 94313 will not have a mandatory introduction. The consumer will always have the right to choose not to use/consume this product.

1.6 Assessment Procedure

Bayer CropScience is submitting this application in anticipation that it will fall within the General Procedure category.

1.7 Exclusive Capturable Commercial Benefit

This application is likely to result in an amendment to the Code that provides exclusive benefits and therefore Bayer CropScience intends to pay the full cost of processing the application.

1.8 International and Other National Standards

1.8(a) International standards

Bayer CropScience makes all efforts to ensure that safety assessments are aligned, as closely as possible, with relevant international standards such as the Codex Alimentarius Commission's *Principles for the Risk Analysis of Foods Derived from Modern Biotechnology* and supporting *Guideline for the Conduct of Food Safety Assessment of Foods Derived from Recombinant-DNA Plants* ([Codex Alimentarius, 2009](#)).

In addition, the composition analysis is conducted in accordance with OECD guidelines and includes the measurement of OECD-defined soybean nutrients and anti-nutrients based on conventional commercial soybean varieties ([OECD, 2012](#)).

1.8(b) Other national standards or regulations

Bayer CropScience has submitted a food and feed safety and nutritional assessment summary for MON 94313 to the United States Food and Drug Administration (FDA) and has also requested a Regulatory Status Review (RSR) for a determination of plant pest risk potential of MON 94313, including all progenies derived from crosses between MON 94313 and conventional soybean, or deregulated biotechnology-derived soybean by the Animal and Plant Health Inspection Service (APHIS) of the U.S. Department of Agriculture (USDA).

Consistent with our commitments to the Excellence Through Stewardship® (ETS) Program¹, regulatory submissions have been or will be made to countries that import significant soybean or food and feed products derived from North and South America soybeans and have functional regulatory review processes in place.

¹ Excellence Through Stewardship is a registered trademark of Excellence Through Stewardship, Washington, DC. (<http://www.excellencethroughstewardship.org>)

PART 2 SPECIFIC DATA REQUIREMENTS FOR SAFETY ASSESSMENT

A. TECHNICAL INFORMATION ON THE GM FOOD

A.1 Nature and Identity of the Genetically Modified Food

A.1(a) A description of the new GM organism from which the new GM food is derived

Bayer has developed herbicide tolerant MON 94313 soybean, which is tolerant to the herbicides glufosinate (2-amino-4-(hydroxymethylphosphinyl) butanoic acid), dicamba (3,6-dichloro-2-methoxybenzoic acid), 2,4-D (2,4-dichlorophenoxyacetate), and mesotrione (2-[4-(methylsulfonyl)-2-nitrobenzoyl]-1,3-cyclohexanedione). MON 94313 contains the phosphinothricin N-acetyltransferase (*pat*) gene from *Streptomyces viridochromogenes* that expresses the PAT protein to confer tolerance to glufosinate herbicide, a demethylase gene from *Stenotrophomonas maltophilia* that expresses a dicamba mono-oxygenase (DMO) protein to confer tolerance to dicamba herbicide, the *ft t.1* gene, a modified version of the R-2,4-dichlorophenoxypropionate dioxygenase (*RdpA*) gene from *Sphingobium herbicidovorans* that expresses a FOPs and 2,4-D dioxygenase protein (FT_T.1) to confer tolerance to 2,4-D herbicide, and the *TDO* gene from *Oryza sativa* that expresses the triketone dioxygenase (TDO) protein to confer tolerance to mesotrione herbicide.

A.1(b) Name, line number and OECD Unique Identifier of each of the new lines or strains of GM organism from which the food is derived

In accordance with OECD's "Guidance for the Designation of a Unique Identifier for Transgenic Plants" MON 94313 has been assigned the unique identifier MON-94313-8.

A.1(c) The name the food will be marketed under (if known)

Soybean containing the transformation event MON 94313 will be produced in North and South America. There are currently no plans to produce this product in Australia and New Zealand. A commercial trade name for the product has not been determined at the time of this submission and will be available prior to commercial launch of the product in North America.

A.2 History of Use of the Host and Donor Organisms

A.2(a) For the donor organism(s) from which the genetic elements are derived:

A.2(a)(i) Any known pathogenicity, toxicity or allergenicity relevance to the food

A.2(a)(i)(i) Source of the *dmo* Gene Introduced into MON 94313

The *dmo* gene is derived from the bacterium *Stenotrophomonas maltophilia* strain DI-6, isolated from soil at a dicamba manufacturing plant (Krueger *et al.*, 1989). *S. maltophilia* is ubiquitously present in the environment (Mukherjee and Roy, 2016), including in water and dairy products (An and Berg, 2018; Okuno *et al.*, 2018; Todaro *et al.*, 2011). These bacteria have been used as an effective biocontrol agent against plant and animal pathogenesis (Mukherjee and Roy, 2016), and have antibacterial activity against both gram-positive and gram-negative bacteria (Dong *et al.*, 2015). *S. maltophilia* has been found in healthy individuals without any hazard to human health (Heller *et al.*, 2016; Lira *et al.*, 2017), although these bacteria can form biofilms that become resistant to antibiotics (Berg and Martinez, 2015; Brooke *et al.*, 2017). The opportunistic pathogenicity of *S. maltophilia* is mainly associated with hosts with compromised immune systems rather than with any specific virulence genes of these bacteria. Thus, documented occurrences of *S. maltophilia* infections have been limited to immune-compromised individuals in hospital settings (Lira *et al.*, 2017).

Other than the potential to become an opportunistic pathogen in immune-compromised hosts, *S. maltophilia* is not known for human or animal pathogenicity. *S. maltophilia*'s history of safe exposure has been extensively reviewed during the evaluation of several dicamba-tolerant events with no safety or allergenicity issues identified by FSANZ or other regulatory agencies (e.g., MON 88701 cotton [A1080], MON 87708 soybean [A1063], MON 87419 maize [A1118], and MON 87429 maize [A1192]).

A.2(a)(i)(ii) Identity and Source of the *pat* Gene Introduced into MON 94313

The *pat* gene is derived from the bacterium *Streptomyces viridochromogenes* (Wohlleben *et al.*, 1988). *Streptomyces* species are widespread in the environment and present no known allergenic or toxicity issues (Kämpfer, 2006; Kutzner, 1981), though human exposure is quite common (Goodfellow and Williams, 1983). *S. viridochromogenes* is not considered pathogenic to plants, humans or other animals (Cross, 1989; Goodfellow and Williams, 1983; Locci, 1989). *S. viridochromogenes* is widespread in the environment and the history of safe use is discussed in Hérouet *et al.* (2005). This organism has been extensively reviewed during the evaluation of several glufosinate-tolerant events (e.g., A2704-12 and A5547-127 soybean [A481], MON 87419 [A1118] and MON 87429 [A1192]) with no safety or allergenicity issues identified by FSANZ or other regulatory agencies.

A.2(a)(i)(iii) Identity and Source of the *ft_t.1* Gene Introduced into MON 94313

MON 94313 contains the *ft_t.1* gene, a modified version of the *RdpA* gene from *Sphingobium herbicidovorans*, that expresses the FT_T.1 protein. FT_T.1 is therefore a modified version of the R-2,4-dichlorophenoxypropionate dioxygenase (RdpA) protein (Müller *et al.*, 2006). *S. herbicidovorans* is a common gram-negative, rod-shaped, non-motile, non-spore-forming soil

bacterium ([Takeuchi et al., 2001](#); [Zipper et al., 1996](#)), which is strictly aerobic and chemo-organotrophic, and not known to be associated with human disease.

Members of the genus *Sphingobium* have been isolated from a wide variety of habitats including soil and freshwater ([Chaudhary et al., 2017](#)). *Sphingobium* species have also been isolated from food products such as corn ([Rijavec et al., 2007](#)), papaya ([Thomas et al., 2007](#)) and tomato ([Enya et al., 2007](#)). The biosynthetic and biodegrading properties of this genus have been exploited in the food industry ([Fialho et al., 2008](#); [Pozo et al., 2007](#)), bioremediation ([Alarcón et al., 2008](#); [Jin et al., 2013](#)), and biofuel industries ([Varman et al., 2016](#)). The ubiquitous presence of *Sphingobium* species in the environment has resulted in widespread human and animal exposure without any known adverse safety or allergenicity reports. This organism was reviewed during the evaluation of MON 87429 maize [A1192] with no safety or allergenicity issues identified by the FSANZ.

A.2(a)(i)(iv) Identity and Source of the *TDO* Gene Introduced into MON 94313

The *TDO* gene is derived from Asian (japonica) rice, *Oryza sativa* ([Maeda et al., 2019](#)), which is a crop plant with a long history as food and feed. It is one of the most important crops in the world serving as a primary food source for more than half of the world's population ([Khush, 1997](#)). Rice is cultivated in more than 80 countries around the world (USDA Foreign Agriculture Service - https://apps.fas.usda.gov/psdonline/downloads/psd_grains_pulses_csv.zip), being one of three major staple crops after maize and with a total production similar to wheat. *Oryza sativa* has two subspecies, *indica* and *japonica*, which account for almost all global rice production ([Khush, 1997](#)). Brown, milled, polished and parboiled rice are the major rice products consumed by humans in the form of grain after being cooked. Rice is also consumed as food ingredients which are part of food products. For example, rice flour is used in cereals, baby food, and snacks. The primary nutrients provided by rice are carbohydrates and proteins ([OECD, 2016](#)).

Rice is also widely used as feed for livestock. This is fed in various forms such rice grain, hulls, bran, straw, polishings, and whole crop silage ([OECD, 2016](#)).

Generally, rice is considered to be a safe source of food and feed, and is not considered by allergists to be a common source of allergens. There are very few compounds in rice which are considered unfavourable for human or animal food/feed, and these compounds have not been observed to exist at levels in rice-based foods that would be a concern for food or feed safety ([OECD, 2016](#)).

The binary vector PV-GMHT529103 was used for the transformation of conventional soybean to produce MON 94313. PV-GMHT529103 contains two separate T-DNAs, each delineated by Left and Right Border regions and the vector backbone sequences. The first T-DNA, designated as T-DNA I, contains the *dmo*, *pat*, *ft_t.1*, and *TDO* expression cassettes.

A.2(a)(i)(v) Identity and Source of Other Genetic Material Introduced into MON 94313

The *dmo* expression cassette is regulated by the *ubq3-At1* promoter from *Arabidopsis thaliana*, the *apg6-At1* targeting sequence from *Arabidopsis thaliana*, and the *sali3-2-Mt1* 3' untranslated region (UTR) from *Medicago truncatula*. The *pat* expression cassette is regulated by the *GSP579* promoter developed from multiple promoter sequences from *Arabidopsis thaliana*, the *GSII02* intron developed from multiple intron sequences from *Arabidopsis thaliana*, and the *Hsp20-Mt-1*

3' UTR from *Medicago truncatula*. The *ft_t.1* expression cassette is regulated by the *ubq10-At1* promoter from *Arabidopsis thaliana* and the *guf-Mt2* 3' UTR from *Medicago truncatula*. The *TDO* expression cassette is regulated by the *GSP576* promoter developed from multiple promoter sequences from *Arabidopsis thaliana*, the *GSII7* intron developed from multiple intron sequences from *Arabidopsis thaliana*, and the *GST7* 3' UTR developed from multiple 3' UTR sequences from *Zea mays*.

Arabidopsis thaliana, *Medicago truncatula* and *Zea mays* coding sequences have been used in GM event previously and have a long history of safe use. *A. thaliana* and *M. truncatula* are popular model organism in plant biology and genetics, and legume biology, whose genomes had been extensively studied. *Zea mays* (maize) has been a staple of the human diet for centuries, and its processed fractions are consumed in a multitude of food and animal feed products.

The second T-DNA, designated as T-DNA II, contains the *splA* expression cassette and *aadA* expression cassette. The *splA* expression cassette is regulated by the *Usp* promoter from *Vicia faba* and the *nos* 3' UTR from *Agrobacterium tumefaciens*. The *aadA* expression cassette is regulated by the *FMV* enhancer of figwort mosaic virus, the *EF-1a* promoter from *Arabidopsis thaliana*, the *CTP2* targeting sequence from *Arabidopsis thaliana*, and the *E9* 3' UTR from *Pisum sativum*. T-DNA II is fully removed and absent in MON 94313.

A.2(a)(ii) History of use of the organism in food supply or history of human exposure to the organism through other than intended food use (e.g. as a normal contaminant)

As described in Section A.2(a)(i), *Stenotrophomonas maltophilia* is ubiquitously present in the environment ([Mukherjee and Roy, 2016](#)), including in water and dairy products ([An and Berg, 2018](#); [Okuno et al., 2018](#); [Todaro et al., 2011](#)). It been found in healthy individuals without any hazard to human health ([Heller et al., 2016](#); [Lira et al., 2017](#)), although these bacteria can form biofilms that become resistant to antibiotics ([Berg and Martinez, 2015](#); [Brooke et al., 2017](#)).

Streptomyces viridochromogenes is widespread in the environment and presents no known allergenic or toxicity issues ([Kämpfer, 2006](#); [Kutzner, 1981](#)), though human exposure is quite common ([Goodfellow and Williams, 1983](#)). *S. viridochromogenes* is not considered pathogenic to plants, humans or other animals ([Cross, 1989](#); [Goodfellow and Williams, 1983](#); [Locci, 1989](#)).

Sphingobium herbicidovorans is a common gram-negative, rod-shaped, non-motile, non-spore-forming soil bacterium ([Takeuchi et al., 2001](#); [Zipper et al., 1996](#)), which is strictly aerobic and chemo-organotrophic, and not known to be associated with human disease. *Sphingobium* species have also been isolated from food products such as corn ([Rijavec et al., 2007](#)), papaya ([Thomas et al., 2007](#)) and tomato ([Enya et al., 2007](#)).

Oryza sativa ([Maeda et al., 2019](#)) is a crop plant with a long history as food and feed. It is one of the most important crops in the world serving as a primary food source for more than half of the world's population ([Khush, 1997](#)). Generally, rice is considered to be a safe source of food and feed, and is not considered by allergists to be a common source of allergens.

A.2(b) For the host organism into which the genes were transferred:**A.2(b)(i) Its history of safe use for food**

Soybean is the most widely grown oilseed in the world, with approximately 368 million metric tons (MMT) of harvested seed produced in 2020/2021, which represented 61% of world oilseed production that year ([ASA, 2021](#)). Soybean is grown as a commercial crop in over 35 countries. The major producers of soybean are Brazil, U.S, Argentina, China, Paraguay, India and Canada, which accounted for approximately 79% of the global soybean production in 2020/2021 ([ASA, 2021](#)). Approximately 31% of the 2020/2021 world soybean production was produced in the U.S. ([ASA, 2021](#)). With 61.5 MMT exported, the U.S. was second to Brazil (81.5 MMT) in world soybean exports. Approximately 58.3 MMT of soybeans were crushed in the U.S. in 2020/2021 and used to supply the feed industry for livestock use or the food industry for edible vegetable oil and soybean protein isolates ([ASA, 2021](#)).

Soybean is the second most planted field crop in the U.S. after corn. According to data from USDA-NASS, soybean was planted on approximately 87.2 million acres in the U.S. in 2021, producing 120.7 MMT of soybean ([ASA, 2021](#)).

A.2(b)(ii) The part of the organism typically used as food

Soybean is used in various food products, including tofu, soy sauce, soymilk, energy bars, and meat products. A major food use for soybean is purified oil, for use in margarines, shortenings, cooking, and salad oils. Soybean oil generally has a smaller contribution to soybean's overall value compared to soybean meal because the oil constitutes just 18 to 19% of the soybean's weight. Nonetheless, soybean oil accounted for approximately 29% of all the vegetable oils consumed globally in 2021, and was the second largest source of vegetable oil worldwide, slightly behind palm oil at approximately 36% share ([ASA, 2021](#)).

A.2(b)(iii) The types of products likely to include the food or food ingredient

Soybean meal is a high-value component obtained from processing of soybean, and is used as a supplement in feed rations for livestock. Industrial edible and industrial uses of soybean range from a carbon/nitrogen source in the production of yeasts via fermentation to the manufacture of soaps, inks, paints, disinfectants, and biodiesel. Industrial uses of soybean have been summarized by the American Soybean Association ([ASA, 2021](#)).

A.2(b)(iv) Whether special processing is required to render food safe to eat

In general, soyfoods can be roughly classified into four major categories ([Liu, 2004](#)).

Traditional soyfoods, primarily made from whole soybean: The non-fermented traditional soyfoods include soymilk, tofu, and soybean sprouts, whereas the fermented soyfoods include soybean paste (miso), soybean sauce, natto, and tempeh.

Soybean oil: soybean oil constitutes approximately 29% of global consumption of vegetable oil, and is the second largest source of vegetable oil worldwide slightly behind palm oil at approximately 36% share ([ASA, 2021](#)).

Refined, bleached, and deodorized (RDB) soybean oil can be further processed and utilized in the manufacture of cooking oils, shortening, margarine, mayonnaise, salad dressings, and a wide variety of products that are either based entirely on fats and oils or contain fat or oil as a principal ingredient. Soybean oil is comprised primarily of five major fatty acids: saturated fatty acids; 16:0 palmitic and 18:0 stearic acids, monounsaturated; 18:1 oleic acid, and the PUFAs; 18:2 linoleic and 18:3 linolenic acids. These five major fatty acids have very different oxidative stabilities and chemical functionalities. Conventional soybean oil typically contains 60-65% PUFAs, mostly in the form of 18:2 linoleic acid. This composition makes soybean oil unsuitable for certain food applications since the high concentrations of PUFAs in the oil are susceptible to oxidation and degradation at high temperature resulting in off-flavors and odors. Therefore, hydrogenation of soybean oil is necessary to reduce levels of polyunsaturated fatty acids by converting them to saturated fatty acids resulting in higher stability oil suitable for a range of food uses.

Soybean protein products: soybean protein products are made from defatted soybean flakes, and include soybean flour, soybean protein concentrate, and soybean protein isolate. Soybean flour has a protein content of approximately 50% and is used mainly as an ingredient in the bakery industry. Soybean protein concentrate has a protein content of approximately 70% and is used widely in the meat industry as a key ingredient of meat alternative products such as soybean burgers and meatless “meatballs.” Soybean protein isolate has a protein content of 90%, and possesses many functional properties such as gelation and emulsification. As a result, it can be used in a wide range of food applications, including soups, sauce bases, energy bars, nutritional beverages, infant formula, and dairy replacements.

Dietary supplements: soybean is a rich source of certain phytochemicals used as dietary supplements, which include isoflavones and tocopherols. Isoflavones have been shown to inhibit the growth of cancer cells, lower cholesterol levels, and inhibit bone resorption ([Messina, 1999](#)). Tocopherols have long been recognized as a free radical scavenging antioxidant whose deficiency impairs mammalian fertility. In addition, biological activities have been reported for the desmethyl tocopherols, such as γ -tocopherol, which possess anti-inflammatory, antineoplastic, and natriuretic functions ([Hensley et al., 2004](#); [Schafer et al., 2003](#)). Detailed reviews of soybean fractions and soybean-derived phytochemicals have been published ([Liu, 2004](#)).

A.3 The Nature of the Genetic Modification

Characterisation of the genetic modification in MON 94313 was conducted using a combination of sequencing, PCR, and bioinformatics. The results of this characterisation demonstrate that MON 94313 contains a single copy of the intended T-DNA I containing the *dmo*, *pat*, *ft_t.1*, and *TDO* expression cassettes that is stably integrated at a single locus and is inherited according to Mendelian principles over multiple generations. These conclusions are based on the following:

- Molecular characterisation of MON 94313 by NGS demonstrated that MON 94313 contained a single copy of T-DNA I insert. These whole-genome sequence analyses ([Kovalic et al., 2012](#)) provided a comprehensive assessment of MON 94313 to determine the presence of sequences derived from PV-GMHT529103 and demonstrated that MON 94313 contained a single copy of T-DNA I insert with no detectable backbone or T-DNA II sequences.

PART 2: SPECIFIC DATA REQUIREMENTS FOR SAFETY ASSESSMENT

- Directed sequencing (locus-specific PCR, DNA sequencing and analyses) performed on MON 94313 was used to determine the complete sequence of the single DNA insert from PV-GMHT529103, the adjacent flanking DNA, and the 5' and 3' insert-to-flank junctions. This analysis confirmed that the sequence and organization of the DNA insert is identical to the corresponding region in the PV-GMHT529103 T-DNA I. Furthermore, the genomic organization at the insertion site was assessed by comparing the T-DNA I insert and sequences flanking the T-DNA I insert in MON 94313 to the sequence of the insertion site in conventional soybean. This analysis identified a 40 bp deletion that likely occurred during integration of the T-DNA sequence and determined that no major DNA rearrangement occurred at the insertion site in MON 94313 upon DNA integration.
- Generational stability analysis by NGS demonstrated that the single PV-GMHT529103 T-DNA I insert in MON 94313 has been maintained through five breeding generations, thereby confirming the stability of the T-DNA I in MON 94313.
- Segregation data confirm that the inserted T-DNA I segregated following Mendelian inheritance patterns, which corroborates the insert stability demonstrated by NGS and independently establishes the nature of the T-DNA I at a single chromosomal locus.

Taken together, the characterisation of the genetic modification in MON 94313 demonstrates that a single copy of the intended T-DNA I was stably integrated at a single locus of the soybean genome and that no T-DNA II or plasmid backbone sequences were present in MON 94313.

A.3(a) A description of the method used to transform the host organism

MON 94313 was created through an *Agrobacterium*-mediated transformation in A3555 soybean meristem explants with the PV-GMHT529103 binary plasmid vector DNA based on the methods described by Ye *et al.* (2008). After co-culturing with *Agrobacterium* AB30 strain carrying the plasmid vector, meristem explants were placed on selection medium containing spectinomycin to select for transgenic events, and carbenicillin, cefotaxime and timentin to inhibit the overgrowth of *Agrobacterium*. The putative transgenic plants (R0) with normal phenotypic characteristics were selected and screened using copy number assay and linkage analysis. Events which passed the advancement criteria (such as a single copy of the T-DNA I insert unlinked with the selectable markers, no presence of vector backbone, no insertion into repetitive regions or gene sequences) were selected and transferred to soil for growth and further assessment.

The R0 plants generated through the transformation process described above were self-pollinated to produce R1 seed, and the unlinked insertions of T-DNA I (containing the expression cassettes) and T-DNA II (containing the selectable marker genes) were segregated. The *splA* phenotype (wrinkled seed) and polymerase chain reaction (PCR) analyses to evaluate presence/absence of the *aadA* coding sequence and to eliminate any seeds or plants from further development that contain T-DNA II. Subsequently, R1 plants homozygous for T-DNA I were selected for further development and their progenies were subjected to further molecular analysis, herbicide tolerance/efficacy testing and phenotypic assessments. As is typical of a commercial event production and selection process, hundreds of different transformation events (regenerants) were generated in the laboratory using PV-GMHT529103. After careful selection and evaluation of these events in the laboratory, greenhouse and field, MON 94313 was selected as the lead event based on superior agronomic, phenotypic, and molecular characteristics. Studies on MON 94313 were initiated to further characterize the genetic insertion and the expressed products, and to establish the food and feed safety and unaltered environmental risk compared to commercial soybean. The major development steps of MON 94313 are depicted in Figure 1.

PART 2: SPECIFIC DATA REQUIREMENTS FOR SAFETY ASSESSMENT

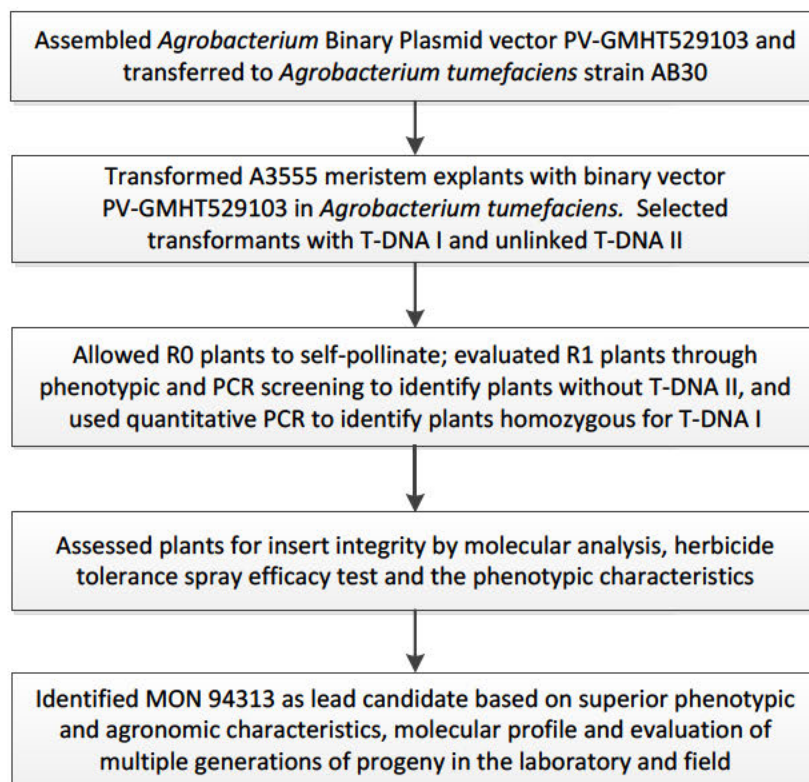


Figure 1. Schematic of the Development of MON 94313

A.3(b) A description of the construct and the transformation vectors used, including:**A.3(b)(i) The size, source and function of all the genetic components including marker genes, regulatory and other elements**

Plasmid vector PV-GMHT529103 was used for the transformation of conventional soybean to produce MON 94313 and its plasmid map is shown in Figure 2. A description of the genetic elements and their prefixes (e.g. B, P, TS, CS, T, I, OR, and E) in PV-GMHT529103 is provided in Table 1. PV-GMHT529103 is approximately 24.5 kb and contains two separate T-DNAs, each delineated by Left and Right Border regions and the vector backbone sequences. The first T-DNA, designated as T-DNA I, contains the *dmo*, *pat*, *ft_t.1*, and *TDO* expression cassettes. The second T-DNA, designated as T-DNA II, contains the *splA* and *aadA* expression cassettes. When *splA* is expressed during embryo development, it interferes with sucrose metabolism, leading to a recognizable wrinkled seed phenotype to provide a visual demonstration that T-DNA II is present (Piper *et al.*, 1999). The expression of *aadA* provides antibiotics resistance and a second method for selecting transformants carrying T-DNA II. During transformation, both T-DNAs were inserted into the soybean genome. Subsequently, segregation, selection and screening were used to isolate those plants that contained the *dmo*, *pat*, *ft_t.1*, and *TDO* expression cassettes (T-DNA I) and did not contain T-DNA II containing the selectable marker genes *splA* and *aadA* or the backbone sequences from the transformation vector.

The individual elements controlling the gene expression cassettes of T-DNA I and T-DNA II were described in Section A.2(a)(i) and further documented in Table 1. Additionally, the backbone region of PV-GMHT529103 contains two origins of replication for maintenance of the plasmid vector in bacteria (*ori-pRi*, *ori-pBR322*), a bacterial selectable marker gene (*nptII*) controlled by a promoter of the ribosomal RNA operon from *Agrobacterium tumefaciens* that drives transcription in plant cells, a non-functional portion of the bacterial selectable marker gene *ble1*, and a coding sequence for repressor of primer (ROP) protein for the maintenance of the plasmid vector copy number in *Escherichia coli* (*E. coli*).

A.3(b)(i)(i) The *dmo* Coding Sequence and DMO Protein

The *dmo* expression cassette contains the *dmo* gene encoding a precursor protein of 408 amino acids (340 amino acids encoded by the *dmo* gene and 68 amino acids encoded by the *APG6* gene for targeting the DMO protein into chloroplasts). MON 94313 expresses a ~35.6 kDa mature DMO protein as observed by Coomassie stain of SDS-PAGE and western blot analysis. The *dmo* coding sequence in the expression cassette includes a codon optimized sequence from *S. maltophilia* that encodes the DMO protein (Herman *et al.*, 2005; Wang *et al.*, 1997). The expression of the DMO protein confers tolerance to dicamba herbicide.

PART 2: SPECIFIC DATA REQUIREMENTS FOR SAFETY ASSESSMENT

DMO

1 MATATTTATA AFSGVVSVGT ETRRIYSFSH LQPSAAFPAK PSSFKSLKLK
51 QSARLTRRLD HRPFVVRCML TFVRNAWYVA ALPEELSEKP LGRTILDTPL
101 ALYRQPDGVV AALLDICPHR FAPLSDGILV NGHLQCPYHG LEFDGGGQCV
151 HNPHNGARP ASLNVRSFPV VERDALIWIW PGDPPALADPG AIPDFGCRVD
201 PAYRTVGGYG HVDCNYKLLV DNLMDLGHAQ YVHRANAQTD AFDRLEREVI
251 VGDGEIQALM KIPGGTPSVL MAKFLRGANT PVDAWNDIRW NKVSAMLNFI
301 AVAPEGTPKE QSIHSRGTHI LTPETEASCH YFFGSSRNFG IDDPEMDGVL
351 RSWQAQALVK EDKVVVEAIE RRRAYVEANG IRPAMLSCDE AAVRVSREIE
401 KLEQLEAA

Deduced Amino Acid Sequence of APG6 Chloroplast Targeting Sequence and the DMO Protein

The amino acid sequence of the MON 94313 DMO precursor protein was deduced from the full-length coding nucleotide sequence present in PV-GMHT529103 (See Table 1 for more detail). The first 68 amino acids of the precursor protein (underlined) are the CTP from *APG6* gene. The targeting sequence directs the MON 94313 DMO precursor protein to the chloroplast and is cleaved in the chloroplast producing the mature 340 amino acid DMO protein that begins with the methionine at position 69.

A.3(b)(i)(ii) The *pat* Coding Sequence and PAT Protein

The *pat* expression cassette contains the *pat* gene encoding a protein of 183 amino acids. MON 94313 expresses a 22.4 kDa PAT protein, which consists of a single polypeptide of 182 amino acids after the removal of the lead methionine that is cleaved during a co-translational process in MON 94313 ([Wehrmann et al., 1996](#); [Wohlleben et al., 1988](#)). The *pat* open reading frame in the expression cassette includes sequence from *Streptomyces viridochromogenes* that encodes the PAT protein. The expression of PAT protein confers glufosinate tolerance.

PAT

```

1      MSPERRPVEI RPATAADMAA VCDIVNHYIE TSTVNFRTPEP QTPQEWIDDL
51     ERLQDRYPWL VAEVEGVVAG IAYAGPWKAR NAYDWTVEST VYVSHRHQRL
101    GLGSTLYTHL LKSMEAQGFK SVVAVIGLPN DPSVRLHEAL GYTARGTLRA
151    AGYKHGGWHD VGFWQRDFEL PAPPRPVRPV TQI

```

Deduced Amino Acid Sequence of the PAT Protein

The amino acid sequence of the MON 94313 PAT protein was deduced from the full-length coding nucleotide sequence present in PV-GMHT529103 (See Table 1 for more detail). The lead methionine (boxed) of the PAT protein produced in MON 94313 is cleaved during a co-translational process in MON 94313.

A.3(b)(i)(iii) The *ft_t.1* Coding Sequence and FT_T.1 Protein

The *ft_t.1* expression cassette contains the *ft_t.1* gene encoding a protein of 295 amino acids. MON 94313 expresses a 34 kDa FT_T.1 protein, which consists of a single polypeptide of 295 amino acids. The *ft_t.1* open reading frame in the expression cassette is a modified version of R-2,4-dichlorophenoxypropionate dioxygenase (*RdpA*) gene from *Sphingobium herbicidovorans* that encodes a FOPs and 2,4-D dioxygenase protein (FT_T.1) ([Müller et al., 2006](#)). The expression of FT_T.1 protein confers tolerance to 2,4-D herbicide in soybean.

FT_T.1

```

1      MHAALTPLTN KYRFIDVQPL TGVLGAEITG VDLREPLDDS TWNEILDAFH
51     TYQVIYFPGQ AITNEQHIAF SRRFGPVDPV PILKSIEGYP EVQMIRREAN
101    ESSRYIGDDW HADSTFLDAP PAAVVMRAIE VPEYGGDTGF LSMYSAWETL
151    SPTMQATIEG LNVVHSATKV FGSLYQATNW RFSNTSVKVM DVDAGDRETV
201    HPLVVTHPVT GRRALYCNQV YCQKIQGMTD AESKSLQFL YEHATQDFDT
251    CRVRWKKDQV LVWDNLCTMH RAVPDYAGKF RYLTRTTVAG DKPSR

```

Deduced Amino Acid Sequence of the FT_T.1 Protein

The amino acid sequence of the MON 94313 FT_T.1 protein was deduced from the full-length coding nucleotide sequence present in PV-GMHT529103 (See Table 1 for more detail). FT_T.1 protein is expressed as a mature 295 amino acid FT_T.1 protein that begins with the lead methionine.

A.3(b)(i)(iv) The *TDO* Coding Sequence and *TDO* Protein

The *TDO* expression cassette contains the *TDO* gene encoding a protein of 351 amino acids. MON 94313 expresses a 36.9 kDa *TDO* protein, which consists of a single polypeptide of 350 amino acids after the removal of the lead methionine that is cleaved during a co-translational process in MON 94313 ([Meinzel and Giglione, 2008](#)). The *TDO* open reading frame in the expression cassette includes a codon optimized sequence from *Oryza sativa* that encodes the *TDO* protein. The expression of *TDO* protein confers mesotrione tolerance.

TDO

```

1  MADESWRAPA IVQELAAAGV EEPSPRYLLR EKDRSDVKLV AAELPEPLPV
51  VDLSRLDGAE EATKLRVALQ NWGFFLLTNH GVEASLMDSV MNLSREFFNQ
101 PIERKQKFSN LIDGKNFQIQ GYGTDRVVTQ DQILDWSDRL HLRVEPKKEEQ
151 DLAFWPDHPE SFRDVLNKYA SGTKRIRDDI IQAMAKLLEL DEDYFLDRLN
201 EAPAFARFNY YPPCPRPDLV FGIRPHSDGT LLTILLVDKD VSGLQVQRDG
251 KWSNVEATPH TLLINLGDTM EVMCNGIFRS PVHRVVTNAE KERISLAMLY
301 SVNDEKDIEP AAGLLDENRP ARYRKVSVEE FRAGIFGKFS RGERYIDSLR
351 I

```

Deduced Amino Acid Sequence of the *TDO* Protein

The amino acid sequence of the MON 94313 *TDO* protein was deduced from the full-length coding nucleotide sequence present in PV-GMHT529103 (See Table 1 for more detail). The lead methionine (boxed) of the *TDO* protein produced in MON 94313 is cleaved during a co-translational process in MON 94313.

A.3(b)(i)(v) Regulatory Sequences

The transformation plasmid PV-GMHT529103 contains the *dmo*, *ft_t.1*, *pat*, and *TDO* expression cassettes, and also the expression cassettes for the *splA* and *aadA* selectable markers, each with their own regulatory sequences. The regulatory sequences associated with each cassette are described in Section A.2(a)(i) and Table 1.

A.3(b)(i)(vi) T-DNA Border Regions

PV-GMHT529103 contains Left and Right Border regions (Figure 2 and Table 1) that were derived from *A. tumefaciens* plasmids. The border regions each contain a nick site that is the site of DNA exchange during transformation ([Barker et al., 1983](#); [Depicker et al., 1982](#); [Zambryski et al., 1982](#)). The border regions separate the T-DNA from the plasmid backbone region and are involved in the efficient transfer of T-DNA into the soybean genome.

A.3(b)(i)(vii) Genetic Elements Outside the T-DNA Border Regions

Genetic elements that exist outside of the T-DNA border regions are those that are essential for the maintenance or selection of PV-GMHT529103 in bacteria and are referred to as plasmid backbone. The gene *ble1* is the partial coding sequence of the bleomycin resistance gene from transposon Tn5 that confers antibiotic resistance ([Mazodier et al., 1985](#)), but is non-functional and was not used in the development of MON 94313. The selectable marker gene *nptII* is the coding sequence of the *neo* gene from transposon Tn5 of *E. coli* encoding neomycin phosphotransferase II (NPT II) ([Beck et al., 1982](#)) that confers neomycin and kanamycin resistance in *E. coli* and *Agrobacterium* during molecular cloning ([Fraley et al., 1983](#)). Expression of the *nptII* gene is under control of the *rrn* promoter which is the promoter of the ribosomal RNA operon from *Agrobacterium tumefaciens* that drives transcription in plant cells ([Bautista-Zapanta et al., 2002](#)). The origin of replication, *ori-pBR322*, is required for the maintenance of the plasmid in *E. coli* and is derived from the plasmid vector pBR322. Coding sequence *rop* encodes the repressor of primer protein from the ColE1 plasmid for maintenance of plasmid copy number in *E. coli* ([Giza and Huang, 1989](#)). The origin of replication, *ori-pRi*, is required for the maintenance of the plasmid in *Agrobacterium* ([Ye et al., 2011](#)). Because these elements are outside the border regions, they are not expected to be transferred into the soybean genome. The absence of the backbone and other unintended plasmid sequence in MON 94313 was confirmed by sequencing and bioinformatic analyses.

Table 1. Summary of Genetic Elements in PV-GMHT529103

Genetic Element	Location in Plasmid Vector	Function (Reference)
T-DNA I		
B¹-Right Border Region	1-285	DNA region from <i>Agrobacterium tumefaciens</i> containing the right border sequence used for transfer of the T-DNA (Depicker et al., 1982 ; Zambryski et al., 1982)
Intervening Sequence	286-324	Sequence used in DNA cloning
P²-ubq3-At1	325-1332	Promoter, leader and intron from <i>Arabidopsis thaliana</i> of the polyubiquitin gene <i>ubq3</i> (Norris et al., 1993), which directs transcription in plant cells
TS³-apg6-At1	1333-1536	Targeting sequence of the <i>APG6</i> gene from <i>Arabidopsis thaliana</i> encoding a HSP101 (heat shock protein) homologue and acts as a transit peptide that directs transport of the protein to the chloroplast (Myouga et al., 2006)
CS⁴-dmo	1537-2559	Codon optimized coding sequence for the dicamba mono-oxygenase (DMO) protein of <i>Stenotrophomonas maltophilia</i> that confers dicamba resistance (Herman et al., 2005 ; Wang et al., 1997)
Intervening Sequence	2560-2578	Sequence used in DNA cloning
T⁵-sali3-2-Mt1	2579-3078	3' UTR sequence from <i>Medicago truncatula</i> (barrel medic) of an aluminum-induced Sali3-2 protein that directs polyadenylation of the mRNA (Hunt, 1994)
Intervening Sequence	3079-3156	Sequence used in DNA cloning
P-GSP579	3157-3656	A promoter and 5' UTR that has been developed from multiple promoter and 5' UTR sequences from <i>Arabidopsis thaliana</i> (To et al., 2021) that directs transcription in plant cells.
I⁶-GSI102	3657-3966	An intron that has been developed from multiple intron sequences from <i>Arabidopsis thaliana</i> (To et al., 2021) that is involved in regulating gene expression
Intervening Sequence	3967-3972	Sequence used in DNA cloning

PART 2: SPECIFIC DATA REQUIREMENTS FOR SAFETY ASSESSMENT

CS-pat	3973-4524	Codon optimized coding sequence for the phosphinothricin N-acetyltransferase (PAT) protein of <i>Streptomyces viridochromogenes</i> that confers tolerance to glufosinate (Wehrmann et al., 1996 ; Wohlleben et al., 1988)
Intervening Sequence	4525-4532	Sequence used in DNA cloning
T-Hsp20-Mt1	4533-5032	3' UTR sequence from <i>Medicago truncatula</i> (barrel medic) of a putative <i>Hsp20</i> gene encoding a heat shock protein that directs polyadenylation of the mRNA (Hunt, 1994)
Intervening Sequence	5033-5115	Sequence used in DNA cloning
P-ubq10-At1	5116-6317	Promoter, leader and intron from <i>Arabidopsis thaliana</i> of the polyubiquitin gene <i>ubq10</i> (Norris et al., 1993), which directs transcription in plant cells
Intervening Sequence	6318-6323	Sequence used in DNA cloning
CS-ft_t.1	6324-7211	Modified version of R-2,4 dichlorophenoxypropionate dioxygenase (<i>RdpA</i>) gene of <i>Sphingobium herbicidovorans</i> that expresses a modified FOPs and 2,4-D dioxygenase protein (FT_T.1) that confers tolerance to 2,4-D herbicide in soybean (Larue et al., 2019).
Intervening Sequence	7212-7219	Sequence used in DNA cloning
T-guf-Mt2	7220-7719	3' UTR from an expressed gene of <i>Medicago truncatula</i> of unknown function that directs polyadenylation of mRNA (Hunt, 1994)
Intervening Sequence	7720-7857	Sequence used in DNA cloning
P-GSP576	7858-8357	A promoter and 5' UTR that has been developed from multiple promoter and 5' UTR sequences from <i>Arabidopsis thaliana</i> (To et al., 2021) that directs transcription in plant cells.
I-GSII7	8358-8657	An intron that has been developed from multiple intron sequences from <i>Arabidopsis thaliana</i> (To et al., 2021) that is involved in regulating gene expression
Intervening Sequence	8658-8692	Sequence used in DNA cloning

PART 2: SPECIFIC DATA REQUIREMENTS FOR SAFETY ASSESSMENT

CS-TDO	8693-9748	Codon optimized coding sequence for the triketone dioxygenase (TDO) protein of <i>Oryza sativa</i> that confers tolerance to mesotrione (Maeda et al., 2019)
Intervening Sequence	9749-9778	Sequence used in DNA cloning
T-GST7	9779-10078	A 3' UTR that has been developed from multiple 3' UTR sequences from <i>Zea mays</i> (maize) (To et al., 2021) that directs polyadenylation of the mRNA.
Intervening Sequence	10079-10178	Sequence used in DNA cloning
B-Left Border Region	10179-10620	DNA region from <i>Agrobacterium tumefaciens</i> containing the left border sequence used for transfer of the T-DNA (Barker et al., 1983)
Vector Backbone		
Intervening Sequence	10621-10657	Sequence used in DNA cloning
CS-ble1	10658-10809	Partial coding sequence of the bleomycin resistance gene from transposon Tn5 that confers antibiotic resistance (Mazodier et al., 1985)
Intervening Sequence	10810-10829	Sequence used in DNA cloning
CS-nptII	10830-11624	Coding sequence of the <i>neo</i> gene from transposon Tn5 of <i>E. coli</i> encoding neomycin phosphotransferase II (NPT II) (Beck et al., 1982) that confers neomycin and kanamycin resistance (Fraley et al., 1983)
P-rrn	11625-11849	Promoter of the ribosomal RNA operon from <i>Agrobacterium tumefaciens</i> (Bautista-Zapanta et al., 2002) that drives transcription in plant cells.
Intervening Sequence	11850-11925	Sequence used in DNA cloning
OR⁷-ori-pBR322	11926-12514	Origin of replication from plasmid pBR322 for maintenance of plasmid in <i>E. coli</i> (Sutcliffe, 1979)
Intervening Sequence	12515-12941	Sequence used in DNA cloning
CS-rop	12942-13133	Coding sequence for repressor of primer protein from the ColE1 plasmid for maintenance of plasmid copy number in <i>E. coli</i> (Giza and Huang, 1989)
Intervening Sequence	13134-13321	Sequence used in DNA cloning

PART 2: SPECIFIC DATA REQUIREMENTS FOR SAFETY ASSESSMENT

OR-ori-pRi	13322-17435	Origin of replication from plasmid pRi for maintenance of plasmid in <i>Agrobacterium</i> (Ye et al., 2011)
Intervening Sequence	17436-17442	Sequence used in DNA cloning
T-DNA II		
B-Left Border Region	17443-17761	DNA region from <i>Agrobacterium tumefaciens</i> containing the left border sequence used for transfer of the T-DNA (Barker et al., 1983)
Intervening Sequence	17762-17793	Sequence used in DNA cloning
T-nos	17794-18046	3' UTR sequence of the <i>nopaline synthase</i> (<i>nos</i>) gene from <i>Agrobacterium tumefaciens</i> pTi encoding NOS that directs polyadenylation (Bevan et al., 1983 ; Fraleley et al., 1983)
Intervening Sequence	18047-18062	Sequence used in DNA cloning
CS-splA	18063-19520	Coding sequence of the <i>splA</i> gene from <i>Agrobacterium tumefaciens</i> strain C58 encoding the sucrose phosphorylase protein that catalyzes the conversion of sucrose to fructose and glucose-1-phosphate (Piper et al., 1999)
Intervening Sequence	19521-19532	Sequence used in DNA cloning
P-Usp	19533-20711	5' UTR, promoter, and enhancer sequence of an unknown seed protein gene from <i>Vicia faba</i> (broad bean) encoding an unknown seed protein that is involved in regulating gene expression (Bäumlein et al., 1991)
Intervening Sequence	20712-20762	Sequence used in DNA cloning
T-E9	20763-21405	3' UTR sequence from <i>Pisum sativum</i> (pea) <i>rbcS</i> gene family encoding the small subunit of ribulose biphosphate carboxylase protein (Coruzzi et al., 1984) that directs polyadenylation of the mRNA
Intervening Sequence	21406-21420	Sequence used in DNA cloning
aadA	21421-22212	Coding sequence for an aminoglycoside-modifying enzyme, 3'(9)- <i>O</i> -nucleotidyltransferase from the transposon Tn7 (Fling et al., 1985) that confers spectinomycin and streptomycin resistance
TS-CTP2	22213-22440	Targeting sequence of the <i>ShkG</i> gene from <i>Arabidopsis thaliana</i> encoding the EPSPS

PART 2: SPECIFIC DATA REQUIREMENTS FOR SAFETY ASSESSMENT

		transit peptide region that directs transport of the protein to the chloroplast (Herrmann, 1995 ; Klee et al., 1987)
Intervening Sequence	22441-22449	Sequence used in DNA cloning
P-<i>EF-1α</i>	22450-23597	Promoter, leader , and intron sequences of the <i>EF-1α</i> gene from <i>Arabidopsis thaliana</i> encoding elongation factor EF-1α (Axelos et al., 1989) that directs transcription in plant cells
Intervening Sequence	23598-23620	Sequence used in DNA cloning
E⁸-<i>FMV</i>	23621-24157	Enhancer from the 35S RNA of figwort mosaic virus (FMV) (Richins et al., 1987) that enhances transcription in most plant cells (Rogers, 2000)
Intervening Sequence	24158-24203	Sequence used in DNA cloning
B-Right Border Region	24204-24534	DNA region from <i>Agrobacterium tumefaciens</i> containing the right border sequence used for transfer of the T-DNA (Depicker et al., 1982 ; Zambryski et al., 1982)
Vector Backbone		
Intervening Sequence	24535-24549	Sequence used in DNA cloning

¹ B, Border

² P, Promoter

³ TS, Targeting Sequence

⁴ CS, Coding Sequence

⁵ T, Transcription Termination Sequence

⁶ I, Intron

⁷ OR, Origin of Replication

⁸ E, Enhancer

A.3(b)(ii) A detailed map of the location and orientation of all genetic elements contained within the construct and vector, including the location of relevant restriction sites

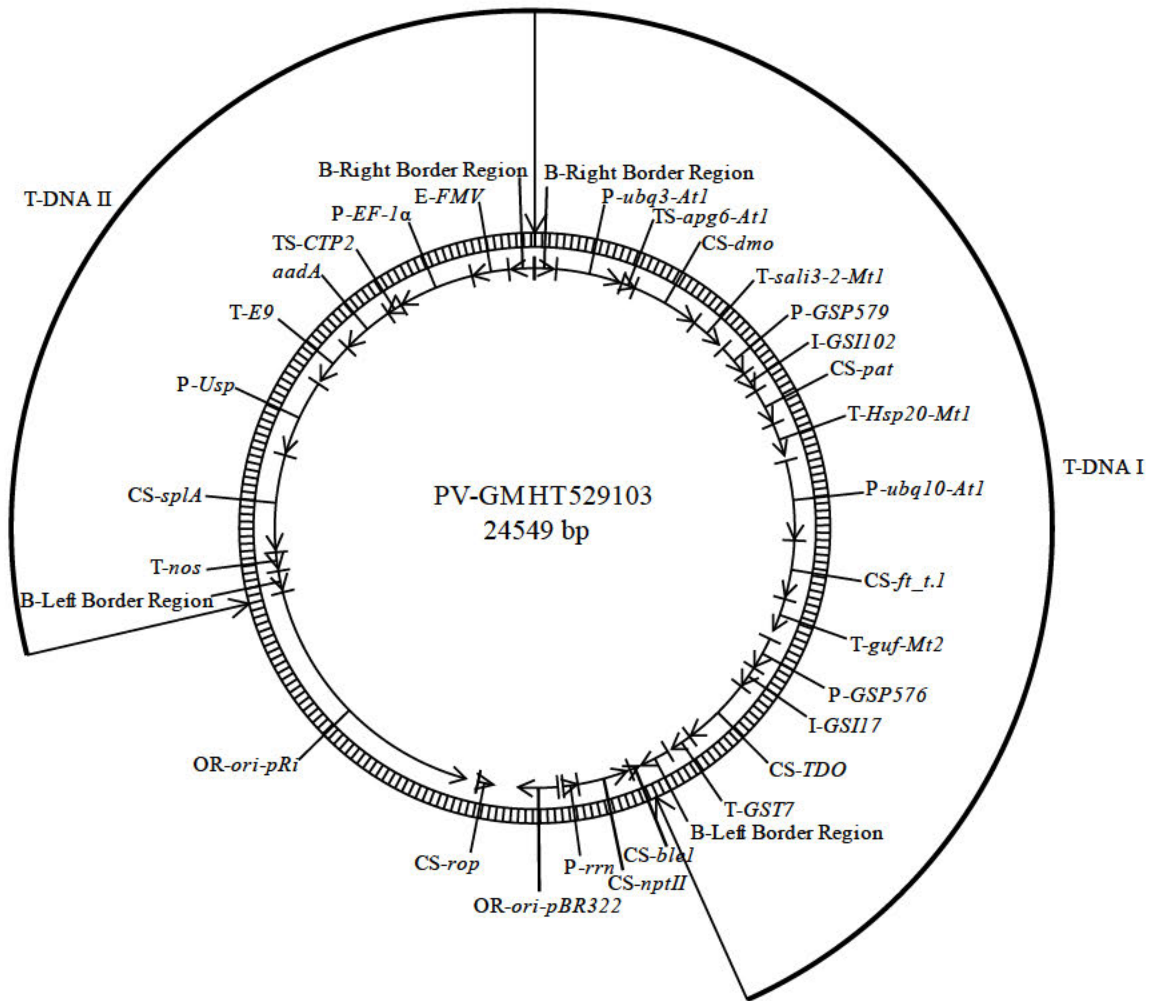


Figure 2. Circular Map of PV- GMHT529103

A circular map of PV-GMHT529103 used to develop MON 94313 is shown. PV-GMHT529103 contains two T-DNAs. Genetic elements are shown on the exterior of the map.

A.3(c) A full molecular characterisation of the genetic modification in the new organism, including:

A.3(c)(i) Identification of all transferred genetic material and whether it has undergone any rearrangements

This section describes the methods and results of a comprehensive molecular characterisation of the genetic modification present in MON 94313. It provides information on the DNA insertion(s) into the plant genome of MON 94313, and additional information regarding the arrangement and stability of the introduced genetic material. The information provided in this section addresses the relevant factors in Codex Plant Guidelines, Section 4, paragraphs 30, 31, 32, and 33 ([Codex Alimentarius, 2009](#)).

A schematic representation of the next generation sequencing (NGS) methodology and the basis of the characterisation using NGS and PCR sequencing are illustrated in Figure 3 below.

For details, please refer to Appendix 1.

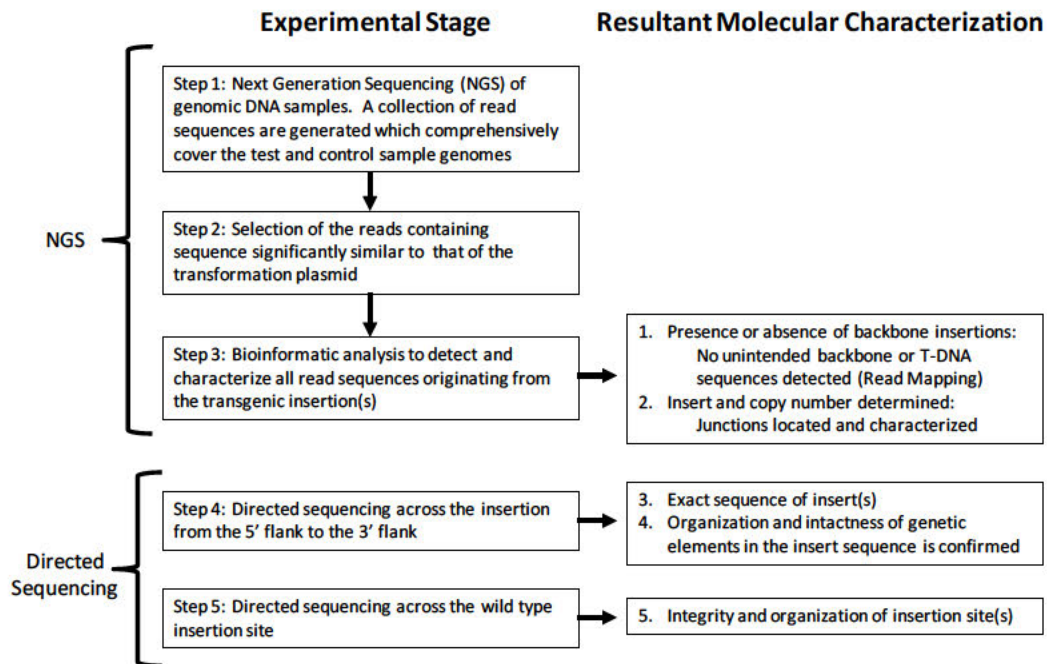


Figure 3. Molecular Characterisation using Sequencing and Bioinformatics

Genomic DNA from MON 94313 soybean (test) and the conventional control was sequenced using technology that produces a set of short, randomly distributed sequence reads that comprehensively cover the test and control genomes (Step 1). Utilizing these genomic sequence reads, bioinformatics searches are conducted to identify all sequence reads that are significantly similar to the transformation plasmid (Step 2). These captured reads are then mapped and analyzed to determine the presence/absence of transformation plasmid backbone or T-DNA II sequences, identify insert junctions, and to determine the insert and copy number (Step 3). Overlapping PCR products are also produced which span any identified insert and their

PART 2: SPECIFIC DATA REQUIREMENTS FOR SAFETY ASSESSMENT

corresponding wild type locus (Step 4 and Step 5 respectively); these overlapping PCR products are sequenced to allow for detailed characterisation of the inserted DNA and insertion site.

The NGS method was used to characterize the genomic DNA from MON 94313 and the conventional control by generating short (~150 bp) randomly distributed sequence fragments (sequencing reads) generated in sufficient number to ensure comprehensive coverage of the sample genomes. It has been previously demonstrated that whole genome sequencing at 75× depth of coverage is adequate to provide comprehensive coverage and ensure detection of inserted DNA ([Kovalic *et al.*, 2012](#)). To confirm sufficient sequence coverage of the genome, the 150 bp sequence reads are analyzed to determine the coverage of a known single-copy endogenous soybean gene. This establishes the depth of coverage (the median number of times each base of the genome is independently sequenced). The level of sensitivity of this method was demonstrated by detection of a positive control plasmid DNA sampled at 1 and 1/10th copy-per-genome equivalent. This confirms the method's ability to detect any sequences derived from the transformation plasmid. Bioinformatics analysis was then used to select sequencing reads that contained sequences similar to the transformation plasmid, and these were analysed in depth to determine the number of DNA inserts. NGS was run on five breeding generations of MON 94313 and the appropriate conventional controls. Results of NGS are shown in Sections A.3(c)(ii) and A.3(e)(i).

The DNA inserts of MON 94313 were characterized by mapping of sequencing reads to the transformation plasmid and identifying junctions and unpaired read mappings adjacent to the junctions. Examples of five types of NGS reads are shown in Figure 4. The junctions of the DNA insert and the flanking DNA are unique for each insertion ([Kovalic *et al.*, 2012](#)). Therefore, insertion sites can be recognized by analyzing for sequence reads containing such junctions.

Directed sequencing (locus-specific PCR and DNA sequencing analyses, Figure 3, step 4) complements the NGS characterisation. Sequencing of the insert and flanking DNA determines the complete sequence of the insert and flanks; by evaluating if the sequence of the insert is identical to the corresponding sequence in the plasmid vector, and if each genetic element in the insert is intact. Furthermore, the genomic organization at the insertion site was assessed by comparing the insert and flanking sequence to the sequence of the insertion site in conventional soybean. Results are described in Sections A.3(c)(ii) and A.3(c)(iii).

For details, please refer to Appendix 1.

Mapping of Plasmid Sequence Alignments

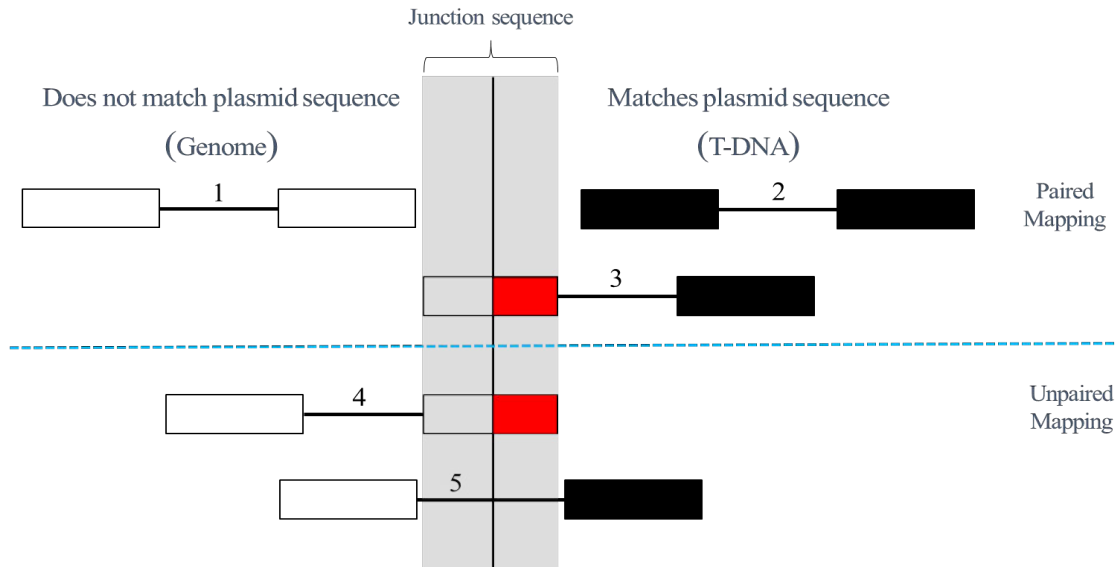


Figure 4. Five Types of NGS Reads

NGS yields data in the form of read pairs where sequence from each end of a size selected DNA fragment is returned. Depicted above are five types of sequencing reads/read pairs generated by NGS sequencing which can be found spanning or outside of junction points. Sequence boxes are color-filled if it matches with plasmid sequence, and empty if it matches with genomic sequence. Grey highlighting indicates sequence reads spanning the junction. Junctions are detected by examining the NGS data for reads having portions of plasmid sequences that span less than the full read, as well as reads mapping adjacent to the junction points where their mate pair does not map to the plasmid sequence. The five types of sequencing reads/read pairs being (1) Paired and unpaired reads mapping to genomic sequence outside of the insert, greater than 99.999% of collected reads fall into this category and are not evaluated in this analysis, (2) Paired reads mapping entirely to the transformation plasmid sequence, such reads reveal the presence of transformation sequence *in planta*, (3) Paired reads where one read maps entirely within the inserted DNA and the other read maps partially to the insert (indicating a junction point), (4) Single read mapping partially to the transformation plasmid DNA sequence (indicating a junction point) where its mate maps entirely to the genomic flanking sequence and (5) Single read mapping entirely to the transformation plasmid DNA sequence where its mate maps entirely to genomic flanking sequence, such reads are part of the junction signature.

A.3(c)(ii) A determination of number of insertion sites, and the number of copies at each insertion site

The number of inserted DNA sequences from PV-GMHT529103 in MON 94313 was assessed by generating a comprehensive collection of reads via NGS of MON 94313 genomic DNA using the R3 generation (Figure 8). A plasmid map of PV-GMHT529103 is shown in Figure 2 and descriptions of the genetic elements present in MON 94313 show in Table 2. A schematic representation of the insert and flanking sequences in MON 94313 is shown in Figure 5.

For details, please refer to Appendix 1.

A.3(c)(ii)(i) Next Generation Sequencing for MON 94313 and Conventional Control Genomic DNA

Genomic DNA from five breeding generations of MON 94313 (Figure 6) and conventional controls were isolated from seed and prepared for sequencing. These genomic DNA libraries were used to generate short (~150 bp) randomly distributed sequencing reads of the soybean genome (Figure 3, Step 1).

To demonstrate sufficient sequence coverage the 150 bp sequence reads were analyzed by mapping all reads to a known single-copy endogenous gene (*Glycine max* lectin (*Le1*), GenBank accession version: K00821.1). The analysis showed that the depth of coverage (*i.e.*, the mean number of times any base of the genome is expected to be independently sequenced) was 75× or greater for the five generations of MON 94313 (R₃, R₄, R₅, R₆, and R₇) and the conventional control (Appendix 1). It has previously been demonstrated that 75× coverage of the soybean genome is adequate to provide comprehensive coverage and ensure detection of inserted DNA ([Kovalic et al., 2012](#)).

To demonstrate the method's ability to detect any sequences derived from the PV-GMHT529103 transformation plasmid, a sample of PV-GMHT529103 DNA was sequenced by NGS following the same processes outlined for all samples. The resulting PV_GMHT529103 reads were randomly selected to achieve a depth of one and 1/10th genome equivalence relative to the mean coverage of the A3555 conventional control. (Appendix 1). This result demonstrates that all nucleotides of PV-GMHT529103 are observed by the sequencing and bioinformatic assessments performed and that a detection level of at least 1/10th genome equivalent was achieved for the plasmid DNA sequence assessment.

Table 2. Summary of Genetic Elements in MON 94313

Genetic Element	Location in Sequence	Function (Reference)
Flanking DNA	1-1000	DNA sequence flanking the 5' end of the insert
B ¹ -Right Border Region ^{r1}	1001-1071	DNA region from <i>Agrobacterium tumefaciens</i> containing the right border sequence used for transfer of the T-DNA (Depicker et al., 1982 ; Zambryski et al., 1982)
Intervening Sequence	1072-1110	Sequence used in DNA cloning
P ² - <i>ubq3-At1</i>	1111-2118	Promoter, leader and intron from <i>Arabidopsis thaliana</i> of the polyubiquitin gene <i>ubq3</i> (Norris et al., 1993), which directs transcription in plant cells
TS ³ - <i>apg6-At1</i>	2119-2322	Targeting sequence of the <i>APG6</i> gene from <i>Arabidopsis thaliana</i> encoding a HSP101 (heat shock protein) homologue and acts as a transit peptide that directs transport of the protein to the chloroplast (Myouga et al., 2006)
CS ⁴ - <i>dmo</i>	2323-3345	Codon optimized coding sequence for the dicamba mono-oxygenase (DMO) protein of <i>Stenotrophomonas maltophilia</i> that confers dicamba resistance (Herman et al., 2005 ; Wang et al., 1997)
Intervening Sequence	3346-3364	Sequence used in DNA cloning
T ⁵ - <i>sali3-2-Mt1</i>	3365-3864	3' UTR sequence from <i>Medicago truncatula</i> (barrel medic) of an aluminum-induced Sali3-2 protein that directs polyadenylation of the mRNA (Hunt, 1994)
Intervening Sequence	3865-3942	Sequence used in DNA cloning
P- <i>GSP579</i>	3943-4442	A promoter and 5' UTR that has been developed from multiple promoter and 5' UTR sequences from <i>Arabidopsis thaliana</i> (To et al., 2021) that directs transcription in plant cells.
I ⁶ - <i>GSII02</i>	4443-4752	An intron that has been developed from multiple intron sequences from <i>Arabidopsis thaliana</i> (To et al., 2021) that is involved in regulating gene expression
Intervening Sequence	4753-4758	Sequence used in DNA cloning
CS- <i>pat</i>	4759-5310	Codon optimized coding sequence for the phosphinothricin N-acetyltransferase (PAT) protein of <i>Streptomyces viridochromogenes</i> that confers

PART 2: SPECIFIC DATA REQUIREMENTS FOR SAFETY ASSESSMENT

		tolerance to glufosinate (Wehrmann et al., 1996 ; Wohlleben et al., 1988)
Intervening Sequence	5311-5318	Sequence used in DNA cloning
<i>T-Hsp20-Mt1</i>	5319-5818	3' UTR sequence from <i>Medicago truncatula</i> (barrel medic) of a putative <i>Hsp20</i> gene encoding a heat shock protein that directs polyadenylation of the mRNA (Hunt, 1994)
Intervening Sequence	5819-5901	Sequence used in DNA cloning
<i>P-ubq10-At1</i>	5902-7103	Promoter, leader and intron from <i>Arabidopsis thaliana</i> of the polyubiquitin gene (Norris et al., 1993), which directs transcription in plant cells
Intervening Sequence	7104-7109	Sequence used in DNA cloning
<i>CS-ft_t.1</i>	7110-7997	Modified version of R-2,4 dichlorophenoxypropionate dioxygenase (<i>rdpA</i>) gene of <i>Sphingobium herbicidovorans</i> that expresses a modified FOPs and 2,4-D dioxygenase protein (FT_T.1) that confers tolerance to 2,4-D herbicide in soybean (Larue et al., 2019)
Intervening Sequence	7998-8005	Sequence used in DNA cloning
<i>T-guf-Mt2</i>	8006-8505	3' UTR from an expressed gene of <i>Medicago truncatula</i> of unknown function that directs polyadenylation of mRNA (Hunt, 1994)
Intervening Sequence	8506-8643	Sequence used in DNA cloning
<i>P-GSP576</i>	8644-9143	A promoter and 5' UTR that has been developed from multiple promoter and 5' UTR sequences from <i>Arabidopsis thaliana</i> (To et al., 2021) that directs transcription in plant cells.
<i>I-GSII7</i>	9144-9443	An intron that has been developed from multiple intron sequences from <i>Arabidopsis</i> (To et al., 2021) that is involved in regulating gene expression
Intervening Sequence	9444-9478	Sequence used in DNA cloning
<i>CS-TDO</i>	9479-10534	Codon optimized coding sequence for the triketone dioxygenase (TDO) protein of <i>Oryza sativa</i> that confers tolerance to mesotrione (Maeda et al., 2019)
Intervening Sequence	10535-10564	Sequence used in DNA cloning

PART 2: SPECIFIC DATA REQUIREMENTS FOR SAFETY ASSESSMENT

T- <i>GST7</i>	10565-10864	A 3' UTR that has been developed from multiple 3' UTR sequences from <i>Zea mays</i> (maize) (To et al., 2021) that directs polyadenylation of the mRNA.
Intervening Sequence	10865-10964	Sequence used in DNA cloning
B-Left Border Region ^{r1}	10965-11196	DNA region from <i>Agrobacterium tumefaciens</i> containing the left border sequence used for transfer of the T-DNA (Barker et al., 1983)
Flanking DNA	11197-12196	DNA sequence flanking the 3' end of the insert

¹ B, Border

² P, Promoter

³ TS, Targeting Sequence

⁴ CS, Coding Sequence

⁵ T, Transcription Termination Sequence

⁶ I, Intron

^{r1} Superscript in the Left and Right Border Regions indicates that the sequence in MON 94313 was truncated compared to the sequences in PV-GMHT529103

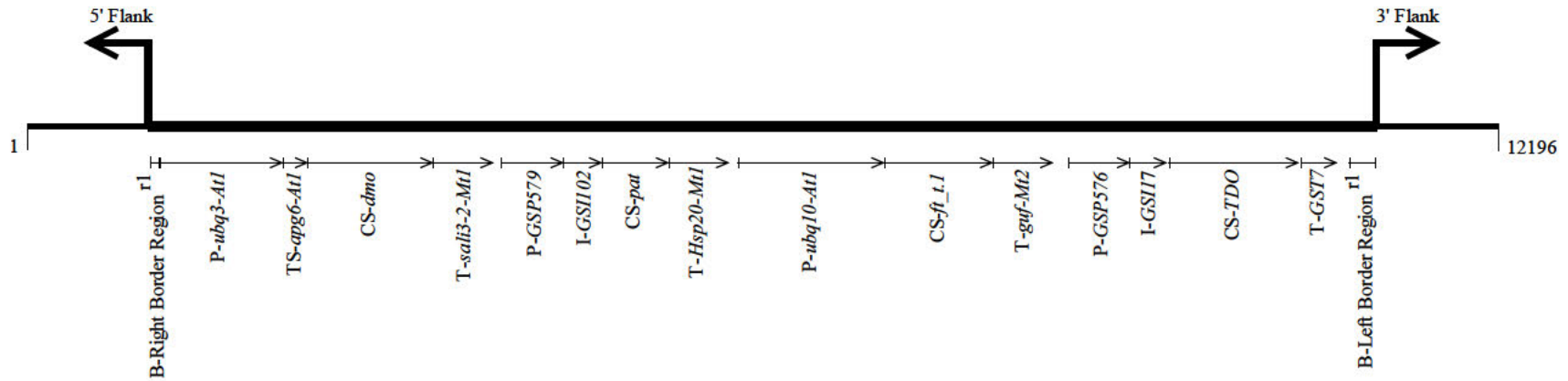


Figure 5. Schematic Representation of the Insert and Flanking Sequences in MON 94313

DNA derived from T-DNA I of PV-GMHT529103 integrated in MON 94313. Right-angled arrows indicate the ends of the integrated T-DNA and the beginning of the flanking sequence. Identified on the map are genetic elements within the insert. This schematic diagram may not be drawn to scale.

^{r1} Superscript in the Left and Right Border Regions indicates that the sequence in MON 94313 was truncated compared to the sequences in PV-GMHT529103

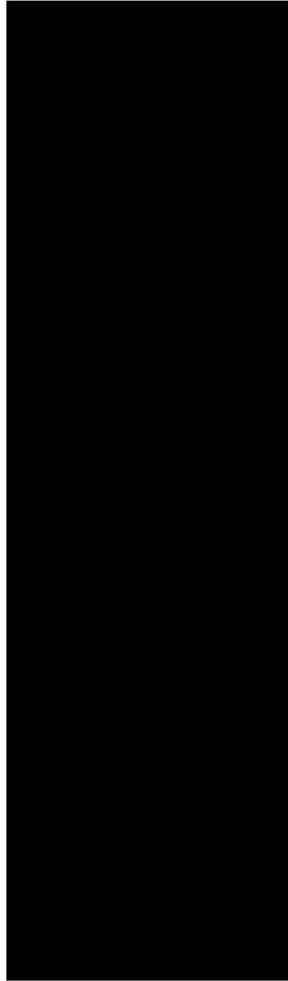


Figure 6. Breeding History of MON 94313

The generations used for molecular characterisation and insert stability analyses are indicated in bold text. R0 corresponds to the transformed plant, ⊗ designates self-pollination.

¹ Generation used for molecular characterisation

² Generations used to confirm insert stability

³ Generation used for commercial development of MON 94313

A.3(c)(ii)(ii) Selection of Sequence Reads that Align to PV-GMHT529103

PV-GMHT529103 was transformed into the parental variety A3555 to produce MON 94313. Consequently, any DNA inserted into MON 94313 will consist of sequences that are similar to the PV-GMHT529103 DNA sequence. Therefore, to fully characterize the DNA from PV-GMHT529103 inserted in MON 94313, it is sufficient to completely analyze only the sequence reads that have similarity to PV-GMHT529103 (Figure 3, Step 2).

Using established criteria (described in the materials and methods of Appendix 1), sequence reads similar to PV-GMHT529103 were selected from MON 94313 sequence datasets and were then used as input data for bioinformatic junction sequence analysis. PV-GMHT529103 sequences were also compared against the conventional control sequence dataset.

A.3(c)(ii)(iii) Determination of T-DNA Copy Number and Presence or Absence of Plasmid Vector Backbone

Mapping sequence reads relative to the transformation plasmid allows for the identification of junction signatures, the presence or absence of plasmid backbone and T-DNA II sequences, and the number of T-DNA I insertions. For a single copy T-DNA I insert sequence at a single genomic locus, a single junction signature pair and few, if any, reads aligning with the transformation plasmid backbone sequences are expected.

When reads from the control A3555 dataset were aligned with the transformation plasmid sequence, a small number of reads mapped sporadically across the plasmid sequence. In T-DNA I a single paired read mapped to the junction between *TS-*apg6-At1** and *CS-*dmo**, and three overlapping paired reads mapped to a portion of the T-DNA I B-Left Border, plasmid backbone intervening sequences and *CS-*ble1** (Figure 7). Additionally, a single paired and unpaired read mapped to the backbone sequences associated with intervening sequence and the *OR-ori-pRi* origin of replication respectively. The sporadic low-level detection of plasmid sequences has previously been described ([Zastrow-Hayes *et al.*, 2015](#)).

When reads from the MON 94313 (R3) dataset were aligned with the transformation plasmid sequence, large numbers of reads mapped to the intended T-DNA I sequence and no reads mapped to T-DNA II or the transformation plasmid backbone sequences (Figure 8). This analysis indicates that MON 94313 (R3) does not contain inserted sequence from T-DNA II or transformation plasmid backbone. The mapping of large numbers of reads from the MON 94313 (R3) dataset to the intended T-DNA sequence is expected and fully consistent with the presence of the inserted DNA.

To determine the insert number in MON 94313 (R3), selected reads mapping to T-DNA I were analyzed to identify junctions. This bioinformatic analysis is used to find and classify partially matched reads characteristic of the ends of insertions. The number of unique junctions determined by this analysis are shown in Table 3.

Table 3. Unique Junction Sequence Results

Sample	Junctions Detected
MON 94313 (R3)	2
A3555	0

Detailed mapping information of the junction sequences is shown in Figure 8. There are two junctions identified in MON 94313. Both junctions contain the T-DNA I border sequence joined to flanking genomic sequence, indicating that they represent the sequences at the junctions of the intended T-DNA insert and the soybean genome. As described earlier, no junctions were detected in the control sample (Figure 7).

Considered together, the absence of plasmid backbone and T-DNA II sequences and the presence of two junctions (joining T-DNA I borders and flanking sequences) indicate a single intended T-DNA at a single locus in the genome of MON 94313. Both junctions originate from the same locus of the MON 94313 genome and are linked by contiguous, known and expected DNA sequence. This is demonstrated by complete coverage of the sequenced reads spanning the interval between the junctions and the directed sequencing of overlapping PCR products described in Section A.3(c)(iii).

Based on the comprehensive NGS and junction identification it is concluded that MON 94313 contains one copy of T-DNA I inserted into a single locus, as shown in Figure 5. This conclusion is confirmed by the sequencing and analysis of overlapping PCR products from this locus as described in Section A.3(c)(iii).

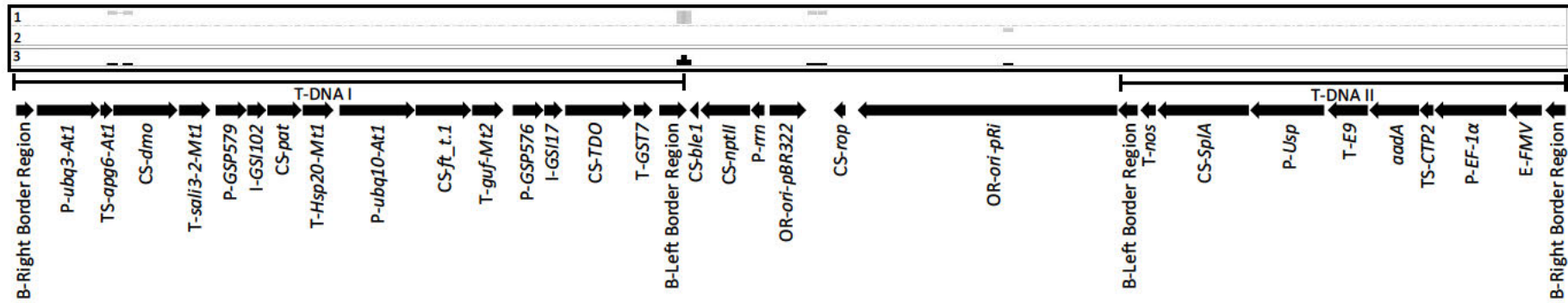


Figure 7. Read Mapping of Conventional Soybean A3555 Versus PV-GMHT529103

Panel 1 shows the location of left to right oriented paired reads. Panel 2 shows unpaired reads and panel 3 is a representation of combined read depth for unpaired and paired reads with a read depth range from 0 to 6.

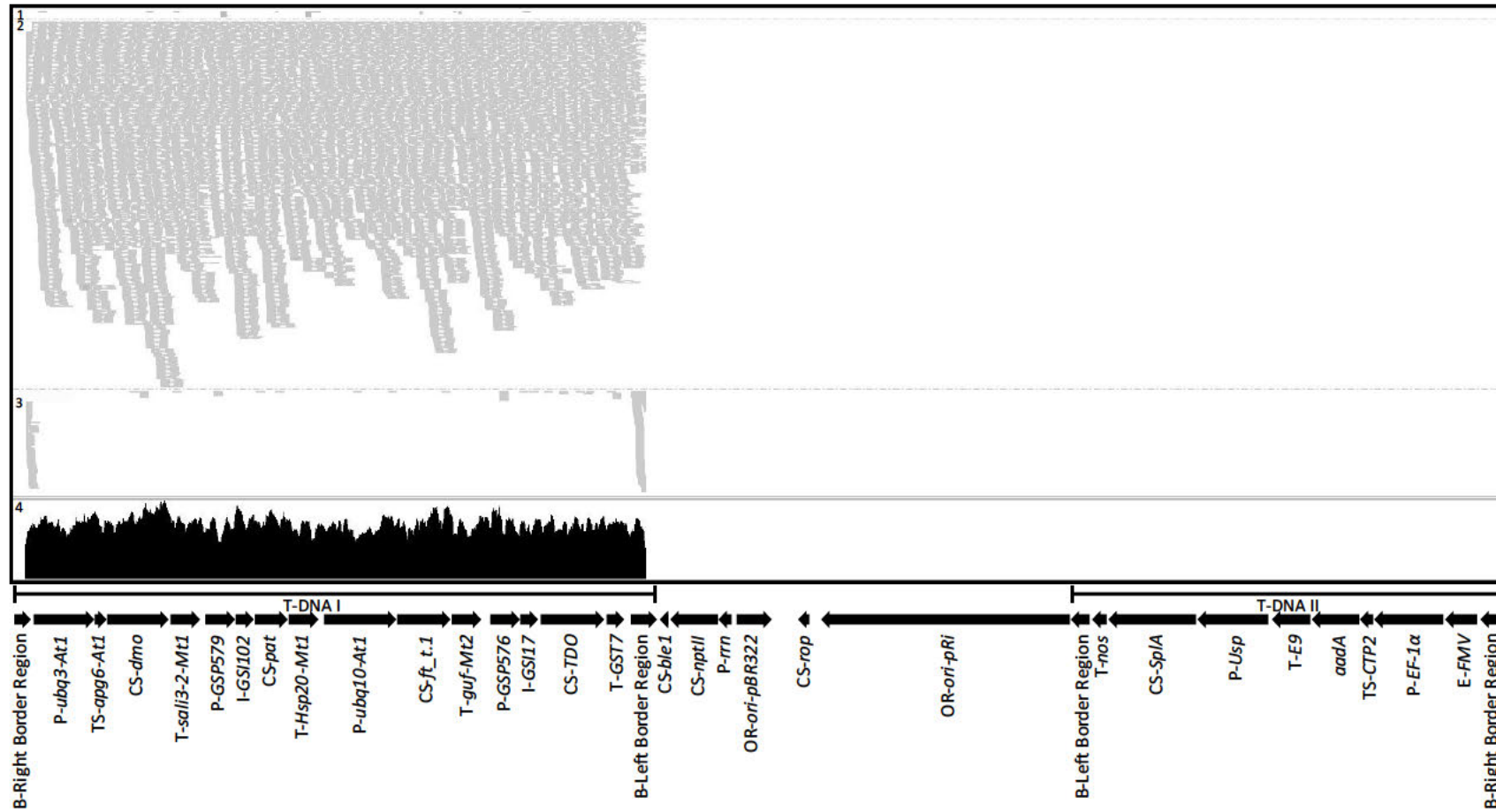


Figure 8. Read Mapping of MON 94313 (R3) Versus PV-GMHT529103

Panel 1 shows the location of right to left oriented paired reads. Panel 2 shows the location of left to right oriented paired reads. Panel 3 shows unpaired reads and panel 4 is a representation of combined read depth for unpaired and paired reads with a read depth range from 0 to 194. Comparable results were observed when read mapping the R4, R5, R6, and R7 generations of MON 94313 versus PV-GMHT529103 (See Appendix 1).

A.3(c)(iii) Full DNA sequence of each insertion site, including junction regions with the host DNA

A.3(c)(iii)(i) Organization and Sequence of the Insert and Adjacent DNA in MON 94313

The organization of the elements within the DNA insert and the adjacent genomic DNA was assessed using directed DNA sequence analysis (Figure 3, Step 4). PCR primers were designed to amplify two overlapping regions of the MON 94313 genomic DNA that span the entire length of the insert and the adjacent DNA flanking the insert (Figure 9). The amplified PCR products were subjected to DNA sequencing analyses. The results of this analysis confirm that the insert is 10,196 bp and that each genetic element within the insert is intact compared to PV-GMHT529103, with the exception of the border regions. The border regions both contain small terminal deletions with the remainder of the inserted border regions being identical to the sequence in PV-GMHT529103. The sequence and organization of the insert was also shown to be identical to the corresponding T-DNA I of PV-GMHT529103 as intended. This analysis also shows that only T-DNA I elements (described in Table 2) were present. In addition, 1000 base pairs flanking the 5' end of the MON 94313 insert (Table 2, bases 1-1000) and 1000 base pairs flanking the 3' end of the MON 94313 insert (Table 2, bases 11,197-12,196) were determined.

PART 2: SPECIFIC DATA REQUIREMENTS FOR SAFETY ASSESSMENT

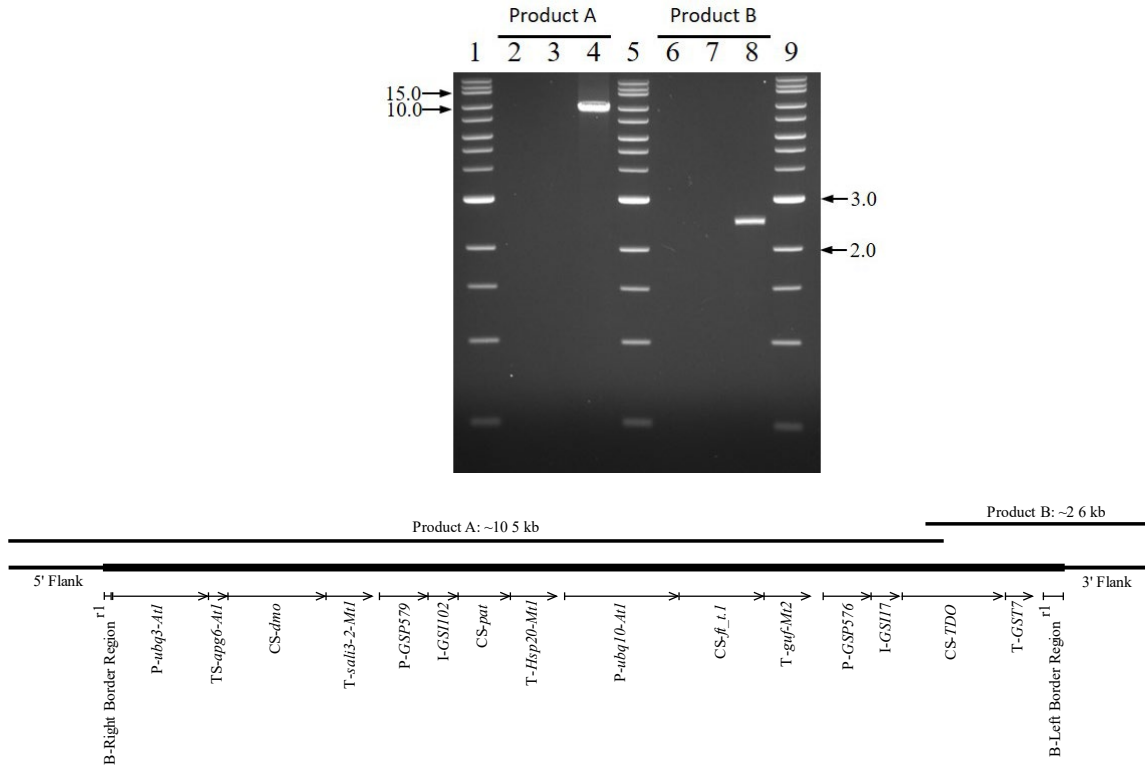


Figure 9. Analysis of Overlapping PCR Analysis Across the Insert in MON 94313

PCR was performed on both conventional control genomic DNA and genomic DNA of the R3 generation of MON 94313 using two pairs of primers to generate overlapping PCR fragments from MON 94313 for sequencing analysis. To verify the PCR products, 2 µl of each of the PCR reactions was loaded on the gel. The expected product size for each amplicon is provided in the illustration of the insert in MON 94313 that appears at the bottom of the figure. This figure is a representative of the data generated in the study. Lane designations are as follows:

Lane	
1	1 Kb Extend DNA Ladder
2	No template control
3	A3555 Conventional Control
4	MON 94313
5	1 Kb Extend DNA Ladder
6	No template control
7	A3555 Conventional Control
8	MON 94313
9	1 Kb Extend DNA Ladder

Arrows on the agarose gel photograph denote the size of the DNA, in kilobase pairs, obtained from the 1 Kb Extend DNA Ladder (New England BioLabs) on the ethidium bromide stained gel.

^{r1} Superscript in the Right and Left Border Region indicates that the sequence in MON 94313 was truncated compared to the sequences in PV-GMHT529103.

A.3(c)(iii)(ii) Sequencing of the MON 94313 Insertion Site

PCR and sequence analysis were performed on genomic DNA extracted from the conventional control to examine the insertion site in conventional soybean (Figure 3, Step 5). The PCR was performed with one primer specific to the genomic DNA sequence flanking the 5' end of the MON 94313 insert paired with a second primer specific to the genomic DNA sequence flanking the 3' end of the insert (Figure 10). A sequence comparison between the PCR product generated from the conventional control and the sequence generated from the 5' and 3' flanking sequences of MON 94313 indicates that 40 bases of soybean genomic DNA were deleted during integration of the T-DNA. Such changes are common during plant transformation ([Anderson *et al.*, 2016](#)) and these changes presumably result from double stranded break repair mechanisms in the plant during *Agrobacterium*-mediated transformation process ([Salomon and Puchta, 1998](#)). The remainder of the soybean genomic DNA sequences flanking the insert in MON 94313 are identical to the conventional control.

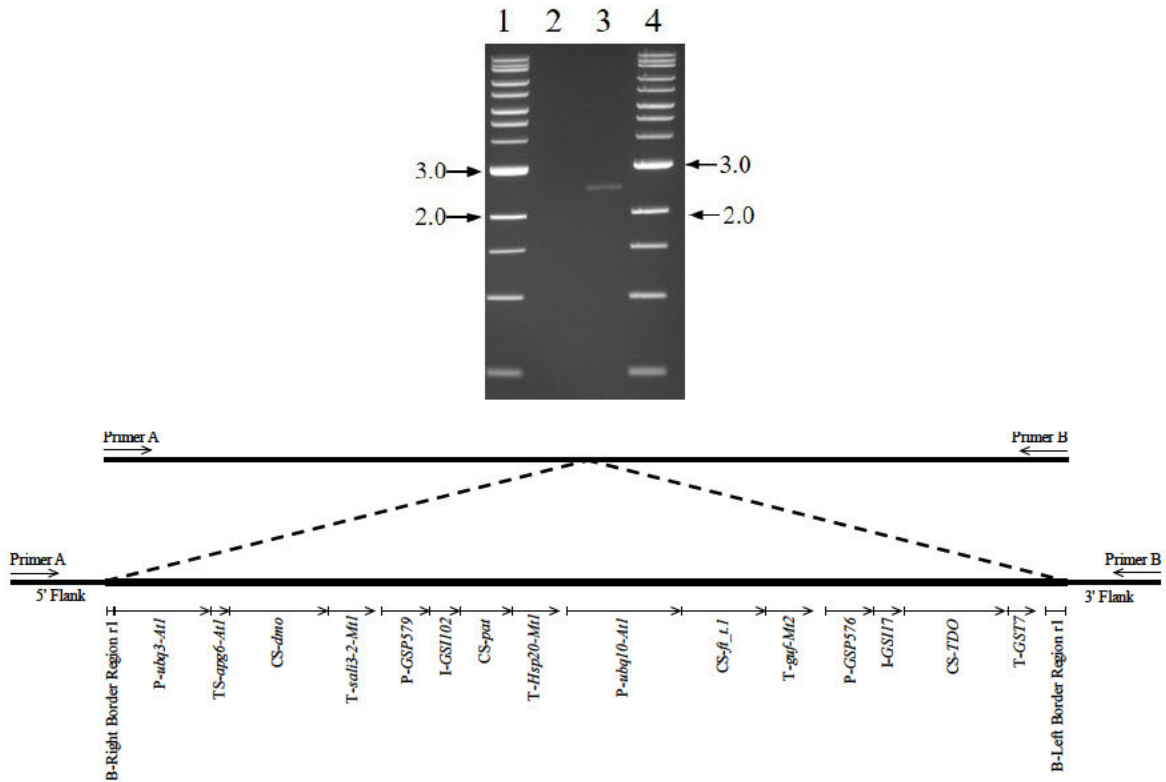


Figure 10. PCR Amplification of the MON 94313 Insertion Site

PCR analysis was performed to evaluate the insertion site. PCR was performed on conventional control DNA using Primer A, specific to the 5' flanking sequence, and Primer B, specific to the 3' flanking sequence of the insert in MON 94313. The expected PCR product size is ~2.5 kb. The DNA generated from the conventional control PCR was used for sequencing analysis. This illustration depicts the MON 94313 insertion site in the conventional control (upper panel) and the MON 94313 insert (lower panel). Approximately 6 µl of each of the PCR reactions were loaded on the gel. This figure is representative of the data generated in the study. Lane designations are as follows:

Lane	
1	1 Kb Plus DNA Ladder
2	No template control
3	A3555 Conventional Control
4	1 Kb Extend DNA Ladder

Arrows on the agarose gel photograph denote the size of the DNA, in kilobase pairs, obtained from the 1 Kb Extend DNA Ladder (New England BioLabs) on the ethidium bromide stained gel.

¹¹ Superscript in Right and Left Border Regions indicates that the sequence in MON 94313 was truncated compared to the sequences in PV-GMHT529103.

A.3(c)(iv) A map depicting the organisation of the inserted genetic material at each insertion site

PCR and DNA sequence analyses performed on MON 94313 and the conventional control determined the organisation of the genetic elements within the insert as given in Figure 10.

A.3(c)(v) Details of an analysis of the insert and junction regions for the occurrence of any open reading frames (ORFs)

In addition to the bioinformatic analyses conducted on MON 94313 DMO, PAT, FT_T.1 and TDO protein sequences (Sections B.2(a)(i) and B.2(b)(ii)), bioinformatic analyses were also performed on the MON 94313 insert to assess the potential for allergenicity, toxicity, or biological activity of putative polypeptides encoded by all six reading frames present in the MON 94313 insert DNA, as well as ORFs present in the 5' and 3' flanking sequence junctions. These various bioinformatic evaluations are depicted in Figure 11. ORFs spanning the 5' and 3' soybean genomic DNA-inserted DNA junctions were translated from stop codon to stop codon in all six reading frames (three forward reading frames and three reading frames in reverse orientation)². Polypeptides of eight amino acids or greater from each reading frame were then compared to toxin, allergen and all proteins databases using bioinformatic tools. Similarly, the entire T-DNA sequence was translated in all six reading frames and the resulting deduced amino acid sequence was subjected to bioinformatic analyses. The data generated from these analyses confirm that even in the highly unlikely occurrence that a translation product other than MON 94313 DMO, PAT, FT_T.1 and TDO proteins were derived from frames one to six of the insert DNA or the ORFs spanning the insert junctions, they would not share a sufficient degree of sequence similarity with other proteins to indicate they would be potentially allergenic, toxic, or have other safety implications. Therefore, there is no evidence for concern regarding the relatedness of the putative polypeptides for MON 94313 to known toxins, allergens, or biologically active putative peptides.

A.3(c)(v)(i) Bioinformatics Evaluation of the T-DNA Insert in MON 94313

Bioinformatic analyses were performed to assess the potential of toxicity, allergenicity or biological activity of any putative peptides encoded by translation of reading frames 1 through 6 of the inserted DNA in MON 94313 (Figure 11).

The FASTA sequence alignment tool was used to assess structural relatedness between the query sequences and any protein sequences in the AD_2022, TOX_2022, and PRT_2022 databases. Structural similarities shared between each putative polypeptide with each sequence in the database were examined. The extent of structural relatedness was evaluated by detailed visual inspection of the alignment, the calculated percent identity and alignment length to ascertain if alignments exceeded Codex ([Codex Alimentarius, 2009](#)) thresholds for FASTA searches of the AD_2022 database, and the *E*-score. Alignments having an *E*-score less than 1×10^{-5} are deemed significant because they may reflect shared structure and function among sequences. In addition

² An evaluation of sequence translated from stop codon to stop codon represents the most conservative approach possible for flank junction analysis as it does not take into consideration that a start codon is necessary for the production of a protein sequence.

to structural similarity, each putative polypeptide was screened for short polypeptide matches using a pair-wise comparison algorithm.

The results of the search comparisons showed that no relevant structural similarity to known allergens and toxins were observed for any of the putative polypeptides when compared to proteins in the allergen (AD_2022) or toxin (TOX_2022) databases. Furthermore, no short (eight amino acid) polypeptide matches were shared between any of the putative polypeptides and proteins in the allergen database that had biological relevance.

Taken together, these data demonstrate the lack of relevant similarities between known allergens or toxins for putative peptides derived from all six reading frames from the inserted DNA sequence of MON 94313. As a result, in the unlikely event that a translation product other than DMO, PAT, FT_T.1 and TDO proteins were derived from reading frames 1 to 6, these putative polypeptides are not expected to be cross-reactive allergens, toxins, or display adverse biological activity.

A.3(c)(v)(ii) Bioinformatics Evaluation of the DNA Sequences Flanking the 5' and 3' Junctions of the MON 94313 Insert: Assessment of Putative Peptides

Analyses of putative polypeptides encoded by DNA spanning the 5' and 3' genomic junctions of the MON 94313 inserted DNA were performed using a bioinformatic comparison strategy. The purpose of the assessment is to evaluate the potential for novel open reading frames (ORFs) that may have homology to known allergens, toxins, or proteins that display adverse biological activity. Sequences spanning the 5' and 3' genomic DNA-insert DNA junctions, (Figure 11) were translated from stop codon to stop codon in all six reading frames. Putative polypeptides from each reading frame, that were eight amino acids or greater in length, were compared to AD_2022, TOX_2022, and PRT_2022 databases using FASTA and to the AD_2022 database using an eight amino acid sliding window search. A total of 8 putative peptides were compared to allergen (AD_2022), toxin (TOX_2022), and all protein (PRT_2022) databases using bioinformatic tools.

The FASTA sequence alignment tool was used to assess the relatedness between the query sequences and any protein sequence in the AD_2022, TOX_2022, and PRT_2022 databases. Similarities shared between the sequence with each sequence in the database were examined. The extent of relatedness was evaluated by detailed visual inspection of the alignment, the calculated percent identity, and the *E*-score. Alignments having *E*-scores of $\leq 1e-5$ (1×10^{-5}) are deemed significant because they may reflect shared structure and function among sequences. In addition to sequence similarity, sequences were screened for short peptide matches using a pair-wise comparison algorithm. In these analyses, eight contiguous and identical amino acids were defined as immunologically relevant, where eight represents the typical minimum sequence length likely to represent an immunological epitope ([Silvanovich et al., 2006](#)).

The results of these data indicate that no biologically relevant sequence similarities were observed between the translated putative flank junction sequences and allergens, toxins, or biologically active proteins associated with adverse effects for human or animal health. The bioinformatic analyses performed using the putative sequences translated from junctions is theoretical. Likewise, other than translation of DMO, PAT, FT_T.1 and TDO no evidence exists to indicate that any other sequence from the T-DNA is translated. Rather, the results of these bioinformatic analyses indicate that in the unlikely occurrence that any of the putative flank junction sequences

analyzed herein is found *in planta*, or translation of sequence other than the intended protein products was to occur, none would share significant similarity or identity to known allergens, toxins, or other biologically active proteins that could affect human or animal health.

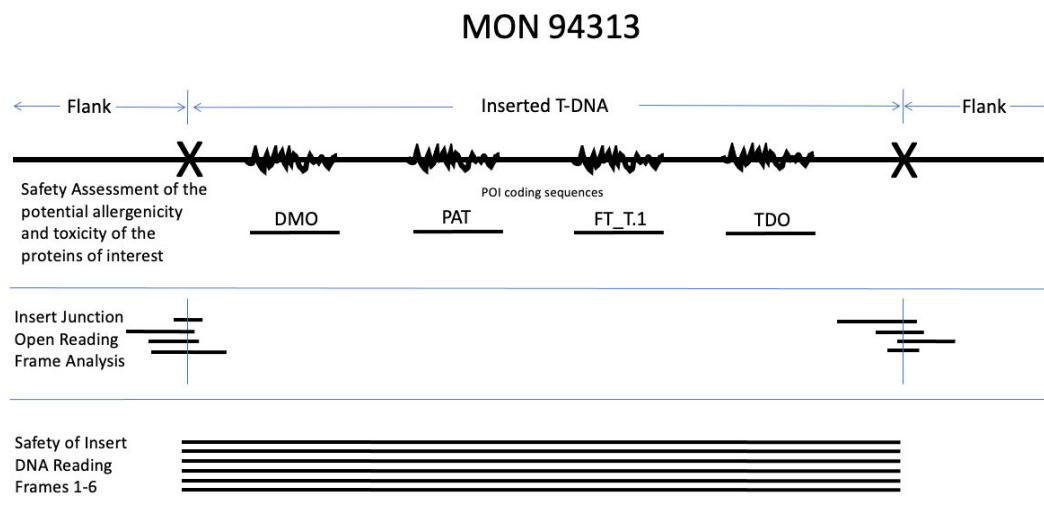


Figure 11. Schematic Summary of MON 94313 Bioinformatic Analyses

A.3(c)(v)(iii) Bioinformatic Evaluation of Putative Open Reading Frames of MON 94313 Insert and Flanking Sequences Summary and Conclusions

A conservative bioinformatic assessment of potential allergenicity, toxicity and adverse biological activity for putative polypeptides derived from different reading frames of the entire insert MON 94313 or that span the 5' and 3' insert junctions was conducted. There are no analytical data that indicate any putative polypeptides subjected to bioinformatic evaluation are produced by MON 94313. Moreover, the data generated from these analyses confirm that even in the highly unlikely occurrence that a translation product other than DMO, PAT, FT_T.1 and TDO proteins was derived from frames 1 to 6 of the insert DNA, or the ORFs spanning the insert junctions; they would not share a sufficient degree of sequence similarity with other proteins to indicate they would be potentially allergenic, toxic, or have other safety implications. Therefore, there is no evidence for concern regarding the putative polypeptides for MON 94313 relatedness to known toxins, allergens, or biologically active putative peptides.

For details, please refer to Appendix 2 and Appendix 3.

A.3(d) A description of how the line or strain from which food is derived was obtained from the original transformant (i.e. provide a family tree or describe the breeding process) including which generations have been used for each study

MON 94313 was derived from a single plant transformant of variety A3555. A3555 was used as the conventional soybean comparator to support the safety assessment of MON 94313.

MON 94313 and the conventional control A3555 have similar genetic backgrounds with the exception of the *dmo*, *pat*, *ft_t.1* and *TDO* expression cassettes. Thus, the effect of the *dmo*, *pat*, *ft_t.1* and *TDO* expression cassettes and the expressed DMO, PAT, FT_T.1 and TDO proteins can be assessed in an unbiased manner in comparative safety assessments. Where appropriate, commercial reference soybean materials were used to establish a range of variability or responses representative of commercial soybean.

For more details, see MON 94313 breeding history Figure 6.

A.3(e) Evidence of the stability of the genetic changes, including:

A.3(e)(i) The pattern of inheritance of the transferred gene(s) and the number of generations over which this has been monitored

In order to demonstrate the stability of the T-DNA I present in MON 94313 through multiple breeding generations, NGS was performed using DNA obtained from five breeding generations of MON 94313. The breeding history of MON 94313 is presented in Figure 6, and the specific generations tested are indicated in the figure legend. The MON 94313 (R3) generation was used for the molecular characterisation analyses discussed in Sections A.3(c)(ii) and A.3(c)(iii). To assess stability, four additional generations were evaluated by NGS, and compared to the fully characterized MON 94313 (R3) generation. The conventional control used for the generational stability analysis was A3555, which has a genetic background similar to the other generations in Table 4 and represents the original transformation line. Genomic DNA isolated from each of the selected generations of MON 94313 and conventional control was used for NGS mapping and subsequent junction identification (Table 4).

Table 4. Junction Sequence Detected

Sample	Junction Sequence Detected
MON 94313 (R3)	2
MON 94313 (R4)	2
MON 94313 (R5)	2
MON 94313 (R6)	2
MON 94313 (R7)	2
A3555	0

As shown by alignments to the full flank/insert sequence obtained from directed sequencing, a single conserved pair of junctions linked by contiguous known and expected DNA sequence is present in MON 94313 (R3). Two identical junctions are found in each of the breeding generations (R3, R4, R5, R6, and R7), confirming the insertion of a single copy of PV-GMHT529103 T-DNA at a single locus in the genome of MON 94313. The consistency of these junctions in the mapping data across all generations tested demonstrates that this single locus is stably maintained throughout the MON 94313 breeding process.

These results demonstrate that the MON 94313 (R3) single locus of integration is found in all subsequent generations of the MON 94313 breeding history, thereby confirming the stability of the insert. Based on this comprehensive sequence data and bioinformatic analysis of NGS data it is concluded that MON 94313 contains a single, stable, inserted T-DNA I.

For details, please refer to Appendix 1. Appendix 4

A.3(e)(ii) The pattern of inheritance and expression of the phenotype over several generations and, where appropriate, across different environments

A.3(e)(ii)(i) Inheritance of the Genetic Insert in MON 94313

The MON 94313 T-DNA I resides at a single locus within the soybean genome and therefore should be inherited according to Mendelian principles of inheritance. During development of lines containing MON 94313, genotypic segregation data were recorded to assess the inheritance and stability of the MON 94313 T-DNA I using Chi square (χ^2) analysis over several generations. The χ^2 analysis is based on comparing the observed segregation ratio to the expected segregation ratio according to Mendelian principles.

The MON 94313 breeding path for generating segregation data is described in Figure 12. The transformed R0 plant was self-pollinated to generate R1 seed. An individual plant homozygous for the MON 94313 T-DNA I (homozygous positive) was identified in the R1 segregating population via a Real-Time TaqMan[®] PCR assay.

The homozygous positive R1 plant was self-pollinated to give rise to R2 seed, and a homozygous positive R2 plant was self-pollinated to give rise to R3 seed. The homozygous positive R3 plants were crossed via traditional breeding techniques to a Bayer CropScience LP proprietary elite variety that did not contain the T-DNA I coding sequences to produce hemizygous F1 seed. The hemizygous F1 plants were self-pollinated to produce F2 seed. The F2 generation was tested for the presence of MON 94313 T-DNA I by Qualitative End Point TaqMan[®] PCR assay for the T-*Sali3-2-Mt1* genetic element. Qualitative End Point TaqMan[®] PCR assays detect the fluorescence of amplified PCR products specific to the TaqMan probe target sequence at the conclusion of PCR cycling.

The inheritance of the MON 94313 T-DNA I was assessed in the F2 generation and in subsequent F3 and F4 generations. In all generations, the MON 94313 T-DNA was predicted to segregate at a 1:2:1 ratio (homozygous positive: hemizygous positive: homozygous negative) according to Mendelian inheritance principles.

A Pearson's chi-square (χ^2) analysis was used to compare the observed segregation ratios of the MON 94313 T-DNA I to the expected ratios.

The Chi-square was calculated as:

$$\chi^2 = \sum [(|o - e|)^2 / e]$$

where o = observed frequency of the genotype or phenotype and e = expected frequency of the genotype or phenotype. The level of statistical significance was predetermined to be 5% ($\alpha = 0.05$).

The results of the χ^2 analysis of the segregating progeny of MON 94313 are presented in Table 5. The χ^2 value in the F2, F3, and F4 generations indicated no statistically significant difference between the observed and expected segregation ratios of MON 94313 T-DNA I. These results support the conclusion that the MON 94313 T-DNA I resides at a single locus within the soybean genome and is inherited according to Mendelian principles of inheritance. These results are also consistent with the molecular characterisation data indicating that MON 94313 contains a single intact copy of the T-DNA I inserted at a single locus in the soybean genome (Sections A.3(c)(ii), A.3(c)(iii) and A.3(e)(i)).

For details, please refer to Appendix 4.

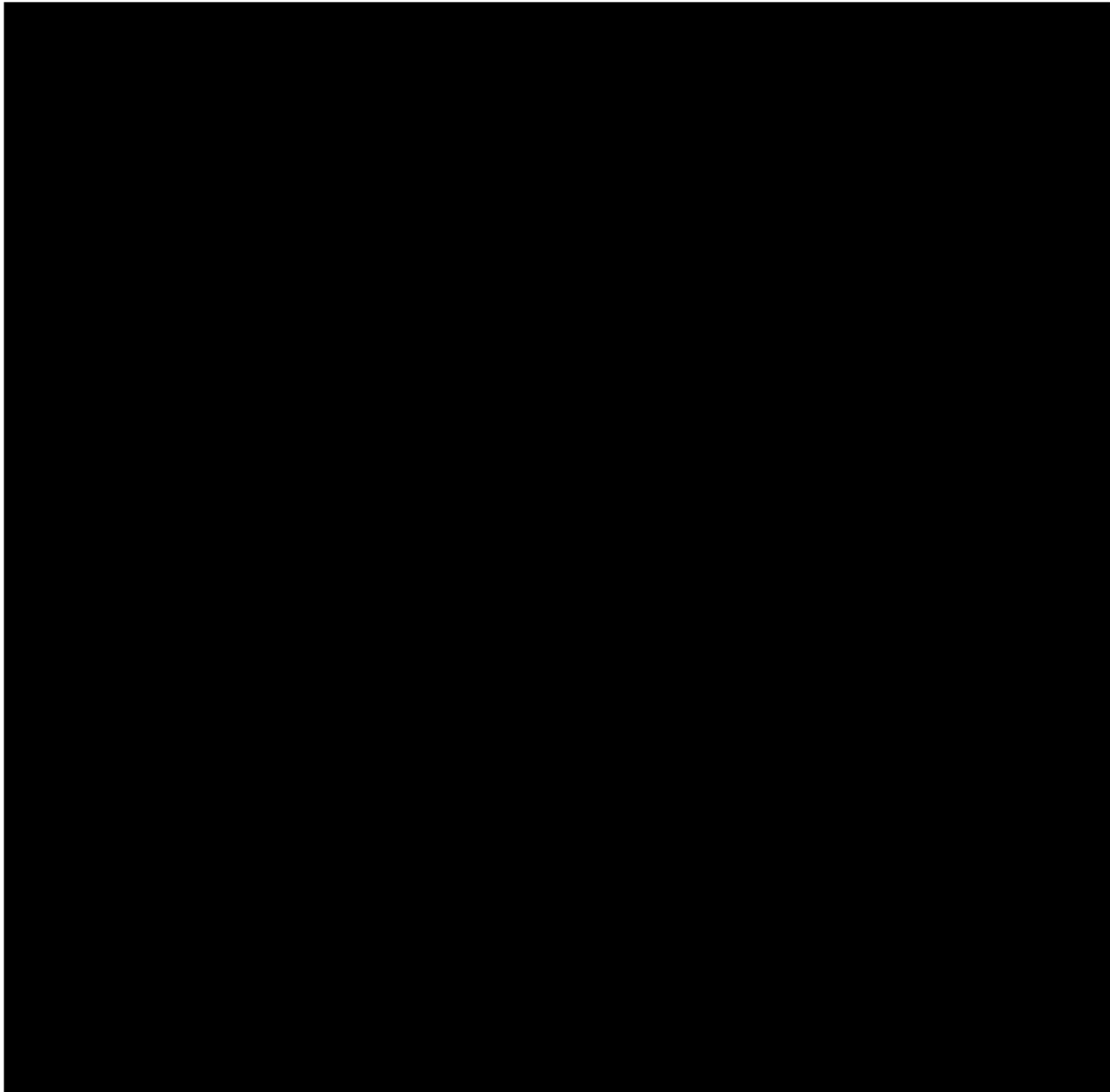


Figure 12. Breeding Path for Generating Segregation Data for MON 94313

PART 2: SPECIFIC DATA REQUIREMENTS FOR SAFETY ASSESSMENT

*Chi-square analysis was conducted on segregation data from F2, F3, and F4 generations (bolded text).

⊗: Self- Pollinated

Table 5. Segregation of the T-DNA I During the Development of MON 94313

Generation	Total Plants	Observed # Plant Homozygous Positive	Observed # Plant Hemizygous Positive	Observed # Plant Homozygous Negative	1:2:1 Segregation			χ^2	p-value
					Expected # Plant Homozygous Positive	Expected # Plant Hemizygous Positive	Expected # Plant Homozygous Negative		
F2	262	68	131	63	65.50	131.00	65.50	0.19	0.909
F3	527	134	251	142	131.75	263.50	131.75	1.43	0.489
F4	291	76	144	71	72.75	145.50	72.75	0.20	0.904

A.3(e)(ii)(ii) Expression of the genetic insert

In order to assess the presence of the DMO, PAT, FT_T.1 and TDO protein in MON 94313 across multiple breeding generations, western blot analysis was conducted on seed tissue collected from generations R3, R4, R5, R6, and R7 of MON 94313, using seed tissue of the conventional control (A3555) as negative control.

The presence of the DMO protein was demonstrated in five breeding generations of MON 94313 using western blot analysis. The *E. coli*-produced DMO protein reference standard (10 ng) was used as a reference for the positive identification of the DMO protein (Figure 13, lane 3). The presence of the DMO protein in seed tissue samples of MON 94313 was determined by visual comparison of the bands detected in five breeding generations (Figure 13, lanes 5-9) to the *E. coli*-produced DMO protein reference standard. The MON 94313-produced DMO protein migrated indistinguishably from that of the *E. coli*-produced protein standard analyzed on the same western blot. The slightly smeared background associated with protein of interest might be a combination of heavy soy matrix effect and antibody detection. Nevertheless, as expected, the DMO protein was not detected in the conventional control seed extract (Figure 13, lane 4).

The presence of the PAT protein was demonstrated in five breeding generations of MON 94313 using western blot analysis. The *E. coli*-produced PAT protein reference standard (2 ng) was used as a reference for the positive identification of the PAT protein (Figure 14, lane 3). The presence of the PAT protein in seed tissue samples of MON 94313 was determined by visual comparison of the bands detected in five breeding generations (Figure 14, lanes 5-9) to the *E. coli*-produced PAT protein reference standard. The MON 94313-produced PAT protein migrated indistinguishably from that of the *E. coli*-produced protein standard analyzed on the same western blot. The light additional bands observed across control and test samples are likely a combination of soy matrix effects and non-specific binding of the PAT antibody. Nevertheless, as expected, the PAT protein was not detected in the conventional control seed extract (Figure 14, lane 4).

The presence of the FT_T.1 protein was demonstrated in five breeding generations of MON 94313 using western blot analysis. The *E. coli*-produced FT_T.1 protein reference standard (1 ng) was used as a reference for the positive identification of the FT_T.1 protein (Figure 15, lane 3). The presence of the FT_T.1 protein in seed tissue samples of MON 94313 was determined by visual comparison of the bands detected in five breeding generations (Figure 15, lanes 5-9) to the *E. coli*-produced FT_T.1 protein reference standard. The MON 94313-produced FT_T.1 protein migrated indistinguishably from that of the *E. coli*-produced protein standard analyzed on the same western blot. The weaker low MW signals in the two generations (Figure 15, lanes 6-7) might be due to a few variabilities, such as the seed grinding process, protein stability, or matrix effects. Nevertheless, as expected, the FT_T.1 protein was not detected in the conventional control seed extract (Figure 15, lane 4).

The presence of the TDO protein was demonstrated in five breeding generations of MON 94313 using Western blot analysis. The *E. coli*-produced TDO protein reference standard (1 ng) was used as a reference for the positive identification of the TDO protein (Figure 16, lane 3). The presence of the TDO protein in seed tissue samples of MON 94313 was determined by visual comparison of the bands detected in five breeding generations (Figure 16, lanes 5-9) to the *E. coli*-produced TDO protein reference standard. The MON 94313-produced TDO protein

PART 2: SPECIFIC DATA REQUIREMENTS FOR SAFETY ASSESSMENT

migrated indistinguishably from that of the *E. coli*-produced protein standard analyzed on the same western blot. The weaker signal intensity of TDO proteins in the early two generations might be due to a few variabilities – powder fineness from the seed grinding process, protein stability, tissue moisture/composition, matrix masking effects, and other potential variables not cited here. Additional bands observed across control and test samples are likely a combination of soy matrix effects and non-specific binding of the TDO antibody. Nevertheless, as expected, the TDO protein was not detected in the conventional control seed extract (Figure 16, lane 9).

For details, please refer to Appendix 5.

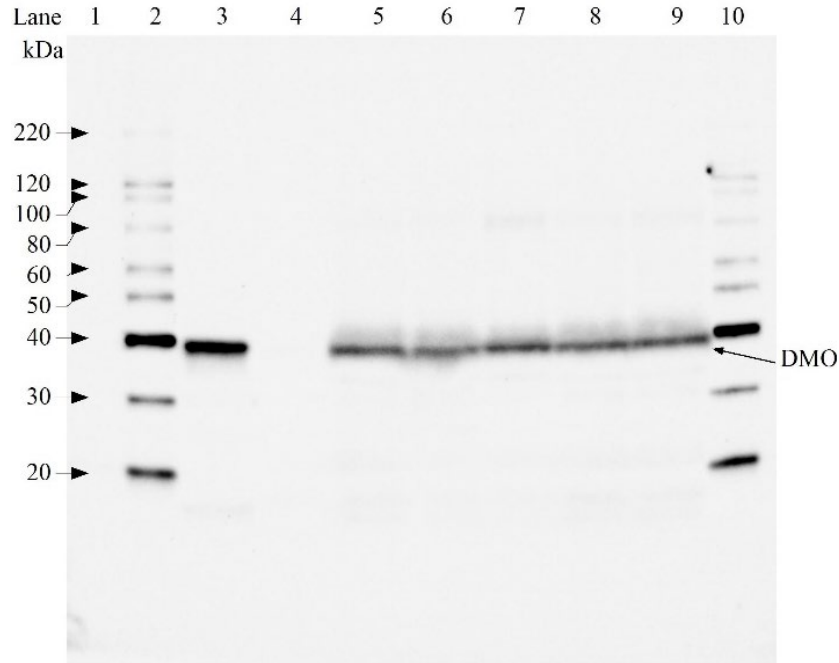


Figure 13. Presence of DMO Protein in Multiple Generations of MON 94313

Blot probed with monoclonal anti-DMO primary antibodies and HRP conjugated anti-mouse IgG secondary antibodies. The 5 second exposure image is shown. The approximate MWs (kDa) of the MagicMark™ Protein Standards are shown on the left. Lane designations are as follows:

Lane	Description	Amount Loaded
1	Precision Plus™ Protein Standards	5 µl
2	MagicMark™ Protein Standards	2 µl
3	<i>E. coli</i> -produced DMO protein	10 ng
4	Conventional Control, 11511575	10 µl
5	MON 94313, R3, 11518561	10 µl
6	MON 94313, R4, 11510914	10 µl
7	MON 94313, R5, 11511576	10 µl
8	MON 94313, R6, 11521043	10 µl
9	MON 94313, R7, 11521045	10 µl
10	MagicMark™ Protein Standards	2 µl

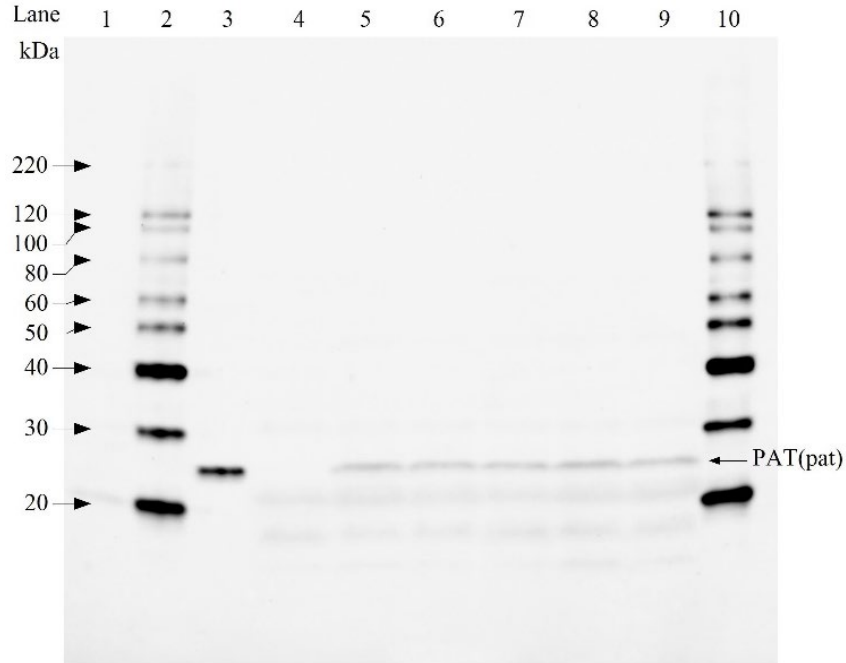


Figure 14. Presence of PAT Protein in Multiple Generations of MON 94313

Blot probed with monoclonal anti-PAT primary antibodies and HRP conjugated anti-mouse IgG secondary antibodies. The 30 second exposure image is shown. The approximate MWs (kDa) of the MagicMark™ Protein Standards are shown on the left. Lane designations are as follows:

Lane	Description	Amount Loaded
1	Precision Plus™ Protein Standards	5 µl
2	MagicMark™ Protein Standards	2 µl
3	<i>E. coli</i> -produced PAT protein	2 ng
4	Conventional Control, 11511575	10 µl
5	MON 94313, R3, 11518561	10 µl
6	MON 94313, R4, 11510914	10 µl
7	MON 94313, R5, 11511576	10 µl
8	MON 94313, R6, 11521043	10 µl
9	MON 94313, R7, 11521045	10 µl
10	MagicMark™ Protein Standards	2 µl

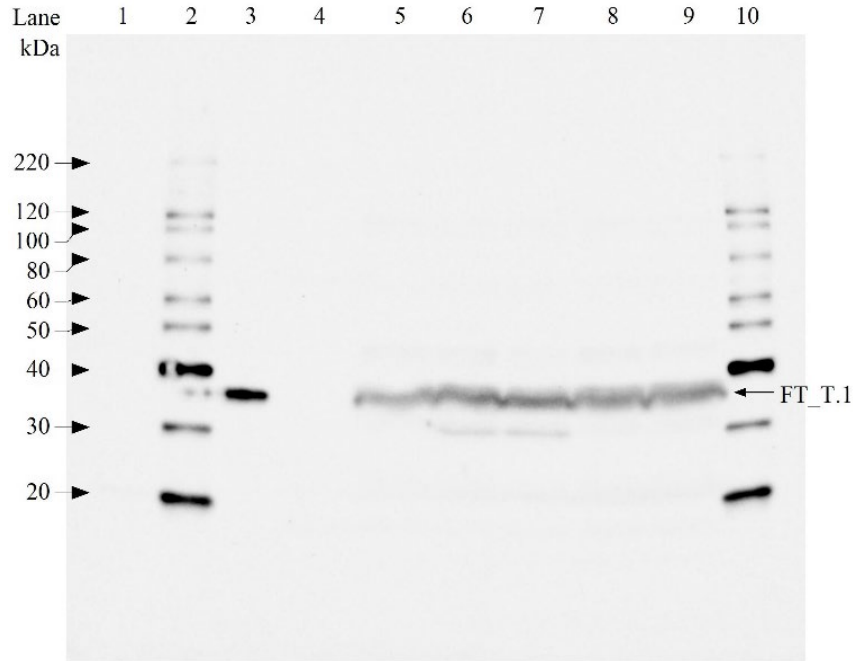


Figure 15. Presence of FT_T.1 Protein in Multiple Generations of MON 94313

Blot probed with monoclonal anti-FT_T.1 primary antibodies and HRP conjugated anti-mouse IgG secondary antibodies. The 5 second exposure image is shown. The approximate MWs (kDa) of the MagicMark™ Protein Standards are shown on the left. Lane designations are as follows:

Lane	Description	Amount Loaded
1	Precision Plus™ Protein Standards	5 µl
2	MagicMark™ Protein Standards	2 µl
3	<i>E. coli</i> -produced FT_T.1 protein	1 ng
4	Conventional Control, 11511575	10 µl
5	MON 94313, R3, 11518561	10 µl
6	MON 94313, R4, 11510914	10 µl
7	MON 94313, R5, 11511576	10 µl
8	MON 94313, R6, 11521043	10 µl
9	MON 94313, R7, 11521045	10 µl
10	MagicMark™ Protein Standards	2 µl

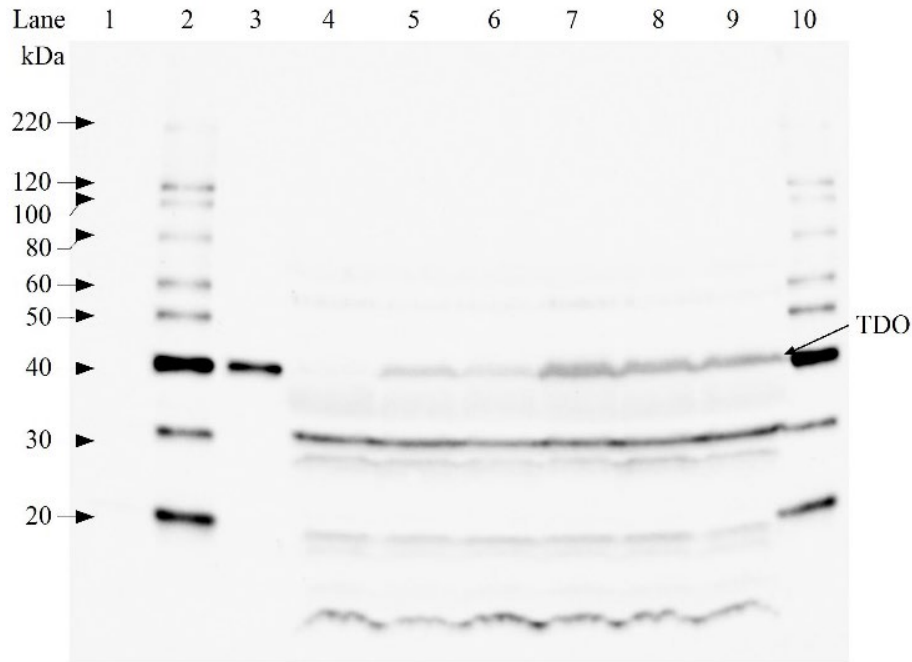


Figure 16. Presence of TDO Protein in Multiple Generations of MON 94313

Blot probed with a monoclonal anti-TDO primary antibody and HRP conjugated anti-mouse IgG secondary antibodies. The 5 second exposure image is shown. The approximate MWs (kDa) of the MagicMark™ Protein Standards are shown on the left. Lane designations are as follows:

Lane	Description	Amount Loaded
1	Precision Plus™ Protein Standards	5 µl
2	MagicMark™ Protein Standards	2 µl
3	<i>E. coli</i> -produced TDO protein	1 ng
4	Conventional Control, 11511575	10 µl
5	MON 94313, R3, 11518561	10 µl
6	MON 94313, R4, 11510914	10 µl
7	MON 94313, R5, 11511576	10 µl
8	MON 94313, R6, 11521043	10 µl
9	MON 94313, R7, 11521045	10 µl
10	MagicMark™ Protein Standards	2 µl

A.3(f) An analysis of the expressed RNA transcripts, where RNA interference has been used

Not relevant for this product.

B. CHARACTERISATION AND SAFETY ASSESSMENT OF NEW SUBSTANCES**B.1 Characterisation and Safety Assessment of New Substances**

B.1(a) Full description of the biochemical and phenotypic effects of all new substances (e.g. a protein or an untranslated RNA) that are expressed in the new GM organism, including their levels and site of accumulation, particularly in edible portions

B.1(a)(i) Description, mode-of-action, and specificity of DMO, PAT, FT_T.1 and TDO proteins expressed in MON 94313

B.1(a)(i)(i) DMO protein expressed in MON 94313

B.1(a)(i)(i)(i) General description

Wild type DMO was initially purified from *Stenotrophomonas maltophilia* (*S. maltophilia*) strain DI-6 ([Herman et al., 2005](#); [Palleroni and Bradbury, 1993](#)), isolated from soil at a dicamba manufacturing plant ([Krueger et al., 1989](#)). DMO is targeted to the chloroplast by a chloroplast transit peptide (CTP) to allow co-localization with the endogenous reductase and ferredoxin enzymes that supply electrons for the DMO demethylation reaction as described by Behrens *et al.* (2007). In the construction of the plasmid vector used in the development of MON 94313, PV-GMHT529103, a CTP coding sequence from *Arabidopsis thaliana* (APG6) was joined to the *dmo* coding sequence; this additional coding sequence results in the production of a precursor protein consisting of the DMO protein and a N-terminal 68 amino acid APG6 CTP that is utilized to target the precursor protein to the chloroplast ([Herrmann, 1995](#); [Klee et al., 1987](#)). Typically, transit peptides are precisely removed from the precursor protein following delivery to the targeted plastid ([della-Cioppa et al., 1986](#)) resulting in the full length protein. However, there are examples in the literature of alternatively processed forms of a protein targeted to a plant's chloroplast ([Behrens et al., 2007](#); [Clark and Lamppa, 1992](#)). Data from N-terminal sequencing analysis of the MON 94313-produced DMO indicate that processing of the DMO precursor protein expressed in MON 94313 produced a single isoform of the mature MON 94313 DMO protein with no additional N-terminal residues remaining from partial processing of the of the APG6 transit peptide. Except for an additional leucine at position two, the MON 94313 DMO protein has an identical sequence to the wild-type DMO protein from the DI-6 strain of *S. maltophilia* ([Herman et al., 2005](#)).

DMO protein produced in MON 94313 is also present in MON 88701 cotton [A1080], MON 87708 soybean [A1063], MON 87419 maize [A1118], and MON 87429 maize [A1192] submitted to FSANZ. As part of these completed FDA consultations, DMO proteins were assessed following the criteria outlined above, which determined that food and feed products derived from them are as safe and nutritious as food and feed derived from their conventional counterparts. The safety of these proteins has also been reviewed, and products containing the DMO protein were approved in numerous other countries (e.g., Australia/New Zealand, Canada, Colombia, Japan, Korea, Mexico, Taiwan Brazil, European Union, China, Indonesia, for MON 87708 soybean)³. MON 94313 DMO protein is identical in amino acid sequence to the DMO protein expressed in

¹Source: CropLife International Database (<http://www.biotradestatus.com/>)

MON 88701 cotton, MON 87419 maize, and MON 87429 maize except it does not have any additional N-terminal amino acid residues from the partial processing of the chloroplast transit peptide. Except for minor amino acid differences at positions 2 and 112 and the lack of any N-terminal amino acid residues in MON 94313 DMO remaining from partial processing of the chloroplast transit peptide, the amino acid sequence of MON 94313 DMO protein is identical to the DMO protein expressed in MON 87708 soybean.

These minor amino differences between the DMO proteins expressed in MON 94313 soybean, MON 88701 cotton, MON 87419 maize, MON 8729 maize, and MON 87708 soybean are not anticipated to have an effect on the structure of the catalytic site, functional activity, immunoreactivity or specificity of the protein ([D'Ordine et al., 2009](#); [Dumitru et al., 2009](#)).

B.1(a)(i)(ii) Mode-of-Action

MON 94313 contains a demethylase gene from *S. maltophilia* that expresses a DMO protein. As a mono-oxygenase protein, the DMO protein is part of the larger oxygenase family of enzymes that incorporate one or two oxygen atoms into substrates and are widely distributed in many universal metabolic pathways ([Harayama et al., 1992](#)). DMO is a Rieske-type non-heme iron oxygenase and is part of a three component system comprised of a reductase, a ferredoxin, and a terminal oxygenase, which in this case is the DMO protein. In MON 94313 soybean, these three proteins work together to catalyze the demethylation of the broadleaf herbicide dicamba to the non-herbicidal compound 3,6-dichlorosalicylic acid (DCSA) and formaldehyde, thus conferring dicamba resistance ([Chakraborty et al., 2005](#)). This three-component redox system is presented in Figure 17.

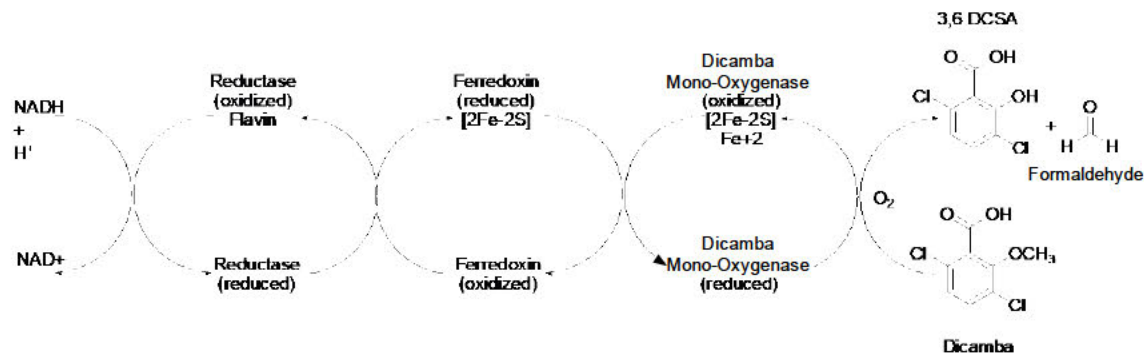


Figure 17. Three Components of the DMO Oxygenase System

Depicted is the electron transport chain that starts with NADH and ends with DMO resulting in the demethylation of dicamba to form DCSA.

The crystal structure of a C-terminal histidine tagged DMO protein, which is identical to wild-type DMO except for an additional alanine at position two and a C-terminal polyhistidine tag has been solved ([D'Ordine et al., 2009](#); [Dumitru et al., 2009](#)). The addition of a polyhistidine tag fused to the N- or C-terminus of a protein of interest is commonly used as a tool to aid in protein purification ([Hochuli et al., 1988](#)). The crystal structure of active DMO was determined to be a trimer comprised of three identical DMO monomers ([D'Ordine et al., 2009](#); [Dumitru et al., 2009](#)). Each DMO monomer contains a Rieske [2Fe-2S] cluster domain and a non-heme iron center domain ([D'Ordine et al., 2009](#); [Dumitru et al., 2009](#)) that are typical of all Rieske-type mono-oxygenases ([Ferraro et al., 2005](#)). To catalyze the demethylation of dicamba, electrons transferred from NADH are shuttled through endogenous reductase and ferredoxin to the terminal DMO protein. The electrons are received by the Rieske [2Fe-2S] cluster of one DMO protein molecule in the trimer and transferred to the non-heme iron center at the catalytic site of an adjacent DMO protein molecule in the trimer ([D'Ordine et al., 2009](#); [Dumitru et al., 2009](#)), where it reductively activates oxygen to catalyze the final demethylation of dicamba. Electron transport from the Rieske [2Fe-2S] cluster domain to the non-heme iron center domain cannot occur within a monomer since the distance is too great ([D'Ordine et al., 2009](#); [Dumitru et al., 2009](#)). As a result of the demethylation reaction, the non-herbicidal compound DCSA and formaldehyde are formed from dicamba. DCSA is a known metabolite found in cotton, soybean, soil, and livestock whose safety has been evaluated by the FAO-WHO and EPA ([FAO-WHO, 2011b](#); [FAO-WHO, 2011a](#); [U.S. EPA, 2009](#)). The other reaction product, formaldehyde, is found naturally in many plants and edible fungi at levels up to several hundred ppm ([Adrian-Romero et al., 1999](#); [Tashkov, 1996](#)). Thus, neither DCSA nor formaldehyde generated by the action of DMO on dicamba pose a significant food or feed safety risk.

B.1(a)(i)(i)(iii) Specificity

The substrate specificity of DMO expressed in MON 94313 was evaluated to understand potential interactions DMO may have with endogenous compounds structurally similar to dicamba that are found in plants. The literature indicates the specificity of DMO for dicamba is due to the specific interactions that occur at the catalytic site between the substrate and the protein ([D'Ordine et al., 2009](#); [Dumitru et al., 2009](#)). Dicamba interacts with amino acids in the catalytic site of DMO through the carboxylate moiety, the ring structure and the chlorine atoms of dicamba, which are primarily involved in orienting the substrate in the catalytic site. These chlorine atoms are required for catalysis to occur ([D'Ordine et al., 2009](#); [Dumitru et al., 2009](#)). The compound 2-methoxy benzoic acid (*o*-anisic acid), which is identical in structure to dicamba except for the absence of chlorines, was tested as a potential substrate of DMO by two independent laboratories ([D'Ordine et al., 2009](#); [Dumitru et al., 2009](#)). No significant turnover was detected under standard assay conditions using HPLC or through liquid chromatography/mass spectrometry methods where picomole levels of products can be observed. Given the limited existence of chlorinated compounds with structures similar to dicamba in plants and other eukaryotes ([Gribble, 2010](#)), it is unlikely that DMO produced in MON 94313 will catalyze the conversion of endogenous compounds.

The potential for DMO to metabolize endogenous plant compounds was evaluated previously through *in vitro* experiments in support of MON 87708 [A1063]. A set of potential endogenous substrates was selected for evaluation based on structural similarity of the compounds to dicamba and their presence in cotton, corn, or soybean ([Buchanan et al., 2000](#); [Janas et al., 2000](#); [Lege et](#)

al., 1995; [Schmelz et al.](#), 2003). The potential substrates tested were *o*-anisic acid (2-methoxybenzoic acid), vanillic acid (4-hydroxy-3-methoxybenzoic acid), syringic acid (3,5-dimethoxy-4-hydroxybenzoic acid), ferulic acid [3-(4-hydroxy-3-methoxy-phenyl)prop-2-enoic acid] and sinapic acid [3-(4-hydroxy-3,5-dimethoxyphenyl)prop-2-enoic acid] (Figure 18). The assay mixture included NADH, reductase, ferredoxin and DMO. Dicamba was first used as a positive control to demonstrate that the assay system was functional. The disappearance of potential substrates and the formation of potential oxidation products were monitored using liquid chromatography-ultraviolet (LC-UV) and liquid chromatography-mass spectrometry (LC-MS). None of the tested substrates, except dicamba, were metabolized by the histidine tagged DMO in these *in vitro* experiments.

In order to confirm the specificity of the MON 94313 DMO protein for dicamba, and to demonstrate that the minor differences in amino acid sequences present in the MON 94313 DMO protein relative to the DMO proteins expressed in previous biotechnology-derived crops do not impact the activity or selectivity for dicamba herbicide as compared to potential endogenous substrates, the potential for MON 94313 DMO to catabolize dicamba and *o*-anisic acid was evaluated using the same qualitative assay used to evaluate the selectivity of MON 87708 DMO. *O*-anisic acid was chosen for this confirmatory experiment since it is the most structurally similar to dicamba among the five substrates used in the original study, which included ferulic acid, *o*-anisic acid, sinapic acid, syringic acid, and vanillic acid. The results from this assessment were similar to the previously reported results for MON 87708 DMO in that the DCSA product was observed using dicamba as the substrate whereas no demethylated products were observed with *o*-anisic acid as the substrate, confirming that the MON 94313 DMO did not metabolize *o*-anisic acid. Thus, MON 94313 DMO is active and has a high specificity for dicamba as a substrate.

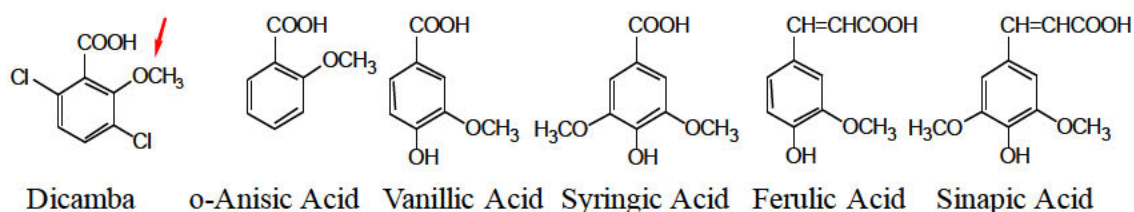


Figure 18. Dicamba and Potential Endogenous Substrates Tested through Previous *In Vitro* Experiments with DMO

The arrow indicates methyl group removed by DMO.

B.1(a)(i)(ii) PAT Protein Expressed in MON 94313

B.1(a)(i)(ii)(i) General description

PAT proteins conferring tolerance to glufosinate herbicide (2-amino-4-(hydroxymethylphosphiny) butanoic acid) have been isolated from two separate species of *Streptomyces*, *S. hygroscopicus* ([Thompson et al.](#), 1987) and *S. viridochromogenes* ([Wohlleben et al.](#), 1988). The PAT protein isolated from *S. hygroscopicus* is encoded by the *bar* gene, and the PAT protein isolated from *S. viridochromogenes* is encoded by the *pat* gene. Both PAT (*bar*) and PAT (*pat*) proteins are comprised of 183 amino acids which share 85% identity at the amino acid level ([Wehrmann et al.](#), 1996). Based on previous studies ([Wehrmann](#)

[et al., 1996](#)) that have extensively characterized PAT proteins produced from both the *bar* and *pat* genes, OECD recognizes both the proteins to be equivalent with regard to function and safety ([OECD, 1999](#)). In addition, the EPA has issued a tolerance exemption for the PAT protein regardless of the encoding gene or crop ([U.S. EPA, 1997](#)). The safety of PAT proteins present in biotechnology-derived crops has been extensively assessed ([Hérouet et al., 2005](#); [ILSI-CERA, 2011](#)), leading to a conclusion that there is a reasonable certainty of no harm resulting from the consumption of PAT proteins in human food or animal feed ([Hérouet et al., 2005](#)).

The PAT protein produced in MON 94313 is from the *pat* gene, and is identical to the wild type PAT (*pat*) protein encoded by *S. viridochromogenes*, except for the first methionine that is removed due to co-translational processing in MON 94313. N-terminal methionine cleavage is common and naturally occurs in the vast majority of proteins ([Meinzel and Gigliione, 2008](#)). The resulting MON 94313-produced PAT protein is a single polypeptide of 182 amino acids that has an apparent molecular weight of 25.5 kDa. The PAT protein in MON 94313 is identical to the PAT protein expressed in several commercially available glufosinate tolerant products.

B.1(a)(i)(ii)(ii) Mode-of-Action

The mode-of-action for PAT protein has been extensively assessed, as numerous glufosinate-tolerant products have been reviewed by the FSANZ (A2704-12 and A5547-127 soybean [A481], MON 87419 [A1118] and MON 87429 [A1192]), including the PAT protein produced in MON 94313, is an enzyme classified as an acetyltransferase that acetylates glufosinate in the presence of acetyl-CoA to form the non-herbicidal compound N-acetyl glufosinate. Glufosinate is a racemic mixture of the D- and L-forms of phosphinothricin. The herbicidal activity of glufosinate results from the binding of L-phosphinothricin to glutamine synthetase ([OECD, 1999](#); [OECD, 2002a](#)). Glutamine synthetase is responsible for the assimilation of ammonia generated during photorespiration. The binding of L-phosphinothricin to glutamine synthetase results in the inactivation of glutamine synthetase and a subsequent toxic build-up of ammonia within the plant, resulting in death of the plant ([Manderscheid and Wild, 1986](#); [OECD, 1999](#); [OECD, 2002a](#); [Wild and Manderscheid, 1984](#)). Thus, expression of the PAT protein in MON 94313 soybean results in the ability to convert L-phosphinothricin to the non-herbicidal N-acetyl-L-phosphinothricin, thus conferring glufosinate resistance to the crop.

B.1(a)(i)(ii)(iii) Specificity

The PAT protein expressed in MON 94313 is highly specific for glufosinate. Enzyme assays have demonstrated that the PAT protein is unable to acetylate other common L-amino acids that are structurally similar to L-phosphinothricin, and substrate competition assays showed no inhibition of glufosinate acetylation in the presence of high concentrations of L-amino acids that are structurally similar to L-phosphinothricin (including the glufosinate analog L-glutamate) ([Wehrmann et al., 1996](#)). Recent metabolic profiling reported some non-specific PAT-mediated acetylation of two amino acids (amino adipate and tryptophan) in senescent leaf extracts from *A. thaliana* and also in PAT-expressing soybean ([Christ et al., 2017](#)). However, the activity level for these two amino acids was very low relative to the activity for glufosinate, indicating that PAT has a very high level of specificity for the herbicidal molecule ([Christ et al., 2017](#)).

B.1(a)(i)(iii) FT_T.1 Protein Expressed in MON 94313**B.1(a)(i)(iii)(i) General description**

The FT_T.1 protein produced in MON 94313 is encoded by the *ft_t.1* gene that provides tolerance to 2,4-D herbicide. FT_T.1 in MON 94313 soybean is a modified version of the FT_T protein present in MON 87429 maize [A1192]. The FT_T protein is itself a modified version of RdpA, an Fe(II)/alpha-ketoglutarate-dependent dioxygenase from the common soil bacterium *Sphingobium herbicidovorans*. FT_T was created through modifications to the RdpA amino acid sequence to improve the enzyme activity towards herbicide substrates, including 2,4-D, and to maintain high activity at temperatures experienced during the hotter summer growing months (Larue *et al.*, 2019). In contrast to conventional maize, which displays some natural tolerance to 2,4-D herbicide, dicots, such as soybeans, are highly sensitive to 2,4-D. Thus, FT_T was further modified to enhance its enzymatic activity towards 2,4-D herbicide. The result was FT_T.1, which provides the 2,4-D tolerance in MON 94313 soybean necessary for in-crop herbicide applications ((Larue *et al.*, 2019); FT_T.1 in this article is referred to as FT_Tv7).

The FT_T.1 protein in MON 94313 soybean differs from the FT_T protein in MON 87429 maize by 3 amino acids, and is >98% identical at the amino acid level. Figure 19 shows the relationship between the original RdpA protein and the modifications introduced to generate FT_T and FT_T.1.

```

1   MHAALTPLTN  KYRFIDVQPL  TGVLGAEITG  VDLREPLDDS  TWNEILDAFH
51  TYQVIYFPGQ  AITNEQHIAF  SRRFGPVDPV  PILKSIEGYP  EVQMIRREAN
101 ESSRYIGDDW  HADSTFLDAP  PAAVVMRAIE  VPEYGGDTGF  LSMYSAWETL
151 SPTMQATIEG  LNVVHSATKV  FGSLYQATNW  RFSNTSVKVM  DVDAGDRETV
201 HPLVVTHPVT  GRRALYCNQV  YCQKIQGMTD  AESKSLLQFL  YEHATQFDFT
251 CRVRWKKDQV  LVWDNLCTMH  RAVPDYAGKF  RYLTRTTVAG  DKPSR

```

Figure 19. Amino Acid Sequence Comparison between FT_T.1, FT_T and RdpA

The amino acid sequence of the MON 94313 FT_T.1 protein is presented. The shaded amino acid residues indicate the three modifications introduced into the FT_T protein to create FT_T.1, which were F105Y, T112A and K246Q, where the first letter denotes the original amino acids followed by the position and the new amino acid. The number counts start from methionine corresponding to start codon. The single underline shows the 30 amino acid substitutions introduced into RdpA to create FT_T. The substitutions are S6T, S9T, Q10N, R11K, F12Y, E13R, R14F, A16D, L82I, G103S, V105F, D130E, H134Y, T145S, R169K, Q178T, R180W, G209V, S210T, K213R, G214A, V217C, R224K, E226Q, P235S, R246K, G289A, V291D, R292K, and A294S.

B.1(a)(i)(iii)(ii) Mode-of-Action

RdpA protein has been characterized as an Fe(II)/alpha-ketoglutarate-dependent dioxygenase (Müller *et al.*, 2006), and given their structural similarity, the FT_T.1 protein is also an Fe(II)/alpha-ketoglutarate-dependent dioxygenase. Fe(II)/alpha-ketoglutarate-dependent dioxygenase belong to a diverse superfamily of Fe(II)/alpha-ketoglutarate dependent hydroxylases that catalyze a range of oxygenation reactions in synthesis and decomposition reactions that include hydroxylation reactions, desaturations, demethylations, ring expansions, ring formations

and other oxidative reactions ([Hausinger, 2004](#)). This protein superfamily is broadly distributed across the plant, animal and bacterial kingdoms, therefore environmental exposure to Fe(II)/alpha-ketoglutarate dependent hydroxylases is ubiquitous. Members of this superfamily share a common double-stranded, beta-helix protein fold with three metal-binding ligands found in a His₁-X-Asp/Glu-X_n-His₂ motif. In oxygenation reactions, alpha-ketoglutarate (α KG) chelates Fe(II) using its C1-carboxylate and C2-ketone. Decarboxylation of α KG results in the formation of succinate and carbon dioxide, which leads to the generation of an Fe(IV)-oxo or other activated oxygen species that subsequently hydroxylate the primary substrate, e.g., quizalofop ([Bugg, 2003](#); [De Carolis and De Luca, 1994](#); [Hausinger, 2004](#)). Thus, the FT_T.1 protein catalyzes the dioxygenase reaction that degrades 2,4-dichlorophenoxyacetic acid (2,4-D), a synthetic auxin herbicide, into herbicidally-inactive 2,4-dichlorophenol (2,4-DCP) and glyoxylic acid in the presence of alpha-ketoglutarate and oxygen (Figure 20). Succinate and carbon dioxide are released as products of this reaction. The safety of 2,4-D and its relevant metabolites have been assessed by US EPA. US EPA concluded that there is a reasonable certainty that no harm will result to the general population, or to infants and children from aggregate exposure to 2,4-D ([U.S. EPA, 2017](#)) residues or their metabolites.

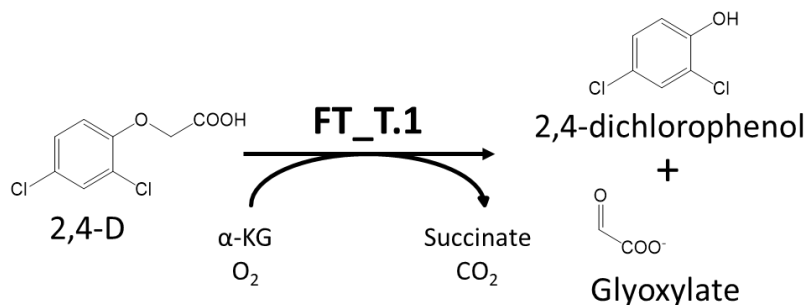


Figure 20. Substrate and Metabolites of FT_T.1 Protein Reaction with 2,4-D

B.1(a)(i)(iii)(iii) Specificity

The amino acid changes introduced into FT_T.1 do not have an impact the substrate specificity of FT_T.1 relative to RdpA or FT_T, and all three proteins are still active on the same herbicide substrate molecules. Like the other two enzymes, FT_T.1 maintains activity on both FOPs and 2,4-D-type herbicides, although FT_T.1 displays higher enzymatic activity for 2,4-D than either enzyme (([Larue et al., 2019](#)), Table 6). As noted, this increase in activity is important as soybean is highly sensitive to 2,4-D, whereas all soybeans are naturally tolerant to FOPs herbicide chemistries. Like the specificity, the integrity and stability of the FT_T.1 protein was not affected by the targeted amino acids changes, as evidenced by the fact that like FT_T, FT_T.1 maintains elevated *in vitro* protein melting temperature compared to the RdpA. The heat stability of these enzymes is important in maintaining herbicide tolerance at the higher seasonal temperatures observed in maize and soybean growing regions (([Larue et al., 2019](#)); Table 6).

Table 6. Comparison of RdpA, FT_T, and FT_T.1 Activity on Different Herbicide Substrates

			RdpA	FT_T	FT_T.1 (FT_Tv7)
Protein melting temp (°C)	Buffer		43	58	57
	Buffer (Fe and α -KG)		53	62	61
FOP	Quizalofop	V_{max}	2.76 (0.11)	1.62 (0.05)	1.53 (0.05)
		K_m	0.09 (0.01)	0.12 (0.01)	0.14 (0.01)
		k_{cat}/K_m	1.04	0.46	0.37
Synthetic auxins	Dichlorprop	V_{max}	5.32 (0.09)	2.09 (0.03)	1.04 (0.01)
		K_m	0.06 (0.004)	0.03 (0.002)	0.03 (0.002)
	2,4-D	V_{max}	0.25 (0.01)	1.17 (0.01)	2.91 (0.04)
		K_m	0.13 (0.02)	0.03 (0.002)	0.07 (0.004)
		k_{cat}/K_m	0.06	1.33	1.42
	MCPA	V_{max}	0.20 (0.01)	1.23 (0.02)	2.93 (0.06)
	Mecoprop	V_{max}	4.11 (0.15)	3.04 (0.07)	1.28 (0.02)

FT_T and FT_T.1 variants and RdpA as a control are characterized for enzyme temperature stability and enzyme kinetics with FOP and synthetic auxin herbicides. Protein melting is recorded as the temperature in which the protein is 50% denatured in buffer alone or with supplemental Fe(II) and α -ketoglutarate (α -KG). Enzyme kinetic parameters are recorded for representative FOP and synthetic auxin herbicides with V_{max} ($\mu\text{mol}/\text{mg}^{-1} \text{min}^{-1}$), K_m (mM) and k_{cat}/K_m ($\text{M}^{-1} \text{min}^{-1}$) shown. The standard error is shown in parenthesis. ND, not determined (Adapted from [Larue et al., 2019](#)). FT_T.1 is called FT_Tv7 in this article).

B.1(a)(i)(iv) TDO Protein Expressed in MON 94313

B.1(a)(i)(iv)(i) General description

MON 94313 soybean expresses triketone dioxygenase (TDO) protein encoded by the *TDO* gene that provides tolerance to mesotrione. *TDO* is a codon-optimized version of the *HPPD INHIBITOR SENSITIVE 1 (HIS1)* gene from rice that has the same amino acid sequence as the HIS1 protein (Figure 21). Mesotrione, a β -triketone herbicide, is an inhibitor of 4-hydroxyphenylpyruvate dioxygenase (HPPD; EC: 1.13.11.27) which catalyzes the first committed step of tyrosine catabolism in plants. Inhibition of HPPD in plants leads to a depletion of key downstream metabolites, most notably tocopherols and plastoquinone. Plastoquinone is critical for the functioning of photosystem II and carotenoid biosynthesis ([Mitchell et al., 2001](#)). Carotenoids and tocopherols are in turn, key molecules in protecting the photosynthetic machinery from oxidative damage. As a result of the reduction in levels of these protective molecules after application of mesotrione to susceptible plants, characteristic bleaching occurs, ultimately leading to plant death. Natural tolerance to β -triketone herbicides in certain *Oryza sativa* (rice) cultivars was determined to be a result of the presence of the HIS1 protein, which includes motifs conserved

in Fe(II)/alpha-ketoglutarate-dependent dioxygenases and was shown to oxidize the mesotrione herbicide molecule (Maeda *et al.*, 2019). Expression of the codon-optimized *TDO* gene in MON 94313 soybean results in soybean plants that are capable of tolerating in-crop applications of mesotrione through oxidation of the mesotrione molecule.

MON 94313 TDO	- ADESWRAPA	IVQELAAAGV	EEPPSRYLLR	EKDRSDVKLV	AAELPEPLPV	VDLSRLDGAE	59
<i>O. sativa</i> HIS1	MADESWRAPA	IVQELAAAGV	EEPPSRYLLR	EKDRSDVKLV	AAELPEPLPV	VDLSRLDGAE	60
MON 94313 TDO	EATKLRVALQ	NWGFFLLTNH	GVEASLMDSV	MNLSREFFNQ	PIERKQKFSN	LIDGKNFQIQ	119
<i>O. sativa</i> HIS1	EATKLRVALQ	NWGFFLLTNH	GVEASLMDSV	MNLSREFFNQ	PIERKQKFSN	LIDGKNFQIQ	120
MON 94313 TDO	GYGTDRVVTQ	DQILDWSDRL	HLRVEPKEEQ	DLAFWPDHPE	SFRDVLNKYA	SGTKRIRDDI	179
<i>O. sativa</i> HIS1	GYGTDRVVTQ	DQILDWSDRL	HLRVEPKEEQ	DLAFWPDHPE	SFRDVLNKYA	SGTKRIRDDI	180
MON 94313 TDO	IQAMAKLLEL	DEDYFLDRLN	EAPAFARFNY	YPPCPRPDLV	FGIRPHSDGT	LLTILLVDKD	239
<i>O. sativa</i> HIS1	IQAMAKLLEL	DEDYFLDRLN	EAPAFARFNY	YPPCPRPDLV	FGIRPHSDGT	LLTILLVDKD	240
MON 94313 TDO	VSGLQVQRDG	KWSNVEATPH	TLLINLGDTM	EVMCNGIFRS	PVHRVVTNAE	KERISLAMLY	299
<i>O. sativa</i> HIS1	VSGLQVQRDG	KWSNVEATPH	TLLINLGDTM	EVMCNGIFRS	PVHRVVTNAE	KERISLAMLY	300
MON 94313 TDO	SVNDEKDI EP	AAGLLDENRP	ARYRKVSVEE	FRAGIFGKFS	RGERYIDSLR	I	350
<i>O. sativa</i> HIS1	SVNDEKDI EP	AAGLLDENRP	ARYRKVSVEE	FRAGIFGKFS	RGERYIDSLR	I	351

Figure 21. Alignment of MON 94313 TDO and *Oryza sativa* HIS1

Alignment of amino acid sequences of TDO from MON 94313 soybean and the HIS1 protein (Os02g0280700) from rice (<https://www.uniprot.org/uniprot/A3A5K1>). TDO and rice HIS1 are identical at the amino acid level, except for the N-terminal M at position 1 which is cleaved in MON 94313 soybean TDO during protein processing in the cytosol.

B.1(a)(i)(iv)(ii) Mode-of-Action

Like other Fe (II)/alpha-ketoglutarate-dependent dioxygenases, TDO uses iron and alpha-ketoglutarate as cofactors in the oxidation of its substrate, producing succinate and the oxidized product. Alpha-ketoglutarate-dependent non-heme iron dioxygenases share a common double-stranded, beta-helix protein fold with three metal-binding ligands found in a His₁-X-Asp/Glu-X_n-His₂ motif. In oxygenation reactions, alpha-ketoglutarate (α KG) chelates Fe(II) using its C-1 carboxylate and C2-ketone. Decarboxylation of α KG results in the formation of succinate and carbon dioxide, which leads to the generation of an Fe(IV)-oxo or other activated oxygen species that subsequently hydroxylate the primary substrate, e.g., mesotrione (Bugg, 2003; De Carolis and De Luca, 1994; Hausinger, 2004). *In vitro* studies of recombinant TDO show that the initial oxidation of mesotrione takes place at the 5'C, yielding 5' hydroxy-mesotrione. A second oxidation, followed by a spontaneous loss of a water molecule, creates oxy-mesotrione (Figure 22). *In vitro* assays demonstrated that hydroxy-mesotrione is less inhibitory to HPPD than mesotrione, and oxy-mesotrione had virtually no impact on the activity of HPPD. Thus, the oxidative capabilities of TDO provide a mechanism by which mesotrione is neutralized and prevented from inhibiting the native soybean HPPD activity.

Studies of soybean expressing the TDO protein show that the plants can tolerate in-crop applications of mesotrione (Dai *et al.*, 2022). Metabolic analysis of soybean leaves expressing TDO demonstrated that tolerance is accomplished through rapid conversion of mesotrione

primarily to hydroxy-mesotrione, hydroxy-xanthone, and downstream glucosyl and malonyl conjugates (oxy-mesotrione is not detected in TDO-expressing soybean, likely due to non-enzymatic cyclization to hydroxy-xanthone). In addition, mesotrione is not translocated from the treated tissues in TDO-expressing soybean, thus preventing inhibition of HPPD in newly developing apex or root tissues. In contrast, apical and root tissues of treated conventional soybean accumulate mesotrione, resulting in the inhibition of HPPD and the bleaching phenotype typical of β -triketone treatments of susceptible plants ([Dai et al., 2022](#)).

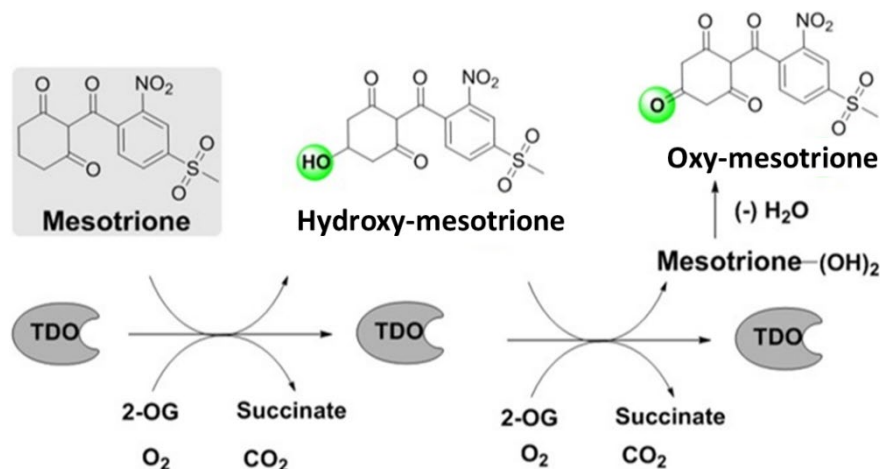


Figure 22. MON 94313 TDO Biochemical Mode of Action

TDO oxidizes mesotrione sequentially, yielding hydroxy-mesotrione in the first round of oxidation, followed by oxy-mesotrione after the second oxidative step and the loss of a water molecule. Hydroxy- and oxy-mesotrione are progressively less inhibitory to HPPD than the parent mesotrione molecule, providing MON 94313 soybean with tolerance to in-crop application of mesotrione. Oxy-mesotrione is not detected in treated leaves, likely due to non-enzymatic conversion to hydroxy-xanthone, which is further metabolized to glucosyl and malonyl conjugates ([Dai et al., 2022](#)) (2-OG = alpha-ketoglutarate).

B.1(a)(i)(iv)(iii) Specificity

To assess the specificity of TDO, an *in silico* screen was conducted to identify potential soybean endogenous molecules that could be substrates for TDO. This consisted of a 2D and 3D screen of the NAPRALERT[®] plant metabolite database, including soybean metabolites, for molecules that met criteria set by a known TDO substrate (mesotrione) and expectations of the mesotrione conformation in the TDO active site. A schematic of the *in silico* screening approach is shown in Figure 23. 59 plant metabolites from the database were identified as highest probability of being a substrate for TDO. Commercially available candidate compounds identified in the plant metabolite database (a total of 32 molecules), the positive control (mesotrione) and other potential HPPD herbicide substrates were tested *in vitro* to assess the specificity of the TDO protein. The results showed that TDO had no significant activity with any of the putative plant substrates, but was specific to the β -triketone class of HPPD herbicide compounds (e.g. mesotrione, tembotrione, and sulcotrione) (Table 7).

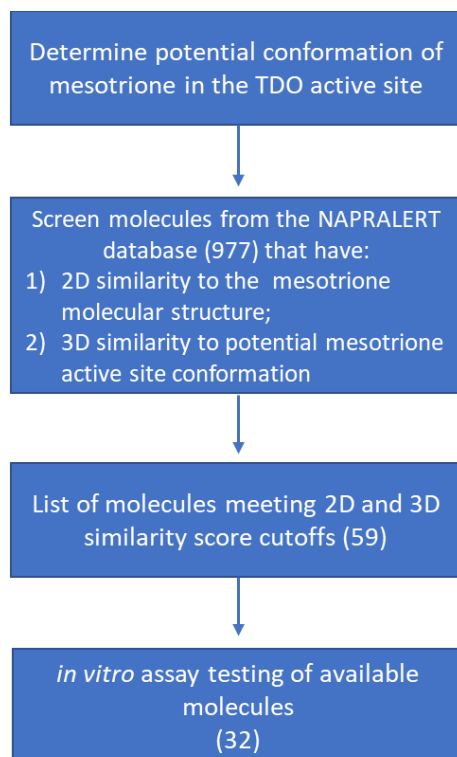


Figure 23. *In silico* and *In vitro* Protocol for TDO Endogenous Substrate Specificity Screen

Overview of the screening and testing scheme to identify putative endogenous plant small molecules that could act as substrates for the TDO enzyme.

Table 7. Results of *in vitro* TDO Assays with Available Plant Metabolites Identified in the *in silico* Screen

PubChem ID	PubChem Common Name/ IUPAC Name	Mean ^a	Estimate ^b	StdErr	p-value ^c	Sig ^d
176907	Dihydrodaidzein	-0.000064333	0.2974	0.5124	0.577	
5281254	Hispidol	-0.000017889	-1.1079	0.5124	0.0612	
86223063	Chitinase-IN-1	-0.000039778	-0.07912	0.1096	0.48	
25200808	Indole-3-acetyl-glutamate(2-)	-0.000034556	-0.211	0.1096	0.0708	
6436348	Germacrone	-0.000042889	0.004319	0.1096	0.969	
5317750	Glycitein	-0.000114889	0.5093	0.5124	0.3483	
5280373	Biochanin A	-0.000045167	0.08054	0.1245	0.5262	
6781	Diethyl phthalate	-0.000041222	-0.03704	0.1096	0.7395	
74706	Indole-3-acetic acid	-0.000036	-0.1721	0.1096	0.1345	
84098	Isoxaflutole	-0.000062889	0.1877	0.5124	0.7232	
62428	Ethyl 1-naphthaleneacetate	-0.000042444	-0.0066	0.1096	0.9527	
	DMSO	-0.000043111				
	Mesotrione	-0.000158889	1.2798	0.1096	<.0001	*
3080590	Oxindole-3-acetic acid	-0.000026	0.1013	0.2944	0.7337	
4947	Propyl gallate	-0.000028444	0.2025	0.2944	0.4978	
5281576	Zearalenone	-0.000035778	0.2464	0.2944	0.4106	
896	Melatonin	-0.000019111	-0.1913	0.2944	0.5218	
8554	Dimethyl phthalate	-0.000023667	-0.04499	0.2944	0.8798	
5870	Estrone	-0.000027567	0.173	0.2944	0.562	
5281708	Daidzein	-0.000042222	0.5873	0.2944	0.0571	
5281707	Coumestrol	-0.000023167	-0.0012	0.3324	0.9972	
5280460	Scopoletin	-0.000023333	0.02116	0.2944	0.9433	
5280961	Genistein	-0.000028667	0.2146	0.2944	0.4729	
13067	1H-Indole-3-acetic acid, ethyl ester	-0.000021111	-0.08247	0.2944	0.7817	
	DMSO	-0.000023778				
	Mesotrione	-0.000127444	1.7007	0.2944	<.0001	*
92383	Pyrazoxyfen	-0.000044667	0.1917	0.1298	0.1509	

PART 2: SPECIFIC DATA REQUIREMENTS FOR SAFETY ASSESSMENT

PubChem ID	PubChem Common Name/ IUPAC Name	Mean ^a	Estimate ^b	StdErr	p-value ^c	Sig ^d
11556911	Tembotrione	-0.000131111	1.2794	0.1298	<.0001	*
91760	Sulcotrione	-0.000124444	1.2287	0.1298	<.0001	*
932	Naringenin	-0.000033667	-0.08098	0.1298	0.5377	
6985	2',4'-Dimethylacetophenone	-0.000036556	0.006742	0.1298	0.9589	
441140	Griseofulvin	-0.000040333	0.1025	0.1298	0.4365	
730037	Indole-3-(4'-oxo)butyric acid	-0.000040333	0.09884	0.1298	0.4527	
170551	Lacinilene C	-0.000032778	-0.1043	0.1298	0.4282	
5280385	Sinapine	-0.000036	-0.01244	0.1298	0.9243	
11302979	Topramezone	-0.000031111	-0.1869	0.1298	0.1609	
	DMSO	-0.000036333				
	Mesotrione	-0.000147778	1.4006	0.1298	<.0001	*
493570	Riboflavin	-8.74997E-05	-0.03105	0.03589	0.8039	
5280378	Formononetin	-0.000085395	-0.04679	0.03589	0.9001	
8441	Dimethyl terephthalate	-8.73703E-05	-0.02213	0.03589	0.7295	
5281704	7-hydroxy-6-methoxy-3-(4-methoxyphenyl)-4H-chromen-4-one	-0.000083938	-0.0672	0.03589	0.9657	
86223064	Chitinase-IN-2	-8.61973E-05	-0.04682	0.03589	0.9002	
	DMSO	-8.98513E-05				
	Mesotrione	-0.000394938	1.3657	0.08844	<.0001	*

Enzymatic activity assays were conducted for each potential plant metabolite and six HPPD inhibitor herbicidal molecules (mesotrione, isoxaflutole, pyrazoxyfen, tembotrione, sulcotrione, and topramezone). The table represents four different sets of data, each containing a mesotrione positive control (shaded in green) and a dimethyl sulfoxide (DMSO) negative control.

^aMean data represents the average change in absorbance of the assays for that molecule.

^bThe estimate is the difference in absorbance change between the test compound and the DMSO control (log transformed).

^cStatistical analysis was conducted for each molecule to determine if the response was significantly different than the negative control.

^dStatistical significance was based on a p value score <0.05.

B.1(a)(ii) Characterisation of the DMO, PAT, FT_T.1 and TDO Proteins**B.1(a)(ii)(i) Characterisation of the MON 94313 DMO protein**

The safety assessment of crops derived through biotechnology includes characterisation of the physicochemical and functional properties of and confirmation of the safety of the introduced protein(s). For the safety data generated using *E. coli*-produced MON 94313 DMO to be applied to MON 94313 DMO protein (plant-produced DMO), the equivalence of the plant- and *E. coli*-produced proteins must first be demonstrated. To assess the equivalence between MON 94313-produced DMO and *E. coli*-produced MON 94313 DMO proteins, a small quantity of the MON 94313 DMO protein was purified from seed of MON 94313. The MON 94313-produced DMO protein was characterized and the equivalence of the physicochemical characteristics and functional activity between the MON 94313-produced DMO and the *E. coli*-produced MON 94313 DMO proteins was assessed using a panel of six analytical tests as shown in Table 8. Taken together, these data provide a detailed characterisation of the MON 94313-produced DMO protein and establish the equivalence of MON 94313-produced DMO and *E. coli*-produced MON 94313 DMO proteins.

For details, please refer to Appendix 6.

Table 8. Summary of MON 94313 DMO Protein Identity and Equivalence

Analytical Test Assessment	Analytical Test Outcome
1. N-terminal sequence	<ul style="list-style-type: none"> The N-terminal sequences for MON 94313-produced DMO protein was observed by Nono LC-MS/MS¹
2. Nano LC-MS/MS ¹	<ul style="list-style-type: none"> Nano LC-MS/MS¹ analysis yielded peptide masses consistent with the peptide masses from the theoretical trypsin digest of the MON 94313-produced DMO sequence
3. Western blot analysis	<ul style="list-style-type: none"> MON 94313-produced DMO protein identity was confirmed using a western blot probed with an antibody specific for DMO protein Immunoreactive properties of the MON 94313-produced DMO and the <i>E. coli</i>-produced DMO proteins were shown to be equivalent
4. Apparent molecular weight (MW)	<ul style="list-style-type: none"> Electrophoretic mobility and apparent molecular weight of the MON 94313-produced DMO and the <i>E. coli</i>-produced DMO proteins were shown to be equivalent
5. Glycosylation analysis	<ul style="list-style-type: none"> MON 94313-produced DMO and the <i>E. coli</i>-produced DMO proteins were not glycosylated and were shown to be equivalent
6. Functional activity	<ul style="list-style-type: none"> Functional activity of the MON 94313-produced DMO and the <i>E. coli</i>-produced DMO proteins were shown to be equivalent

¹ Nano LC-MS/MS = Nanoscale liquid chromatography coupled to tandem mass spectrometry

B.1(a)(ii)(i)(i) Results of the N-terminal sequencing analysis

The expected N-terminal sequence for the DMO protein deduced from the *dmo* gene present in MON 94313 was observed by LC-MS/MS. The N-terminal sequence for MON 94313-produced DMO protein was consistent with the N-terminal sequence for the *E. coli*-produced DMO protein observed by LC-MS/MS (Figure 24). Hence, the sequence information confirms the identity of the DMO protein isolated from the seed of MON 94313.

Amino Acids Residue # from the N-terminus	→	1	2	3	4	5	6	7	8	9	10	11	12	13	14	15
<i>E. coli</i> -produced DMO sequence	→	M	L	T	F	V	R	N	A	W	Y	V	A	A	L	P
Expected DMO Sequence	→	M	L	T	F	V	R	N	A	W	Y	V	A	A	L	P
MON 94313 Experimental Sequence	→	M	L	T	F	V	R	N	A	W	Y	V	A	A	L	P

Figure 24. N-terminal Sequence of the MON 94313-Produced DMO Protein

The experimental sequence obtained from the MON 94313 produced DMO was compared to the expected sequence deduced from the *dmo* gene present in MON 94313. The N-terminal sequence of the *E. coli*-produced MON 94313 DMO protein was also obtained by Nano LC-MS/MS peptide analysis. The single letter International Union of Pure and Applied Chemistry International Union of Biochemistry (IUPAC-IUB) amino acid code is M, methionine; L, leucine; T, threonine; F, phenylalanine; V, valine; R, arginine; N, asparagine; A, alanine; W, tryptophan; Y, tyrosine; P, proline.

B.1(a)(ii)(i)(ii) Results of nano LC-MS/MS mass fingerprint analysis

Peptide mass fingerprint analysis is a standard technique used for confirming the identity of proteins. The ability to identify a protein using this method is dependent upon matching a sufficient number of observed tryptic peptide fragment masses with predicted tryptic peptide fragment masses. In general, protein identification made by peptide mapping is considered to be reliable if >40% of the protein sequence was identified by matching experimental masses observed for the tryptic peptide fragments to the expected masses for the fragments ([Biron et al., 2006](#); [Krause et al., 1999](#)). The identity of the MON 94313-produced DMO protein was confirmed by LC-MS/MS analysis of peptide fragments produced by the trypsin digestion of the MON 94313-produced DMO protein.

There were 37 unique peptides identified that corresponded to the masses expected to be produced by trypsin digestion of the MON 94313-produced DMO protein (

Table 9). The identified masses were used to assemble a coverage map of the MON 94313-produced DMO protein (Figure 25). The experimentally determined coverage of the MON 94313-produced DMO substance was 85% (291 out of 340 amino acids, Figure 25A). This analysis further confirms the identity of MON 94313-produced DMO protein.

There were 38 unique peptides identified that corresponded to the masses expected to be produced by trypsin digestion of the *E. coli*-produced DMO protein (Table 10). The identified masses were used to assemble a coverage map of the *E. coli*-produced DMO protein (Figure 25). The experimentally determined coverage of the *E. coli*-produced DMO protein was 85% (291 out of 340 amino acids, Figure 25B). This analysis further confirms the identity of the *E. coli*-produced DMO protein.

Table 9. Summary of the Tryptic Masses Identified for the MON 94313-Produced DMO Using Nano LC-MS/MS¹

Experimental Mass ²	Calculated Mass ³	Difference ⁴	Fragment ⁵	Sequence ⁶
765.4193	765.4207	-0.0014	1 - 6	MLTFVR
2905.5163	2905.5160	0.0003	1 - 25	MLTF...PLGR
634.3800	634.3802	-0.0002	2 - 6	LTFVR
2142.1100	2142.1109	-0.0009	7 - 25	NAWY...PLGR
1274.7236	1274.7234	0.0002	26 - 36	TILD...ALYR
1759.9027	1759.9039	-0.0012	37 - 52	QPDG...CPHR
832.4451	832.4443	0.0008	99 - 105	SFPVVER
2722.3248	2722.3214	0.0034	106 - 130	DALI...FGCR
3423.6557	3423.6710	-0.0153	106 - 136	DALI...PAYR
719.3598	719.3602	-0.0004	131 - 136	VDPAYR
1468.6408	1468.6405	0.0003	137 - 149	TVGG...CNYK
1993.0198	1993.0204	-0.0006	150 - 166	LLVD...YVHR
1107.4964	1107.4945	0.0019	167 - 176	ANAQ...AFDR
1505.7247	1505.7222	0.0025	167 - 179	ANAQ...RLER
1516.7807	1516.7807	0.0000	180 - 193	EVIV...ALMK
2668.4141	2668.4180	-0.0039	180 - 205	EVIV...LMAK
1169.6478	1169.6478	0.0000	194 - 205	IPGG...LMAK
1585.9006	1585.9014	-0.0008	194 - 208	IPGG...KFLR
1843.9376	1843.9329	0.0047	206 - 221	FLRG...NDIR
1427.6819	1427.6793	0.0026	209 - 221	GANT...NDIR
2188.1381	2188.1350	0.0031	222 - 241	WNKV...GTPK
1759.9179	1759.9178	0.0001	225 - 241	VSAM...GTPK
2581.3259	2581.3322	-0.0063	225 - 248	VSAM...IHSR
855.4205	855.4199	0.0006	242 - 248	EQSIHSR
2396.0885	2396.0856	0.0029	249 - 269	GTHI...GSSR
1592.7154	1592.7141	0.0013	270 - 283	NFGI...GVLR
2604.2629	2604.2642	-0.0013	270 - 292	NFGI...ALVK
1029.5627	1029.5607	0.0020	284 - 292	SWQA...ALVK
1401.7242	1401.7252	-0.0010	284 - 295	SWQA...KEDK
2297.2371	2297.2379	-0.0008	284 - 303	SWQA...AIER
1285.6874	1285.6878	-0.0004	293 - 303	EDKV...AIER
913.5243	913.5233	0.0010	296 - 303	VVVEAIER
1225.7244	1225.7255	-0.0011	296 - 305	VVVE...ERRR
2308.1046	2308.0940	0.0106	306 - 326	AYVE...AAVR
517.2734	517.2748	-0.0014	330 - 333	EIEK
1271.6609	1271.6608	0.0001	330 - 340	EIEK...LEAA
772.3953	772.3967	-0.0014	334 - 340	LEQLEAA

PART 2: SPECIFIC DATA REQUIREMENTS FOR SAFETY ASSESSMENT

¹ All imported values were rounded to four decimal places.

² Only experimental masses that matched calculated masses with the highest scores are listed in the table.

³ The calculated mass is the exact molecular mass calculated from the matched peptide sequence.

⁴ The calculated difference = experimental mass – calculated mass.

⁵ Position refers to amino acid residues within the predicted MON 94313-produced DMO sequence.

⁶ For peptide matches greater than nine amino acids in length, the first four residues and last four residues are shown separated by three dots (...).

Table 10. Summary of the Tryptic Masses Identified for *E. coli*-Produced DMO Protein Using Nano LC-MS/MS¹

Experimental Mass ²	Calculated Mass ³	Difference ⁴	Fragment ⁵	Sequence ⁶
765.4205	765.4207	-0.0002	1 - 6	MLTFVR
634.3786	634.3802	-0.0016	2 - 6	LTFVR
2142.1131	2142.1109	0.0022	7 - 25	NAWY...PLGR
1274.7241	1274.7234	0.0007	26 - 36	TILD...ALYR
3016.6223	3016.6168	0.0055	26 - 52	TILD...CPHR
1759.9035	1759.9039	-0.0004	37 - 52	QPDG...CPHR
832.4438	832.4443	-0.0005	99 - 105	SFPVVER
3536.7526	3536.7551	-0.0025	99 - 130	SFPV...FGCR
2722.3228	2722.3214	0.0014	106 - 130	DALI...FGCR
3423.6623	3423.6710	-0.0087	106 - 136	DALI...PAYR
719.3601	719.3602	-0.0001	131 - 136	VDPAYR
1468.6395	1468.6405	-0.0010	137 - 149	TVGG...CNYK
1993.0232	1993.0204	0.0028	150 - 166	LLVD...YVHR
1107.4967	1107.4945	0.0022	167 - 176	ANAQ...AFDR
1505.7205	1505.7222	-0.0017	167 - 179	ANAQ...RLER
1899.0141	1899.0135	0.0006	177 - 193	LERE...ALMK
1500.7859	1500.7858	0.0001	180 - 193	EVIV...ALMK
2652.4235	2652.4230	0.0005	180 - 205	EVIV...LMAK
1169.6483	1169.6478	0.0005	194 - 205	IPGG...LMAK
1585.9023	1585.9014	0.0009	194 - 208	IPGG...KFLR
1427.6803	1427.6793	0.0010	209 - 221	GANT...NDIR
2172.1395	2172.1401	-0.0006	222 - 241	WNKV...GTPK
1743.9286	1743.9229	0.0057	225 - 241	VSAM...GTPK
2581.3342	2581.3322	0.0020	225 - 248	VSAM...IHSR
855.4197	855.4199	-0.0002	242 - 248	EQSIHSR
2396.0863	2396.0856	0.0007	249 - 269	GTHI...GSSR
1576.7186	1576.7192	-0.0006	270 - 283	NFGL...GVLR
1029.5608	1029.5607	0.0001	284 - 292	SWQA...ALVK
1401.7241	1401.7252	-0.0011	284 - 295	SWQA...KEDK
2297.2410	2297.2379	0.0031	284 - 303	SWQA...AIER
1285.6883	1285.6878	0.0005	293 - 303	EDKV...AIER
1441.7888	1441.7889	-0.0001	293 - 304	EDKV...IERR
913.5237	913.5233	0.0004	296 - 303	VVVEAIER
1069.6249	1069.6244	0.0005	296 - 304	VVVE...IERR
2448.2019	2448.2002	0.0017	305 - 326	RAYV...AAVR
2292.0992	2292.0990	0.0002	306 - 326	AYVE...AAVR
1271.6604	1271.6608	-0.0004	330 - 340	EIEK...LEAA
772.3973	772.3967	0.0006	334 - 340	LEQLEAA

PART 2: SPECIFIC DATA REQUIREMENTS FOR SAFETY ASSESSMENT

¹All imported values were rounded to 4 decimal places.

²Only experimental masses that matched calculated masses with the highest scores (Mascot ion score) are listed in the table.

³The calculated mass is the exact molecular mass calculated from the matched peptide sequence.

⁴The calculated difference = experimental mass – calculated mass.

⁵Position refers to amino acid residues within the predicted *E. coli*-produced DMO sequence.

⁶For peptide matching greater than nine amino acids in length, the first 4 residues and last 4 residues are shown separated by three dots (...).

(A)

1 MLTFVRNAWY VAALPEELSE KPLGRTILDT PLALYRQPDG VVAALLDICE
 51 HRFAPLSDGI LVNGHLQCPY HGLEFDGGGQ CVHNPHGNGA RPASLNVRSE
 101 PVVERDALIW IWPGDPALAD PGAIPDFGCR VDPAYRTVGG YGHVDCNYKL
 151 LVDNLMDLGH AQYVHRANAQ TDAFDRLERE VIVGDGEIQA LMKIPGGTSP
 201 VLMAKFLRGA NTPVDAWNDI RWNKVSAMLN FIAVAPEGTP KEQSIHSRGT
 251 HILTPETEAS CHYFFGSSRN FGIDPEMDG VLRWQAQAL VKEDKVVVEA
 301 IERRRAYVEA NGIRPAMLSC DEAAVRVSR E IEKLEQLEAA

(B)

1 MLTFVRNAWY VAALPEELSE KPLGRTILDT PLALYRQPDG VVAALLDICE
 51 HRFAPLSDGI LVNGHLQCPY HGLEFDGGGQ CVHNPHGNGA RPASLNVRSE
 101 PVVERDALIW IWPGDPALAD PGAIPDFGCR VDPAYRTVGG YGHVDCNYKL
 151 LVDNLMDLGH AQYVHRANAQ TDAFDRLERE VIVGDGEIQA LMKIPGGTSP
 201 VLMAKFLRGA NTPVDAWNDI RWNKVSAMLN FIAVAPEGTP KEQSIHSRGT
 251 HILTPETEAS CHYFFGSSRN FGIDPEMDG VLRWQAQAL VKEDKVVVEA
 301 IERRRAYVEA NGIRPAMLSC DEAAVRVSR E IEKLEQLEAA

Figure 25. Peptide Map of the MON 94313-Produced DMO and *E. coli*-Produced DMO

(A) The amino acid sequence of the MON 94313-produced DMO protein was deduced from the *dmo* gene present in MON 94313. Boxed regions correspond to peptides that were identified from the MON 94313-produced DMO protein sample using Nano LC-MS/MS. In total, 85% coverage (291 out of 340 amino acids) of the expected protein sequence was covered by the identified peptides.

(B) The amino acid sequence of the *E. coli*-produced DMO protein was deduced from the *dmo* gene that is contained on the expression plasmid. Boxed regions correspond to peptides that were identified from the *E. coli*-produced DMO protein sample using Nano LC-MS/MS. In total, 85% (291 out of 340 amino acids) of the expected protein sequence was identified.

B.1(a)(ii)(i)(iii) Results of western blot analysis of the DMO protein isolated from the grain of MON 94313 and immunoreactivity comparison to *Bt*-produced DMO

Western blot analysis was conducted using a mouse anti-DMO monoclonal antibody as additional means to confirm the identity of the DMO protein isolated from the seed of MON 94313 and to assess the equivalence of the immunoreactivity of the MON 94313-produced and *E. coli*-produced DMO proteins.

The results showed that immunoreactive bands with the same electrophoretic mobility were present in all lanes loaded with the MON 94313-produced and *E. coli*-produced DMO proteins (Figure 26). For each amount loaded, comparable signal intensity was observed between the MON 94313-produced and *E. coli*-produced DMO protein bands. As expected, the signal intensity increased with increasing load amounts of the MON 94313-produced and *E. coli*-produced DMO proteins, thus supporting identification of MON 94313-produced DMO protein.

To compare the immunoreactivity of the MON 94313-produced and *E. coli*-produced DMO proteins, densitometric analysis was conducted on the bands that migrated at the expected apparent MW for DMO proteins (~ 35.6 kDa). The signal intensity (reported in OD) of the band of interest in lanes loaded with MON 94313-produced and *E. coli*-produced DMO proteins was measured (Table 11). Because the mean signal intensity of the MON 94313-produced DMO protein was within $\pm 35\%$ of the mean signal intensity of the *E. coli*-produced DMO protein, the MON 94313-produced DMO and *E. coli*-produced DMO proteins were determined to have equivalent immunoreactivity.

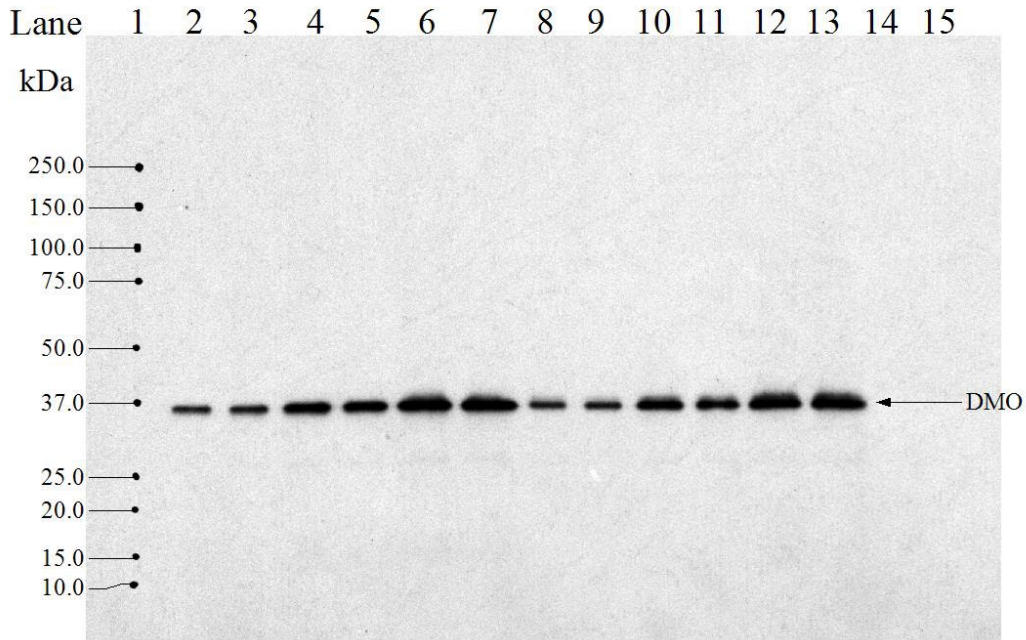


Figure 26. Western Blot Analysis of MON 94313-Produced and *E. coli*-Produced DMO Proteins

Aliquots of the MON 94313-produced DMO protein and the *E. coli*-produced DMO protein were subjected to SDS-PAGE and electrotransferred to a nitrocellulose membrane. Proteins were detected using mouse anti-DMO monoclonal antibody and then horse anti-mouse polyclonal antibody conjugated with peroxidase. Immunoreactive bands were visualized using an ECL system. The approximate MW (kDa) of the standards are shown on the left. The 30 second image is shown. Lane designations are as follows:

<u>Lane</u>	<u>Sample</u>	<u>Amount (ng)</u>
1	Precision Plus Protein™ Standards	-
2	<i>E. coli</i> -produced DMO	1.0
3	<i>E. coli</i> -produced DMO	1.0
4	<i>E. coli</i> -produced DMO	2.5
5	<i>E. coli</i> -produced DMO	2.5
6	<i>E. coli</i> -produced DMO	5.0
7	<i>E. coli</i> -produced DMO	5.0
8	MON 94313-produced DMO	1.0
9	MON 94313-produced DMO	1.0
10	MON 94313-produced DMO	2.5
11	MON 94313-produced DMO	2.5
12	MON 94313-produced DMO	5.0
13	MON 94313-produced DMO	5.0
14	Blank	-

Table 11. Immunoreactivity of the MON 94313-Produced DMO Protein and *E. coli*-Produced DMO Protein

Mean Signal Intensity from MON 94313-Produced DMO ¹ (OD)	Mean Signal Intensity from <i>E. coli</i> -Produced DMO ¹ (OD)	Acceptance Limits ² (OD)
3,405.15	3,691.79	2399.66 – 4983.92

¹ Each value represents the mean of six values (n = 6).

² The acceptance limits are for the MON 94313-produced DMO protein and are based on the interval between -35% ($3691.79 \times 0.65 = 2399.66$) and +35 % ($3691.79 \times 1.35 = 4983.92$) of the mean of the *E. coli*-produced DMO signal intensity across all loads.

B.1(a)(ii)(i)(iv) Results of the DMO protein molecular weight and purity analysis

For apparent MW and purity determination, the MON 94313-produced DMO and the *E. coli*-produced DMO proteins were subjected to SDS-PAGE. Following electrophoresis, the gel was stained with Brilliant Blue G-Colloidal stain and analyzed by densitometry. The MON 94313-produced DMO protein (Figure 27, lanes 3-8) migrated to the same position on the gel as the *E. coli*-produced DMO protein (Figure 27, lane 2) and the apparent MW was calculated to be 35.6 kDa (Table 12). Because the experimentally determined apparent MW of the MON 94313-produced DMO protein was within the acceptance limits for equivalence (Table 13), the MON 94313-produced and *E. coli*-produced DMO proteins were determined to have equivalent apparent molecular weights.

The purity of the MON 94313-produced DMO protein was calculated based on the six lanes loaded on the gel (Figure 27, lanes 3-8). The average purity was determined to be 93% (Table 12).

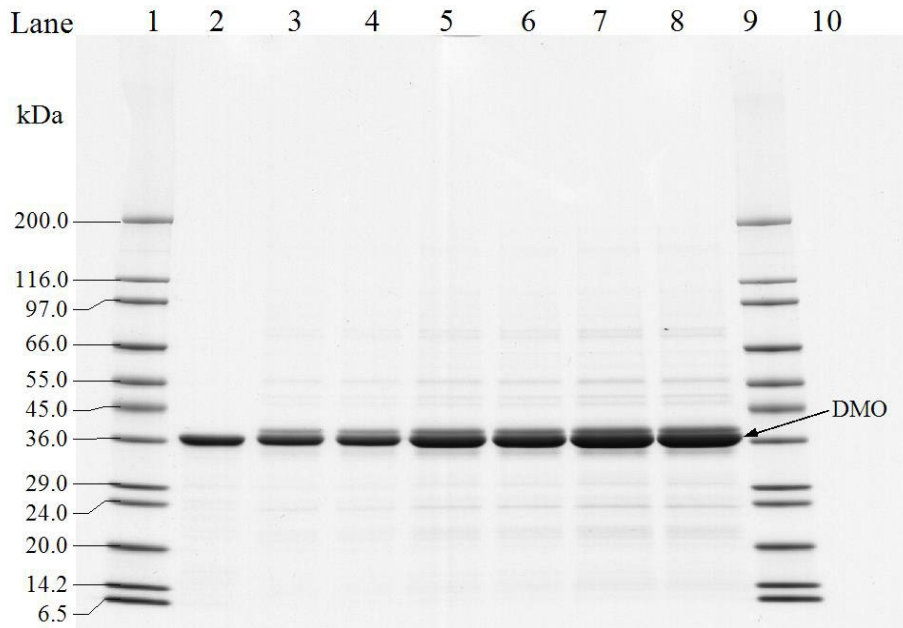


Figure 27. Purity and Apparent Molecular Weight Analysis of the MON 94313-Produced DMO Protein

Aliquots of the *E. coli*-produced and the MON 94313-produced DMO proteins were subjected to SDS-PAGE and the gel was stained with Brilliant Blue G-Colloidal stain. The MWs (kDa) are shown on the left and correspond to the standards loaded in lanes 1 and 9. The DMO protein is indicated with an arrow in the image. Lane designations are as follows:

<u>Lane</u>	<u>Sample</u>	<u>Amount (µg)</u>
1	SigmaMarker™ MW Standard	-
2	<i>E. coli</i> -produced DMO	1.0
3	MON 94313-produced DMO	1.0
4	MON 94313-produced DMO	1.0
5	MON 94313-produced DMO	2.0
6	MON 94313-produced DMO	2.0
7	MON 94313-produced DMO	3.0
8	MON 94313-produced DMO	3.0
9	SigmaMarker™ MW Standard	-
10	Blank	

Table 12. Apparent Molecular Weight and Purity Analysis of the MON 94313-Produced DMO Protein

	Apparent MW ¹ (kDa)	Purity ² (%)
Average (n=6)	35.6	93

¹Final MW was rounded to one decimal place.

²Average % purity was rounded to the nearest whole number.

Table 13. Apparent Molecular Weight Comparison Between the MON 94313-Produced DMO and *E. coli*-Produced DMO Proteins

Apparent MW of MON 94313-Produced DMO Protein (kDa) ¹	Apparent MW of <i>E. coli</i> -Produced DMO Protein (kDa)	Acceptance Limits ² (kDa)
35.6	35.6	34.7 – 36.5

¹ Value refers to mean calculated based on n=6.

²Data obtained for the *E. coli*-produced DMO protein was used to generate the prediction interval (Appendix 6).

B.1(a)(ii)(i)(v) DMO glycosylation analysis

Eukaryotic proteins can be post-translationally modified with carbohydrate moieties ([Rademacher et al., 1988](#)). To test whether the MON 94313 DMO protein was glycosylated when expressed in the seed of MON 94313, the MON 94313-produced DMO protein was analyzed using an ECL™ glycoprotein detection method. To assess equivalence of the MON 94313-produced to *E. coli*-produced DMO proteins, the *E. coli*-produced DMO protein was also analyzed.

A clear glycosylation signal was observed at the expected molecular weight (~80 kDa) in the lanes containing the positive control (transferrin) and the band intensity increased with increasing concentration (Figure 28A). In contrast, no glycosylation signal was observed in the lanes containing the *E. coli*-produced DMO protein or MON 94313-produced DMO protein (Figure 28A).

To confirm that MON 94313-produced DMO and *E. coli*-produced DMO proteins were appropriately loaded for glycosylation analysis, a second membrane with identical loadings and transfer time was stained with Coomassie Blue R-250 for protein detection. Both the MON 94313-produced and *E. coli*-produced DMO proteins were detected (Figure 28B). These data indicate that the glycosylation status of MON 94313-produced DMO protein is equivalent to that of the *E. coli*-produced DMO protein and that neither is glycosylated.

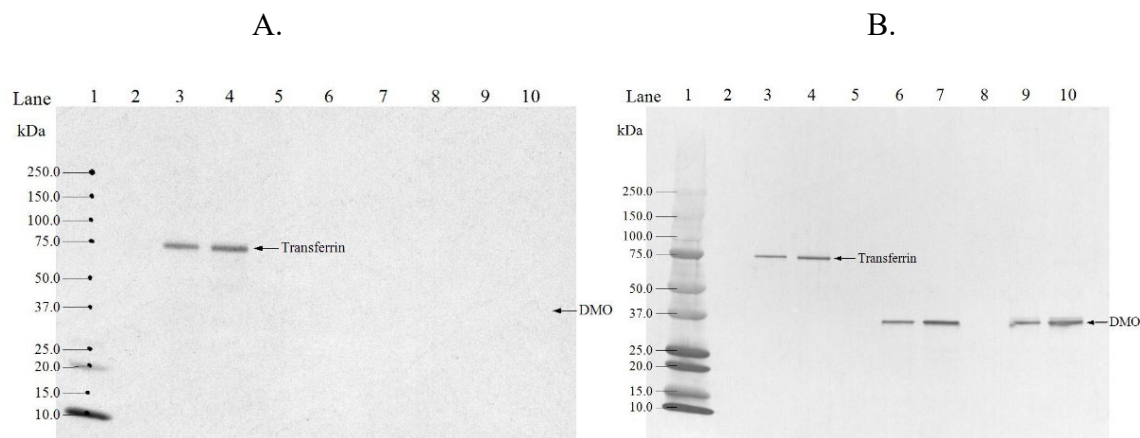


Figure 28. Glycosylation Analysis of the MON 94313-Produced DMO Protein and *E. coli*-Produced DMO Protein

Aliquots of the transferrin (positive control), *E. coli*-produced DMO and MON 94313-produced DMO were subjected to SDS-PAGE and electrotransferred to a PVDF membrane. The MWs (kDa) correspond to the Precision Plus Protein™ Standards. The arrows show the expected migration of the MON 94313-produced and *E. coli*-produced DMO proteins and transferrin. (A) Where present, the labeled carbohydrate moieties were detected by addition of streptavidin conjugated to HRP followed by a luminol-based the detection using ECL reagents. The 2 minute exposure is shown. (B) An equivalent blot was stained with Coomassie Blue R250 to confirm the presence of proteins. Lane designations are as follows:

<u>Lane</u>	<u>Sample</u>	<u>Amount (ng)</u>
1	Precision Plus Protein™ Standards	-
2	Blank	-
3	Transferrin (positive control)	100
4	Transferrin (positive control)	200
5	Blank	-
6	<i>E. coli</i> -produced DMO	100
7	<i>E. coli</i> -produced DMO	200
8	Blank	-
9	MON 94313-produced DMO	100
10	MON 94313-produced DMO	200

B.1(a)(ii)(i)(vi) DMO functional activity

The functional activity of the MON 94313-produced DMO and *E. coli*-produced DMO proteins was determined by measuring the amount of dicamba that was converted to DSCA via HPLC separation and fluorescence detection. In this assay, activity is expressed as specific activity and reported as $\text{nmol} \times \text{minute}^{-1} \times \text{mg}^{-1}$. The MON 94313-produced DMO and *E. coli*-produced DMO proteins were considered functionally equivalent if the specific activity of both were within acceptance limits of 80.0 to 347.4 (the prediction interval calculated from data obtained for the *E. coli*-produced DMO protein activity, Appendix 6).

The specific activity of the MON 94313-produced and *E. coli*-produced DMO proteins were determined to be 202.5 and 255.7 $\text{nmol} \times \text{minute}^{-1} \times \text{mg}^{-1}$ respectively (Table 14). Because the specific activity of MON 94313-produced and *E. coli*-produced DMO proteins were within the acceptance limits, the proteins were determined to have equivalent functional activity.

Table 14. Functional Activity Comparison of MON 94313-Produced DMO and *E. coli*-Produced DMO Proteins

MON 94313-Produced DMO¹ ($\text{nmol} \times \text{minute}^{-1} \times \text{mg}^{-1}$)	<i>E. coli</i>-Produced DMO¹ ($\text{nmol} \times \text{minute}^{-1} \times \text{mg}^{-1}$)	Acceptance Limits² ($\text{nmol} \times \text{minute}^{-1} \times \text{mg}^{-1}$)
202.5	255.7	80.0 – 347.4

¹ Value refers to mean calculated based on $n = 5$.

² Data obtained for the *E. coli*-produced DMO was used to generate a prediction interval for setting the acceptance limits (Appendix 6).

B.1(a)(ii)(i)(vii) MON 94313 DMO protein identity and equivalence conclusion

The MON 94313-produced DMO protein purified from MON 94313 seed was characterized, and a comparison of the physicochemical and functional properties between the MON 94313-produced and the *E. coli*-produced DMO proteins was conducted following a panel of analytical tests: 1) the N-terminal sequence of the MON 94313-produced DMO protein was confirmed by Nano LC-MS/MS analysis; 2) Nano LC-MS/MS analysis yielded peptide masses consistent with the expected peptide masses from the theoretical trypsin digest of the *dmo* gene product present in MON 94313; 3) the MON 94313-produced and the *E. coli*-produced DMO proteins were both detected on a western blot probed with antibodies specific for DMO protein and the immunoreactive properties of both proteins was shown to be equivalent; 4) the electrophoretic mobility and apparent molecular weight of the MON 94313-produced and *E. coli*-produced DMO proteins were shown to be equivalent; 5) the glycosylation status of MON 94313-produced and *E. coli*-produced DMO proteins was determined to be equivalent and neither to be glycosylated; and 6) the functional activity of the MON 94313-produced and *E. coli*-produced DMO was demonstrated to be equivalent. These results demonstrate that the MON 94313-produced DMO protein and the *E. coli*-produced DMO protein are equivalent. This demonstration of protein equivalence confirms that the *E. coli*-produced DMO protein is appropriate for use in the evaluation of the safety of the MON 94313-produced DMO protein.

B.1(a)(ii)(ii) Characterisation of the MON 94313 PAT protein

As previously described, the safety assessment of crops derived through biotechnology includes characterisation of the physicochemical and functional properties of and confirmation of the safety of the introduced protein(s). For the safety data generated using *E. coli*-produced PAT to be applied to PAT protein produced in MON 94313, the equivalence of the plant- and *E. coli*-produced proteins must be established. To assess the equivalence between MON 94313-produced and *E. coli*-produced PAT proteins, a small quantity of the PAT protein was purified from seed of MON 94313. The MON 94313-produced PAT protein was characterized and the equivalence of the physicochemical characteristics and functional activity between the MON 94313-produced and the *E. coli*-produced PAT proteins was assessed using a panel of six analytical tests as shown in Table 15. Taken together, these data provide a detailed characterisation of the MON 94313-produced PAT protein and establish the equivalence of MON 94313-produced PAT and *E. coli*-produced PAT proteins.

For details, please refer to Appendix 7 .

Table 15. Summary of MON 94313 PAT Protein Identity and Equivalence

Analytical Test Assessment	Analytical Test Outcome
1. N-terminal sequence	<ul style="list-style-type: none"> The expected N-terminal sequence was confirmed
2. Nano LC-MS/MS ¹	<ul style="list-style-type: none"> Nano LC-MS/MS¹ analysis yielded peptide masses consistent with the expected peptide masses from the theoretical trypsin digest of the MON 94313-produced PAT sequence
3. Western blot analysis	<ul style="list-style-type: none"> MON 94313-produced PAT protein identity was confirmed using a western blot probed with an antibody specific for PAT proteins Immunoreactive properties of the MON 94313-produced PAT and the <i>E. coli</i>-produced PAT proteins were shown to be equivalent
4. Apparent molecular weight (MW)	<ul style="list-style-type: none"> Electrophoretic mobility and apparent molecular weight of the MON 94313-produced PAT and the <i>E. coli</i>-produced PAT proteins were shown to be equivalent
5. Glycosylation analysis	<ul style="list-style-type: none"> MON 94313-produced PAT and the <i>E. coli</i>-produced PAT proteins were not glycosylated and were shown to be equivalent
6. Functional activity	<ul style="list-style-type: none"> Functional activity of the MON 94313-produced PAT and the <i>E. coli</i>-produced PAT proteins were shown to be equivalent

¹ Nano LC-MS/MS = Nanoscale liquid chromatography coupled to tandem mass spectrometry

² SDS-PAGE = sodium dodecyl sulfate-polyacrylamide gel electrophoresis

B.1(a)(ii)(i) Results of the N-terminal sequencing analysis

The expected N-terminal sequence for the PAT protein deduced from the *pat* gene present in soybean of MON 94313 was observed by Nano LC-MS/MS minus the initiator methionine (Figure 29, MON 94313 experimental sequence). The removal of the initiator methionine (M) was expected for the MON 94313-produced PAT protein which is expressed in the cytoplasm. The cleavage of the N-terminal methionine from proteins *in vivo* by methionine aminopeptidase is thought to occur in all organisms ([Bradshaw et al., 1998](#); [Giglione et al., 2004](#)) and is observed with high frequency when the penultimate amino acid residue is a serine ([Frottin et al., 2006](#)) as is the case for the PAT protein. The N-terminal sequencing results for MON 94313-produced PAT protein were consistent with the sequencing results for the *E. coli*-produced PAT protein (Figure 29). Hence, the sequence information confirms the identity of the PAT protein isolated from the seed of MON 94313.

Amino Acids Residue # from the N- terminus	→	1	2	3	4	5	6	7	8	9	10	11	12	13	14	15
<i>E. coli</i> - produced PAT Sequence	→	M	S	P	E	R	R	P	V	E	I	R	P	A	T	A
Expected PAT sequence	→															
MON 94313 Experiment Sequence	→	-	S	P	E	R	R	P	V	E	I	R	P	A	T	A

Figure 29. N-terminal Sequence of the MON 94313-Produced PAT Protein

The experimental sequence obtained from the MON 94313-produced PAT was compared to the expected sequence deduced from the *pat* gene present in MON 94313. The removal of the initiator methionine (M) was confirmed for the MON 94313-produced PAT protein which is expressed in the cytoplasm. The single letter International Union of Pure and Applied Chemistry- International Union of Biochemistry (IUPAC-IUB) amino acid code is M, methionine; S, serine; P, proline; E, glutamic acid; R, arginine; V, valine; I, isoleucine; A, alanine; T, threonine.

B.1(a)(ii)(ii)(ii) Results of nano LC-MS/MS mass fingerprint analysis

The identity of the MON 94313-produced PAT protein was confirmed by Nano LC-MS/MS analysis of peptide fragments produced by the trypsin digestion of the MON 94313-produced PAT protein.

There were 22 unique peptides identified that corresponded to the masses expected to be produced by trypsin digestion of the MON 94313-produced PAT protein (Table 16). The identified masses were used to assemble a coverage map of the entire PAT protein (Figure 30A). The experimentally determined coverage of the PAT protein was 99% (Figure 30A, 182 out of 183 amino acids, the lead methionine is cleaved during a co-translational process in MON 94313). This analysis further confirms the identity of MON 94313-produced PAT protein.

There were 11 unique peptides identified that corresponded to the masses expected to be produced by trypsin digestion of the *E. coli*-produced PAT protein (Table 17) by MALDI-TOF MS analysis during the protein characterisation. The identified masses were used to assemble a coverage map of the entire PAT protein (Figure 30B). The experimentally determined coverage of the *E. coli*-produced PAT protein was 86% (Figure 30B, 159 out of 183 amino acids). This analysis further confirms the identity of *E. coli*-produced PAT protein.

Table 16. Summary of the Tryptic Masses Identified for the MON 94313-Produced PAT Using Nano LC-MS/MS¹

Experimental Mass ^{1,2}	Calculated Mass ³	Difference ⁴	Fragment ⁵	Sequence ⁶
487.2388	487.2390	-0.0002	2 - 5	SPER
3615.7922	3615.7926	-0.0004	6 - 37	RPVE...VNFR
1855.8581	1855.8588	-0.0007	38 - 52	TEPQ...DLER
2368.1354	2368.1295	0.0059	38 - 56	TEPQ...LQDR
530.2812	530.2813	-0.0001	53 - 56	LQDR
2886.5051	2886.5068	-0.0017	53 - 78	LQDR...GPWK
2374.2374	2374.2361	0.0013	57 - 78	YPWL...GPWK
2153.0363	2153.0290	0.0073	79 - 96	ARNA...VSHR
1925.8889	1925.8908	-0.0019	81 - 96	NAYD...VSHR
1836.0374	1836.0370	0.0004	97 - 112	HQRL...HLLK
1414.8186	1414.8184	0.0002	100 - 112	LGLG...HLLK
896.4067	896.4062	0.0005	113 - 120	SMEAQGFK
2400.2455	2400.2471	-0.0016	113 - 135	SMEA...PSVR
1521.8518	1521.8515	0.0003	121 - 135	SVVA...PSVR
2633.4314	2633.4289	0.0025	121 - 145	SVVA...YTAR
1129.5876	1129.5880	-0.0004	136 - 145	LHEA...YTAR
1556.8429	1556.8423	0.0006	136 - 149	LHEA...GTLR
445.2652	445.2649	0.0003	146 - 149	GTLR
935.5197	935.5188	0.0009	146 - 154	GTLR...AGYK
508.2642	508.2645	-0.0003	150 - 154	AAGYK
1480.6752	1480.6749	0.0003	155 - 166	HGGW...FWQR
1931.0637	1931.0629	0.0008	167 - 183	DFEL...VTQI

¹ All imported values were rounded to 4 decimal places.

² Only experimental masses that matched calculated masses with the highest scores are listed.

³ The calculated mass is the relative molecular mass calculated from the matched peptide sequence.

⁴ The calculated difference = (experimental mass – calculated mass).

⁵ Position refers to amino acid residues within the predicted MON 94313-produced PAT sequence.

⁶ For peptide matches greater than nine amino acids in length the first 4 residues and last 4 residues are shown separated by dots (...).

Table 17. Summary of the Tryptic Masses Identified for the *E. coli*-Produced PAT Using MALDI-TOF MS¹

Experimental Mass ^{1,2}	Calculated Mass ³	Difference ⁴	Fragment ⁵	Sequence ⁶
3616.7368	3616.7766	-0.0398	6 - 37	RPVE...VNFR
1855.8205	1855.8588	-0.0383	38 - 52	TEPQ...DLER
2886.4400	2886.5068	-0.0668	53 - 78	LQDR...GPWK
2374.1822	2374.2361	-0.0539	57 - 78	YPWL...GPWK
1925.8546	1925.8908	-0.0362	81 - 96	NAYD...VSHR
2347.1682	2347.1094	0.0588	81 - 99	NAYD...RHQR
1414.7882	1414.8184	-0.0302	100 - 112	LGLG...HLLK
1521.8238	1521.8515	-0.0277	121 - 135	SVVA...PSVR
1129.5744	1129.5880	-0.0136	136 - 145	LHEA...YTAR
1480.6502	1480.6749	-0.0247	155 - 166	HGGW...FWQR
1931.0281	1931.0629	-0.0348	167 - 183	DFEL...VTQI

¹ All imported values were rounded to 4 decimal places.

² Only experimental masses that matched calculated masses with the highest scores are listed.

³ The calculated mass is the exact molecular mass calculated from the matched peptide sequence.

⁴ The calculated difference = (experimental mass – calculated mass).

⁵ Position refers to amino acid residues within the predicted *E. coli*-produced PAT sequence.

⁶ For peptide matches greater than nine amino acids in length the first 4 residues and last 4 residues are shown separated by dots (...).

(A)

001 MSPERRPVEI RPATAADMAA VCDIVNHYIE TSTVNRTEP QTPQEWIDDL
 051 ERLQDRYPWL VAEVEGVVAG IAYAGPWKAR NAYDWTVEST VYVSHRHQRL
 101 GLGSTLYTHL LKSMEAQGFK SVVAVIGLPN DPSVRLHEAL GYTARGTLRA
 151 AGYKHGGWHD VGFWQ RDFEL PAPP RPVRPV TQI

(B)

001 MSPERRPVEI RPATAADMAA VCDIVNHYIE TSTVNRTEP QTPQEWIDDL
 051 ERLQDRYPWL VAEVEGVVAG IAYAGPWKAR NAYDWTVEST VYVSHRHQRL
 101 GLGSTLYTHL LKSMEAQGFK SVVAVIGLPN DPSVRLHEAL GYTARGTLRA
 151 AGYKHGGWHD VGFWQ RDFEL PAPP RPVRPV TQI

Figure 30. Peptide Maps of the MON 94313-Produced PAT and *E. coli*-Produced PAT Proteins

(A). The amino acid sequence of the MON 94313-produced PAT protein was deduced from the *pat* gene present in MON 94313. Boxed regions correspond to peptides that were identified from the MON 94313-produced PAT protein sample (trypsin digest) using Nano LC-MS/MS. In total, 99% (182 out of 183 amino acids) of the MON 94313-produced PAT protein sequence was covered by the identified peptides.

(B). The amino acid sequence of the *E. coli*-produced PAT protein was deduced from the *pat* gene that is contained on the expression plasmid. Boxed regions correspond to peptides that were identified from the *E. coli*-produced PAT protein sample using MALDI-TOF MS. In total, 86% coverage (159 out of 183 amino acids) of the expected protein sequence was covered by the identified peptides.

B.1(a)(ii)(iii) Results of western blot analysis of the PAT protein isolated from the grain of MON 94313 and immunoreactivity comparison to *Bt*-produced PAT protein

Western blot analysis was conducted using a mouse anti-PAT (*pat*) monoclonal antibody as additional means to confirm the identity of the PAT protein isolated from the seed of MON 94313 and to assess the equivalence of the immunoreactivity of the MON 94313-produced and *E. coli*-produced PAT proteins.

The results showed that immunoreactive bands with the same electrophoretic mobility were present in all lanes loaded with the MON 94313-produced and *E. coli*-produced PAT proteins (Figure 31). At the higher loadings of MON 94313-produced PAT, a weak band corresponding to the expected position of the PAT dimer was observed on the blot films. For each amount loaded, comparable signal intensity for the principal bands at ~20-25 kDa was observed between the MON 94313-produced and *E. coli*-produced PAT protein bands. As expected, the signal intensity increased with increasing load amounts of the MON 94313-produced and *E. coli*-produced PAT proteins, thus, supporting identification of MON 94313-produced PAT protein.

To compare the immunoreactivity of the MON 94313-produced and the *E. coli*-produced PAT proteins, densitometric analysis was conducted on the bands that migrated at the expected apparent MW for PAT proteins (~25 kDa). The signal intensity (reported in OD) of the band of interest in lanes loaded with MON 94313-produced and the *E. coli*-produced PAT proteins was measured (Table 18). Because the mean signal intensity of the MON 94313-produced PAT protein band was within $\pm 35\%$ of the mean signal of the *E. coli*-produced PAT protein, the MON 94313-produced PAT and *E. coli*-produced PAT proteins were determined to have equivalent immunoreactivity.

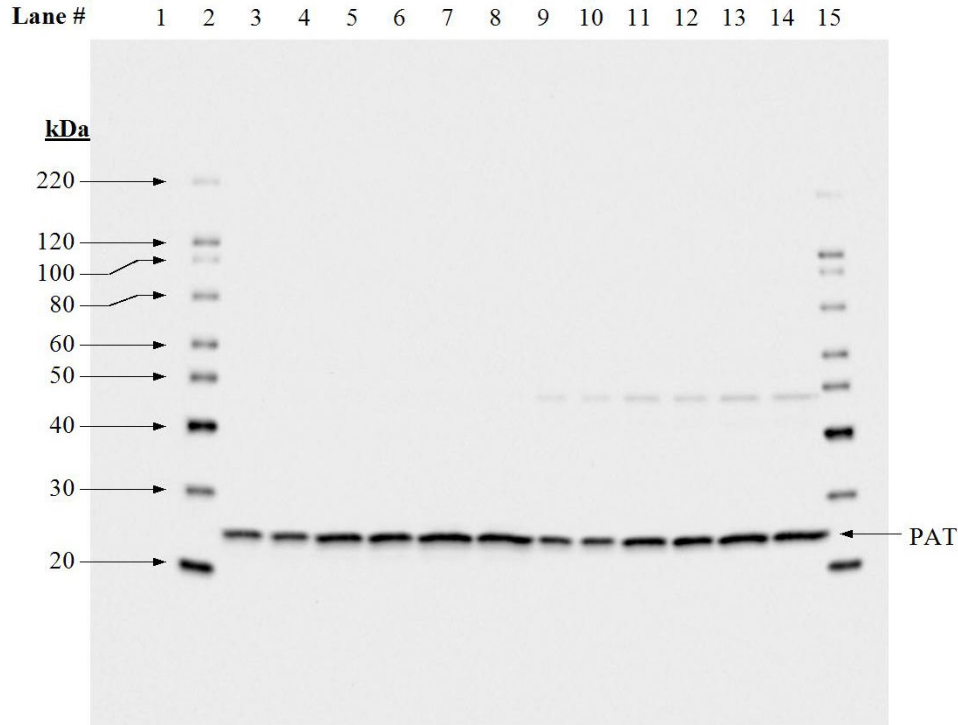


Figure 31. Western Blot Analysis of MON 94313-Produced and *E. coli*-Produced PAT

Aliquots of the MON 94313-produced PAT protein and the *E. coli*-produced PAT protein were subjected to SDS-PAGE and electro-transferred to a nitrocellulose membrane. Proteins were detected using mouse anti-PAT monoclonal antibody and then horse anti-mouse polyclonal antibody conjugated with peroxidase. Immunoreactive bands were visualized using an ECL system. The approximate MW (kDa) of the standards are shown on the left. The 4 second image is shown. Lane designations are as follows:

<u>Lane</u>	<u>Sample</u>	<u>Amount (ng)</u>
1	Precision Plus Protein™ Standards	-
2	Magic Mark™ XP Western Standard	-
3	<i>E. coli</i> -produced PAT	5
4	<i>E. coli</i> -produced PAT	5
5	<i>E. coli</i> -produced PAT	10
6	<i>E. coli</i> -produced PAT	10
7	<i>E. coli</i> -produced PAT	15
8	<i>E. coli</i> -produced PAT	15
9	MON 94313-produced PAT	5
10	MON 94313-produced PAT	5
11	MON 94313-produced PAT	10
12	MON 94313-produced PAT	10
13	MON 94313-produced PAT	15
14	MON 94313-produced PAT	15
15	Magic Mark™ XP Western Standard	-

Table 18. Immunoreactivity of the MON 94313-Produced and *E. coli*-Produced PAT Proteins

Mean Signal Intensity from MON 94313-Produced PAT ¹ (OD)	Mean Signal Intensity from <i>E. coli</i> -Produced PAT ¹ (OD)	Acceptance Limits ² (OD)
2,912,084	3,139,853	2,040,904 – 4,238,801

¹ Each value represents the mean of six values (n = 6).

² The acceptance limits are for the MON 94313-produced PAT protein and are based on the interval between -35% ($3,139,853 \times 0.65 = 2,040,904$) and +35 % ($3,139,853 \times 1.35 = 4,238,801$) of the mean of the *E. coli*-produced PAT signal intensity across all loads.

B.1(a)(ii)(ii)(iv) Results of the MON 94313-PAT protein molecular weight and purity analysis

For apparent MW and purity determination, the MON 94313-produced PAT and the *E. coli*-produced PAT proteins were subjected to SDS-PAGE. Following electrophoresis, the gel was stained with Brilliant Blue G-Colloidal stain and analyzed by densitometry. The MON 94313-produced PAT protein (Figure 32, lanes 3-8) migrated to the same position on the gel as the *E. coli*-produced PAT protein (Figure 32, lane 2) and the apparent MW was calculated to be 22.4 kDa (Table 19). Because the experimentally determined apparent MW of the MON 94313-produced PAT protein was within the acceptance limits for equivalence (Table 20), the MON 94313-produced PAT(*pat*) and *E. coli*-produced PAT proteins were determined to have equivalent apparent molecular weights.

The purity of the MON 94313-produced PAT protein was calculated based on the six lanes loaded on the gel (Figure 32, lanes 3-8). The average purity was determined to be 90% (Table 19).

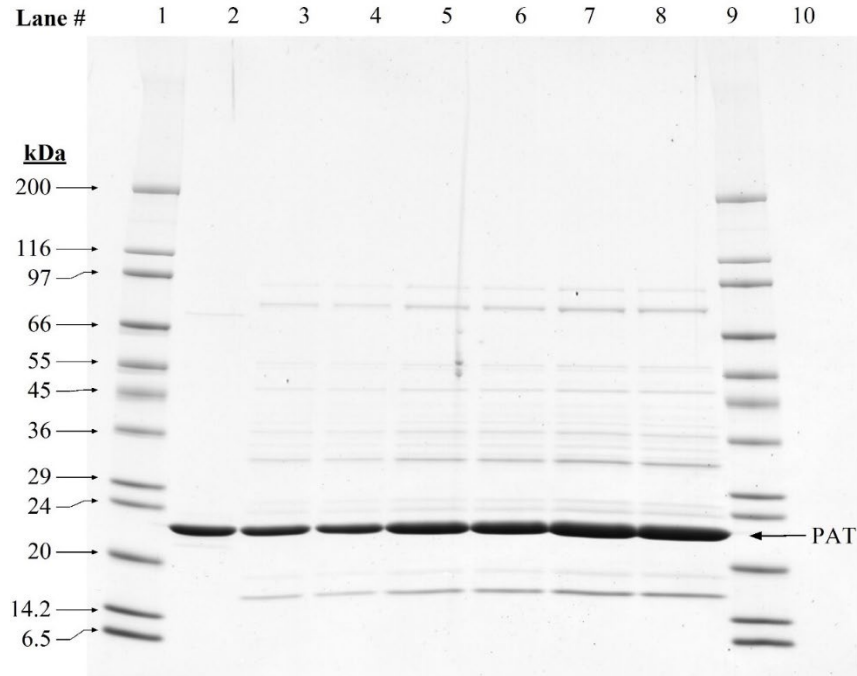


Figure 32. Purity and Apparent Molecular Weight Analysis of the MON 94313-Produced and *E. coli*-Produced PAT Proteins

Aliquots of the MON 94313-produced and the *E. coli*-produced PAT proteins were subjected to SDS-PAGE and the gel was stained with Brilliant Blue G-Colloidal stain. The MWs (kDa) are shown on the left and correspond to the standards loaded in lanes 1 and 9. Lane designations are as follows:

<u>Lane</u>	<u>Sample</u>	<u>Amount (µg)</u>
1	SigmaMarker™ MW Standard	-
2	<i>E. coli</i> -produced PAT	1.0
3	MON 94313-produced PAT	1.0
4	MON 94313-produced PAT	1.0
5	MON 94313-produced PAT	2.0
6	MON 94313-produced PAT	2.0
7	MON 94313-produced PAT	3.0
8	MON 94313-produced PAT	3.0
9	SigmaMarker™ MW Standard	-
10	Blank	-

Table 19. Apparent Molecular Weight and Purity Analysis of the MON 94313-Produced PAT Protein

	Apparent MW ¹ (kDa)	Purity ² (%)
Average (n=6)	22.4	90

¹Final MW was rounded to one decimal place.

²Average % purity was rounded to the nearest whole number.

Table 20. Apparent Molecular Weight Comparison Between the MON 94313-Produced PAT and *E. coli*-Produced PAT Proteins

Apparent MW of MON 94313-Produced PAT Protein (kDa)	Apparent MW of <i>E. coli</i> -Produced PAT Protein (kDa)	Acceptance Limits ¹ (kDa)
22.4	22.5	22.2 – 22.7

¹Data obtained for the *E. coli*-produced PAT protein was used to generate the prediction interval (Appendix 7).

B.1(a)(ii)(v) MON 94313 PAT protein glycosylation analysis

Some eukaryotic proteins are post-translationally modified by the addition of carbohydrate moieties ([Rademacher et al., 1988](#)). To test whether the PAT protein was glycosylated when expressed in the seed of MON 94313, the MON 94313-produced PAT protein was analyzed using an ECL™ glycoprotein detection method. Transferrin, a glycosylated protein, was used as a positive control in the assay. To assess equivalence of the MON 94313-produced and *E. coli*-produced PAT proteins, the *E. coli*-produced PAT protein, previously shown to be free of glycosylation in another equivalence assessment, was also analyzed.

A clear glycosylation signal was observed at the expected molecular weight (~80 kDa) in the lanes containing the positive control (transferrin) and the band intensity increased with increasing concentration (Figure 33A). In contrast, no glycosylation signal was observed in the lanes containing the *E. coli*-produced PAT protein or MON 94313-produced PAT protein (Figure 33A).

To confirm that MON 94313-produced PAT and *E. coli*-produced PAT proteins were appropriately loaded for glycosylation analysis, a second membrane with identical loadings and transfer time was stained with Coomassie Blue R-250 for protein detection. Both the MON 94313-produced and *E. coli*-produced PAT proteins were detected (Figure 33B). These data indicate that the glycosylation status of MON 94313-produced PAT protein is equivalent to that of the *E. coli*-produced PAT protein and that neither is glycosylated.

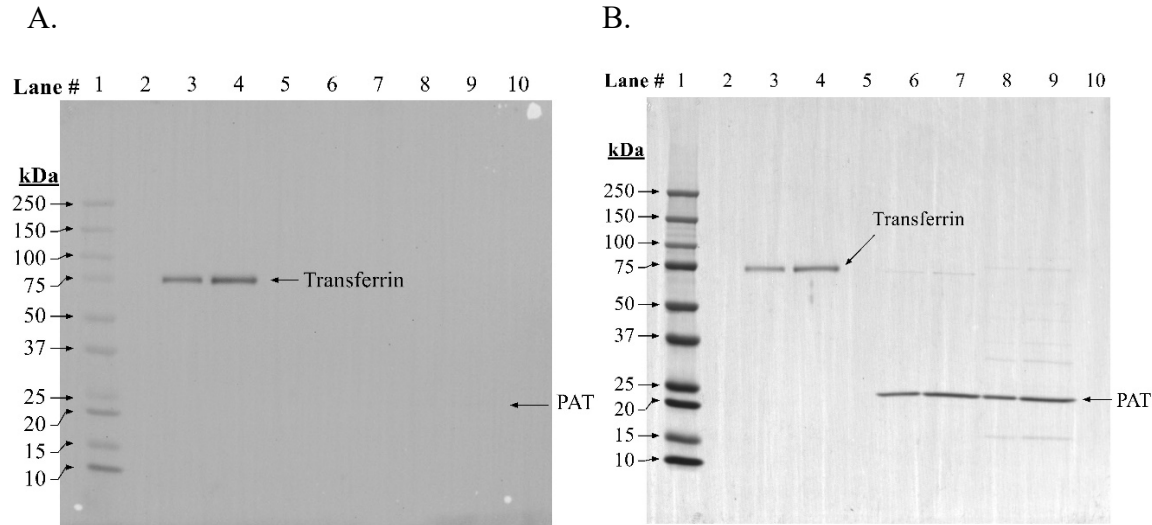


Figure 33. Glycosylation Analysis of the MON 94313-Produced PAT Protein

Aliquots of the transferrin (positive control), *E. coli*-produced PAT and MON 94313-produced PAT were subjected to SDS-PAGE and electro-transferred to a PVDF membrane. The MWs (kDa) correspond to the Precision Plus Dual Color Protein™ Standards. The arrows show the expected migration of the MON 94313-produced and *E. coli*-produced PAT proteins and transferrin. (A) Where present, the labeled carbohydrate moieties were detected by addition of streptavidin conjugated to HRP followed by a luminol-based detection using ECL reagents. The 120 second exposure is shown. (B) An equivalent blot was stained with Coomassie Blue R250 to confirm the presence of proteins. Lane designations are as follows:

<u>Lane</u>	<u>Sample</u>	<u>Amount (ng)</u>
1	Precision Plus Protein™ Standards	-
2	Blank	-
3	Transferrin (positive control)	100
4	Transferrin (positive control)	200
5	Blank	-
6	<i>E. coli</i> -produced PAT	100
7	<i>E. coli</i> -produced PAT	200
8	MON 94313-produced PAT	100
9	MON 94313-produced PAT	200
10	Blank	-

B.1(a)(ii)(ii)(vi) MON 94313 PAT functional activity

The functional activity of the MON 94313-produced and *E. coli*-produced PAT proteins was assessed using a coenzyme A (CoA) release assay. PAT catalyzes the reaction of phosphinothricin (PPT) with acetyl-CoA to form acetyl-PPT and free CoA. CoA released during the reaction can be monitored using the reduction of 5,5'-dithio-bis-(2-nitrobenzoic acid) (DTNB) by CoA to form the colorimetric reagent 5-thio-nitrobenzoate (TNB). In this assay, protein-specific activity is expressed as mmoles TNB released per minute at 30°C per milligram of PAT protein. The MON 94313-produced PAT and *E. coli*-produced PAT proteins were considered to have equivalent functional activity if the specific activity of both were within acceptance limits of 21.7 to 68.7 mmoles \times min⁻¹ \times mg⁻¹ (the prediction interval calculated from a data set based on assays conducted for the *E. coli*-produced PAT protein, Appendix 7).

The experimentally determined specific activity for the MON 94313-produced and *E. coli*-produced PAT proteins are presented in Table 21. The specific activities of MON 94313-produced and *E. coli*-produced PAT proteins were 36 and 39 μ moles \times min⁻¹ \times mg⁻¹ PAT protein, respectively. Because the specific activities of MON 94313-produced and *E. coli*-produced PAT proteins fall within the preset acceptance limits (Table 21), the MON 94313-produced PAT protein was considered to have equivalent functional activity to that of the *E. coli*-produced PAT protein.

Table 21. Functional Activity of MON 94313-Produced and *E. coli*-Produced PAT Proteins

MON 94313-Produced PAT ¹ (μ moles \times min ⁻¹ \times mg ⁻¹)	<i>E. coli</i> -Produced PAT ¹ (μ moles \times min ⁻¹ \times mg ⁻¹)	Acceptance Limits ² (μ moles \times min ⁻¹ \times mg ⁻¹)
36	39	21.7 – 68.7

¹ Value refers to mean calculated based on 3 data points (n = 3) within each assay.

² Data obtained for the *E. coli*-produced PAT(pat) protein were used to generate a prediction interval for setting the acceptance limits (Appendix 7).

B.1(a)(ii)(ii)(vii) MON 94313 PAT Protein Identity and Equivalence Conclusion

The PAT protein purified from seed of MON 94313 was characterized and the equivalence of the immunoreactive and physicochemical characteristics and functional activity between the MON 94313-produced and the *E. coli*-produced PAT proteins was established using a panel of analytical tests: 1) the N-terminal sequence of the MON 94313-produced PAT protein was confirmed by Nano LC-MS/MS analysis; 2) Nano LC-MS/MS analysis yielded peptide masses consistent with the expected peptide masses from the theoretical trypsin digest of the MON 94313-produced PAT sequence; 3) MON 94313-produced PAT protein was detected on a western blot probed with antibodies specific for PAT protein and the immunoreactive properties of the MON 94313-produced and *E. coli*-produced PAT proteins were shown to be equivalent; 4) the electrophoretic mobility and apparent molecular weight of the MON 94313-produced and *E. coli*-produced PAT proteins were shown to be equivalent; 5) the glycosylation status of MON 94313-produced and *E. coli*-produced PAT proteins were determined to be equivalent and

neither to be glycosylated; and 6) functional activities of the MON 94313-produced and *E. coli*-produced PAT proteins were demonstrated to be equivalent.

Taken together, these data provide a detailed characterisation of the MON 94313-produced PAT protein and establish the equivalence of the MON 94313-produced and the *E. coli*-produced PAT proteins. This equivalence justifies the use of the *E. coli*-produced PAT protein in studies to establish the safety of the PAT protein expressed in MON 94313.

B.1(a)(ii)(iii) Characterisation of the MON 94313 FT_T.1 protein

The safety assessment of crops derived through biotechnology includes characterisation of the physicochemical and functional properties and confirmation of the safety of the introduced protein(s). For the safety data generated using the *E. coli*-produced FT_T.1 protein to be applied to the MON 94313-produced ([Wehrmann et al., 1996](#)) FT_T.1 protein (plant-produced FT_T.1), the equivalence of the plant- and *E. coli*-produced proteins must first be demonstrated. To assess the equivalence between the MON 94313-produced FT_T.1 and *E. coli*-produced FT_T.1 proteins, a small quantity of the MON 94313-produced FT_T.1 protein was purified from MON 94313 seed. The MON 94313-produced FT_T.1 protein was characterized and the equivalence of the physicochemical characteristics and functional activity between the MON 94313-produced and *E. coli*-produced FT_T.1 proteins was assessed using a panel of six analytical tests; as shown in Table 22. Taken together, these data provide a detailed characterisation of the MON 94313-produced FT_T.1 protein and establish the equivalence of the MON 94313-produced FT_T.1 and *E. coli*-produced FT_T.1 proteins. Based on this established equivalence, conclusions derived from digestibility, heat susceptibility and oral acute toxicology studies conducted with *E. coli*-produced FT_T.1 protein are applicable to MON 94313-produced FT_T.1 protein.

For details, please refer to Appendix 8.

Table 22. Summary of MON 94313 FT_T.1 Protein Identity and Equivalence

Analytical Test	Analytical Test Outcome
1. N-terminal sequence	<ul style="list-style-type: none"> The expected N-terminal sequence for MON 94313-produced FT_T.1 was observed by Nano LC-MS/MS¹
2. Nano LC-MS/MS ¹	<ul style="list-style-type: none"> Nano LC-MS/MS¹ analysis of trypsin and Asp-N digested peptides from for MON 94313-produced FT_T.1 protein yielded peptide masses consistent with expected peptide masses from the theoretical trypsin or Asp-N digest of the amino acid sequence
3. Western blot analysis	<ul style="list-style-type: none"> MON 94313-produced FT_T.1 protein identity was confirmed using a western blot probed with antibodies specific for FT_T.1 protein Immunoreactive properties of the MON 94313-produced FT_T.1 and the <i>E. coli</i>-produced FT_T.1 proteins were shown to be equivalent
4. Apparent molecular weight (MW)	<ul style="list-style-type: none"> Electrophoretic mobility and apparent molecular weight of the MON 94313-produced FT_T.1 and the <i>E. coli</i>-produced FT_T.1 proteins were shown to be equivalent
5. Glycosylation analysis	<ul style="list-style-type: none"> Glycosylation status of MON 94313-produced FT_T.1 and <i>E. coli</i>-produced FT_T.1 proteins were not glycosylated and were shown to be equivalent
6. Functional activity	<ul style="list-style-type: none"> Functional activity of the MON 94313-produced FT_T.1 and the <i>E. coli</i>-produced FT_T.1 proteins were shown to be equivalent

¹ Nano LC-MS/MS = Nanoscale liquid chromatography-tandem mass spectrometry

B.1(a)(ii)(iii)(i) Results of the N-terminal sequencing analysis

The expected N-terminal sequence for the FT_T.1 protein deduced from the *ft_t.1* gene present in soybean of MON 94313 was confirmed by Nano LC-MS/MS. The experimentally determined sequence corresponds to the deduced FT_T.1 protein beginning at the initial alanine position (Figure 34). The N-terminal sequencing results for MON 94313 -produced FT_T.1 protein were consistent with the sequencing results for the *E. coli*-produced FT_T.1 protein (Figure 34). Hence, the sequence information confirms the identity of the FT_T.1 protein isolated from the seed of MON 94313.

Amino Acids Residue # from the N- terminus	→	1	2	3	4	5	6	7	8	9	10	11	12	13	14	15
<i>E. coli</i> - produced FT_T.1 Sequence	→	M	H	A	A	L	T	P	L	T	N	K	Y	R	F	I
Expected FT_T.1 sequence	→	M	H	A	A	L	T	P	L	T	N	K	Y	R	F	I
MON 94313 produced FT_T.1 Sequence	→	M	H	A	A	L	T	P	L	T	N	K	Y	R	F	I

Figure 34. N-Terminal Sequence of the MON 94313-Produced FT_T.1 Protein

The experimental sequence obtained from the MON 94313-produced FT_T.1 was compared to the expected sequence of the mature protein deduced from the *ft_t.1* gene. The single letter International Union of Pure and Applied Chemistry- International Union of Biochemistry (IUPAC-IUB) amino acid code is A, alanine; M, methionine; H, histidine; L, leucine; T, threonine; P, proline; N, asparagine; K, lysine; Y, tyrosine; R, arginine; F, phelyalanine; I, isoleucine.

B.1(a)(ii)(iii)(ii) Results of nano LC-MS/MS mass fingerprint analysis

Peptide mass fingerprint analysis is a standard technique used for confirming the identity of proteins. The identity of the MON 94313-produced FT_T.1 protein was confirmed by Nano LC-MS/MS analysis of peptide fragments produced by the trypsin and Asp-N digestion of the MON 94313-produced FT_T.1 protein.

There were 57 unique peptides identified that corresponded to the masses expected to be produced by trypsin and Asp-N digestion of the MON 94313-produced FT_T.1 protein (Table 23). The identified masses were used to assemble a coverage map of the FT_T.1 protein (Figure 35A). The experimentally determined coverage of the FT_T.1 protein was 100% (Figure 35A 295 out of 295 amino acids). This analysis further confirms the identity of MON 94313-produced FT_T.1 protein.

There were 44 unique peptides identified that corresponded to the masses expected to be produced by trypsin digestion of the *E. coli*-produced FT_T.1 protein (Table 24) by Nano LC-MS/MS analysis during the protein characterisation. The identified masses were used to assemble a coverage map of the FT_T.1 protein (Figure 35B). The experimentally determined coverage of the *E. coli*-produced FT_T.1 protein was 100% (Figure 35B, 295 out of 295 amino acids). This analysis further confirms the identity of *E. coli*-produced FT_T.1 protein.

PART 2: SPECIFIC DATA REQUIREMENTS FOR SAFETY ASSESSMENT

Table 23. Summary of the Tryptic and Asp-N Masses Identified for the MON 94313-Produced FT T.1 Using Nano LC-MS/MS

Experimental Mass ^{1,2}	Calculated Mass ³	Difference ⁴	Fragment ⁵	Sequence ⁶
1237.6494	1237.6489	0.0005	1 - 11	MHAA...LTNK
1790.9477	1790.9501	-0.0024	1 - 15	MHAA...YRFI
3382.7990	3382.7959	0.0031	1 - 31	MHAA...ITGV
1064.5982	1064.5978	0.0004	2 - 11	HAAL...LTNK
1643.9155	1643.9147	0.0008	2 - 15	HAAL...YRFI
2212.2130	2212.2104	0.0026	14 - 34	FIDV...VDLR
1567.8467	1567.8458	0.0009	16 - 31	DVQP...ITGV
2291.2401	2291.2373	0.0028	16 - 37	DVQP...REPL
2406.2667	2406.2642	0.0025	16 - 38	DVQP...EPLD
741.4021	741.4021	0.0000	32 - 37	DLREPL
856.4293	856.4290	0.0003	32 - 38	DLREPLD
1814.8696	1814.8686	0.0010	32 - 46	DLRE...NEIL
4465.1237	4465.1291	-0.0054	35 - 72	EPLD...AFSR
1091.4781	1091.4771	0.0010	38 - 46	DDST...NEIL
976.4504	976.4502	0.0002	39 - 46	DSTWNEIL
3608.7954	3608.7953	0.0001	47 - 77	DAFH...FGPV
1336.7873	1336.7867	0.0006	73 - 84	RFGP...PILK
1180.6861	1180.6856	0.0005	74 - 84	FGPV...PILK
2583.3737	2583.3771	-0.0034	74 - 96	FGPV...QMIR
3445.7667	3445.7663	0.0004	78 - 107	DPVP...RYIG
1436.6977	1436.6969	0.0008	85 - 96	SIEG...QMIR
1576.8028	1576.8031	-0.0003	85 - 97	SIEG...MIRR
947.4416	947.4420	-0.0004	97 - 104	REANESSR
791.3410	791.3409	0.0001	98 - 104	EANESSR
2546.1917	2546.1900	0.0017	105 - 127	YIGD...VVMR
642.2400	642.2398	0.0002	108 - 112	DDWHA
1205.4990	1205.4989	0.0001	108 - 117	DDWH...STFL
2520.2234	2520.2206	0.0028	113 - 136	DSTF...EYGG
1940.9680	1940.9666	0.0014	118 - 136	DAPP...EYGG
7971.8565	7971.8573	-0.0008	118 - 190	DAPP...VKVM
4532.1461	4532.1403	0.0058	128 - 169	AIEV...SATK
6048.9022	6048.9013	0.0009	137 - 190	DTGF...VKVM
1440.7162	1440.7150	0.0012	170 - 181	VFGS...TNWR
781.3971	781.3970	0.0001	182 - 188	FSNTSVK
992.4233	992.4233	0.0000	189 - 197	VMDV...AGDR
2615.3146	2615.3126	0.0020	189 - 212	VMDV...VTGR
4026.0141	4026.0139	0.0002	196 - 229	DRET...QGMT
1640.8999	1640.8999	0.0000	198 - 212	ETVH...VTGR
1601.7456	1601.7442	0.0014	213 - 224	RALY...YCQK

Table 23. Summary of the Tryptic and Asp-N Masses Identified for the MON 94313-Produced FT_T.1 Using Nano LC-MS/MS (Continued)

Experimental Mass ^{1,2}	Calculated Mass ³	Diff ⁴	Fragment ⁵	Sequence ⁶
1445.6434	1445.6431	0.0003	214 - 224	ALYC...YCQK
1094.4919	1094.4914	0.0005	225 - 234	IQGM...AESK
2126.0321	2126.0320	0.0001	230 - 247	DAES...ATQF
2275.0739	2275.0732	0.0007	235 - 252	SLLQ...FTCR
1394.7246	1394.7241	0.0005	248 - 257	DFTC...RWKK
2135.1115	2135.1099	0.0016	248 - 263	DFTC...VLVW
1913.9223	1913.9240	-0.0017	257 - 271	KDQV...TMHR
1801.8266	1801.8240	0.0026	258 - 271	DQVL...TMHR
758.3954	758.3963	-0.0009	258 - 263	DQVLVW
2068.9850	2068.9823	0.0027	258 - 274	DQVL...RAVP
1312.6034	1312.6016	0.0018	264 - 274	DNLC...RAVP
3112.5275	3112.5335	-0.0060	264 - 290	DNLC...TVAG
819.4135	819.4127	0.0008	272 - 279	AVPDYAGK
1122.5823	1122.5822	0.0001	272 - 281	AVPD...GKFR
1817.9426	1817.9424	0.0002	275 - 290	DYAG...TVAG
551.3067	551.3067	0.0000	282 - 285	YLTR
1030.5410	1030.5407	0.0003	286 - 295	TTVA...KPSR
601.3189	601.3184	0.0005	291 - 295	DKPSR

¹ All imported values were rounded to 4 decimal places.

² Only experimental masses that matched calculated masses with the highest scores are listed.

³ The calculated mass is the exact molecular mass calculated from the matched peptide sequence.

⁴ The calculated difference = (experimental mass – calculated mass).

⁵ Position refers to amino acid residues within the predicted MON 94313-produced FT_T.1 sequence.

⁶ For peptide matches greater than nine amino acids in length the first 4 residues and last 4 residues are shown separated by dots (...).

Table 24. Summary of the Tryptic Masses Identified for *E. coli*-produced FT_T.1 using Nano LC-MS/MS¹

Experimental Mass ^{1,2}	Calculated Mass ³	Difference ⁴	Fragment ⁵	Sequence ⁶
1195.6377	1195.6383	-0.0006	1 - 11	MHAA...LTNK
1514.8061	1514.8027	0.0034	1 - 13	MHAA...NKYR
1064.5975	1064.5978	-0.0003	2 - 11	HAAL...LTNK
2212.2135	2212.2104	0.0031	14 - 34	FIDV...VDLR
6659.3308	6659.3289	0.0019	14 - 72	FIDV...AFSR
4465.1321	4465.1291	0.0030	35 - 72	EPLD...AFSR
4621.2287	4621.2302	-0.0015	35 - 73	EPLD...FSRR
5783.8933	5783.9053	-0.0120	35 - 84	EPLD...PILK
1336.7867	1336.7867	0.0000	73 - 84	RFGP...PILK
1180.6858	1180.6856	0.0002	74 - 84	FGPV...PILK
2583.3766	2583.3771	-0.0005	74 - 96	FGPV...QMIR
1420.7024	1420.7020	0.0004	85 - 96	SIEG...QMIR
1576.8032	1576.8031	0.0001	85 - 97	SIEG...MIRR
947.4420	947.4420	0.0000	97 - 104	REANESSR
791.3409	791.3409	0.0000	98 - 104	EANESSR
3319.5236	3319.5204	0.0032	98 - 127	EANE...VVMR
2546.1913	2546.1900	0.0013	105 - 127	YIGD...VVMR
4500.1532	4500.1505	0.0027	128 - 169	AIEV...SATK
5922.8571	5922.8549	0.0022	128 - 181	AIEV...TNWR
6686.2454	6686.2414	0.0040	128 - 188	AIEV...TSVK
1440.7164	1440.7150	0.0014	170 - 181	VFGS...TNWR
3162.5165	3162.5193	-0.0028	170 - 197	VFGS...AGDR
781.3970	781.3970	0.0000	182 - 188	FSNTSVK
1739.8172	1739.8149	0.0023	182 - 197	FSNT...AGDR
3362.7114	3362.7042	0.0072	182 - 212	FSNT...VTGR
976.4287	976.4284	0.0003	189 - 197	VMDV...AGDR
2599.3180	2599.3177	0.0003	189 - 212	VMDV...VTGR
2755.4191	2755.4188	0.0003	189 - 213	VMDV...TGRR
1640.9005	1640.8999	0.0006	198 - 212	ETVH...VTGR
1797.0028	1797.0010	0.0018	198 - 213	ETVH...TGRR
1601.7403	1601.7442	-0.0039	213 - 224	RALY...YCQK
1445.6434	1445.6431	0.0003	214 - 224	ALYC...YCQK
2506.1283	2506.1290	-0.0007	214 - 234	ALYC...AESK
1078.4969	1078.4965	0.0004	225 - 234	IQGM...AESK
3335.5578	3335.5591	-0.0013	225 - 252	IQGM...FTCR
2275.0733	2275.0732	0.0001	235 - 252	SLLQ...FTCR
2530.2469	2530.2427	0.0042	235 - 254	SLLQ...CRVR
2228.0988	2228.0983	0.0005	255 - 271	WKKD...TMHR
1913.9226	1913.9240	-0.0014	257 - 271	KDQV...TMHR

Table 24. Summary of the Tryptic Masses Identified for *E. coli*-produced FT_T.1 using MALDI-TOF MS (Continued)

Experimental Mass ^{1,2}	Calculated Mass ³	Difference ⁴	Fragment ⁵	Sequence ⁶
1785.8294	1785.8291	0.0003	258 - 271	DQVL...TMHR
819.4127	819.4127	0.0000	272 - 279	AVPDYAGK
1122.5818	1122.5822	-0.0004	272 - 281	AVPD...GKFR
551.3069	551.3067	0.0002	282 - 285	YLTR
1030.5409	1030.5407	0.0002	286 - 295	TTVA...KPSR

¹ All imported values were rounded to 4 decimal places.

² Only experimental masses that matched calculated masses with the highest scores are listed in the table.

³ The calculated mass is the exact molecular mass calculated from the matched peptide sequence.

⁴ The calculated difference = experimental mass - calculated mass.

⁵ Position refers to amino acid residues within the predicted *E. coli*-produced FT_T.1 sequence.

⁶ For peptide matches greater than nine amino acids in length, the first 4 residues and last 4 residues are show separated by three dots (...).

PART 2: SPECIFIC DATA REQUIREMENTS FOR SAFETY ASSESSMENT

(A)

001 MHAALTPLTN KYRFIDVQPL TGVLGAEITG VDLREPLDDS TWNEILDAFH
051 TYQVIYFPGQ AITNEQHIAF SRRFGPVDPV PILKSIEGYP EVQMIRREAN
101 ESSRYIGDDW HADSTFLDAP PAAVVMRAIE VPEYGGDTGF LSMYSAWETL
151 SPTMQATIEG LNVVHSATKV FGSLYQATNW RFSNTSVKVM DVDAGDRETV
201 HPLVVTHPVT GRRALYCNQV YCQKIQGMTD AESKSLLOFL YECHATQDFDT
251 CRVRWKKDQV LVWDNLCTMH RAVPDYAGKF RYLTRTTVAG DKPSR

(B)

001 MHAALTPLTN KYRFIDVQPL TGVLGAEITG VDLREPLDDS TWNEILDAFH
051 TYQVIYFPGQ AITNEQHIAF SRRFGPVDPV PILKSIEGYP EVQMIRREAN
101 ESSRYIGDDW HADSTFLDAP PAAVVMRAIE VPEYGGDTGF LSMYSAWETL
151 SPTMQATIEG LNVVHSATKV FGSLYQATNW RFSNTSVKVM DVDAGDRETV
201 HPLVVTHPVT GRRALYCNQV YCQKIQGMTD AESKSLLOFL YECHATQDFDT
251 CRVRWKKDQV LVWDNLCTMH RAVPDYAGKF RYLTRTTVAG DKPSR

Figure 35. Peptide Map of the MON 94313-Produced FT_T.1 and *E. coli*-Produced FT_T.1 Proteins

(A) For the combined Trypsin and Asp-N digest, the amino acid sequence of the MON 94313-produced FT_T.1 protein was deduced from the *ft_t.1* gene present in MON 94313. Boxed regions correspond to peptides that were identified from the MON 94313-produced FT_T.1 protein sample using Nano LC-MS/MS. In total, 100% coverage (295 out of 295 amino acids) of the expected protein sequence was covered by the identified peptides.

(B) The amino acid sequence of the *E. coli*-produced FT_T.1 protein was deduced from the *ft_t.1* gene that is contained on the expression plasmid. Boxed regions correspond to peptides that were identified from the *E. coli*-produced FT_T.1 protein sample using Nano LC-MS/MS. In total, 100% coverage (295 out of 295 amino acids) of the expected protein sequence was covered by the identified peptides.

B.1(a)(ii)(iii)(iii) Results of western blot analysis of the FT_T.1 protein isolated from the grain of MON 94313 and immunoreactivity comparison to *Bt*-produced FT_T.1 protein

Western blot analysis was conducted using rabbit anti-FT_T.1 polyclonal antibody to provide additional confirmation of the identity of the FT_T.1 protein isolated from the grain of MON 94313 and to assess the equivalence of the immunoreactivity of the MON 94313-produced and *E. coli*-produced FT_T.1 proteins. The results showed that immunoreactive bands with the same electrophoretic mobility were present in all lanes loaded with the MON 94313-produced and *E. coli*-produced FT_T.1 proteins (Figure 36). For each amount loaded, comparable signal intensity was observed between the MON 94313-produced and *E. coli*-produced FT_T.1 protein bands. As expected, the signal intensity increased with increasing load amounts of the MON 94313-produced and *E. coli*-produced FT_T.1 proteins, thus, supporting the identity of the MON 94313-produced FT_T.1 protein.

To compare the immunoreactivity of the MON 94313-produced and the *E. coli*-produced FT_T.1 proteins, densitometric analysis was conducted on the bands that migrated at the expected apparent molecular weight (MW) for FT_T.1 proteins (~34 kDa). The signal intensity (reported in OD) of the band of interest in lanes loaded with MON 94313-produced and the *E. coli*-produced FT_T.1 proteins was measured (Table 25). Because the mean signal intensity of the MON 94313-produced FT_T.1 protein band was within $\pm 35\%$ of the mean signal of the *E. coli*-produced FT_T.1 protein, the MON 94313-produced FT_T.1 and *E. coli*-produced FT_T.1 proteins were determined to have equivalent immunoreactivity.

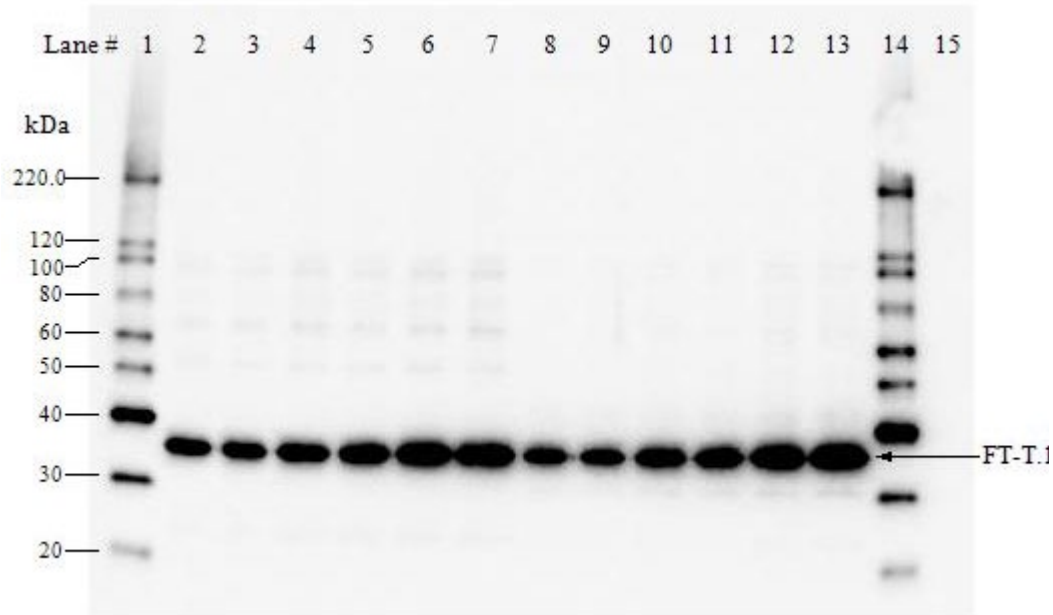


Figure 36. Western Blot Analysis of MON 94313-Produced and *E. coli*-Produced FT_T.1 Proteins

Aliquots of the MON 94313-produced FT_T.1 protein and the *E. coli*-produced FT_T.1 protein were subjected to SDS-PAGE and electrotransferred to a nitrocellulose membrane. Proteins were detected using rabbit anti-FT_T.1 polyclonal antibody and then goat anti-rabbit polyclonal antibody conjugated with peroxidase. Immunoreactive bands were visualized using an ECL system. The approximate MW (kDa) of the standards are shown on the left. The 3 second exposure is shown. Lane designations are as follows:

<u>Lane</u>	<u>Sample</u>	<u>Amount (ng)</u>
1	Magic Mark™ XP Western Standard	-
2	<i>E. coli</i> -produced FT_T.1	5
3	<i>E. coli</i> -produced FT_T.1	5
4	<i>E. coli</i> -produced FT_T.1	10
5	<i>E. coli</i> -produced FT_T.1	10
6	<i>E. coli</i> -produced FT_T.1	20
7	<i>E. coli</i> -produced FT_T.1	20
8	MON 94313-produced FT_T.1	5
9	MON 94313-produced FT_T.1	5
10	MON 94313-produced FT_T.1	10
11	MON 94313-produced FT_T.1	10
12	MON 94313-produced FT_T.1	20
13	MON 94313-produced FT_T.1	20
14	Magic Mark XP™ Western Standard	-
15	Blank	-

Table 25. Immunoreactivity of the MON 94313-Produced and *E. coli*-Produced FT_T.1 Proteins

Mean Signal Intensity from MON 94313-Produced FT_T.1 ¹ (OD)	Mean Signal Intensity from <i>E. coli</i> -Produced FT_T.1 ¹ (OD)	Acceptance Limits ² (OD)
2,336,050	2,307,548	1,499,906 – 3,115,190

¹ Each value represents the mean of six values (n = 6).

² The acceptance limits are for the MON 94313-produced FT_T.1 protein and are based on the interval between -35% ($2,307,548 \times 0.65 = 1,499,906$) and +35 % ($2,307,548 \times 1.35 = 3,115,190$) of the mean of the *E. coli*-produced FT_T.1 signal intensity across all loads.

B.1(a)(ii)(iii)(iv) Results of the FT_T.1 protein molecular weight and purity analysis

For apparent MW and purity determination, the MON 94313-produced FT_T.1 and the *E. coli*-produced FT_T.1 proteins were subjected to SDS-PAGE. Following electrophoresis, the gel was stained with Brilliant Blue G-Colloidal stain and analyzed by densitometry. The MON 94313-produced FT_T.1 protein (Figure 37, lanes 3-8) migrated with the same mobility on the gel as the *E. coli*-produced FT_T.1 protein (Figure 37, lane 2) and the apparent MW was calculated to be 34.0 kDa (Table 26). Because the experimentally determined apparent MW of the MON 94313-produced FT_T.1 protein was within the acceptance limits for equivalence (Table 27), the MON 94313-produced FT_T.1 and *E. coli*-produced FT_T.1 proteins were determined to have equivalent apparent molecular weights.

The purity of the MON 94313-produced FT_T.1 protein was calculated based on the six lanes loaded on the gel (Figure 37, lanes 3-8). The average purity was determined to be 98% (Table 26).

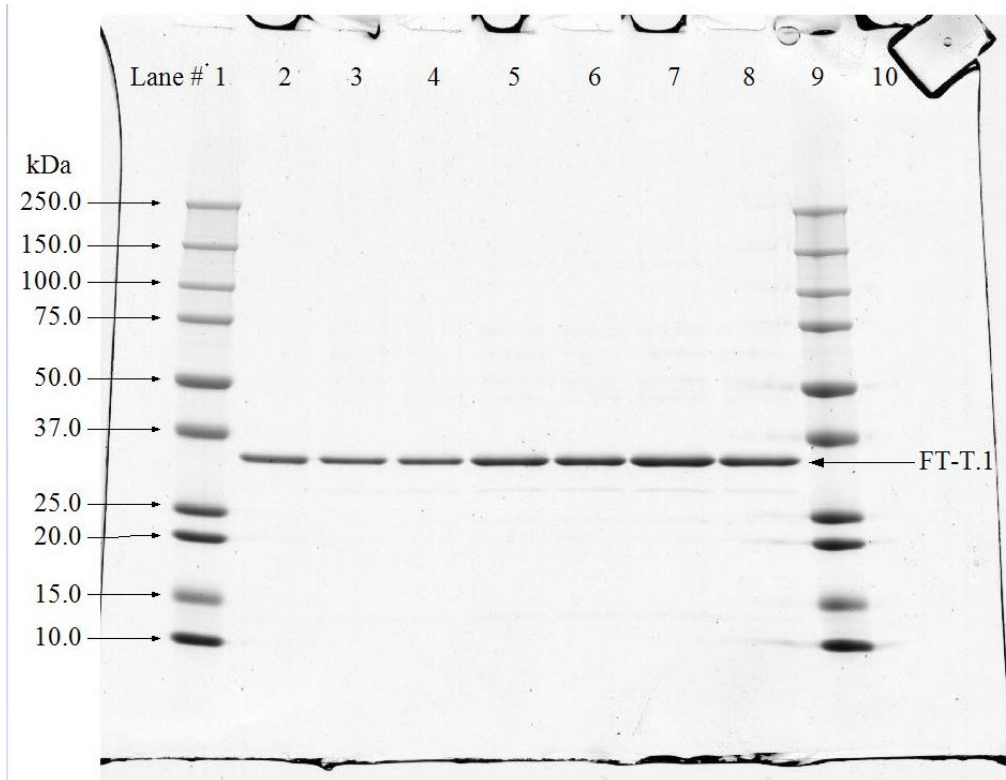


Figure 37. Purity and Apparent Molecular Weight Analysis of the MON 94313-Produced FT_T.1 Protein

Aliquots of the MON 94313-produced and the *E. coli*-produced FT_T.1 proteins were subjected to SDS-PAGE and the gel was stained with Brilliant Blue G-Colloidal stain. The MWs (kDa) are shown on the left and correspond to the standards loaded in lanes 1 and 9. Lane designations are as follows:

<u>Lane</u>	<u>Sample</u>	<u>Amount (µg)</u>
1	Precision Plus Protein™ Standards	-
2	<i>E. coli</i> -produced FT_T.1	1.0
3	MON 94313-produced FT_T.1	1.0
4	MON 94313-produced FT_T.1	1.0
5	MON 94313-produced FT_T.1	2.0
6	MON 94313-produced FT_T.1	2.0
7	MON 94313-produced FT_T.1	3.0
8	MON 94313-produced FT_T.1	3.0
9	Precision Plus Protein™ Standards	-
10	Blank	-

Table 26. Apparent Molecular Weight and Purity Analysis of the MON 94313-Produced FT_T.1 Protein

	Apparent MW ¹ (kDa)	Purity ² (%)
Average (n=6)	34.0	98

¹Final MW was rounded to one decimal place.

²Average % purity was rounded to the nearest whole number.

Table 27. Apparent Molecular Weight Comparison Between the MON 94313-Produced FT_T.1 and *E. coli*-Produced FT_T.1 Proteins

Apparent MW of MON 94313-Produced FT_T.1 Protein (kDa)	Apparent MW of <i>E. coli</i> -Produced FT_T.1 Protein (kDa)	Acceptance Limits ¹ (kDa)
34.0	33.6	33.1 – 34.2

¹ Data obtained from the *E. coli*-produced FT_T.1 protein was used to generate a prediction interval for setting the acceptance limits (Appendix 8).

B.1(a)(ii)(iii)(vi) FT_T.1 glycosylation analysis

Some eukaryotic proteins are post-translationally modified by the addition of carbohydrate moieties ([Rademacher et al., 1988](#)). To test whether the FT_T.1 protein was glycosylated when expressed in the soybean grain of MON 94313, the MON 94313-produced FT_T.1 protein was analyzed using an ECL™ glycoprotein detection method. Transferrin, a glycosylated protein, was used as a positive control in the assay. To assess equivalence of the MON 94313-produced and *E. coli*-produced FT_T.1 proteins, the *E. coli*-produced FT_T.1 protein was also analyzed.

A clear glycosylation signal was observed at the expected molecular weight (~ 80 kDa) in the lanes containing the positive control (transferrin) and the band intensity increased with increasing concentration (Figure 38, panel A). In contrast, no glycosylation signal was observed in the lanes containing the *E. coli*-produced FT_T.1 protein or MON 94313-produced FT_T.1 protein (Figure 38, panel A).

To confirm that MON 94313-produced FT_T.1 and *E. coli*-produced FT_T.1 proteins were appropriately loaded for glycosylation analysis, a second membrane with identical loadings and transfer time was stained with Coomassie Blue R250 for protein detection. Both the MON 94313-produced and *E. coli*-produced FT_T.1 proteins were detected (Figure 38, panel B). These data indicate that the glycosylation status of MON 94313-produced FT_T.1 protein is equivalent to that of the *E. coli*-produced FT_T.1 protein and that neither is glycosylated.

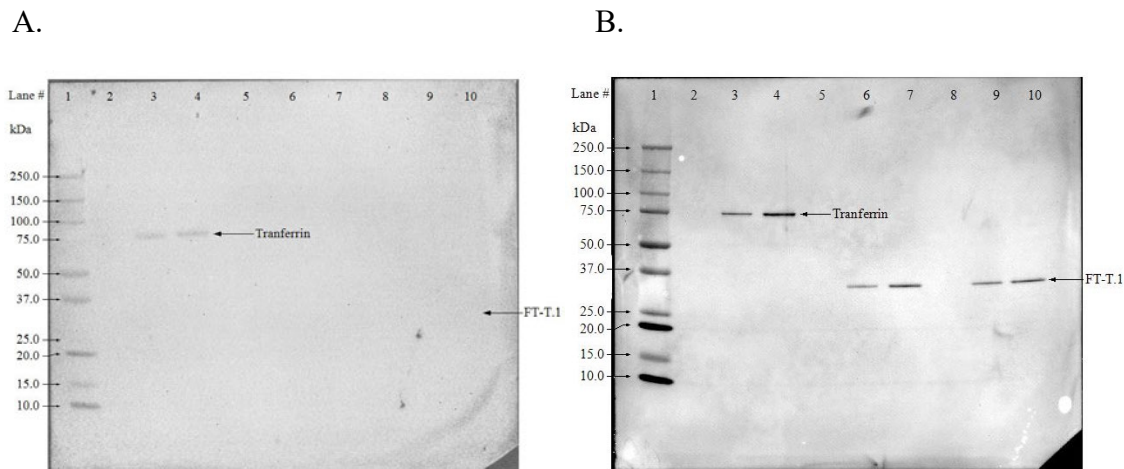


Figure 38. Glycosylation Analysis of the MON 94313-Produced and *E. coli*-Produced FT_T.1 Proteins

Aliquots of the transferrin (positive control), *E. coli*-produced FT_T.1 and MON 94313-produced FT_T.1 were subjected to SDS-PAGE and electrotransferred to a PVDF membrane. The MWs (kDa) correspond to the Precision Plus Dual Color Protein™ Standards. The arrows show the expected migration of the MON 94313-produced and *E. coli*-produced FT_T.1 proteins and transferrin. (A) Where present, the labeled carbohydrate moieties were detected by addition of streptavidin conjugated to HRP followed by a luminol-based detection using ECL reagents. The 120 second exposure is shown. (B) An equivalent blot was stained with Coomassie Blue R250 to confirm the presence of proteins. Lane designations are as follows:

<u>Lane</u>	<u>Sample</u>	<u>Amount (ng)</u>
1	Precision Plus Protein™ Standards	-
2	Blank	-
3	Transferrin (positive control)	100
4	Transferrin (positive control)	200
5	Blank	-
6	<i>E. coli</i> -produced FT_T.1	100
7	<i>E. coli</i> -produced FT_T.1	200
8	Blank	-
9	MON 94313-produced FT_T.1	100
10	MON 94313-produced FT_T.1	200

B.1(a)(ii)(iii)(vi) FT_T.1 functional activity

The functional activities of the MON 94313-produced and *E. coli*-produced FT_T.1 proteins were determined using a colorimetric assay that measures the FT_T.1-catalyzed degradation of 2,4-D to 2,4-DCP. In this assay, protein-specific activity is expressed as units per milligram of protein (U/mg), where a unit (U) is 1 nmole of 2,4-D to 2,4-DCP per min at 25°C. The MON 94313-produced and *E. coli*-produced FT_T.1 proteins were considered to have equivalent functional activity if the specific activity of both were within the preset acceptance limits of 1,135.2 to 2,035.3 U/mg (the prediction interval calculated from a data set of historically determined FT_T.1 protein activity; see Appendix 8, Table 2).

The experimentally determined specific activity for the MON 94313-produced and *E. coli*-produced FT_T.1 proteins are presented in Table 28. The specific activities of MON 94313-produced and *E. coli*-produced FT_T.1 proteins were 1,207.5 U/mg and 1,345.0 U/mg of FT_T.1 protein, respectively. Because the specific activities of MON 94313-produced and *E. coli*-produced FT_T.1 proteins fall within the preset acceptance limits (Table 28), the MON 94313-produced FT_T.1 protein was considered to have equivalent functional activity to that of the *E. coli*-produced FT_T.1 protein.

Table 28. Functional Activity of MON 94313-Produced and *E. coli*-Produced FT_T.1 Proteins

MON 94313-Produced FT_T.1¹ (U/mg)	<i>E. coli</i>-Produced FT_T.1¹ (U/mg)	Acceptance Limits² (U/mg)
1,207.5	1,345.0	1,135.2 – 2,035.3

¹ Value refers to mean calculated based on samples spectrophotometrically read in triplicate plate wells.

² Data obtained from two *E. coli*-produced FT_T.1 lots were used to generate a prediction interval for setting the acceptance limits (Appendix 8).

B.1(a)(ii)(iii)(vii) MON 94313 FT_T.1 protein identity and equivalence conclusion

The MON 94313-produced FT_T.1 protein was purified from MON 94313 grain, was characterized, and a comparison of the physicochemical and functional properties between the MON 94313-produced and the *E. coli*-produced FT_T.1 proteins was conducted following a panel of analytical tests: 1) N-terminal sequence analysis established the same identity for the MON 94313-produced and *E. coli*-produced FT_T.1 proteins; 2) Nano LC-MS/MS analysis yielded peptide masses consistent with the expected peptide masses from the theoretical trypsin digest of the *FT_T.1* gene product present in MON 94313; 3) the MON 94313-produced and the *E. coli*-produced FT_T.1 proteins were both detected on a western blot probed with antibodies specific for FT_T.1 protein and the immunoreactive properties of both proteins was shown to be equivalent; 4) the electrophoretic mobility and apparent molecular weight of the MON 94313-produced and *E. coli*-produced FT_T.1 proteins were shown to be equivalent; 5) the glycosylation status of MON 94313-produced and *E. coli*-produced FT_T.1 proteins was determined to be equivalent; and 6) the functional activity of the MON 94313-produced and *E. coli*-produced FT_T.1 was demonstrated to be equivalent. These results demonstrate that the

MON 94313-produced FT_T.1 protein and the *E. coli*-produced FT_T.1 protein are equivalent. This demonstration of protein equivalence confirms that the *E. coli*-produced FT_T.1 protein is appropriate for use in the evaluation of the safety of the MON 94313-produced FT_T.1 protein.

B.1(a)(ii)(iv) Characterisation of the MON 94313 TDO protein

As previously described, the safety assessment of crops derived through biotechnology includes characterisation of the physicochemical and functional properties of and confirmation of the safety of the introduced protein(s). For the safety data generated using *E. coli*-produced TDO protein to be applied to TDO protein produced in MON 94313, the equivalence of the plant- and *E. coli*-produced proteins must be established. To assess the equivalence between MON 94313-produced and *E. coli*-produced TDO protein, a small quantity of the TDO protein was purified from grain of MON 94313 soybean. The MON 94313-produced TDO protein was characterized and the equivalence of the physicochemical characteristics and functional activity between the MON 94313-produced and the *E. coli*-produced TDO proteins was assessed using a panel of six analytical tests as shown in

Table 29. Taken together, these data provide a detailed characterisation of the MON 94313-produced TDO protein and establish the equivalence of MON 94313-produced TDO and *E. coli*-produced TDO proteins.

For details, please refer to Appendix 9.

Table 29. Summary of MON 94313 TDO Protein Identity and Equivalence

Analytical Test Assessment	Analytical Test Outcome
1. N-terminal sequence	<ul style="list-style-type: none"> The expected N-terminal sequence was confirmed
2. Nano LC-MS/MS ¹	<ul style="list-style-type: none"> Nano LC-MS/MS¹ analysis yielded peptide masses consistent with the expected peptide masses from the theoretical trypsin digest of the MON 94313-produced TDO sequence
3. Western blot analysis	<ul style="list-style-type: none"> MON 94313-produced TDO protein identity was confirmed using a western blot probed with an antibody specific for TDO proteins Immunoreactive properties of the MON 94313-produced TDO and the <i>E. coli</i>-produced TDO proteins were shown to be equivalent
4. Apparent molecular weight (MW)	<ul style="list-style-type: none"> Electrophoretic mobility and apparent molecular weight of the MON 94313-produced TDO and the <i>E. coli</i>-produced TDO proteins were shown to be equivalent
5. Glycosylation analysis	<ul style="list-style-type: none"> MON 94313-produced TDO and the <i>E. coli</i>-produced TDO proteins were not glycosylated and were shown to be equivalent
6. Functional activity	<ul style="list-style-type: none"> Functional activity of the MON 94313-produced TDO and the <i>E. coli</i>-produced TDO proteins were shown to be equivalent

¹ Nano LC-MS/MS = Nanoscale liquid chromatography coupled to tandem mass spectrometry.

² SDS-PAGE = sodium dodecyl sulfate-polyacrylamide gel electrophoresis.

B.1(a)(ii)(iv)(i) Results of the N-terminal sequencing analysis

The expected N-terminal sequence for the TDO protein deduced from the *TDO* gene present in seed of MON 94313 soybean was observed by LC-MS/MS with the exception of the initiator methionine being removed (Figure 39). The cleavage of the N-terminal methionine from proteins *in vivo* by methionine aminopeptidase is thought to occur in all organisms ([Bradshaw et al., 1998](#); [Giglione et al., 2004](#)). The N-terminal methionine is cleaved if the side-chain of the penultimate residue has small size such as serine, alanine etc. ([Wingfield, 2017](#)). Therefore, the removal of the initiator methionine (M) is expected for the MON 94313-produced TDO protein as its penultimate residue is alanine. The N-terminal sequencing results for MON 94313-produced TDO protein were consistent with the sequencing results for the *E. coli*-produced TDO protein (Figure 39). Hence, the sequence information confirms the identity of the TDO protein isolated from the seed of MON 94313.

Amino Acids Residue # from the N- terminus	→	1	2	3	4	5	6	7	8	9	10	11	12	13	14	15
<i>E. coli</i> - produced TDO Sequence	→	-	A	D	E	S	W	R	A	P	A	I	V	Q	E	L
Expected TDO sequence	→	M	A	D	E	S	W	R	A	P	A	I	V	Q	E	L
MON 94313 Experiment Sequence	→	-	A	D	E	S	W	R	A	P	A	I	V	Q	E	L

Figure 39. N-terminal Sequence of the MON 94313-Produced TDO Protein

The experimental sequence obtained from the MON 94313-produced TDO was compared to the expected sequence deduced from the *TDO* gene present in MON 94313. The removal of the initiator methionine (M) *in vivo* was confirmed for the MON 94313-produced TDO protein. The *E. coli*-produced TDO protein sequence was produced with alanine as the N-terminal residue. The single letter International Union of Pure and Applied Chemistry - International Union of Biochemistry (IUPAC-IUB) amino acid code is M, methionine; A, alanine; D, aspartic acid; E, glutamic acid; S, serine; W, tryptophan; R, arginine; P, proline; I, isoleucine; V, valine; Q, glutamine; L, leucine

B.1(a)(ii)(iv)(ii) Results of nano LC-MS/MS mass fingerprint analysis

Peptide mass fingerprint analysis is a standard technique used for confirming the identity of proteins. The identity of the MON 94313-produced TDO protein was confirmed by LC-MS/MS analysis of peptide fragments produced by the trypsin digestion of the MON 94313-produced TDO protein.

There were 47 unique peptides identified that corresponded to the masses expected to be produced by trypsin digestion of the MON 94313-produced TDO protein (Table 30). The identified masses were used to assemble a coverage map of the entire TDO protein (Figure 40A). The experimentally determined coverage of the TDO protein was 88% (Figure 40A, 309 out of 351 amino acids). This analysis further confirms the identity of MON 94313-produced TDO protein.

There were 79 unique peptides identified that corresponded to the masses expected to be produced by trypsin digestion of the *E. coli*-produced TDO protein (Table 31) by Nano LC-MS/MS analysis during the protein characterisation. The identified masses were used to assemble a coverage map of the entire TDO protein (Figure 40B). The experimentally determined coverage of the *E. coli*-produced TDO protein was 100% (Figure 40B, 350 out of 350 amino acids). This analysis further confirms the identity of *E. coli*-produced TDO protein.

Table 30. Summary of the Tryptic Masses Identified for the MON 94313-Produced TDO Using Nano LC-MS/MS

Experimental Mass ^{1,2}	Calculated Mass ³	Diff ⁴	Fragment ⁵	Sequence ⁶
804.3390	804.3402	- 0.0012	2 - 7	ADESWR
2706.3237	2706.3249	- 0.0012	2 - 26	ADES...PPSR
1904.0000	1904.0003	- 0.0003	8 - 26	APAI...PPSR
563.3430	563.3431	- 0.0001	27 - 30	YLLR
546.2763	546.2762	0.0001	31 - 34	EKDR
975.4988	975.4985	0.0003	31 - 38	EKDRSDVK
718.3614	718.3610	0.0004	33 - 38	DRSDVK
447.2330	447.2329	0.0001	35 - 38	SDVK
1817.0300	1817.0298	0.0002	39 - 55	LVAA...DLSR
932.4451	932.4451	0.0000	56 - 64	LDGA...EATK
1201.6289	1201.6302	- 0.0013	56 - 66	LDGA...TKLR
3264.6084	3264.6060	0.0024	67 - 95	VALQ...NLSR
1178.5722	1178.5720	0.0002	96 - 104	EFFN...PIER
1148.6190	1148.6190	0.0000	106 - 115	QKFS...IDGK
892.4652	892.4654	- 0.0002	108 - 115	FSNLIDGK
2172.0598	2172.0600	- 0.0002	108 - 126	FSNL...GTDR
1297.6056	1297.6051	0.0005	116 - 126	NFQL...GTDR
1589.7697	1589.7686	0.0011	127 - 139	VVTQ...WSDR
2109.0969	2109.0967	0.0002	127 - 143	VVTQ...LHLR
471.2693	471.2693	0.0000	144 - 147	VEPK
2455.1478	2455.1444	0.0034	144 - 163	VEPK...ESFR
3024.4638	3024.4617	0.0021	144 - 168	VEPK...VLNK
2001.8860	2001.8857	0.0003	148 - 163	EEQD...ESFR
2571.2028	2571.2030	- 0.0002	148 - 168	EEQD...VLNK
587.3272	587.3279	- 0.0007	164 - 168	DVLNK
625.3070	625.3071	- 0.0001	169 - 174	YASGTK
781.4081	781.4082	- 0.0001	169 - 175	YASGTKR
1428.7872	1428.7871	0.0001	175 - 186	RIRD...AMAK
1288.6803	1288.6809	- 0.0006	176 - 186	IRDD...AMAK
1019.4958	1019.4957	0.0001	178 - 186	DDII...AMAK
1539.7463	1539.7457	0.0006	187 - 198	LLEL...FLDR
2509.2473	2509.2489	- 0.0016	187 - 207	LLEL...AFAR
987.5144	987.5137	0.0007	199 - 207	LNEA...AFAR
1000.5300	1000.5302	- 0.0002	240 - 248	DVSG...QVQR
3565.6601	3565.6640	- 0.0039	249 - 279	DGKW...GIFR
3249.5352	3249.5257	0.0095	252 - 279	WSNV...GIFR
594.3241	594.3238	0.0003	280 - 284	SPVHR
759.4126	759.4127	- 0.0001	285 - 291	VVTNAEK
1044.5559	1044.5564	- 0.0005	285 - 293	VVTN...EKER

Table 30. Summary of the Tryptic Masses Identified for the MON 94313-Produced TDO Using Nano LC-MS/MS (Continued)

Experimental Mass ^{1,2}	Calculated Mass ³	Difference ⁴	Fragment ⁵	Sequence ⁶
1497.7401	1497.7385	0.0016	294 - 306	ISLA...NDEK
3215.6123	3215.6132	- 0.0009	294 - 322	ISLA...RPAR
1735.8852	1735.8853	- 0.0001	307 - 322	DIEP...RPAR
992.5288	992.5291	- 0.0003	325 - 332	KVSVVEEFR
864.4342	864.4341	0.0001	326 - 332	VSVEEFR
591.3377	591.3380	- 0.0003	333 - 338	AGIFGK
765.4018	765.4021	- 0.0003	345 - 350	YIDSLR
878.4862	878.4861	0.0001	345 - 351	YIDSLRI

¹All imported values were rounded to 4 decimal places.

²Only experimental masses that matched calculated masses with the highest scores are listed in the table.

³The calculated mass is the relative molecular mass calculated from the matched peptide sequence.

⁴The calculated difference = experimental mass – calculated mass.

⁵Position refers to amino acid residues within the predicted MON 94313-produced TDO sequence.

⁶For peptide matches greater than nine amino acids in length, the first 4 residues and last 4 residues are show separated by three dots (...).

Table 31. Summary of the Tryptic Masses Identified for the *E. coli*-Produced TDO Using Nano LC-MS/MS

Experimental Mass ^{1,2}	Calculated Mass ³	Difference ⁴	Fragment ⁵	Sequence ⁶
762.3291	762.3297	-0.0006	1 - 6	ADESWR
2648.3218	2648.3194	0.0024	1 - 25	ADES...PPSR
3193.6550	3193.6519	0.0031	1 - 29	ADES...YLLR
1903.9996	1904.0003	-0.0007	7 - 25	APAI...PPSR
2449.3350	2449.3329	0.0021	7 - 29	APAI...YLLR
563.3435	563.3431	0.0004	26 - 29	YLLR
820.4801	820.4807	-0.0006	26 - 31	YLLREK
1091.6087	1091.6087	0.0000	26 - 33	YLLREKDR
546.2762	546.2762	0.0000	30 - 33	EKDR
975.4984	975.4985	-0.0001	30 - 37	EKDRSDVK
718.3609	718.3610	-0.0001	32 - 37	DRSDVK
447.2329	447.2329	0.0000	34 - 37	SDVK
2246.2555	2246.2522	0.0033	34 - 54	SDVK...DLSR
1817.0310	1817.0298	0.0012	38 - 54	LVAA...DLSR
2731.4648	2731.4643	0.0005	38 - 63	LVAA...EATK
3000.6502	3000.6495	0.0007	38 - 65	LVAA...TKLR
932.4463	932.4451	0.0012	55 - 63	LDGA...EATK
1201.6319	1201.6302	0.0017	55 - 65	LDGA...TKLR
3248.6112	3248.6111	0.0001	66 - 94	VALQ...NLSR
4409.1750	4409.1725	0.0025	66 - 103	VALQ...PIER
1178.5714	1178.5720	-0.0006	95 - 103	EFFN...PIER
1306.6673	1306.6670	0.0003	95 - 104	EFFN...IERK
1276.7133	1276.7139	-0.0006	104 - 114	KQKF...IDGK
1148.6192	1148.6190	0.0002	105 - 114	QKFS...IDGK
2428.2161	2428.2135	0.0026	105 - 125	QKFS...GTDR
892.4651	892.4654	-0.0003	107 - 114	FSNLIDGK
2172.0619	2172.0600	0.0019	107 - 125	FSNL...GTDR
3727.8206	3727.8231	-0.0025	107 - 138	FSNL...WSDR
1297.6052	1297.6051	0.0001	115 - 125	NFQI...GTDR
3372.6974	3372.6964	0.0010	115 - 142	NFQI...LHLR
1573.7711	1573.7737	-0.0026	126 - 138	VVTQ...WSDR
2093.1035	2093.1018	0.0017	126 - 142	VVTQ...LHLR
2546.3623	2546.3605	0.0018	126 - 146	VVTQ...VEPK
537.3389	537.3387	0.0002	139 - 142	LHLR
990.5985	990.5974	0.0011	139 - 146	LHLRVEPK
471.2694	471.2693	0.0001	143 - 146	VEPK
2455.1449	2455.1444	0.0005	143 - 162	VEPK...ESFR
3024.4614	3024.4617	-0.0003	143 - 167	VEPK...VLNK
2001.8877	2001.8857	0.0020	147 - 162	EEQD...ESFR

PART 2: SPECIFIC DATA REQUIREMENTS FOR SAFETY ASSESSMENT

Experimental Mass^{1,2}	Calculated Mass³	Difference⁴	Fragment⁵	Sequence⁶
2571.2000	2571.2030	-0.0030	147 - 167	EEQD...VLNK
3178.5019	3178.4996	0.0023	147 - 173	EEQD...SGTK
587.3279	587.3279	0.0000	163 - 167	DVLNK
1194.6249	1194.6244	-0.0003	163 - 173	DVLN...SGTK
1350.7256	1350.7255	0.0001	163 - 174	DVLN...GTKR
625.3072	625.3071	0.0001	168 - 173	YASGTK
781.4082	781.4082	0.0000	168 - 174	YASGTR
1428.7880	1428.7871	0.0009	174 - 185	RIRD...AMAK
1272.6860	1272.6860	0.0000	175 - 185	IRDD...AMAK
1003.5002	1003.5008	-0.0006	177 - 185	DDII...AMAK
1539.7452	1539.7457	-0.0005	186 - 197	LLEL...FLDR
2509.2493	2509.2489	0.0004	186 - 206	LLEL...AFAR
987.5140	987.5137	0.0003	198 - 206	LNEA...AFAR
3712.9455	3712.9440	0.0015	207 - 238	FNYY...LVDK
4695.4645	4695.4636	0.0009	207 - 247	FNYY...QVQR
1000.5300	1000.5302	-0.0002	239 - 247	DVSG...QVQR
3517.6794	3517.6792	0.0002	248 - 278	DGKW...GIFR
3217.5357	3217.5359	-0.0002	251 - 278	WSNV...GIFR
594.3238	594.3238	0.0000	279 - 283	SPVHR
1620.8690	1620.8696	-0.0006	279 - 292	SPVH...EKER
759.4926	759.4927	-0.0001	284 - 290	VVTNAEK
1044.5564	1044.5564	0.0000	284 - 292	VVTN...EKER
2508.2846	2508.2893	-0.0047	284 - 305	VVTN...NDEK
3484.7619	3484.7619	0.0000	291 - 321	ERIS...RPAR
1481.7445	1481.7435	0.0010	293 - 305	ISLA...NDEK
3199.6181	3199.6183	-0.0002	293 - 321	ISLA...RPAR
1735.8844	1735.8853	-0.0009	306 - 321	DIEP...RPAR
2055.0532	2055.0497	0.0035	306 - 323	DIEP...ARYR
1311.6936	1311.6935	0.0001	322 - 331	YRKV...EEFR
992.5286	992.5291	-0.0005	324 - 331	KVSVEEFR
1565.8568	1565.8566	0.0002	324 - 337	KVSV...IFGK
864.4349	864.4349	0.0000	325 - 331	VSVVEEFR
1437.7625	1437.7616	0.0009	325 - 337	VSVE...IFGK
591.3379	591.3380	-0.0001	332 - 337	AGIFGK
981.5395	981.5396	-0.0001	332 - 340	AGIF...KFSR
1323.7049	1323.7048	0.0001	332 - 343	AGIF...RGER
750.3774	750.3773	0.0001	338 - 343	FSRGER
1220.6522	1220.6513	0.0009	349 - 350	GERY...SLRI
765.4024	765.4021	0.0003	344 - 349	YIDSLR
878.4862	878.4861	0.0001	344 - 350	YIDSLRI

PART 2: SPECIFIC DATA REQUIREMENTS FOR SAFETY ASSESSMENT

¹ All imported values were rounded to 2 decimal places.

² Only experimental masses that matched calculated TDO trypsin digested masses are listed in the table.

³ The calculated mass is the exact molecular mass calculated from the matched peptide sequence.

⁴ The calculated difference = experimental mass - calculated mass.

⁵ Position refers to amino acid residues within the predicted *E. coli*-produced TDO sequence.

⁶ For peptide matches greater than nine amino acids in length, the first 4 residues and last 4 residues are show separated by three dots (...).

PART 2: SPECIFIC DATA REQUIREMENTS FOR SAFETY ASSESSMENT

(A)

1 MADESWRAPA IVQELAAAGV EPPSRYLLR EKDRSDVKLV AAELPEPLPV
 51 VDLSRLDGAE EATKLRVALQ NWGFFLLTNH GVEASLMDSV MNLSREFFNQ
 101 PIERKQKFSN LIDGKNFQIQ GYGTDRVVTQ DQILDWSDRL HLRVEPKKEEQ
 151 DLAFWPDHPE SFRDVLNKYA SGTKRIRDDI IQAMAKLLEL DEDYFLDRLN
 201 EAPAFARFNY YPPCPRPDV FGIRPHSDGT LLTILLVDKDV VSGLQVQRDG
 251 KWSNVEATPH TLLINLGD TM EVMCNGIFRS PVHRVVTNAE KERISLAMLY
 301 SVNDEKDIEP AAGLLDENRP ARYRKVSVVEE FRAGIFGKFS RGERYIDSLR
 351 I

(B)

1 ADESWRAPAI VQELAAAGVE EPPSRYLLRE KDRSDVKLVA AELPEPLPVV
 51 DLSRLDGAE EATKLRVALQN WGFFLLTNHG VEASLMDSVM NLSREFFNQP
 101 IERKQKFSNL IDGKNFQIQG YGTDRVVTQD QILDWSDRLH LRVEPKKEEQD
 151 LAFWPDHPES FRDVLNKYAS GTKRIRDDII QAMAKLLELD EDYFLDRLNE
 201 APAFARFNY PPCPRPDV FGIRPHSDGT LLTILLVDKDV SGLQVQRDGK
 251 WSNVEATPHT LLINLGD TME VMCNGIFRSP VHRVVTNAEK ERISLAMLYS
 301 VNDEKDIEPA AGLLDENRPA RYRKVSVEEF RAGIFGKFSR GERYIDSLRI

Figure 40. Peptide Map of the MON 94313-Produced TDO and *E. coli*-Produced TDO

(A). The amino acid sequence of the MON 94313-produced TDO protein was deduced from the *TDO* gene present in MON 94313. Boxed regions correspond to peptides that were identified from the MON 94313-produced TDO protein sample using Nano LC-MS/MS. In total, 88% coverage (309 out of 351 amino acids) of the expected protein sequence was covered by the identified peptides.

(B). The amino acid sequence of the *E. coli*-produced TDO protein was deduced from the *TDO* gene that is contained on the expression plasmid. Boxed regions correspond to peptides that were identified from the *E. coli*-produced TDO protein sample using Nano LC-MS/MS. In total, 100% coverage (350 out of 350 amino acids) of the expected protein sequence was covered by the identified peptides.

B.1(a)(ii)(iv)(iii) Results of western blot analysis of the TDO protein isolated from the grain of MON 94313 and immunoreactivity comparison to *Bt*-produced TDO protein

Western blot analysis was conducted using mouse anti-TDO monoclonal antibody as additional means to confirm the identity of the TDO protein isolated from the seed of MON 94313 and to assess the equivalence of the immunoreactivity of the MON 94313-produced and *E. coli*-produced TDO proteins.

The results showed that immunoreactive bands with the same electrophoretic mobility were present in all lanes loaded with the MON 94313-produced and *E. coli*-produced TDO proteins (Figure 41). For each amount loaded, comparable signal intensity was observed between the MON 94313-produced and *E. coli*-produced TDO protein bands. As expected, the signal intensity increased with increasing load amounts of the MON 94313-produced and *E. coli*-produced TDO proteins, thus, supporting identification of MON 94313-produced TDO protein.

To compare the immunoreactivity of the MON 94313-produced and the *E. coli*-produced TDO proteins, densitometric analysis was conducted on the bands that migrated at the expected apparent MW for TDO proteins (~37 kDa). The signal intensity (reported in OD) of the band of interest in lanes loaded with MON 94313-produced and the *E. coli*-produced TDO proteins was measured (Table 32). Because the mean signal intensity of the MON 94313-produced TDO protein band was within $\pm 35\%$ of the mean signal of the *E. coli*-produced TDO protein, the MON 94313-produced TDO and *E. coli*-produced TDO proteins were determined to have equivalent immunoreactivity.

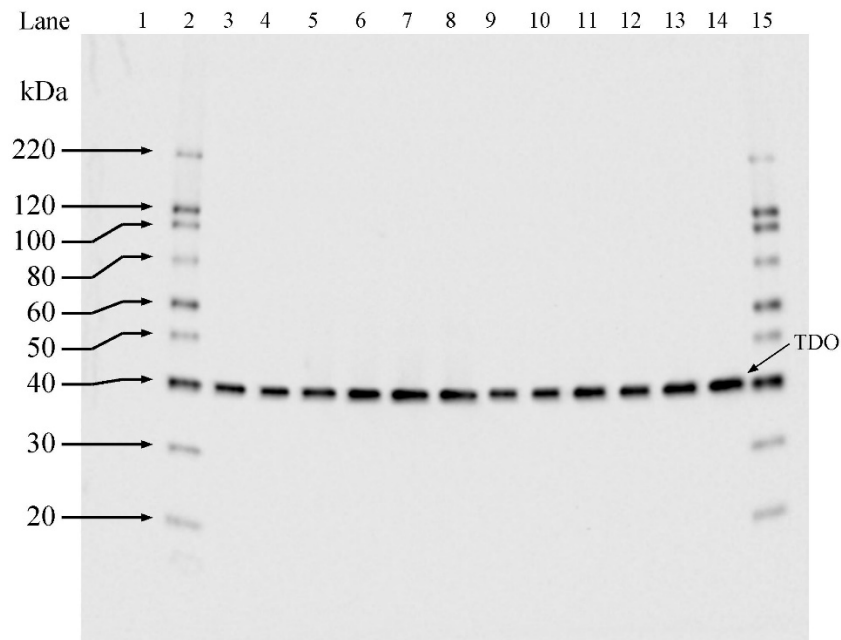


Figure 41. Western Blot Analysis of MON 94313-Produced and *E. coli*-Produced TDO

Aliquots of the MON 94313-produced TDO protein and the *E. coli*-produced TDO protein were subjected to SDS-PAGE and electrotransferred to a nitrocellulose membrane. Proteins were detected using mouse anti-TDO monoclonal antibody and then horse anti-mouse antibody conjugated with peroxidase. Immunoreactive bands were visualized using an ECL system. The 6 second exposure is shown. The approximate MW (kDa) of the standards are shown on the left. Lane designations are as follows:

<u>Lane</u>	<u>Sample</u>	<u>Amount (ng)</u>
1	Precision Plus Protein™ Standards	-
2	Magic Mark™ XP Western Standard	-
3	<i>E. coli</i> -produced TDO	4
4	<i>E. coli</i> -produced TDO	4
5	<i>E. coli</i> -produced TDO	8
6	<i>E. coli</i> -produced TDO	8
7	<i>E. coli</i> -produced TDO	12
8	<i>E. coli</i> -produced TDO	12
9	MON 94313-produced TDO	4
10	MON 94313-produced TDO	4
11	MON 94313-produced TDO	8
12	MON 94313-produced TDO	8
13	MON 94313-produced TDO	12
14	MON 94313-produced TDO	12
15	Magic Mark™ XP Western Standard	-

Table 32. Immunoreactivity of the MON 94313-Produced and *E. coli*-Produced TDO Proteins

Mean Signal Intensity from MON 94313-Produced TDO ¹ (OD)	Mean Signal Intensity from <i>E. coli</i> -Produced TDO ¹ (OD)	Acceptance Limits ² (OD)
3,991,148	4,081,707	2,653,110 – 5,510,304

¹ Each value represents the mean of six values (n = 6).

² The acceptance limits are for the MON 94313-produced TDO protein and are based on the interval between -35% ($4,081,707 \times 0.65 = 2,653,110$) and +35% ($4,081,707 \times 1.35 = 5,510,304$) of the mean of the *E. coli*-produced TDO signal intensity across all loads.

B.1(a)(ii)(iv)(v) Results of the TDO protein molecular weight and purity analysis

For apparent MW and purity determination, the MON 94313-produced TDO and the *E. coli*-produced TDO proteins were subjected to SDS-PAGE. Following electrophoresis, the gel was stained with Brilliant Blue G-Colloidal stain and analyzed by densitometry. The MON 94313-produced TDO protein (Figure 42, lanes 3-8) migrated to the same position on the gel as the *E. coli*-produced TDO protein (Figure 42, lane 2) and the apparent MW was calculated to be 36.9 kDa (Table 33). Because the experimentally determined apparent MW of the MON 94313-produced TDO protein was within the acceptance limits for equivalence (Table 34), the MON 94313-produced TDO and *E. coli*-produced TDO proteins were determined to have equivalent apparent molecular weights.

The purity of the MON 94313-produced TDO protein was calculated based on the six lanes loaded on the gel (Figure 42, lanes 3-8). The average purity was determined to be 71% (Table 33).

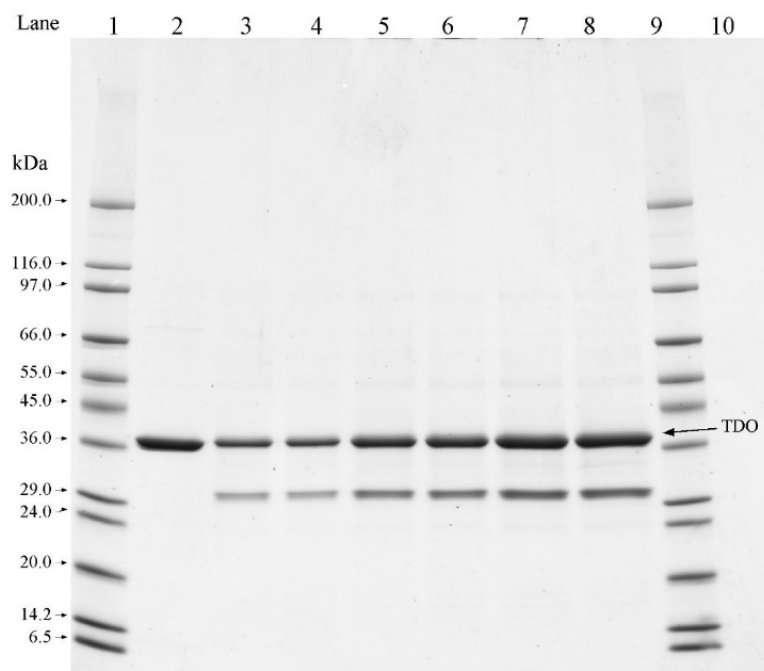


Figure 42. Purity and Apparent Molecular Weight Analysis of the MON 94313-Produced and *E. coli*-Produced TDO Proteins

Aliquots of the MON 94313-produced and the *E. coli*-produced TDO proteins were subjected to SDS-PAGE and the gel was stained with Brilliant Blue G-Colloidal stain. The MWs (kDa) are shown on the left and correspond to the standards loaded in lanes 1 and 9. Lane designations are as follows:

<u>Lane</u>	<u>Sample</u>	<u>Amount (µg)</u>
1	SigmaMarker™ Wide Range Standard	-
2	<i>E. coli</i> -produced TDO	1.0
3	MON 94313-produced TDO	0.5
4	MON 94313-produced TDO	0.5
5	MON 94313-produced TDO	1.0
6	MON 94313-produced TDO	1.0
7	MON 94313-produced TDO	1.5
8	MON 94313-produced TDO	1.5
9	SigmaMarker™ Wide Range Standard	-
10	Blank	

Table 33. Apparent Molecular Weight and Purity Analysis of the MON 94313-Produced TDO Protein

	Apparent MW ¹ (kDa)	Purity ² (%)
Average (n=6)	36.9	71

¹Final MW was rounded to one decimal place.

²Average % purity was rounded to the nearest whole number.

Table 34. Apparent Molecular Weight Comparison Between the MON 94313-Produced TDO and *E. coli*-Produced TDO Proteins

Apparent MW of MON 94313-Produced TDO Protein (kDa)	Apparent MW of <i>E. coli</i> -Produced TDO Protein (kDa)	Acceptance Limits ¹ (kDa)
36.9	37.0	36.6 – 37.4

¹Data obtained for the *E. coli*-produced TDO protein and several plant-produced TDO proteins was used to generate the prediction interval (Appendix 9).

B.1(a)(ii)(iv)(vi) TDO glycosylation analysis

Some eukaryotic proteins are post-translationally modified by the addition of carbohydrate moieties ([Rademacher et al., 1988](#)). To test whether the TDO protein was glycosylated when expressed in the soybean grain of MON 94313, the MON 94313-produced TDO protein was analyzed using an ECL™ glycoprotein detection method. Transferrin, a glycosylated protein, was used as a positive control in the assay. To assess equivalence of the MON 94313-produced and *E. coli*-produced TDO proteins, the *E. coli*-produced TDO protein, previously shown to be free of glycosylation ([Harrison et al., 1996](#)), was also analyzed.

A clear glycosylation signal was observed at the expected molecular weight (~80 kDa) in the lanes containing the positive control (transferrin) and the band intensity increased with increasing concentration (Figure 43A). In contrast, no glycosylation signal was observed in the lanes containing the *E. coli*-produced TDO protein or MON 94313-produced TDO protein (Figure 43A).

To confirm that MON 94313-produced TDO and *E. coli*-produced TDO proteins were appropriately loaded for glycosylation analysis, a second membrane with identical loadings and transfer time was stained with Coomassie Blue R250 for protein detection. Both the MON 94313-produced and *E. coli*-produced TDO proteins were detected (Figure 43B). These data indicate that the glycosylation status of MON 94313-produced TDO protein is equivalent to that of the *E. coli*-produced TDO protein and that neither is glycosylated.

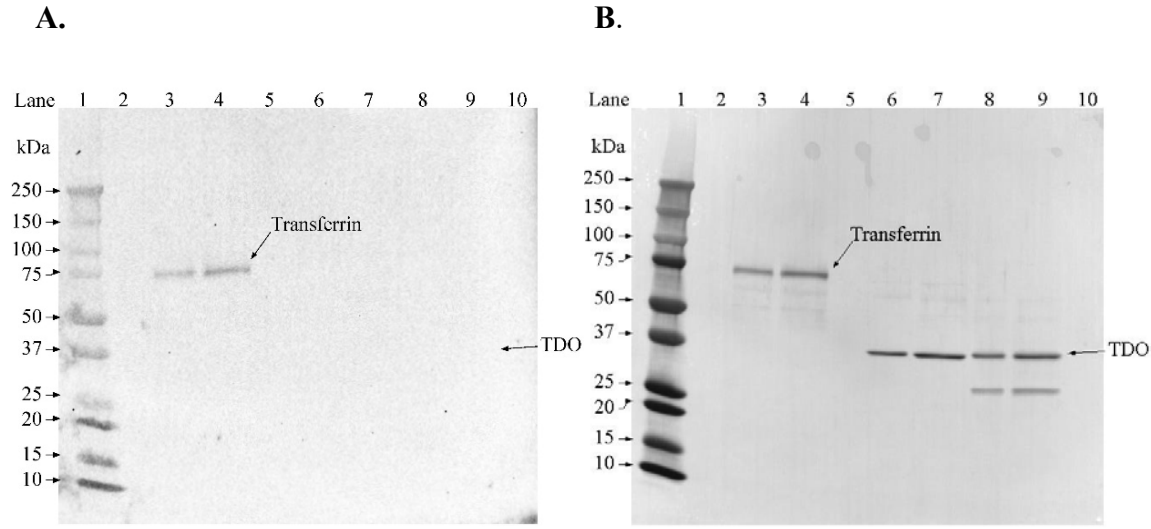


Figure 43. Glycosylation Analysis of the MON 94313-Produced TDO Protein

Aliquots of the transferrin (positive control), *E. coli*-produced TDO and MON 94313-produced TDO were subjected to SDS-PAGE and electrotransferred to a PVDF membrane. The MWs (kDa) correspond to the Precision Plus Protein™ Standards. The arrows show the expected migration of the MON 94313-produced and *E. coli*-produced TDO proteins and transferrin. (A) Where present, the labeled carbohydrate moieties were detected by addition of streptavidin conjugated to HRP followed by a luminol-based the detection using ECL reagents. The 6-minute exposure is shown. (B) An equivalent blot was stained with Coomassie Blue R250 to confirm the presence of proteins. Lane designations are as follows:

<u>Lane</u>	<u>Sample</u>	<u>Amount (ng)</u>
1	Precision Plus Protein™ Standards	-
2	Blank	-
3	Transferrin (positive control)	100
4	Transferrin (positive control)	200
5	Blank	-
6	<i>E. coli</i> -produced TDO	100
7	<i>E. coli</i> -produced TDO	200
8	MON 94313-produced TDO	100
9	MON 94313-produced TDO	200
10	Blank	-

B.1(a)(ii)(iv)(vi) TDO functional activity

The functional activity of the MON 94313-produced and *E. coli*-produced TDO proteins was assessed by measuring the amount of mesotrione that was converted to the oxidized mesotrione products hydroxy-mesotrione and keto-mesotrione over the course of 30 min. In this assay, protein-specific activity is expressed as nmol mesotrione converted per minute per milligram of TDO protein. The MON 94313-produced TDO and *E. coli*-produced TDO proteins were considered to have equivalent functional activity if the specific activity of both TDO proteins were within acceptance limits of 94.0-233.8 nmol × min⁻¹ × mg⁻¹ (the prediction interval calculated from a data set based on assays conducted for the *E. coli*-produced TDO protein; see Appendix 9, Table 2).

The experimentally determined specific activity for the MON 94313-produced and *E. coli*-produced TDO proteins are presented in Table 35. The specific activities of MON 94313-produced and *E. coli*-produced TDO proteins were 118.6 and 156 nmol × min⁻¹ × mg⁻¹, respectively. Because the specific activities of MON 94313-produced and *E. coli*-produced TDO proteins fall within the preset acceptance limits (Table 35), the MON 94313-produced TDO protein was considered to have equivalent functional activity to that of the *E. coli*-produced TDO protein.

Table 35. Functional Activity of MON 94313-Produced and *E. coli*-Produced TDO Proteins

MON 94313-Produced TDO¹ (nmol × min⁻¹ × mg⁻¹)	<i>E. coli</i>-Produced TDO¹ (nmol × min⁻¹ × mg⁻¹)	Acceptance Limits² (nmol × min⁻¹ × mg⁻¹)
118.6	156.0	94.0 – 233.8

¹ Value refers to mean calculated based on triplicate samples (n = 3).

² Data obtained for the *E. coli*-produced TDO was used to generate a prediction interval for setting the acceptance limits (Appendix 9).

B.1(a)(ii)(iv)(vii) MON 94313 TDO protein identity and equivalence conclusion

The TDO protein purified from grain of MON 94313 soybean was characterized and the equivalence of the immunoreactive and physicochemical characteristics and functional activity between the MON 94313-produced and the *E. coli*-produced TDO proteins was established using a panel of analytical tests: 1) the N-terminal sequence of the MON 94313-produced TDO protein was confirmed by Nano LC-MS/MS analysis; 2) Nano LC-MS/MS analysis yielded peptide masses consistent with the expected peptide masses from the theoretical tryptic digest of the MON 94313-produced TDO sequence; 3) MON 94313-produced TDO protein was detected on a western blot probed with antibodies specific for TDO protein and the immunoreactive properties of the MON 94313-produced and *E. coli*-produced TDO proteins were shown to be equivalent; 4) the electrophoretic mobility and apparent molecular weight of the MON 94313-produced and *E. coli*-produced TDO proteins were shown to be equivalent; 5) the glycosylation status of MON 94313-produced and *E. coli*-produced TDO proteins were determined to be equivalent and neither to be glycosylated; and 6) functional activities of the MON 94313-produced and *E. coli*-produced TDO proteins were demonstrated to be equivalent.

Taken together, these data provide a detailed characterisation of the MON 94313-produced TDO protein and establish the equivalence of the MON 94313-produced and the *E. coli*-produced TDO proteins. This equivalence justifies the use of the *E. coli*-produced TDO protein in studies to establish the safety of the TDO protein expressed in MON 94313.

B.1(a)(iii) Expression levels of DMO, PAT, FT_T.1 and TDO proteins in MON 94313

The protein expression levels determined in MON 94313 are used to assess exposure to the introduced proteins via food or feed ingestion and potential environmental exposure. The most appropriate tissues to evaluate DMO, PAT, FT_T.1 and TDO protein levels are forage, grain, leaf, and root tissue samples. Levels of the introduced proteins were determined in forage and grain tissue to evaluate food and feed exposure in humans and animals, where the levels are utilized to also calculate margins of exposure for each protein. Leaf and root tissues are distinct above and below ground plant tissues that are important to estimate environmental exposure. The materials and methods used in the validated immunoassay are described in Appendix 10.

MON 94313 DMO, PAT, FT_T.1 and TDO protein levels in various tissues of MON 94313 relevant to characterisation and risk assessment were determined by validated immunoassays. Tissues of MON 94313 were collected from four replicate plots planted in a randomized complete block field design during the 2020 growing season from the following five field sites in the U.S.: Jefferson County, Iowa (IARL), Butler County, Missouri (MOFI), York County, Nebraska (NEYO), Warren County, Illinois (ILMN), and Walworth County, Wisconsin (WIDL). The field sites were representative of soybean-producing regions suitable for commercial production. Forage, grain, leaf, and root tissue samples were collected from each replicated plot at all field sites treated with dicamba, glufosinate, 2,4-D and mesotrione. Samples were collected at the following growth stages:

PART 2: SPECIFIC DATA REQUIREMENTS FOR SAFETY ASSESSMENT

Tissue type ¹	Growth Stage (BBCH) ¹
Forage	77
Grain	99
Leaf	14-15
Root	77

¹BBCH = Biologische Bundesanstalt, Bundessortenamt und Chemische Industrie; a scale used to identify the phenological development stages of plants ([Meier, 2001](#)).

For details, please refer to Appendix 10.

B.1(a)(iii)(i) Expression levels of DMO protein

MON 94313 DMO protein levels were determined in four tissue types. The results obtained from immunoassays are summarized in Table 36 and the details of the materials and methods are described in Appendix 10. The mean DMO protein levels were determined across five sites treated with dicamba, glufosinate, 2,4-D and mesotrione. Samples with values determined to be less than the LOD or LOQ were not included in mean determinations. The mean DMO protein level in MON 94313 across all sites was highest in forage at 150 µg/g dw and lowest in root at 20 µg/g dw. The mean DMO protein level in MON 94313 was 40 µg/g dw in grain.

Table 36. Summary of DMO Protein Levels in Tissues Collected from MON 94313 Soybean Produced in United States Field Trials During 2020

Tissue Type	Development Stage ¹	Mean (SE) Range (µg/g dw) ²	LOQ/LOD (µg/g dw) ³
Forage	BBCH 77	150 (7.4) 100-230	0.007/0.004
Grain	BBCH 99	40 (1.2) 32-49	0.007/0.004
Leaf	BBCH 14-15	68 (3.7) 45-100	0.007/0.004
Root	BBCH 77	20 (1.1) 10-27	0.007/0.004

¹The crop development stage at which each tissue was collected.

² Protein levels are expressed as the arithmetic mean and standard error (SE) as microgram (µg) of protein per gram (g) of tissue on a dry weight basis (dw). The means, SE, and ranges (minimum and maximum values) were calculated for each tissue across all five sites (n=20).

³LOQ=limit of quantitation, LOD=limit of detection.

B.1(a)(iii)(ii) Expression levels of PAT protein

MON 94313 PAT protein levels were determined in four tissue types. The results obtained from immunoassays are summarized in Table 37 and the details of the materials and methods are described in Appendix 10. The mean PAT protein levels were determined across five sites treated with dicamba, glufosinate, 2,4-D and mesotrione. Samples with values determined to be less than the LOD or LOQ were not included in mean determinations. The mean PAT protein level in MON 94313 across all sites was highest in leaf at 19 µg/g dw and lowest in root at 3.7 µg/g dw. The mean PAT protein level in MON 94313 was 3.8 µg/g dw in grain.

Table 37. Summary of PAT Protein Levels in Tissues Collected from MON 94313 Soybean Produced in United States Field Trials During 2020

Tissue Type	Development Stage¹	Mean (SE) Range (µg/g dw)²	LOQ/LOD (µg/g dw)³
Forage	BBCH 77	12 (0.74)	0.007/0.003
		6.7-18	
Grain	BBCH 99	3.8 (0.14)	0.007/0.003
		2.6-4.6	
Leaf	BBCH 14-15	19 (1.1)	0.014/0.007
		12-29	
Root	BBCH 77	3.7 (0.25)	0.007/0.003
		1.7-5.4	

¹The crop development stage at which each tissue was collected.

² Protein levels are expressed as the arithmetic mean and standard error (SE) as microgram (µg) of protein per gram (g) of tissue on a dry weight basis (dw). The means, SE, and ranges (minimum and maximum values) were calculated for each tissue across all five sites (n=20).

³LOQ=limit of quantitation, LOD=limit of detection.

B.1(a)(iii)(iii) Expression levels of FT_T.1 protein

MON 94313 FT_T.1 protein levels were determined in four tissue types. The results obtained from immunoassays are summarized in

PART 2: SPECIFIC DATA REQUIREMENTS FOR SAFETY ASSESSMENT

Table 38 and the details of the materials and methods are described in Appendix 10. The mean FT_T.1 protein levels were determined across five sites treated with dicamba, glufosinate, 2,4-D and mesotrione. Samples with values determined to be less than the LOD or LOQ were not included in mean determinations. The mean FT_T.1 protein level in MON 94313 across all sites was the highest in leaf at 20 µg/g dw and lowest in root at 4.1 µg/g dw. The mean FT_T.1 protein level in MON 94313 was 6.1 µg/g dw in grain.

Table 38. Summary of FT_T.1 Protein Levels in Tissues Collected from MON 94313 Soybean Produced in United States Field Trials During 2020

Tissue Type	Development Stage ¹	Mean (SE) Range (µg/g dw) ²	LOQ/LOD (µg/g dw) ³
Forage	BBCH 77	11 (0.48) 7.5-15	0.046/0.028
Grain	BBCH 99	6.1 (0.16) 4.7-7.2	0.023/0.014
Leaf	BBCH 14-15	20 (0.60) 14-25	0.023/0.014
Root	BBCH 77	4.1 (0.25) 2.3-6.0	0.023/0.014

¹The crop development stage at which each tissue was collected.

² Protein levels are expressed as the arithmetic mean and standard error (SE) as microgram (µg) of protein per gram (g) of tissue on a dry weight basis (dw). The means, SE, and ranges (minimum and maximum values) were calculated for each tissue across all five sites (n=20).

³LOQ=limit of quantitation, LOD=limit of detection.

B.1(a)(iii)(iv) Expression levels of TDO protein

MON 94313 TDO protein levels were determined in four tissue types. The results obtained from immunoassays are summarized in

PART 2: SPECIFIC DATA REQUIREMENTS FOR SAFETY ASSESSMENT

Table 39 and the details of the materials and methods are described in Appendix 10. The mean TDO protein levels were determined across five sites treated with dicamba, glufosinate, 2,4-D and mesotrione. Samples with values determined to be less than the LOD or LOQ were not included in mean determinations. The mean TDO protein level in MON 94313 across all sites was the highest in leaf at 41 µg/g dw and lowest in root at <LOQ (0.50 µg/g dw for root). The mean TDO protein level in MON 94313 was 5.0 µg/g dw in grain.

Table 39. Summary of TDO Protein Levels in Tissues Collected from MON 94313 Soybean Produced in United States Field Trials During 2020

Tissue Type	Development Stage¹	Mean (SE) Range (µg/g dw)²	LOQ/LOD (µg/g dw)³
Forage	BBCH 77	12 (0.58) 8.8-17	1.0/0.421
Grain	BBCH 99	5.0 (0.36) 2.8-8.1	0.50/0.312
Leaf	BBCH 14-15	41 (1.9) 25-53	1.0/0.413
Root	BBCH 77	<LOQ	0.50/0.341

¹The crop development stage at which each tissue was collected.

² Protein levels are expressed as the arithmetic mean and standard error (SE) as microgram (µg) of protein per gram (g) of tissue on a dry weight basis (dw). The means, SE, and ranges (minimum and maximum values) were calculated for each tissue across all five sites (n=20, except root which had 14 samples expressing <LOQ and 6 positive samples with a mean of 0.91 (0.088) µg/g dw).

³LOQ=limit of quantitation, LOD=limit of detection.

B.1(b) Information about prior history of human consumption of the new substances, if any, or their similarity to substances previously consume in food.

Refer to Section A.2(a)(i) and A.2(a)(ii).

B.1(c) Information on whether any new protein has undergone any unexpected post-translational modification in the new host

Refer to Sections B.1(a)(ii).

B.1(d) Where any ORFs have been identified, bioinformatics analysis to indicate the potential for allergenicity and toxicity of the ORFs

Refer to Section A.3(c)(v).

B.2 New Proteins

B.2(a) Information on the potential toxicity of any new proteins, including:

B.2(a)(i) A bioinformatic comparison of the amino acid sequence of each of the new proteins to know protein toxins and anti-nutrients (e.g. protease inhibitors, lectins)

Potential structural similarities shared between the MON 94313 DMO, PAT, FT_T.1 and TDO proteins with sequences in a protein database were evaluated using the FASTA sequence alignment tool. The FASTA program directly compares amino acid sequences (*i.e.*, primary, linear protein structure) and the alignment data may be used to infer shared higher order structural similarities between two sequences (*i.e.*, secondary and tertiary protein structures). Proteins that share a high degree of similarity throughout the entire sequence are often homologous. Homologous proteins often have common secondary structures, common three-dimensional configuration, and, consequently, may share similar functions ([Caetano-Anollés *et al.*, 2009](#); [Illergård *et al.*, 2009](#)).

FASTA bioinformatic alignment searches using the MON 94313 DMO amino acid sequence, PAT amino acid sequence, FT_T.1 amino acid sequence and TDO amino acid sequence were performed with the toxin database to identify possible homology with proteins that may be harmful to human and animal health. Periodically, the databases used to evaluate proteins are updated. Since the most recent reports were completed, the toxin (TOX_2022) and protein (PRT_2022) databases have been revised and updated. In order to determine if proteins share significant sequence similarity to new sequences contained in the updated toxin database they were used as a queries for a FASTA searches of the TOX_2022 database. The UniProt toxin protein database (TOX_2022) is a subset of sequences derived from the Swiss-Prot database (found at <https://www.uniprot.org/>) that were selected using a keyword search and filtered to remove likely non-toxin proteins.. It is referred to herein as the TOX_2022 database and contains 8,131 sequences.

Using MON 94313 DMO as the query sequence, no alignment with an *E*-score of $\leq 1e-5$ was observed using the TOX_2022 database to run a FASTA search.

Using PAT as the query sequence, no alignment with an *E*-score of $\leq 1e-5$ was observed using the TOX_2022 database to run a FASTA search.

Using FT_T.1 as the query sequence, no alignment with an *E*-score of $\leq 1e-5$ was observed using the TOX_2022 database to run a FASTA search.

Using TDO as the query sequence, no alignment with an *E*-score of $\leq 1e-5$ was observed using the TOX_2022 database to run a FASTA search.

For details, please refer to Appendix 11 and Appendix 12.

B.2(a)(ii) Information on the stability of the proteins to proteolysis in appropriate gastrointestinal model systems**B.2(a)(ii)(i) Digestive fate of the DMO protein****Degradation of the MON 94313 DMO Protein by Pepsin**

Degradation of the *E. coli*-produced DMO protein by pepsin was evaluated over time by analyzing digestion mixtures incubated for targeted time intervals following a standardized protocol validated in an international, multi-laboratory ring study ([Thomas *et al.*, 2004](#)) collected at targeted incubation time points. The susceptibility of the DMO protein to pepsin degradation was assessed by visual analysis of a Brilliant Blue G-Colloidal stained SDS-PAGE gel and by visual analysis of a western blot probed with an anti-DMO antibody. Both visualization methods were run concurrently with separate SDS-PAGE and western blot analyses to estimate the limit of detection (LOD) of the DMO protein for each method.

For SDS-PAGE analysis of the digestibility of the DMO protein in pepsin, the gel was loaded with 1 µg of total test protein (based on pre-digestion protein concentrations) for each of the digestion samples (Figure 44A). The SDS-PAGE gel used to assess the resistance of the DMO protein to pepsin digestion (Figure 44A) was run concurrently with a SDS-PAGE to estimate the LOD of the DMO protein (Figure 44B). The LOD of the DMO protein was approximately 6.3 ng (Figure 44B, lane 8). The LOD was used to calculate the maximum relative amount of DMO protein that could remain visually undetected after digestion, which corresponded to approximately 0.63% ($6.3 / 1000 \times 100\% = 0.63\%$) of the total protein loaded.

Examination of SDS-PAGE data showed that the intact MON 94313 DMO protein was digested within 0.5 min of incubation with pepsin (see Figure 44A, lane 5). A faint band of ~3.5 kDa peptide fragment was observed through 5 min but disappeared by 10 min of the pepsin digestion. Based on the SDS-PAGE LOD for the DMO protein, it can be concluded that more than 99.4% ($100\% - 0.63\% = 99.4\%$) of the intact DMO protein was degraded within 0.5 min. A faint band of ~3.5 kDa peptide fragment was observed through 5 min but disappeared by 10 min of the pepsin digestion.

No change in the DMO protein band intensity was observed in the absence of pepsin in the 0 min No Pepsin Control and 60 min No Pepsin Control samples (Figure 44A, lanes 3 and 12). This indicates that the degradation of the DMO protein was due to the proteolytic activity of pepsin and not due to instability of the protein while incubated in the pepsin test system over the course of the experiment.

The 0 min No Test Protein Control and 60 min No Test Protein Control (Figure VI-30, Panel A, lanes 2 and 13) demonstrated that the pepsin is stable throughout the experimental phase.

A separate SDS-PAGE gel to estimate the LOD of the DMO protein was run concurrently with the SDS-PAGE for the degradation assessment (Figure 44B). The LOD of the intact MON 94313 DMO protein was approximately 6.3 ng (see Figure 44B, lane 8). The LOD was used to calculate the maximum relative amount of the MON 94313 DMO protein that could remain visually undetected after digestion, which corresponded to approximately 0.63% of the MON 94313 DMO

PART 2: SPECIFIC DATA REQUIREMENTS FOR SAFETY ASSESSMENT

protein loaded. Therefore, based on the LOD, more than 99.4% ($100\% - 0.63\% \cong 99.4\%$) of the intact MON 94313 DMO protein was digested within 0.5 min of incubation with pepsin.

For details, please refer to Appendix 13.

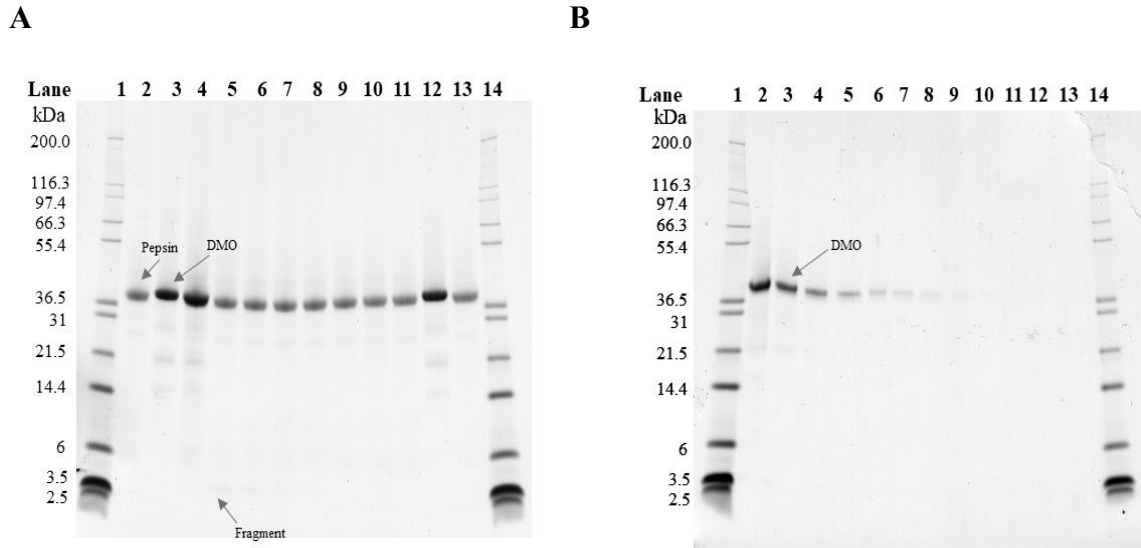


Figure 44. SDS-PAGE Analysis of the Degradation of DMO Protein by Pepsin

Colloidal Brilliant Blue G stained SDS-PAGE gels were used to assess the degradation of the DMO protein by pepsin. Molecular weights (kDa) are shown on the left of each gel, and correspond to the protein markers loaded. Empty lanes were cropped from the images.

A: DMO protein degradation by pepsin. Based on pre-reaction protein concentrations, 1 µg of test protein was loaded in each lane containing MON 94313 DMO protein.

B: LOD determination. Various amounts of the test protein from the Pepsin Treated T0 sample were loaded to estimate the LOD of the MON 94313 DMO protein.

Lane	Sample	Incubation Time (min)	Lane	Sample	Amount (ng)
1	Mark 12™ MWM	-	1	Mark 12™ MWM	-
2	0 min No Test Protein Control	0	2	Pepsin Treated T0	360
3	0 min No Pepsin Control	0	3	Pepsin Treated T0	200
4	Pepsin Treated T0	0	4	Pepsin Treated T0	100
5	Pepsin Treated T1	0.5	5	Pepsin Treated T0	50
6	Pepsin Treated T2	2	6	Pepsin Treated T0	18
7	Pepsin Treated T3	5	7	Pepsin Treated T0	12.5
8	Pepsin Treated T4	10	8	Pepsin Treated T0	6.3
9	Pepsin Treated T5	20	9	Pepsin Treated T0	3.1
10	Pepsin Treated T6	30	10	Pepsin Treated T0	1.3
11	Pepsin Treated T7	60	11	Pepsin Treated T0	0.6
12	60 min No Pepsin Control	60	12	Pepsin Treated T0	0.4
13	60 min No Test Protein Control	60	13	Pepsin Treated T0	0.2
14	Mark 12™ MWM	-	14	Mark 12™ MWM	-
15	Empty	-	15	Empty	-

For western blot analysis of DMO pepsin susceptibility, the DMO protein was loaded with approximately 10 ng per lane of total protein (based on pre-reaction total protein concentrations) for each reaction time point examined. The western blot used to assess the resistance of the DMO protein to pepsin digestion (Figure 45A) was run concurrently with a western blot to estimate the LOD of the DMO protein (Figure 45B). The LOD of the DMO protein was approximately 0.16 ng (Figure 45B, lane 10). The LOD was used to calculate the maximum relative amount of DMO protein that could remain visually undetected after digestion, which corresponded to approximately 1.6% ($0.16 / 10 \times 100\% = 1.6\%$) of the total protein loaded.

Western blot analysis demonstrated that the DMO protein was degraded below the LOD within 0.5 min of incubation in the presence of pepsin (Figure 45A, lane 6). Based on the western blot LOD for the DMO protein, it can be concluded that more than 98.4% ($100\% - 1.6\% = 98.4\%$) of the intact DMO protein was degraded within 0.5 min. No peptide fragments were detected at any timepoint in pepsin by western blot.

No apparent change in the DMO protein band intensity was observed in the absence of pepsin in the 0 min No Pepsin Control and 60 min No Pepsin Control samples (Figure 45A, lanes 4 and 13). This indicates that the degradation of the DMO protein was due to the proteolytic activity of pepsin and not due to instability of the protein while incubated in the assay buffer during the course of the experiment.

No immunoreactive bands were observed in the 0 min No Protein Control and 60 min No Protein Control samples (Figure 45A, lanes 3 and 14). This result indicates that there was no non-specific interaction between the pepsin solution and the DMO-specific antibody under these experimental conditions.

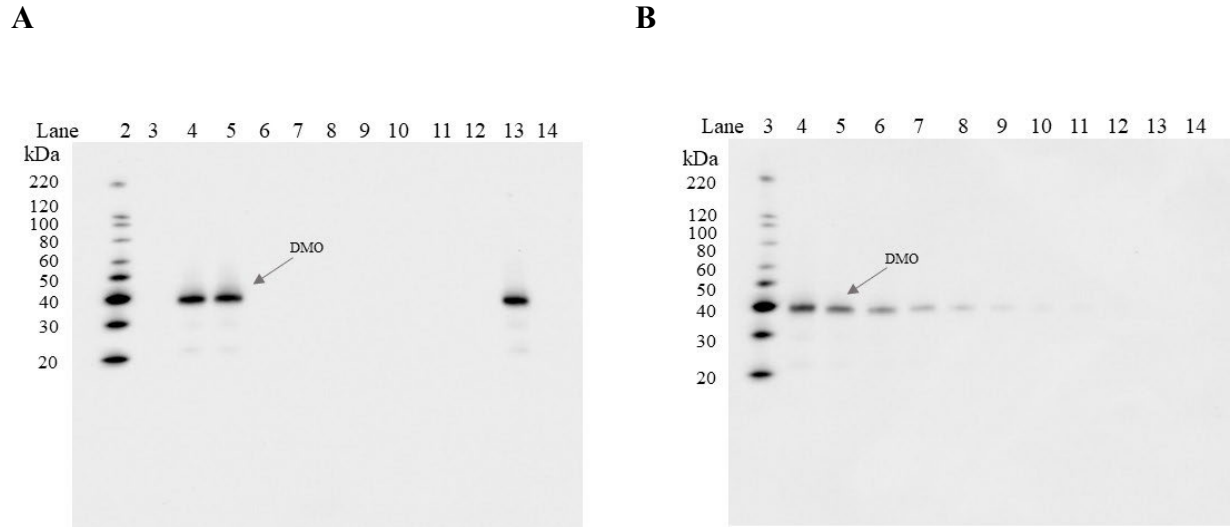


Figure 45. Western Blot Analysis of the Degradation of DMO Protein by Pepsin

Western blots were conducted using an anti-DMO primary antibody. Approximate molecular weights (kDa) are shown on the left of each gel, and correspond to the MagicMark™ XP western protein markers loaded. Empty lanes were cropped from the images. A 203 second exposure is shown.

A: DMO protein degradation by pepsin. Based on pre-reaction protein concentrations, 10 ng of test protein was loaded in each lane containing the MON 94313 DMO protein. Lanes 1 and 15 were cropped from the image.

B: LOD determination. Various amounts of the test protein from the Pepsin Treated T0 sample were loaded to estimate the LOD of the MON 94313 DMO protein. Lanes 1, 2 and 15 were cropped from the image.

Lane	Sample	Incubation Time (min)	Lane	Sample	Amount (ng)
1	Precision Plus™ MWM	-	1	Empty	-
2	MagicMark XP	-	2	Precision Plus™ MWM	-
3	0 min No Test Protein Control	0	3	MagicMark™ XP	-
4	0 min No Pepsin Control	0	4	Pepsin Treated T0	10
5	Pepsin Treated T0	0	5	Pepsin Treated T0	5
6	Pepsin Treated T1	0.5	6	Pepsin Treated T0	2.5
7	Pepsin Treated T2	2	7	Pepsin Treated T0	1.25
8	Pepsin Treated T3	5	8	Pepsin Treated T0	0.63
9	Pepsin Treated T4	10	9	Pepsin Treated T0	0.31
10	Pepsin Treated T5	20	10	Pepsin Treated T0	0.16
11	Pepsin Treated T6	30	11	Pepsin Treated T0	0.08
12	Pepsin Treated T7	60	12	Pepsin Treated T0	0.04
13	60 min No Pepsin Control	60	13	Pepsin Treated T0	0.02
14	60 min No Test Protein Control	60	14	Empty	-
15	Precision Plus™ MWM	-	15	Empty	-

Degradation of the MON 94313 DMO by Pancreatin

The degradation of the DMO protein by pancreatin was assessed by western blot analysis (Figure 46). The total loading of the DMO test protein for each timepoint examined was approximately 10 ng per lane (based on pre-reaction total protein concentrations). The western blot used to assess the DMO protein degradation (Figure 46A) was run concurrently with the western blot used to estimate the LOD (Figure 46B) of the DMO protein. The LOD of the DMO protein was observed at approximately the 0.31 ng protein loading (Figure 46A, lane 9). The LOD was used to calculate the maximum relative amount of DMO protein that could remain visually undetected after digestion, which corresponded to approximately 3.1% ($0.31/10 \times 100\% = 3.1\%$) of the total protein loaded.

Western blot analysis demonstrated that a band corresponding to the DMO protein was degraded to a level below the LOD within 5 min of incubation in the presence of pancreatin (Figure 46A, lane 6), the first timepoint assessed. Therefore, based on the LOD, more than 96.9% ($100\% - 3.1\% = 96.9\%$) of the DMO protein was degraded within 5 min. No peptide fragments were detected at any timepoint in pepsin by western blot.

No apparent change in the intact DMO band intensity was observed in the absence of pancreatin in the 0 h No Pancreatin Control and 24 h No Pancreatin Control samples (Figure 46A, lanes 4 and 14). This indicates that the degradation of all immunoreactive forms of the DMO protein was due to the proteolytic activity of pancreatin and not due to instability of the protein when incubated in 50 mM KH_2PO_4 , pH 7.5 at 37.1°C over the course of the experiment.

No immunoreactive bands were observed in the 0 h No Test Protein Control and 24 h No Test Protein Control samples (Figure 46A, lanes 3 and 15), demonstrating the absence of non-specific antibody interactions with the pancreatin solution.

For details, please refer to Appendix 13.

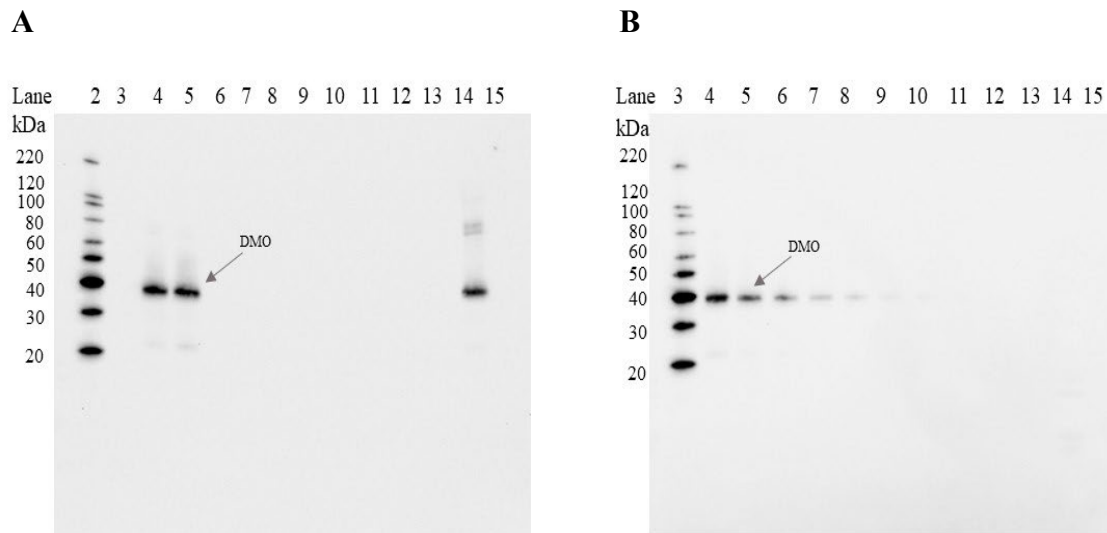


Figure 46. Western Blot Analysis of the Degradation of DMO Protein by Pancreatin

Western blots were conducted using an anti DMO primary antibody. Approximate molecular weights (kDa) are shown on the left of each gel, and correspond to the MagicMark™ XP western protein markers loaded. Empty lanes were cropped from the images. A 160 second exposure is shown.

A: DMO protein degradation by pancreatin. Based on pre-reaction protein concentrations, 10 ng of test protein was loaded in each lane containing the MON 94313 DMO protein. Lane 1 was cropped from the image.

B: LOD determination. Indicated amounts of the test protein from the T0 sample were loaded to estimate the LOD of the DMO protein. Lanes 1 and 2 were cropped from the image.

Lane	Sample	Incubation Time	Lane	Sample	Amount (ng)
1	Precision Plus™ MWM	-	1	Empty	-
2	MagicMark™ XP MWM	-	2	Precision Plus™ MWM	-
3	0 min No Test Protein Control	0	3	MagicMark™ XP	-
4	0 min No Pancreatin Control	0	4	Pancreatin Treated T0	10
5	Pancreatin Treated T0	0	5	Pancreatin Treated T0	5
6	Pancreatin Treated T1	5 min	6	Pancreatin Treated T0	2.5
7	Pancreatin Treated T2	15 min	7	Pancreatin Treated T0	1.25
8	Pancreatin Treated T3	30 min	8	Pancreatin Treated T0	0.63
9	Pancreatin Treated T4	1 h	9	Pancreatin Treated T0	0.31
10	Pancreatin Treated T5	2 h	10	Pancreatin Treated T0	0.16
11	Pancreatin Treated T6	4 h	11	Pancreatin Treated T0	0.08
12	Pancreatin Treated T7	8 h	12	Pancreatin Treated T0	0.04
13	Pancreatin Treated T8	24 h	13	Pancreatin Treated T0	0.02
14	24 h No Pancreatin Control	24 h	14	Precision Plus™ MWM	-
15	24 h No Test Protein Control	24 h	15	Empty	-

Digestive Fate of the DMO Protein Conclusions

The ability of the DMO protein to be degraded by pepsin and by pancreatin was evaluated in this study. The results showed that at least 99.4% of the intact MON 94313 DMO protein was degraded by pepsin within 0.5 min when analyzed by SDS-PAGE and 98.4% of the intact MON 94313 DMO was degraded by pepsin within 0.5 min when analyzed by western blot using a DMO-specific antibody. SDS-PAGE analysis showed that a faint band of ~3.5 kDa peptide fragment was observed through the 5 min of the pepsin digestion but disappeared by 10 min time point.

Greater than 96.9% of the intact DMO protein was degraded within 5 min during incubation with pancreatin when analyzed by western blot. No immunoreactive peptide fragments were observed at any timepoint.

These results show that the intact DMO protein is readily degraded in either pepsin or pancreatin. Rapid degradation of the DMO protein in pepsin and pancreatin indicates that it is highly unlikely that the DMO protein will pose any safety concern to human health.

B.2(a)(ii)(ii) Digestive fate of the PAT protein

Degradation of PAT Protein in the Presence of Pepsin

Degradation of the PAT protein by pepsin was evaluated over time by analyzing digestion mixtures incubated for targeted time intervals following a standardized protocol validated in an international, multi-laboratory ring study ([Thomas *et al.*, 2004](#)) collected at targeted incubation time points. The susceptibility of PAT protein to pepsin degradation was assessed by visual analysis of a Brilliant Blue G-Colloidal stained SDS-PAGE gel and by visual analysis of a western blot probed with an anti-PAT polyclonal antibody. Both visualization methods were run concurrently with separate SDS-PAGE and western blot analyses to estimate the limit of detection (LOD) of the PAT protein for each method.

For SDS-PAGE analysis of the digestibility of the PAT protein in pepsin, the gel was loaded with approximately 1 µg of total test protein (based on pre-digestion protein concentrations) for each of the digestion samples (Figure 47A). Visual examination of SDS-PAGE data showed that the intact PAT protein was completely degraded within 0.5 min of incubation in the presence of pepsin (Figure 47A, Lane 5). A peptide fragment of ~3 kDa was observed for the first 5 min of pepsin treatment with the staining intensity decreasing over time and it was completely degraded within 10 min of incubation. This ~3 kDa peptide fragment is likely a result of a partially digested protein. This is comparable with previously published safety assessments of PAT protein ([Hérouet *et al.*, 2005](#)).

No change in the PAT protein band intensity was observed in the absence of pepsin in the 0 min No Pepsin Control and 60 min No Pepsin Control samples (Figure 47A, lanes 3 and 12). This indicates that the degradation of the PAT protein was due to the proteolytic activity of pepsin and not due to instability of the protein while incubated in the pepsin test system over the course of the experiment.

The 0 min No Test Protein Control and 60 min No Test Protein Control (Figure 47A, lanes 2 and 13) demonstrated that the pepsin is stable throughout the experimental phase.

PART 2: SPECIFIC DATA REQUIREMENTS FOR SAFETY ASSESSMENT

A separate SDS PAGE gel to estimate the LOD of the PAT protein was run concurrently with the SDS PAGE for the degradation assessment (Figure 47B). The LOD of the PAT protein was visually estimated to be approximately 3.6 ng (Figure 47B, lane 8). This LOD is used to calculate the maximum amount of intact PAT protein that could remain visually undetected after degradation, which corresponded to approximately 0.4% ($3.6/1000 \times 100\% = \sim 0.4\%$) of the total protein loaded. Based on that LOD, more than 99.6% ($100\% - 0.4\% = 99.6\%$) of the intact PAT protein was degraded within 0.5 min of incubation in the presence of pepsin.

For details, please refer to Appendix 14.

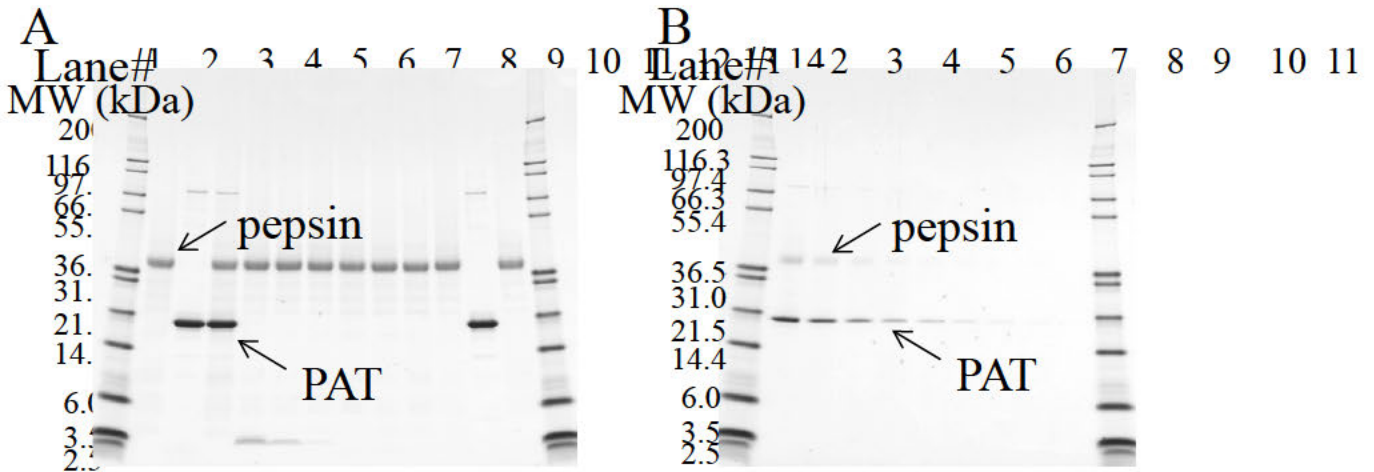


Figure 47. SDS-PAGE Analysis of the Degradation of PAT Protein by Pepsin

Colloidal Brilliant Blue G stained SDS-PAGE gels were used to assess the degradation of PAT protein by pepsin. Molecular weights (kDa) are shown on the left of each gel, and correspond to the markers loaded. In each gel, PAT protein migrated to approximately 21 kDa and pepsin to approximately 38 kDa. Blank lanes were cropped from the images.

A: PAT protein degradation by Pepsin. Based on pre-reaction protein concentrations, 1 µg of test protein was loaded in each lane containing PAT protein.

B: LOD determination. Indicated amounts of the test protein from the Pepsin Treated T0 sample were loaded to estimate the LOD of the PAT protein.

Lane	Sample	Incubation Time (min)	Lane	Sample	Amount (ng)
1	Mark 12™ MWM	-	1	Mark 12™ MWM	-
2	0 min No Test Protein Control	0	2	Pepsin Treated T0	230
3	T 0 min No Pepsin Control	0	3	Pepsin Treated T0	115
4	Pepsin Treated T0	0	4	Pepsin Treated T0	57.5
5	Pepsin Treated T1	0.5	5	Pepsin Treated T0	28.8
6	Pepsin Treated T2	2	6	Pepsin Treated T0	14.4
7	Pepsin Treated T3	5	7	Pepsin Treated T0	7.2
8	Pepsin Treated T4	10	8	Pepsin Treated T0	3.6
9	Pepsin Treated T5	20	9	Pepsin Treated T0	1.8
10	Pepsin Treated T6	30	10	Pepsin Treated T0	0.9
11	Pepsin Treated T7	60	11	Mark 12™ MWM	-
12	60 min No Pepsin Control	60			
13	60 min No Test Protein Control	60			
14	Mark 12™ MWM	-			

PART 2: SPECIFIC DATA REQUIREMENTS FOR SAFETY ASSESSMENT

For western blot analysis of PAT pepsin susceptibility, the PAT protein was loaded with approximately 20 ng per lane of total protein (based on pre-reaction total protein concentrations) for each reaction time point examined. The western blot used to assess the resistance of the PAT protein to pepsin digestion (Figure 48A) was run concurrently with a western blot to estimate the LOD of the PAT protein (Figure 48B). The LOD of the PAT protein was approximately 0.36 ng (Figure 48B, lane 8). The LOD was used to calculate the maximum relative amount of PAT protein that could remain visually undetected after digestion, which corresponded to approximately 1.8% ($0.36/20 \times 100\% = 1.8\%$) of the total protein loaded.

Western blot analysis demonstrated that the PAT protein was degraded below the LOD within 0.5 min of incubation in the presence of pepsin (Figure 48A, lane 5). Based on the western blot LOD for the PAT protein, it can be concluded that more than 98.2% ($100\% - 1.8\% = 98.2\%$) of the intact PAT protein was degraded within 0.5 min. No peptide fragments were detected at any timepoint in pepsin by western blot.

No apparent change in the PAT protein band intensity was observed in the absence of pepsin in the 0 min No Pepsin Control and 60 min No Pepsin Control samples (Figure 48A, lanes 3 and 12). This indicates that the degradation of the PAT protein was due to the proteolytic activity of pepsin and not due to instability of the protein while incubated in the pepsin test system over the course of the experiment.

No immunoreactive bands were observed in the 0 min No Protein Control and 60 min No Protein Control samples (Figure 48A, lanes 2 and 13). This result indicates that there was no non-specific interaction between the pepsin solution and the PAT specific antibody under these experimental conditions.

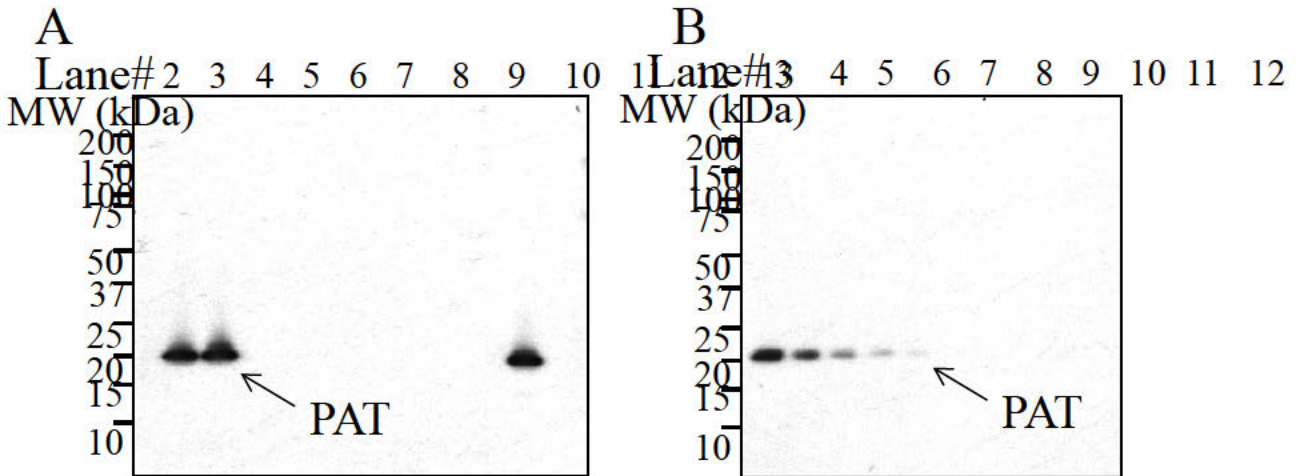


Figure 48. Western Blot Analysis of the Degradation of PAT Protein by Pepsin

Western blots probed with an anti-PAT antibody were used to assess the degradation of PAT by pepsin. Molecular weights (kDa) are shown on the left of each gel, and correspond to the markers loaded (cropped from images). Blank lanes were cropped from the images. A 20 sec exposure is shown.

A: PAT protein degradation by pepsin. Based on pre-reaction protein concentrations, 20 ng of test protein was loaded in each lane containing PAT protein.

B: LOD determination. Indicated amounts of the test protein from the Pepsin Treated T0 sample were loaded to estimate the LOD of the PAT protein.

Lane	Sample	Incubation Time (min)	Lane	Sample	Amount (ng)
1	Precision Plus™ MWM	-	1	Precision Plus™ MWM	-
2	0 min No Test Protein Control	0	2	Empty	-
3	0 min No Pepsin Control	0	3	Pepsin Treated T0	5.8
4	Pepsin Treated T0	0	4	Pepsin Treated T0	2.9
5	Pepsin Treated T1	0.5	5	Pepsin Treated T0	1.44
6	Pepsin Treated T2	2	6	Pepsin Treated T0	0.72
7	Pepsin Treated T3	5	7	Pepsin Treated T0	0.36
8	Pepsin Treated T4	10	8	Pepsin Treated T0	0.18
9	Pepsin Treated T5	20	9	Pepsin Treated T0	0.09
10	Pepsin Treated T6	30	10	Pepsin Treated T0	0.045
11	Pepsin Treated T7	60	11	Pepsin Treated T0	0.022
12	60 min No Pepsin Control	60	12	Pepsin Treated T0	0.011
13	60 min No Test Protein Control	60	13	Empty	-
14	Precision Plus™ MWM	-	14	Precision Plus™ MWM	-

Degradation of PAT Protein in the Presence of Pancreatin

The degradation of the PAT protein by pancreatin was assessed by western blot analysis (Figure 49). The total loading of the PAT test protein for each timepoint examined was approximately 20 ng per lane (based on pre-reaction total protein concentrations). The western blot used to assess the PAT protein degradation (Figure 49A) was run concurrently with the western blot used to estimate the LOD (Figure 49B) of the intact PAT protein. The LOD of the PAT protein was observed at approximately the 0.17 ng protein loading (Figure 49A, lane 8). The LOD was used to calculate the maximum relative amount of the PAT protein that could remain visually undetected after digestion, which corresponded to approximately 0.9% ($0.17/20 \times 100\% = \sim 0.9\%$) of the total protein loaded.

Western blot analysis demonstrated that a band corresponding to the PAT protein was degraded to a level below the LOD within 5 min of incubation in the presence of pancreatin (Figure 49A, lane 5), the first timepoint assessed. Therefore, based on the LOD, more than 99% ($100\% - 0.9\% = 99.1\%$) of the PAT protein was degraded within 5 min. No other immunoreactive bands were detected in any other tested specimens. This is comparable with previously published safety assessments of PAT protein ([Héroutet *et al.*, 2005](#)).

No apparent change in the intact PAT band intensity was observed in the absence of pancreatin in the 0 h No Pancreatin Control and 24 h No Pancreatin Control samples (Figure 49A, lanes 3 and 13). This indicates that the degradation of all immunoreactive forms of the PAT protein was due to the proteolytic activity of pancreatin and not due to instability of the protein when incubated in the pancreatin test system over the course of the experiment.

No immunoreactive bands were observed in the 0 h No Test Protein Control and 24 h No Test Protein Control samples (Figure 49A, lanes 2 and 14), demonstrating the absence of non-specific antibody interactions with the pancreatin solution.

For details, please refer to Appendix 14.

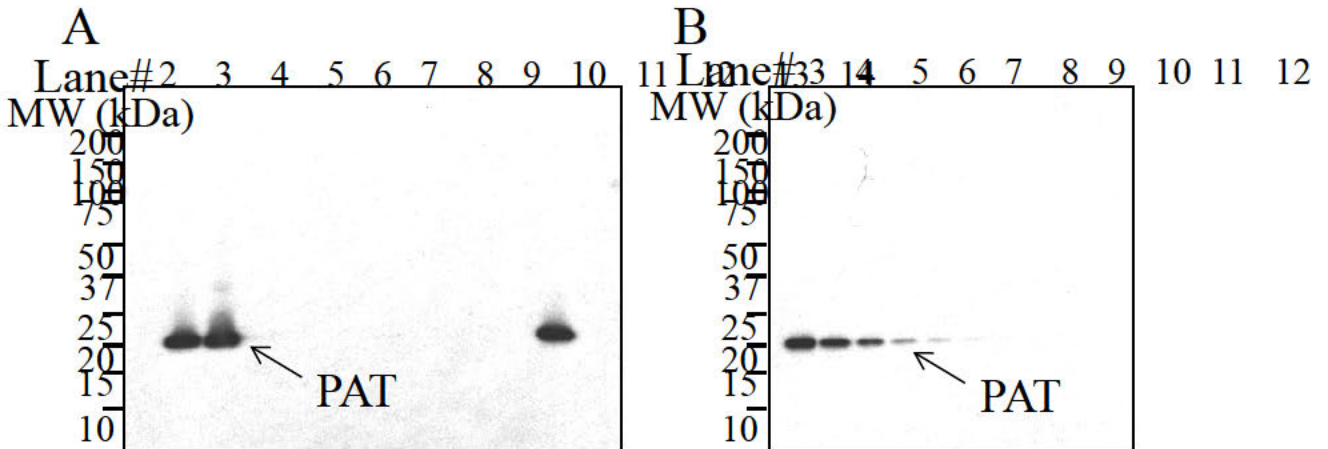


Figure 49. Western Blot Analysis of the Degradation of PAT Protein by Pancreatin

Western blots probed with an anti-PAT antibody were used to assess the degradation of PAT by pancreatin. Molecular weights (kDa) are shown on the left of each gel, and correspond to the markers loaded (cropped from images). Blank lanes were cropped from the images. A 15 sec exposure is shown.

A: PAT protein degradation by pancreatin. Based on pre-reaction protein concentrations, 20 ng of test protein was loaded in each lane containing PAT protein.

B: LOD determination. Indicated amounts of the test protein from the T0 sample were loaded to estimate the LOD of the PAT protein.

Lane	Sample	Incubation Time	Lane	Sample	Amount (ng)
1	Precision Plus™ MWM	-	1	Precision Plus™ MWM	-
2	0 min No Test Protein Control	0	2	Empty	-
3	0 min No Pancreatin Control	0	3	Pancreatin Treated T0	5.6
4	Pancreatin Treated T0	0	4	Pancreatin Treated T0	2.78
5	Pancreatin Treated T1	5 min	5	Pancreatin Treated T0	1.39
6	Pancreatin Treated T2	15 min	6	Pancreatin Treated T0	0.69
7	Pancreatin Treated T3	30 min	7	Pancreatin Treated T0	0.35
8	Pancreatin Treated T4	1 hr	8	Pancreatin Treated T0	0.17
9	Pancreatin Treated T5	2 hr	9	Pancreatin Treated T0	0.087
10	Pancreatin Treated T6	4 hr	10	Pancreatin Treated T0	0.043
11	Pancreatin Treated T7	8 hr	11	Pancreatin Treated T0	0.022
12	Pancreatin Treated T8	24 hr	12	Pancreatin Treated T0	0.011
13	24 hr No Pancreatin Control	24 hr	13	Empty	-
14	24 hr No Test Protein Control	24 hr	14	Precision Plus™ MWM	-
15	Precision Plus™ MWM	-			

Digestive Fate of the PAT Protein Conclusions

The ability of the PAT protein to be degraded by pepsin and by pancreatin was evaluated in this study. The results of the SDS-PAGE analysis demonstrate that greater than 99.6% of the intact PAT protein was degraded by pepsin within 0.5 min and at least 98.2% of the intact PAT protein was degraded by pepsin within 0.5 min when analyzed by western blot using a PAT specific antibody. SDS-PAGE analysis showed that a peptide fragment of ~3 kDa was observed in the 0.5 min time points in the presence of pepsin, but was gone by 10 min.

At least 99.1% of the intact PAT protein was degraded within 5 min during incubation with pancreatin when analyzed by western blot.

These results show that the intact PAT is rapidly degraded by pepsin and pancreatin. Rapid and complete degradation of the PAT protein by pepsin and pancreatin indicates that the PAT protein is highly unlikely to pose any safety concern to human or animal health.

B.2(a)(ii)(iii) Digestive fate of the FT_T.1 protein

Degradation of FT_T.1 Protein in the Presence of Pepsin

Degradation of the FT_T.1 protein by pepsin was evaluated over time by analyzing digestion mixtures incubated for targeted time intervals following a standardized protocol validated in an international, multi-laboratory ring study ([Thomas et al., 2004](#)) collected at targeted incubation time points. The susceptibility of FT_T.1 protein to pepsin degradation was assessed by visual analysis of a Brilliant Blue G-Colloidal stained SDS-PAGE gel and by visual analysis of a western blot probed with an anti-FT_T.1 polyclonal antibody. Both visualization methods were run concurrently with separate SDS-PAGE and western blot analyses to estimate the limit of detection (LOD) of the FT_T.1 protein for each method.

For SDS-PAGE analysis of the digestibility of the FT_T.1 protein in pepsin, the gel was loaded with 1 µg of total test protein (based on pre-digestion protein concentrations) for each of the digestion samples (Figure 50, Panel A). The SDS-PAGE gel for the digestibility assessment was run concurrently with a separate SDS-PAGE gel to estimate the LOD of the FT_T.1 protein (Figure 50, Panel B). The LOD of intact FT_T.1 protein was approximately 6.25 ng (Figure 50, Panel B, lane 7). Visual examination of SDS-PAGE data showed that the intact FT_T.1 protein was digested within 0.5 min of incubation in pepsin (Figure 50, Panel A, lane 5). Therefore, based on the LOD, more than 99.4% ($100\% - 0.6\% = 99.4\%$) of the intact FT_T.1 protein was digested within 0.5 -min of incubation in pepsin. Transiently-stable peptide fragments between 3.5 and 6 kDa were observed through 20 min of the digestion.

No change in the FT_T.1 protein band intensity was observed in the absence of pepsin in the 0 min No Pepsin Control and 60 min No Pepsin Control (Figure 50, lanes 3 and 12). This indicates that the degradation of the FT_T.1 protein was due to the proteolytic activity of pepsin and not due to instability of the protein while incubated in the test system over the course of the experiment.

The 0 min No Test Protein Control and 60 min No Test Protein Control (Figure 50, Panel A, lanes 2 and 13) demonstrated that the pepsin is stable throughout the experimental phase.

For details, please refer to Appendix 15.

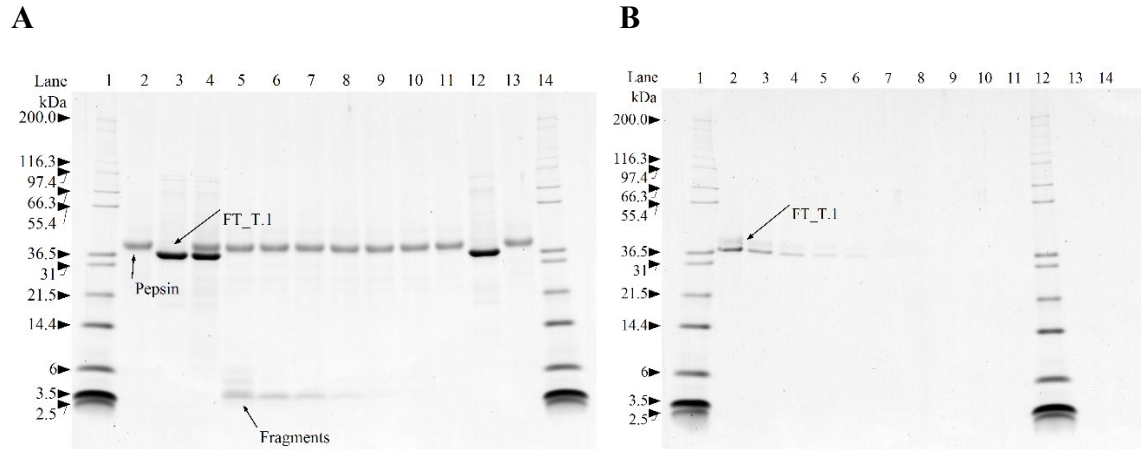


Figure 50. SDS-PAGE Analysis of the Degradation of FT_T.1 Protein by Pepsin

Colloidal Brilliant Blue G stained SDS-PAGE gels were used to assess the degradation of FT_T.1 protein by pepsin. Molecular weights (kDa) are shown on the left of each gel and correspond to the markers loaded. In each gel, the FT_T.1 protein migrated to approximately 33.6 kDa and pepsin to approximately 38 kDa. Empty lanes were cropped from the images.

A: FT_T.1 protein degradation in the presence of pepsin. Based on pre-reaction protein concentrations, 1 µg of test protein was loaded in each lane containing FT_T.1 protein.

B: LOD determination. Indicated amounts of the test protein from the Pepsin Treated T0 sample were loaded to estimate the LOD of the FT_T.1 protein.

Lane	Sample	Incubation Time (min)	Lane	Sample	Amount (ng)
1	Mark12™ MWM	-	1	Mark12™ MWM	-
2	0 min No Test Protein Control	0	2	Pepsin Treated T0	200
3	0 min No Pepsin Control	0	3	Pepsin Treated T0	100
4	Pepsin Treated T0	0	4	Pepsin Treated T0	50
5	Pepsin Treated T1	0.5	5	Pepsin Treated T0	25
6	Pepsin Treated T2	2	6	Pepsin Treated T0	12.5
7	Pepsin Treated T3	5	7	Pepsin Treated T0	62.5
8	Pepsin Treated T4	10	8	Pepsin Treated T0	3.1
9	Pepsin Treated T5	20	9	Pepsin Treated T0	1.6
10	Pepsin Treated T6	30	10	Pepsin Treated T0	0.8
11	Pepsin Treated T7	60	11	Pepsin Treated T0	0.4
12	60 min No Pepsin Control	60	12	Mark12™ MWM	-
13	60 min No Test Protein Control	60	13	Empty	-
14	Mark12™ MWM	-	14	Empty	-
15	Empty	-	15	Empty	-

PART 2: SPECIFIC DATA REQUIREMENTS FOR SAFETY ASSESSMENT

For western blot analysis of FT_T.1 pepsin susceptibility, the FT_T.1 protein was loaded with approximately 10 ng per lane of total protein (based on pre-reaction total protein concentrations) for each reaction time point examined. The western blot used to assess FT_T.1 protein degradation (Figure 51, Panel A) was run concurrently with the western blot used to estimate the LOD (Figure 51, Panel B). The LOD of the FT_T.1 protein was approximately 0.063 ng (Figure 51, Panel B, lane 10). Western blot analysis demonstrated that the intact FT_T.1 protein was degraded below the LOD within 0.5 min of incubation in the presence of pepsin (Figure 51, Panel A, Lane 5). Based on the western blot LOD for the FT_T.1 protein, more than 99.4% ($100\% - 0.6\% = 99.4\%$) of the intact FT_T.1 protein was degraded within 0.5 min. No peptide fragments were detected at the 0.5 min and beyond time points in the western blot analysis.

No change in the FT_T.1 protein band intensity was observed in the absence of pepsin in the 0 min No Pepsin Control and 60 min No Pepsin Control (Figure 51, Panel A, lanes 3 and 12). This indicates that the degradation of the FT_T.1 protein was due to the proteolytic activity of pepsin and not due to instability of the protein while incubated in the test system over the course of the experiment.

No immunoreactive bands were observed in 0 min No Protein Control and 60 min No Protein Control (Figure 51, Panel A, lanes 3 and 14). This result indicates that there was no non-specific interaction between the pepsin solution and the FT_T-specific antibody under these experimental conditions.

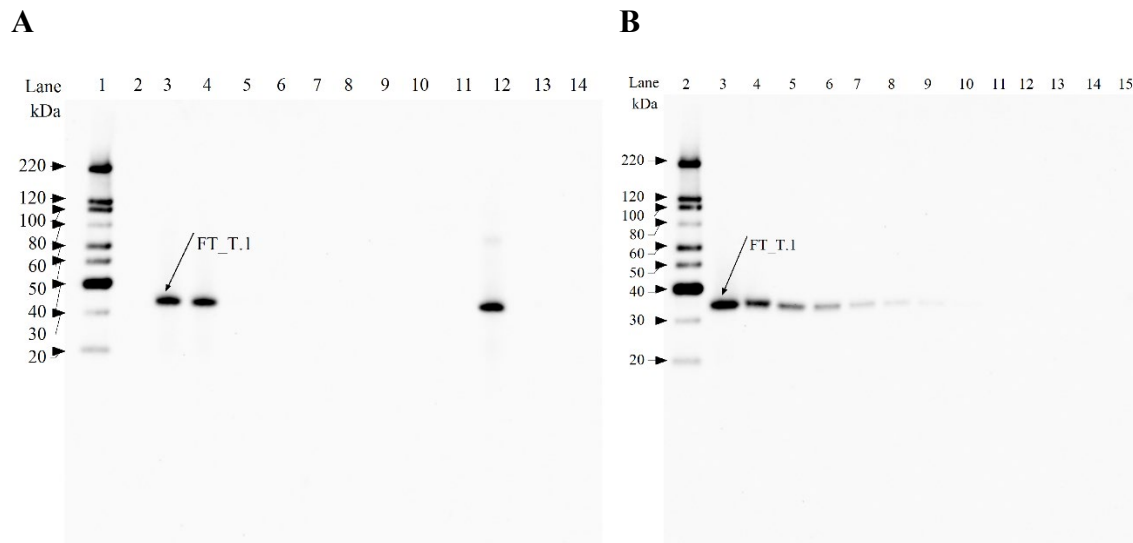


Figure 51. Western Blot Analysis of the Degradation of FT_T.1 Protein by Pepsin

Western blots probed with an anti-FT_T antibody were used to assess the degradation of FT_T.1 by pepsin. Molecular weights (kDa) are shown on the left of each gel and correspond to the MagicMark™ molecular weight marker loaded in two lanes of each gel. Empty lanes and molecular weight markers that were not visible on the film were cropped from the images. A 20 sec exposure is shown.

A: FT_T.1 protein degradation by pepsin. Based on pre-reaction protein concentrations, 10 ng of test protein was loaded in each lane containing FT_T.1 protein.

B: LOD determination. Indicated amounts of the test protein from the Pepsin Treated T0 sample were loaded to estimate the LOD of the FT_T.1 protein.

Lane	Sample	Incubation Time (min)	Lane	Sample	Amount (ng)
1	MagicMark™ MWM	-	1	Precision Plus™ MWM	-
2	0 min No Test Protein Control	0	2	MagicMark™ MWM	-
3	0 min No Pepsin Control	0	3	Pepsin Treated T0	10
4	Pepsin Treated T0	0	4	Pepsin Treated T0	5
5	Pepsin Treated T1	0.5	5	Pepsin Treated T0	2
6	Pepsin Treated T2	2	6	Pepsin Treated T0	1
7	Pepsin Treated T3	5	7	Pepsin Treated T0	0.5
8	Pepsin Treated T4	10	8	Pepsin Treated T0	0.25
9	Pepsin Treated T5	20	9	Pepsin Treated T0	0.13
10	Pepsin Treated T6	30	10	Pepsin Treated T0	0.063
11	Pepsin Treated T7	60	11	Pepsin Treated T0	0.032
12	60 min No Pepsin Control	60	12	Pepsin Treated T0	0.016
13	60 min No Test Protein Control	60	13	Pepsin Treated T0	0.008
14	MagicMark™ MWM	-	14	Pepsin Treated T0	0.004
15	Empty	-	15	Pepsin Treated T0	0.002

Degradation of FT_T.1 Protein in the Presence of Pancreatin

The degradation of the FT_T.1 protein by pancreatin was assessed by western blot analysis (Figure 52). The western blot used to assess the FT_T.1 protein degradation (Figure 52, Panel A) was run concurrently with the western blot used to estimate the LOD (Figure 52, Panel B) of the FT_T.1 protein. The LOD of the FT_T.1 protein was observed at approximate 0.25 ng protein loading (Figure 52, Panel B, lane 8). The LOD was used to calculate the maximum relative amount of FT_T.1 protein that could remain visually undetected after digestion, which corresponded to approximately 2.5% of the total protein loaded.

The gel used to assess degradation of the FT_T.1 protein by western blot was loaded with approximately 10 ng per lane of total protein (based on pre-reaction protein concentrations) for each reaction time point examined. Western blot analysis demonstrated that a band corresponding to the FT_T.1 protein was degraded to a level below the LOD within 5 minutes of incubation with pancreatin (Figure 52, Panel A, lane 5), the first time point assessed. Therefore, based on the LOD, more than 97.5% ($100\% - 2.5\% = 97.5\%$) of the FT_T.1 protein was digested within 5 minutes. No peptide fragments were detected at the 5 min and beyond time points in the western blot analysis.

No significant change in the intact FT_T.1 (~33.6 kDa) band intensity was observed in the absence of pancreatin in the 0 min No Pancreatin Control and 24 hour No Pancreatin Control (Figure 52, Panel A, lanes 3 and 13). This indicates that the degradation of all immunoreactive forms of the FT_T.1 protein was due to the proteolytic activity of pancreatin and not due to instability of the protein when incubated in the test system over the course of the experiment.

No immunoreactive bands were observed in the 0 min No Test Protein Control and 24 hour No Test Protein Control (Figure 52, Panel A, lanes 2 and 14), demonstrating the absence of non-specific antibody interactions with the pancreatin solution.

For details, please refer to Appendix 15.

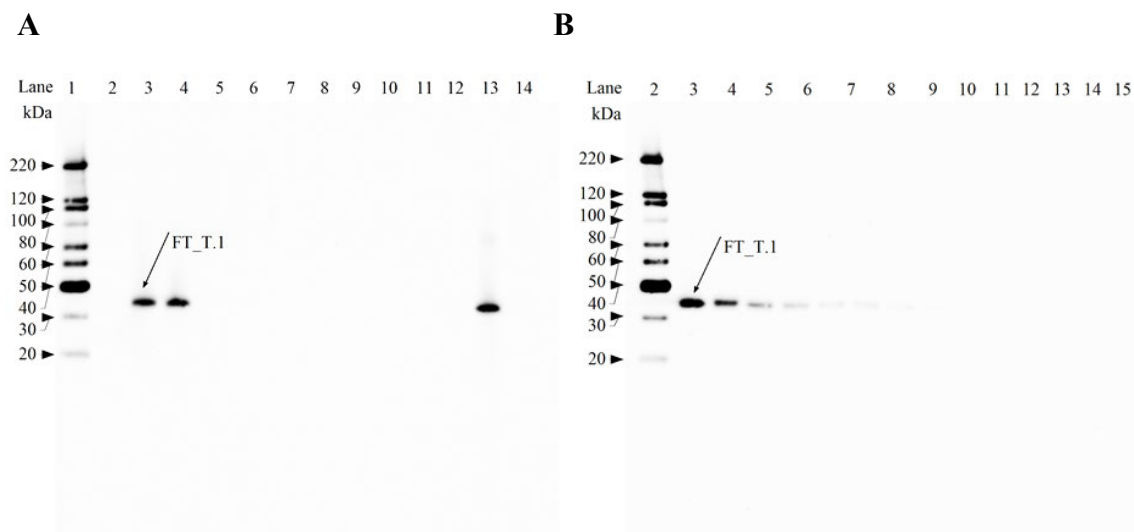


Figure 52. Western Blot Analysis of the Degradation of FT_T.1 Protein by Pancreatin

Western blots probed with an anti-FT_T antibody were used to assess the degradation of FT_T.1 by pancreatin. Molecular weights (kDa) are shown on the left of each gel and correspond to the MagicMark™ molecular weight marker loaded in each gel. Empty lanes and molecular weight markers that were not visible on the film were cropped from the images. A 20 sec exposure is shown.

A: FT_T.1 protein degradation by pancreatin. Based on pre-reaction protein concentrations, 10 ng of test protein was loaded in each lane containing FT_T.1 protein.

B: LOD determination. Indicated amounts of the test protein from the Pancreatin Treated T0 sample were loaded to estimate the LOD of the FT_T.1 protein.

Lane	Sample	Incubation Time	Lane	Sample	Amount (ng)
1	MagicMark™ MWM	-	1	Precision Plus™ MWM	-
2	0 min No Test Protein Control	0	2	MagicMark™ MWM	-
3	0 min No Pancreatin Control	0	3	Pancreatin Treated T0	10
4	Pancreatin Treated T0	0	4	Pancreatin Treated T0	5
5	Pancreatin Treated T1	5 min	5	Pancreatin Treated T0	2
6	Pancreatin Treated T2	15 min	6	Pancreatin Treated T0	1
7	Pancreatin Treated T3	30 min	7	Pancreatin Treated T0	0.5
8	Pancreatin Treated T4	1 h	8	Pancreatin Treated T0	0.25
9	Pancreatin Treated T5	2 h	9	Pancreatin Treated T0	0.13
10	Pancreatin Treated T6	4 h	10	Pancreatin Treated T0	0.063
11	Pancreatin Treated T7	8 h	11	Pancreatin Treated T0	0.032
12	Pancreatin Treated T8	24 h	12	Pancreatin Treated T0	0.016
13	24 h No Pancreatin Control	24 h	13	Pancreatin Treated T0	0.008
14	24 h No Test Protein Control	24 h	14	Pancreatin Treated T0	0.004
15	Precision Plus™ MWM	-	15	Pancreatin Treated T0	0.002

Degradation of FT_T.1 Protein by Pepsin Followed by Pancreatin

To better understand the fate of the transiently-stable peptide fragments between 3.5 and 6 kDa that were observed in the reaction mixtures through the 20 min timepoint of the pepsin digestion of FT_T.1, sequential digestibility of the FT_T.1 protein was conducted. This sequential digestibility was assessed both by visual analysis of a Colloidal Brilliant Blue G stained SDS-PAGE gel, and visual analysis of a western blot probed with an anti FT_T-polyclonal antibody.

For the sequential degradation assay, the FT_T.1 protein was incubated with pepsin for 2 min, followed by incubation with pancreatin. For the Colloidal Brilliant Blue G stained SDS-PAGE assessment, the gel was loaded with 1 µg of FT_T.1 protein (based on pre-digestion protein concentrations) for each of the digestion samples. Examination of SDS-PAGE data showed that the intact FT_T.1 protein was digested within 2 min of incubation in pepsin followed by pancreatin (Figure 53, Panel A, lane 7).

No change in the fragment band intensities was observed in the absence of pancreatin in the SEQ 0 min No Pancreatin Control and SEQ 2 hour No Pancreatin Control (Figure 53, Panel A, lanes 5 and 14). This indicates that the digestion of the fragments was due to the proteolytic activity of pancreatin and not due to instability of the fragment when incubated in the test system over the course of the experiment.

The SEQ 0 min No Test Protein Control and SEQ 2 hour No Test Protein Control (Figure 53, Panel A, lanes 4 and 15) demonstrated the integrity of the pancreatin over the course of the experiment.

The sequential digestion of the FT_T.1 protein was also assessed by western blot (Figure 53, Panel B), with 10 ng of the test protein (based on total protein pre-digestion concentrations) loaded per lane. No bands were detected in the 2 min Pepsin Treated sample (Figure 53, Panel B, lane 3).

For details, please refer to Appendix 15.

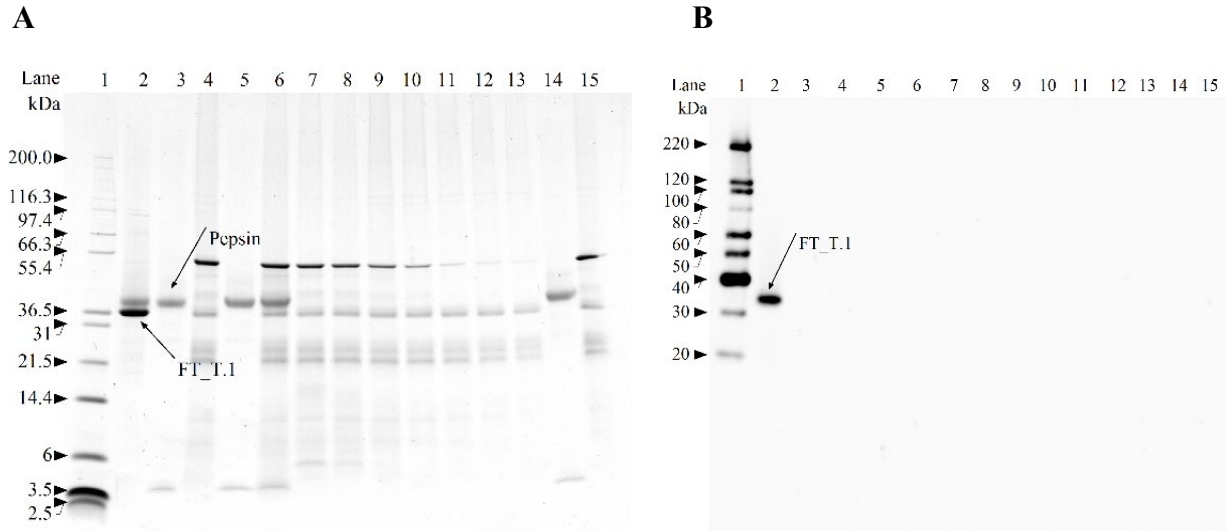


Figure 53. SDS-PAGE and Western Blot Analysis of the Degradation of FT_T.1 Protein by Sequential Digestion

SDS-PAGE and western blot analysis were used to assess the degradation of FT_T.1 in sequential digestion. Molecular weights (kDa) are shown on the left of each gel and correspond to the markers loaded (cropped in panel B).

A: Colloidal Brilliant Blue G stained SDS-PAGE gel analysis of FT_T.1 in sequential digestion. Based on pre-digestion protein concentrations, 1 µg of test protein was loaded in each lane containing FT_T.1 protein.

B: Western blot analysis of FT_T.1 in sequential digestion. Based on pre-digestion protein concentrations, 10 ng of test protein was loaded in each lane containing FT_T.1 protein. A 20 sec exposure is shown.

Lane	Sample	Incubation Time	Lane	Sample	Incubation Time
1	Mark12™ MWM	-	1	MagicMark™ MWM	-
Pepsin Degradation			Pepsin Degradation		
2	0 min Pepsin Treated	0 min	2	0 min Pepsin Treated	0 min
3	2 min Pepsin Treated	2 min	3	2 min Pepsin Treated	2 min
Pancreatin Degradation			Pancreatin Degradation		
4	SEQ 0 min No Test Protein Control	0 min	4	SEQ 0 min No Test Protein Control	0 min
5	SEQ 0 min No Pancreatin Control	0 min	5	SEQ 0 min No Pancreatin Control	0 min
6	SEQ T0	0 min	6	SEQ T0	0 min
7	SEQ T1	0.5 min	7	SEQ T1	0.5 min
8	SEQ T2	2 min	8	SEQ T2	2 min
9	SEQ T3	5 min	9	SEQ T3	5 min
10	SEQ T4	10 min	10	SEQ T4	10 min
11	SEQ T5	30 min	11	SEQ T5	30 min
12	SEQ T6	1 h	12	SEQ T6	1 h
13	SEQ T7	2 h	13	SEQ T7	2 h
14	SEQ 2 h No Pancreatin Control	2 h	14	SEQ 2 h No Pancreatin Control	2 h
15	SEQ 2 h No Test Protein Control	2 h	15	SEQ 2 h No Test Protein Control	2 h

Digestive Fate of the FT_T.1 Protein Conclusions

The ability of FT_T.1 protein to be degraded by pepsin and by pancreatin was evaluated in this study. The results showed that at least 99.4% of the intact FT_T.1 protein was degraded by pepsin within 0.5 min when analyzed by SDS-PAGE and at least 99.4% of the intact FT_T.1 was degraded by pepsin within 0.5 min when analyzed by western blot using a FT_T specific antibody. SDS-PAGE analysis showed that transient peptide fragments between 3.5 and 6 kDa were observed through the 20 min time point of the pepsin digestion. At least 97.5% of the intact FT_T.1 protein was degraded by pancreatin within 5 min when analyzed by western blot. These results show that the full-length FT_T.1 is rapidly degraded by pepsin and pancreatin. The transient fragments between 3.5 and 6 kDa were rapidly degraded by sequential digestion, indicating that gastrointestinal digestion is sufficient to degrade the intact FT_T.1 protein and any fragments thereof. Rapid and complete degradation of the FT_T.1 protein by pancreatin alone and pepsin followed by pancreatin indicates that the FT_T.1 protein poses no meaningful risk to human or animal health.

B.2(a)(ii)(iv) Digestive fate of the TDO protein

Degradation of TDO Protein in the Presence of Pepsin

Degradation of the TDO protein by pepsin was evaluated over time by analyzing digestion mixtures incubated for targeted time intervals following a standardized protocol validated in an international, multi-laboratory ring study ([Thomas et al., 2004](#)) collected at targeted incubation time points. The susceptibility of TDO protein to pepsin degradation was assessed by visual analysis of a Brilliant Blue G-Colloidal stained SDS-PAGE gel and by visual analysis of a western blot probed with an anti-TDO polyclonal antibody. Both visualization methods were run concurrently with separate SDS-PAGE and western blot analyses to estimate the limit of detection (LOD) of the TDO protein for each method.

For SDS-PAGE analysis of the digestibility of the TDO protein in pepsin, the gel was loaded with 1 µg of total test protein (based on pre-digestion protein concentrations) for each of the digestion samples (Figure 54, Panel A). The SDS-PAGE gel for the digestibility assessment was run concurrently with a separate SDS-PAGE gel to estimate the LOD of the TDO protein (Figure 54, Panel B). The LOD of intact TDO protein was approximately 12.5 ng (Figure 54, Panel B, lane 7). Visual examination of SDS-PAGE data showed that the intact TDO protein was digested within 0.5 min of incubation in pepsin (Figure 54, Panel A, lane 5). Therefore, based on the LOD, more than 98.8% ($100\% - 1.25\% = 98.75\%$) of the intact TDO protein was digested within 0.5 min of incubation in pepsin. A transiently-stable peptide fragment of ~3.5 kDa was observed through 5 min but disappeared by 10 min of the digestion.

No change in the TDO protein band intensity was observed in the absence of pepsin in the 0 min No Pepsin Control and 60 min No Pepsin Control (Figure 54, Panel A, lanes 3 and 12). This indicates that the degradation of the TDO protein was due to the proteolytic activity of pepsin and not due to instability of the protein while incubated in the test system over the course of the experiment.

The 0 min No Test Protein Control and 60 min No Test Protein Control (Figure 54, Panel A, lanes 2 and 13) demonstrated that the pepsin is stable throughout the experimental phase.

For details, please refer to Appendix 16.

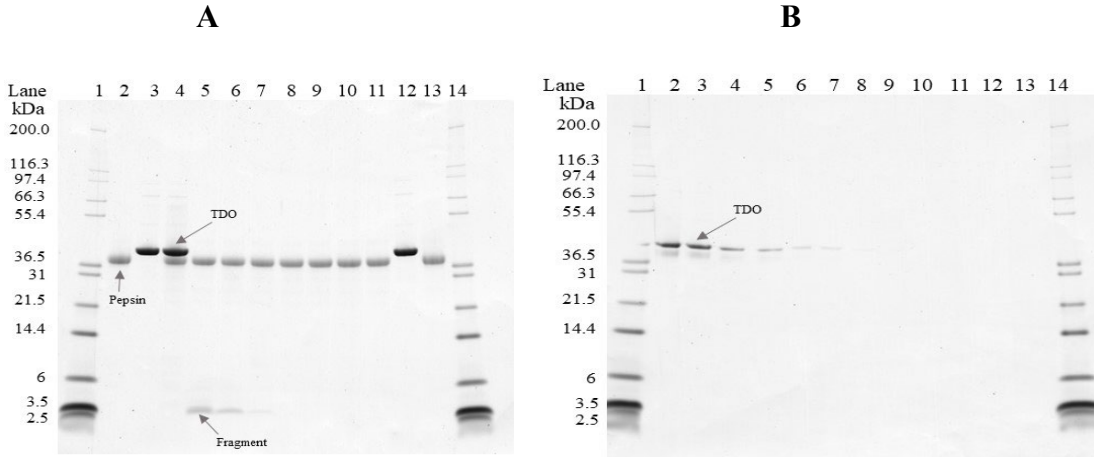


Figure 54. SDS-PAGE Analysis of the Degradation of TDO Protein by Pepsin

Colloidal Brilliant Blue G stained SDS-PAGE gels were used to assess the degradation of TDO protein by pepsin. Molecular weights (kDa) are shown on the left of each gel and correspond to the markers loaded. In each gel, the TDO protein migrated to approximately 37 kDa, above pepsin band. Empty lanes were cropped from the images.

Panel A: TDO protein degradation in the presence of pepsin. Based on pre-reaction protein concentrations, 1 µg of test protein was loaded in each lane containing TDO protein.

Panel B: LOD determination. Indicated amounts of the test protein from the Pepsin Treated T0 sample were loaded to estimate the LOD of the TDO protein.

Lane	Sample	Incubation Time (min)	Lane	Sample	Amount (ng)
1	Mark12™ MWM	-	1	Mark12™ MWM	-
2	0 min No Test Protein Control	0	2	Pepsin Treated T0	400
3	0 min No Pepsin Control	0	3	Pepsin Treated T0	200
4	Pepsin Treated T0	0	4	Pepsin Treated T0	100
5	Pepsin Treated T1	0.5	5	Pepsin Treated T0	50
6	Pepsin Treated T2	2	6	Pepsin Treated T0	25
7	Pepsin Treated T3	5	7	Pepsin Treated T0	12.5
8	Pepsin Treated T4	10	8	Pepsin Treated T0	6.3
9	Pepsin Treated T5	20	9	Pepsin Treated T0	3.1
10	Pepsin Treated T6	30	10	Pepsin Treated T0	1.6
11	Pepsin Treated T7	60	11	Pepsin Treated T0	0.8
12	60 min No Pepsin Control	60	12	Pepsin Treated T0	0.4
13	60 min No Test Protein Control	60	13	Pepsin Treated T0	0.2
14	Mark12™ MWM	-	14	Mark12™ MWM	-
15	Empty	-	15	Empty	-

PART 2: SPECIFIC DATA REQUIREMENTS FOR SAFETY ASSESSMENT

For western blot analysis of TDO pepsin susceptibility, the TDO protein was loaded with approximately 5 ng per lane of total protein (based on pre-reaction total protein concentrations) for each reaction time point examined. The western blot used to assess TDO protein degradation (Figure 55, Panel A) was run concurrently with the western blot used to estimate the LOD (Figure 55, Panel B). The LOD of the TDO protein was approximately 0.08 ng (Figure 55, Panel B, lane 9). Western blot analysis demonstrated that the intact TDO protein was degraded below the LOD within 0.5 min of incubation in the presence of pepsin (Figure 55, Panel A, lane 6). Based on the western blot LOD for the TDO protein, more than 98.4% ($100\% - 1.6\% = 98.4\%$) of the intact TDO protein was degraded within 0.5 min. No peptide fragments were detected at the 0.5 min and beyond time points in the western blot analysis.

No change in the TDO protein band intensity was observed in the absence of pepsin in the 0 min No Pepsin Control and 60 min No Pepsin Control (Figure 55, Panel A, lanes 4 and 13). This indicates that the degradation of the FT_T.1 protein was due to the proteolytic activity of pepsin and not due to instability of the protein while incubated in the test system over the course of the experiment.

No immunoreactive bands were observed in 0 min No Protein Control and 60 min No Protein Control (Figure 55, Panel A, lanes 3 and 14). This result indicates that there was no non-specific interaction between the pepsin solution and the TDO-specific antibody under these experimental conditions.

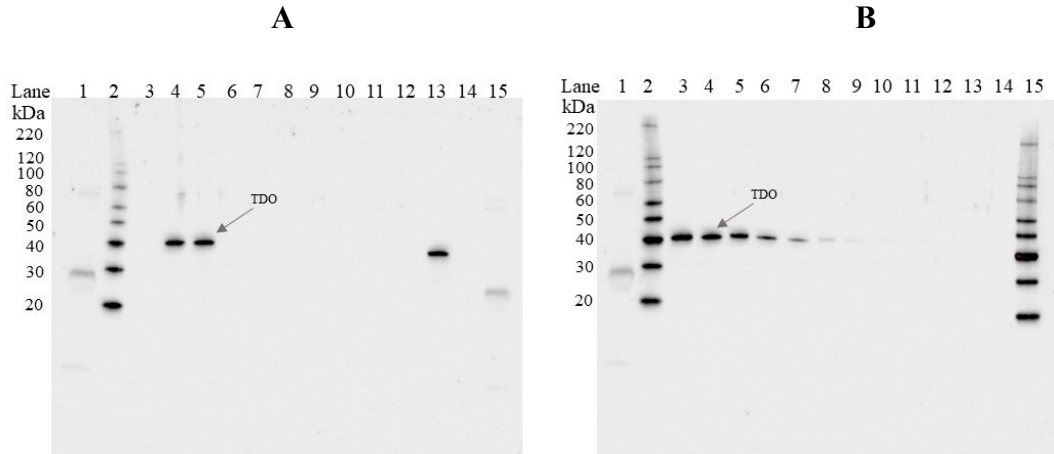


Figure 55. Western Blot Analysis of the Degradation of the Produced TDO Protein by Pepsin

Western blots probed with an anti-TDO antibody were used to assess the degradation of TDO by pepsin. Molecular weights (kDa) are shown on the left of each gel, and correspond to the markers loaded (cropped from images). Molecular weights (kDa) are shown on the left of each gel and correspond to the MagicMark™ molecular weight marker. A 20 sec exposure is shown.

Panel A: TDO protein degradation by pepsin. Based on total pre-reaction protein concentrations, 5 ng of test substance was loaded in each lane containing TDO protein.

Panel B: LOD determination. Indicated amounts of the TDO protein from the Pepsin Treated T0 sample were loaded to estimate the LOD of the TDO protein. Lane designations are as follows:

Lane	Sample	Incubation Time (min)	Lane	Sample	Amount (ng)
1	Precision Plus™ MWM	-	1	Precision Plus™ MWM	-
2	MagicMark™ MWM	-	2	MagicMark™ MWM	-
3	0 min No Test Protein Control	0	3	Pepsin Treated T0	5
4	0 min No Pepsin Control	0	4	Pepsin Treated T0	2.5
5	Pepsin Treated T0	0	5	Pepsin Treated T0	1.25
6	Pepsin Treated T1	0.5	6	Pepsin Treated T0	0.63
7	Pepsin Treated T2	2	7	Pepsin Treated T0	0.31
8	Pepsin Treated T3	5	8	Pepsin Treated T0	0.16
9	Pepsin Treated T4	10	9	Pepsin Treated T0	0.08
10	Pepsin Treated T5	20	10	Pepsin Treated T0	0.04
11	Pepsin Treated T6	30	11	Pepsin Treated T0	0.02
12	Pepsin Treated T7	60	12	Pepsin Treated T0	0.01
13	60 min No Pepsin Control	60	13	Pepsin Treated T0	0.005
14	60 min No Test Protein Control	60	14	Pepsin Treated T0	0.002
15	Precision Plus™ MWM	-	15	MagicMark™ MWM	-

Degradation of TDO Protein in the Presence of Pancreatin

The degradation of the TDO protein by pancreatin was assessed by western blot analysis (Figure 56). The western blot used to assess the TDO protein degradation (Figure 56, Panel A) was run concurrently with the western blot used to estimate the LOD (Figure 56, Panel B) of the TDO protein. The LOD of the TDO protein was observed at approximate 0.16 ng protein loading (Figure 56, Panel B, lane 8). The LOD was used to calculate the maximum relative amount of TDO protein that could remain visually undetected after digestion, which corresponded to approximately 3.2% of the total protein loaded.

The gel used to assess degradation of the TDO protein by western blot was loaded with approximately 5 ng per lane of total protein (based on pre-reaction protein concentrations) for each reaction time point examined. Western blot analysis demonstrated that a band corresponding to the TDO protein was degraded to a level below the LOD within 5 minutes of incubation with pancreatin (Figure 56, Panel A, lane 6), the first time point assessed. Therefore, based on the LOD, more than 96.8% ($100\% - 3.2\% = 96.8\%$) of the TDO protein was digested within 5 minutes. No peptide fragments were detected at the 5 min and beyond time points in the western blot analysis.

No significant change in the intact TDO (~37.0 kDa) band intensity was observed in the absence of pancreatin in the 0 min No Pancreatin Control and 24 hour No Pancreatin Control (Figure 56, Panel A, lanes 4 and 14). This indicates that the degradation of all immunoreactive forms of the TDO protein was due to the proteolytic activity of pancreatin and not due to instability of the protein when incubated in the test system over the course of the experiment.

No immunoreactive bands were observed in the 0 min No Test Protein Control and 24 hour No Test Protein Control (Figure 56, Panel A, lanes 3 and 15), demonstrating the absence of non-specific antibody interactions with the pancreatin solution.

For details, please refer to Appendix 16.

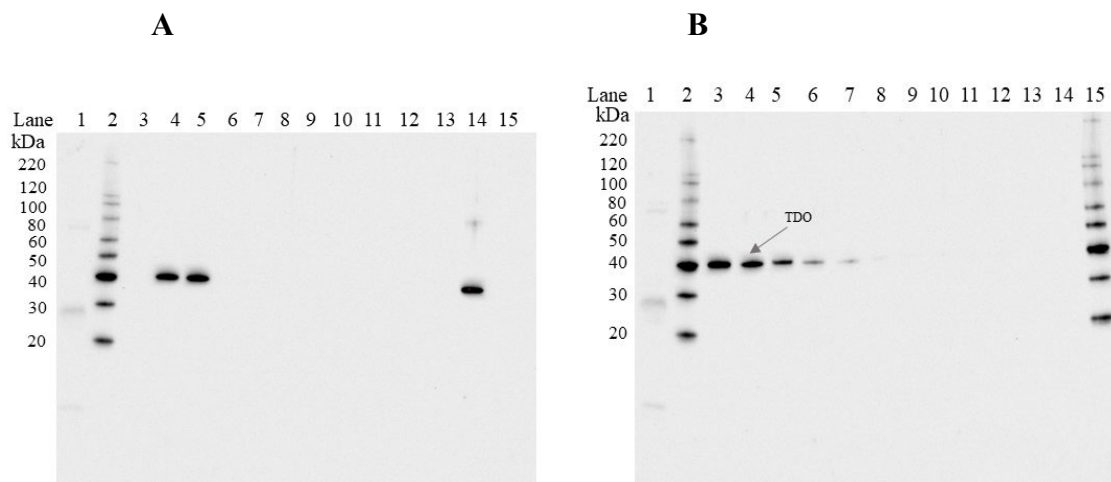


Figure 56. Western Blot Analysis of the TDO Protein Degradation in Pancreatin

Western blots probed with an anti-TDO antibody was used to assess the degradation of TDO by pancreatin. Molecular weights (kDa) are shown on the left of each gel and correspond to the MagicMark™ molecular weight marker. A 25 sec exposure is shown.

A: TDO protein degradation by pancreatin. Based on pre-reaction protein concentrations, 5 ng of test protein was loaded in each lane containing TDO protein.

B: LOD determination. Indicated amounts of the test protein from the Pancreatin Treated T0 sample were loaded to estimate the LOD of the TDO Protein.

Lane	Sample	Incubation Time	Lane	Sample	Amount (ng)
1	Precision Plus™ MWM	-	1	Precision Plus™ MWM	-
2	MagicMark™ MWM	-	2	MagicMark™ MWM	-
3	0 min No Test Protein Control	0	3	Pancreatin Treated T0	5
4	0 min No Pancreatin Control	0	4	Pancreatin Treated T0	2.5
5	Pancreatin Treated T0	0	5	Pancreatin Treated T0	1.25
6	Pancreatin Treated T1	5 min	6	Pancreatin Treated T0	0.63
7	Pancreatin Treated T2	15 min	7	Pancreatin Treated T0	0.31
8	Pancreatin Treated T3	30 min	8	Pancreatin Treated T0	0.16
9	Pancreatin Treated T4	1 h	9	Pancreatin Treated T0	0.08
10	Pancreatin Treated T5	2 h	10	Pancreatin Treated T0	0.04
11	Pancreatin Treated T6	4 h	11	Pancreatin Treated T0	0.02
12	Pancreatin Treated T7	8 h	12	Pancreatin Treated T0	0.01
13	Pancreatin Treated T8	24 h	13	Pancreatin Treated T0	0.005
14	24 h No Pancreatin Control	24 h	14	Pancreatin Treated T0	0.002
15	24 h No Test Protein Control	24 h	15	MagicMark MWM	-

Digestive Fate of the TDO Protein Conclusions

The ability of TDO protein to be degraded by pepsin and by pancreatin was evaluated in this study. The results showed that at least 98.8% of the intact TDO protein was degraded by pepsin within 0.5 min when analyzed by SDS-PAGE and at least 98.4% of the intact TDO was degraded by pepsin within 0.5 min when analyzed by western blot using a TDO specific antibody. SDS-PAGE analysis showed that a peptide fragment of ~3.5 kDa was observed through the 5 min time point of the pepsin digestion but disappeared by 10 min time point. At least 96.8% of the intact TDO protein was degraded by pancreatin within 5 min when analyzed by western blot. These results show that the full-length TDO is rapidly degraded by pepsin and pancreatin. Rapid and complete degradation of the TDO protein by pepsin and pancreatin indicates that the TDO protein poses no meaningful risk to human or animal health.

B.2(a)(iii) An animal toxicity study if the bioinformatic comparison and biochemical studies indicate either a relationship with known protein toxins/anti-nutrients or resistance to proteolysis

Not relevant for this product.

B.2(b) Information on the potential allergenicity of any new proteins, including:

B.2(b)(i) Source of the new proteins

B.2(b)(i)(i) Identity and Source of the *dmo* Gene Introduced into MON 94313

The *dmo* gene is derived from the bacterium *Stenotrophomonas maltophilia* strain DI-6, isolated from soil at a dicamba manufacturing plant ([Krueger et al., 1989](#)). *S. maltophilia* is ubiquitously present in the environment ([Mukherjee and Roy, 2016](#)), including in water and dairy products ([An and Berg, 2018](#); [Okuno et al., 2018](#); [Todaro et al., 2011](#)). These bacteria have been used as an effective biocontrol agent against plant and animal pathogenesis ([Mukherjee and Roy, 2016](#)), and have antibacterial activity against both gram-positive and gram-negative bacteria ([Dong et al., 2015](#)). *S. maltophilia* has been found in healthy individuals without any hazard to human health ([Heller et al., 2016](#); [Lira et al., 2017](#)), although these bacteria can form biofilms that become resistant to antibiotics ([Berg and Martinez, 2015](#); [Brooke et al., 2017](#)). The opportunistic pathogenicity of *S. maltophilia* is mainly associated with hosts with compromised immune systems rather than with any specific virulence genes of these bacteria. Thus, documented occurrences of *S. maltophilia* infections have been limited to immune-compromised individuals in hospital settings ([Lira et al., 2017](#)).

Other than the potential to become an opportunistic pathogen in immune-compromised hosts, *S. maltophilia* is not known for human or animal pathogenicity. *S. maltophilia*'s history of safe exposure has been extensively reviewed during the evaluation of several dicamba-tolerant events with no safety or allergenicity issues identified by FSANZ or other regulatory agencies (e.g., MON 88701 cotton [A1080], MON 87708 soybean [A1063], MON 87419 maize [A1118], and MON 87429 maize [A1192]).

B.2(b)(i)(ii) Identity and Source of the *pat* Gene Introduced into MON 94313

The *pat* gene is derived from the bacterium *Streptomyces viridochromogenes* ([Wohlleben et al., 1988](#)). *Streptomyces* species are widespread in the environment and present no known allergenic or toxicity issues ([Kämpfer, 2006](#); [Kutzner, 1981](#)), though human exposure is quite common ([Goodfellow and Williams, 1983](#)). *S. viridochromogenes* is not considered pathogenic to plants, humans or other animals ([Cross, 1989](#); [Goodfellow and Williams, 1983](#); [Locci, 1989](#)). *S. viridochromogenes* is widespread in the environment and the history of safe use is discussed in [Hérouet et al. \(2005\)](#). This organism has been extensively reviewed during the evaluation of several glufosinate-tolerant events (e.g., A2704-12 and A5547-127 soybean [A481], MON 87419 [A1118] and MON 87429 [A1192]) with no safety or allergenicity issues identified by FSANZ or other regulatory agencies.

B.2(b)(i)(iii) Identity and Source of the *ft_t.1* Gene Introduced into MON 94313

MON 94313 contains the *ft_t.1* gene, a modified version of the *RdpA* gene from *Sphingobium herbicidovorans*, that expresses the FT_T.1 protein. FT_T.1 is therefore a modified version of the R-2,4-dichlorophenoxypropionate dioxygenase (RdpA) protein ([Müller et al., 2006](#)). *S. herbicidovorans* is a common gram-negative, rod-shaped, non-motile, non-spore-forming soil bacterium ([Takeuchi et al., 2001](#); [Zipper et al., 1996](#)), which is strictly aerobic and chemo-organotrophic, and not known to be associated with human disease.

Members of the genus *Sphingobium* have been isolated from a wide variety of habitats including soil and freshwater ([Chaudhary et al., 2017](#)). *Sphingobium* species have also been isolated from food products such as corn ([Rijavec et al., 2007](#)), papaya ([Thomas et al., 2007](#)) and tomato ([Enya et al., 2007](#)). The biosynthetic and biodegrading properties of this genus have been exploited in the food industry ([Fialho et al., 2008](#); [Pozo et al., 2007](#)), bioremediation ([Alarcón et al., 2008](#); [Jin et al., 2013](#)), and biofuel industries ([Varman et al., 2016](#)). The ubiquitous presence of *Sphingobium* species in the environment has resulted in widespread human and animal exposure without any known adverse safety or allergenicity reports. This organism was reviewed during the evaluation of MON 87429 maize [A1192] with no safety or allergenicity issues identified by the FSANZ.

B.2(b)(i)(iv) Identity and Source of the TDO Gene Introduced into MON 94313

The *TDO* gene is derived from Asian (japonica) rice, *Oryza sativa* ([Maeda et al., 2019](#)), which is a crop plant with a long history as food and feed. It is one of the most important crops in the world serving as a primary food source for more than half of the world's population ([Khush, 1997](#)). Rice is cultivated in more than 80 countries around the world (USDA Foreign Agriculture Service - https://apps.fas.usda.gov/psdonline/downloads/psd_grains_pulses_csv.zip), being one of three major staple crops after maize and with a total production similar to wheat. *Oryza sativa* has two subspecies, *indica* and *japonica*, which account for almost all global rice production ([Khush, 1997](#)). Brown, milled, polished and parboiled rice are the major rice products consumed by humans in the form of grain after being cooked. Rice is also consumed as food ingredients which are part of food products. For example, rice flour is used in cereals, baby food, and snacks. The primary nutrients provided by rice are carbohydrates and proteins ([OECD, 2016](#)).

Rice is also widely used as feed for livestock. This is fed in various forms such rice grain, hulls, bran, straw, polishings, and whole crop silage ([OECD, 2016](#)).

Generally, rice is considered to be a safe source of food and feed, and is not considered by allergists to be a common source of allergens. There are very few compounds in rice which are considered unfavourable for human or animal food/feed, and these compounds have not been observed to exist at levels in rice-based foods that would be a concern for food or feed safety ([OECD, 2016](#)).

B.2(b)(ii) A bioinformatics comparison of the amino acid sequence to known allergens

Structural similarity of the DMO, PAT, FT_T.1 and TDO proteins to known allergens

The Codex guidelines for the evaluation of the allergenicity potential of introduced proteins ([Codex Alimentarius, 2009](#)) are based on the comparison of amino acid sequences between introduced proteins and allergens, where allergenic cross-reactivity may exist if the introduced protein is found to have at least 35% amino acid identity with an allergen over any segment of at least 80 amino acids. The Codex guideline also suggests that a sliding window search with a scientifically justified peptide size be used to identify immunologically relevant peptides in otherwise unrelated proteins. Therefore, the extent of sequence similarities between the MON 94313 DMO, PAT, FT_T.1 and TDO proteins sequence and known allergens, gliadins, and glutenins was assessed using the FASTA sequence alignment tool along with an eight-amino acid sliding window search ([Codex Alimentarius, 2009](#); [Thomas et al., 2005](#)). The methods used are summarized below and detailed in Appendix 11 and Appendix 12. The data generated from these analyses confirm that the MON 94313 DMO, PAT, FT_T.1 and TDO proteins do not share amino acid sequence similarities with known allergens, gliadins, or glutenins.

The FASTA program directly compares amino acid sequences (i.e., primary, linear protein structure). This alignment data may be used to infer shared higher order structural similarities between two sequences (i.e., secondary and tertiary protein structures). Proteins that share a high degree of similarity throughout the entire sequence are often homologous. By definition, homologous proteins have common secondary structures, and three-dimensional configuration, and, consequently, may share similar functions. The allergen, gliadin, and glutenin protein sequence database (AD_2022) was obtained as the "COMprehensive Protein Allergen REsource" (COMPARE) database from the Health and Environmental Sciences Institute (HESI) and was used for the evaluation of sequence similarities shared between the DMO, PAT, FT_T.1 and TDO proteins and all proteins in the database. The AD_2022 database contains 2,463 sequences. When used to align the sequence of the introduced protein to each protein in the database, the FASTA algorithm produces an *E*-score (expectation score) for each alignment. The *E*-score is a statistical measure of the likelihood that the observed similarity score could have occurred by chance in a search. A larger *E*-score indicates a low degree of similarity between the query sequence and the sequence from the database. Typically, alignments between two sequences which have an *E*-score of less than or equal to 1×10^{-5} are considered to have meaningful homology. Results indicate that the DMO, PAT, FT_T.1 and TDO proteins sequences do not share meaningful similarity with sequences in the allergen database. No alignment met or exceeded the threshold of 35% identity over 80 amino acids recommended by Codex Alimentarius ([2009](#)), shared an eight amino acid match, or had an *E*-score of less than or equal to 1×10^{-5} .

The bioinformatic results demonstrated there were no biologically relevant sequence similarities to allergens when the DMO, PAT, FT_T.1 and TDO proteins sequences were used as a query for a FASTA search of the AD_2022 database. Furthermore, no short (eight amino acid) polypeptide matches were shared between the DMO, PAT, FT_T.1 and TDO proteins sequences and proteins

in the allergen database. These data show that DMO, PAT, FT_T.1 and TDO proteins sequences lack both structurally and immunologically relevant similarities to known allergens, gliadins, and glutenins.

For details, please refer to Appendix 11 and Appendix 12.

B.2(b)(iii) The new protein's structural properties, including, but not limited to, its susceptibility to enzymatic degradation (e.g. proteolysis), heat and/or acid stability

B.2(b)(iii)(i) Heat susceptibility of the MON 94313 DMO protein

Temperature can have a profound effect on the structure and function of proteins. Heat treatment is widely used in the preparation of foods derived from soybean ([Hammond and Jez, 2011](#)). It is reasonable that such processing will have an effect on the functional activity and structure of DMO protein when consumed in different food products derived from MON 94313, thus reducing any potential safety concerns posed by the protein. Therefore, an assessment of the effect of heating was conducted as a surrogate for the conditions encountered during the preparation of foods from MON 94313.

The effect of heat treatment on the activity of the DMO protein was evaluated using purified protein expressed in *E. coli*. Heat treated samples and an unheated control sample of DMO protein were analyzed: 1) using a functional assay to assess the impact of temperature on the enzymatic activity of the DMO protein; and 2) using SDS-PAGE to assess the impact of temperature on protein integrity.

Aliquots of DMO protein were heated to 25, 37, 55, 75 and 95 °C for either 15 or 30 minutes, while a separate aliquot of DMO protein was maintained on ice for the duration of the heat treatments to serve as a temperature control. The effect of heat treatment on the activity of DMO was evaluated using a functional activity assay. The effect of heat treatment on the integrity of the DMO protein was evaluated using SDS-PAGE analysis of the heated and temperature control DMO protein samples.

Results of the functional activity assay for the DMO protein incubated for 15 and 30 minutes are listed in Table 40 and

Table 41, respectively. The control sample had an activity of 181 and 259 $\text{nmol} \times \text{minute}^{-1} \times \text{mg}^{-1}$ of DMO protein for the 15- and 30-minute incubation periods, respectively, demonstrating that protein activity was maintained during incubation on ice. Protein activity was retained when incubated for 15 and 30 minutes at a temperature of 25°C (103% and 102% of activity compared to the control for 15 and 30 minutes, respectively) and 37°C (93% and 105% of activity compared to the control for 15 and 30 minutes, respectively). At temperatures of 55°C and above, the functional activity of the MON 94313 DMO protein was reduced to 0% relative to the control MON 94313 DMO protein activity whether heated for 15 or 30 minutes.

The results of the SDS-PAGE analysis of the heat-treated samples incubated for 15- and 30-minutes are illustrated in Figure 57 and Figure 58, respectively. The control sample loaded on each gel (Figure 57 and Figure 58, lane 2) showed equivalent ~36 kDa band intensity to the 100% reference standard (Figure 57 and Figure 58, lane 8), demonstrating that the DMO protein was stable on wet ice during the incubation period. No apparent decrease in band intensity of the ~36 kDa MON 94313 DMO protein was observed when heated at temperatures of 25, 37, and 55°C for 15 minutes (Figure 57, lanes 3-5) or 30 minutes (Figure 58, lanes 3-5). A decrease in the band intensity of the DMO protein was observed when heated at an increased temperature from 75°C to 95 °C with increased time from 15 to 30 minutes (Figure 57 and Figure 58, lanes 6–7). When heated at 95°C, lower molecular weight fragments were observed (Figure 57 and Figure 58, lane 7) , likely due to degradation of the MON 94313 DMO protein when heated at 95°C for 15 or 30 minutes.

Higher molecular weight aggregates were observed when the MON 94313 DMO protein samples were heated to 55, 75, and 95°C for 15 and 30 minutes (Figure 57 and Figure 58, lanes 5-7), and the band intensities of these higher molecular weight aggregates increased and became more diffuse with increased heat treatment temperature and duration. These higher molecular weight aggregates may be due to aggregation of the MON 94313 DMO protein when exposed to high temperatures.

These data demonstrate that the DMO protein behaves with a predictable tendency toward protein denaturation and loss of functional activity at elevated temperatures. Heat treatment is widely used in the preparation of foods containing components derived from soybean grain. Therefore, it is reasonable to conclude that DMO protein would not be consumed as an active protein in food or feed products due to standard processing practices that include heat treatment.

For details, please refer to Appendix 17.

Table 40. Dicamba Functional Activity of Heat-Treated *E. coli*-Produced DMO Protein after 15 Minutes

Treatment	Specific Activity ($\text{nmol} \times \text{minute}^{-1} \times \text{mg}^{-1}$) ¹	Relative Activity (% of control sample) ³
Control Treatment (wet ice)	181	100 ²
25 °C	186	103
37 °C	169	93
55 °C	0	0

PART 2: SPECIFIC DATA REQUIREMENTS FOR SAFETY ASSESSMENT

75 °C	0	0
95 °C	0	0

¹ Mean specific activity rounded to nearest whole number determined from n=5.

² DMO protein activity of control samples was assigned 100% active.

³ Relative Activity = [specific activity of sample/specific activity of control sample] x 100

Table 41. Dicamba Functional Activity of Heat-Treated *E. coli*-Produced DMO Protein After 30 Minutes

Treatment	Specific Activity (nmol × minute ⁻¹ × mg ⁻¹) ¹	Relative Activity (% of control sample) ³
Control Treatment (wet ice)	259	100 ²
25 °C	264	102
37 °C	271	105
55 °C	0	0
75 °C	0	0
95 °C	0	0

¹ Mean specific activity rounded to nearest whole number determined from n=5.

² DMO protein activity of control samples was assigned 100% active.

³ Relative Activity = [specific activity of sample/specific activity of control sample] x 100

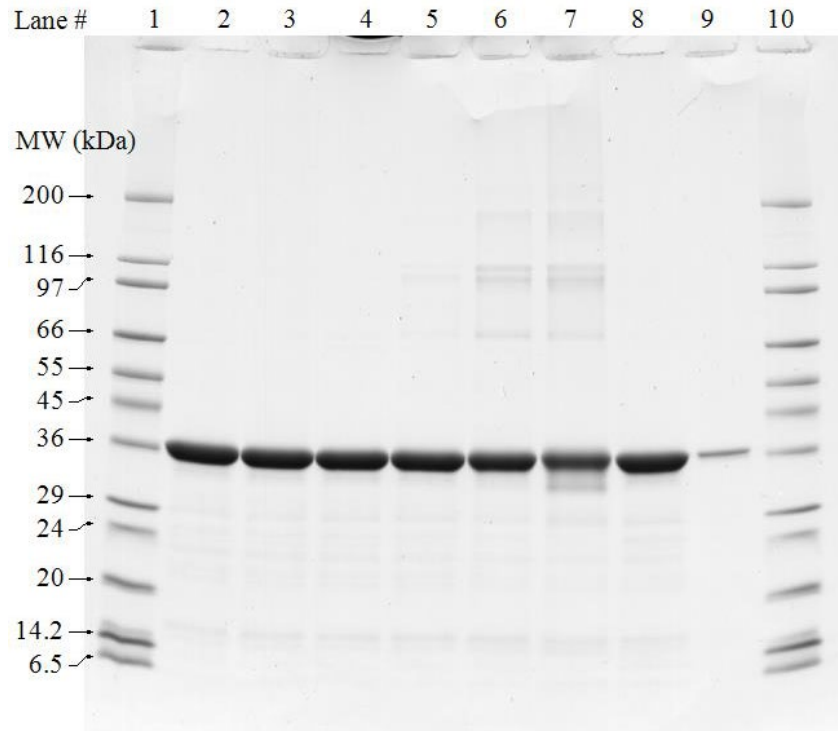


Figure 57. SDS-PAGE of *E. coli*-Produced DMO Protein Demonstrating the Effect After 15 Minutes at Elevated Temperatures on Protein Structural Stability

Heat-treated samples of *E. coli*-produced DMO (3.0 µg total protein) separated on a Tris-glycine 4-20% polyacrylamide gel under denaturing and reducing conditions. The gel was stained with Brilliant Blue G-Colloidal. Molecular weights (kDa) are shown on the left and correspond to molecular weight markers in lanes 1 and 10.

Lane	Description	Total Amount
1	SigmaMarker™ Wide Range Molecular Weight Marker	-
2	<i>E. coli</i> -produced DMO Protein Control	3.0 µg
3	<i>E. coli</i> -produced DMO Protein 25 °C	3.0 µg
4	<i>E. coli</i> -produced DMO Protein 37 °C	3.0 µg
5	<i>E. coli</i> -produced DMO Protein 55 °C	3.0 µg
6	<i>E. coli</i> -produced DMO Protein 75 °C	3.0 µg
7	<i>E. coli</i> -produced DMO Protein 95 °C	3.0 µg
8	<i>E. coli</i> -produced DMO Protein Reference 100 % Equivalence	3.0 µg
9	<i>E. coli</i> -produced DMO Protein Reference 10 % Equivalence	0.3 µg
10	SigmaMarker™ Wide Range Molecular Weight Marker	-

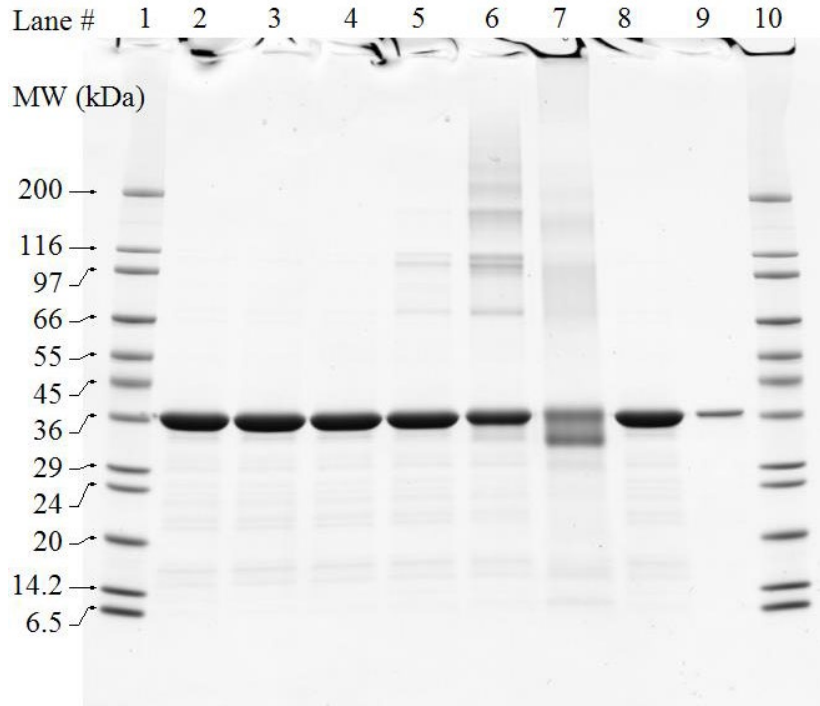


Figure 58. SDS-PAGE of *E. coli*-Produced DMO Protein Demonstrating the Effect After 30 Minutes at Elevated Temperatures on Protein Structural Stability

Heat-treated samples of *E. coli*-produced DMO (3.0 µg total protein) separated on a Tris-glycine 4-20 % polyacrylamide gel under denaturing and reducing conditions. The gel was stained with Brilliant Blue G-Colloidal. Molecular weights (kDa) are shown on the left and correspond to molecular weight markers in lanes 1 and 10.

Lane	Description	Total Amount
1	SigmaMarker™ Wide Range Molecular Weight Marker	-
2	<i>E. coli</i> -produced DMO Protein Control	3.0 µg
3	<i>E. coli</i> -produced DMO Protein 25 °C	3.0 µg
4	<i>E. coli</i> -produced DMO Protein 37 °C	3.0 µg
5	<i>E. coli</i> -produced DMO Protein 55 °C	3.0 µg
6	<i>E. coli</i> -produced DMO Protein 75 °C	3.0 µg
7	<i>E. coli</i> -produced DMO Protein 95 °C	3.0 µg
8	<i>E. coli</i> -produced DMO Protein Reference 100 % Equivalence	3.0 µg
9	<i>E. coli</i> -produced DMO Protein Reference 10 % Equivalence	0.3 µg
10	SigmaMarker™ Wide Range Molecular Weight Marker	-

B.2(b)(iii)(ii) Heat susceptibility of MON 94313 PAT protein

Temperature can have a profound effect on the structure and function of proteins. Heat treatment is widely used in the preparation of foods derived from soybean ([Hammond and Jez, 2011](#)). It is reasonable that such processing will have an effect on the functional activity and structure of PAT protein when consumed in different food products derived from MON 94313, thus reducing any potential safety concerns posed by the protein. Therefore, an assessment of the effect of heating was conducted as a surrogate for the conditions encountered during the preparation of foods from MON 94313.

The effect of heat treatment on the activity of MON 94313-produced PAT protein was evaluated using the *E. coli*-produced PAT protein. Heat-treated samples and an unheated control sample of *E. coli*-produced PAT protein were analyzed: 1) using a functional assay to assess the impact of temperature on the enzymatic activity of PAT protein; and 2) using SDS-PAGE to assess the impact of temperature on protein integrity.

Aliquots of *E. coli*-produced PAT protein were heated to 25, 37, 55, 75, and 95 °C for either 15 or 30 minutes, while a separate aliquot of *E. coli*-produced PAT protein was maintained on ice for the duration of the heat treatments to serve as a temperature control. The effect of heat treatment on the activity of PAT protein was evaluated using a functional activity assay. The effect of heat treatment on the integrity of the PAT protein was evaluated using SDS-PAGE analysis of the heated and temperature control PAT protein samples.

The effects of heating on the functional activity of *E. coli*-produced PAT are presented in Table 42 and Table 43. The functional activity of PAT protein was unaffected at 25 and 37 °C for 15 and 30 minutes. The functional activity of the PAT protein was reduced by approximately 90% or greater relative to the activity of control PAT protein whether heated at 55°C and above for 15 or 30 min. These results suggest that temperature has a considerable effect on the functional activity of PAT protein.

Analysis by SDS-PAGE stained with Brilliant Blue G-Colloidal demonstrated that the PAT control treatment and reference standard contain a major band at ~25 kDa, corresponding to the PAT protein (Figure 59 and Figure 60, Lanes 2 and 8). No apparent decrease in the intensity of this band was observed in heat-treated PAT protein at 25, 37, 55, 75 and 95 °C for 15 minutes (Figure 59, Lanes 3-7) or 30 minutes (Figure 60, Lanes 3-7). However, PAT protein heated to 95°C for 15 and 30 minutes (Figure 59 and Figure 60, Lane 7) showed some appearance of higher molecular weight species, which may be due to slight aggregation of the PAT protein when exposed to high temperatures.

These data demonstrate that PAT protein remains intact, but is deactivated at 55 °C and above. This is comparable with what has been previously published on the safety assessment of PAT protein ([Hérout et al., 2005](#)). Therefore, it is reasonable to conclude that PAT protein would not be consumed as an active protein in food or feed products due to standard processing practices that include heat treatment.

For details, please refer to Appendix 18.

Table 42. Functional Activity of PAT Protein after 15 Minutes at Elevated Temperatures

Temperature	Specific Activity ($\mu\text{mol} \times \text{minute}^{-1} \times \text{mg}^{-1}$) ¹	Relative Activity (% of control sample) ^{2,3}
0 °C (control)	24.5	100 %
25 °C	26.7	109 %
37 °C	26.9	110 %
55 °C	2.8	11 %
75 °C	0.9	4 %
95 °C	1.1	4 %

¹ Mean specific activity determined from n=3.

² PAT protein activity of control samples was assigned 100 % active.

³ Relative Activity = [specific activity of sample/specific activity of control sample] × 100

Table 43. Functional Activity of PAT Protein after 30 Minutes at Elevated Temperatures

Temperature	Specific Activity ($\mu\text{mol} \times \text{minute}^{-1} \times \text{mg}^{-1}$) ¹	Relative Activity (% of control sample) ^{2,3}
0 °C (control)	24.5	100 %
25 °C	31.2	127 %
37 °C	29.8	122 %
55 °C	1.0	4 %
75 °C	1.1	4 %
95 °C	1.3	5 %

¹ Mean specific activity determined from n=3.

² PAT protein activity of control sample was assigned 100 % active.

³ Relative Activity = [specific activity of sample/specific activity of control sample] × 100

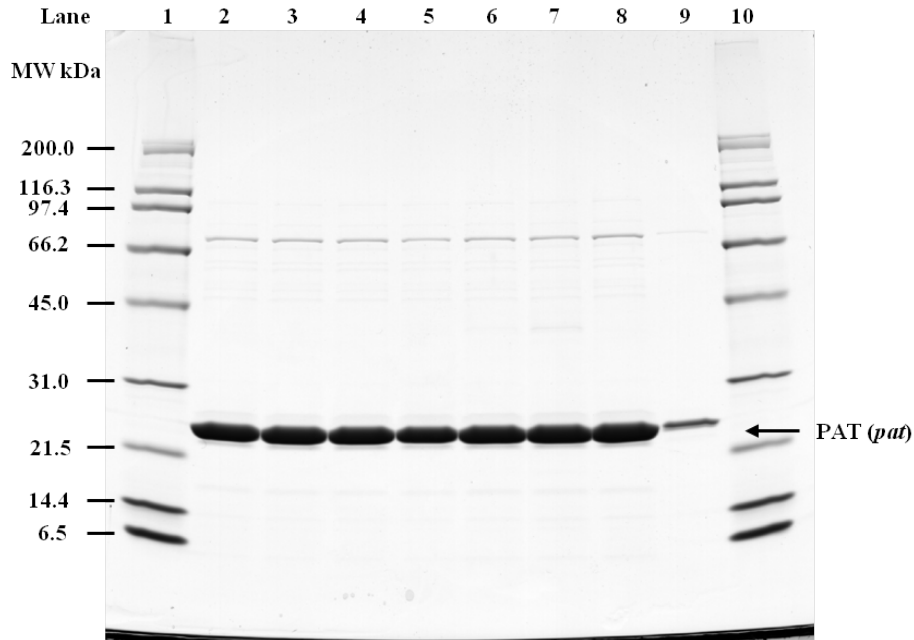


Figure 59. SDS-PAGE of *E. coli*-Produced PAT Protein Following Heat Treatment for 15 Minutes

Heat treated samples of *E. coli*-produced PAT (3.0 µg total protein) separated on a Tris-glycine 4-20 % polyacrylamide gel under denaturing and reducing conditions. The gel was stained with Brilliant Blue G-Colloidal. Molecular weights (kDa) are shown on the left and correspond to molecular weight markers in lanes 1 and 10.

Lane	Description	Total Amount
1	Broad Range™ Molecular Weight Markers	-
2	<i>E. coli</i> -produced PAT Protein Control	3.0
3	<i>E. coli</i> -produced PAT Protein 25 °C	3.0
4	<i>E. coli</i> -produced PAT Protein 37 °C	3.0
5	<i>E. coli</i> -produced PAT Protein 55 °C	3.0
6	<i>E. coli</i> -produced PAT Protein 75 °C	3.0
7	<i>E. coli</i> -produced PAT Protein 95 °C	3.0
8	<i>E. coli</i> -produced PAT Protein Reference 100 % Equivalence	3.0
9	<i>E. coli</i> -produced PAT Protein Reference 10 % Equivalence	0.3
10	Broad Range Molecular Weight Markers	-

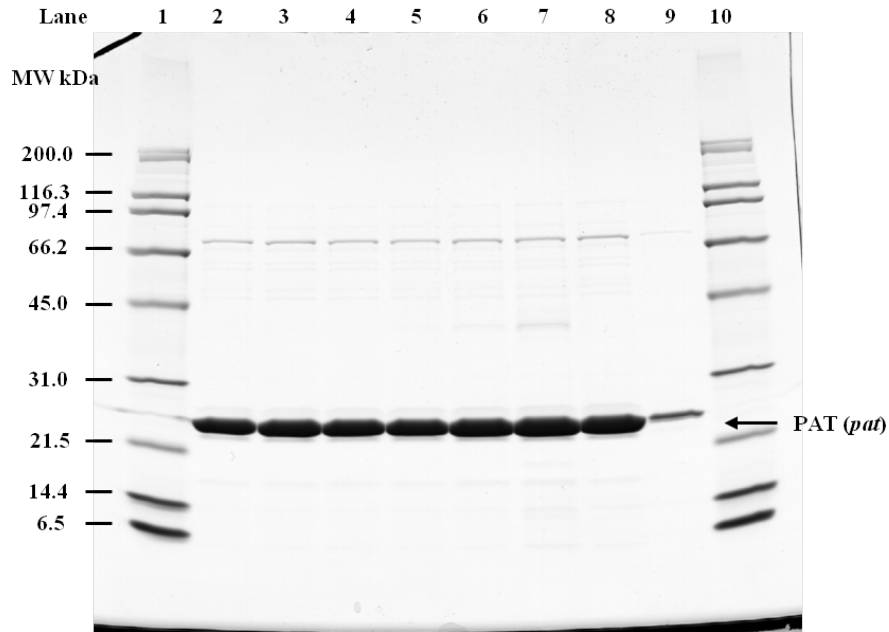


Figure 60. SDS-PAGE of *E. coli*-Produced PAT Protein Following Heat Treatment for 30 Minutes

Heat treated samples of *E. coli*-produced PAT (3.0 µg total protein) separated on a Tris-glycine 4-20 % polyacrylamide gel under denaturing and reducing conditions. The gel was stained with Brilliant Blue G-Colloidal. Molecular weights (kDa) are shown on the left and correspond to molecular weight markers in lanes 1 and 10.

Lane	Description	Total Amount
1	Broad Range™ Molecular Weight Markers	-
2	<i>E. coli</i> -produced PAT Protein Control	3.0
3	<i>E. coli</i> -produced PAT Protein 25 °C	3.0
4	<i>E. coli</i> -produced PAT Protein 37 °C	3.0
5	<i>E. coli</i> -produced PAT Protein 55 °C	3.0
6	<i>E. coli</i> -produced PAT Protein 75 °C	3.0
7	<i>E. coli</i> -produced PAT Protein 95 °C	3.0
8	<i>E. coli</i> -produced PAT Protein Reference 100 % Equivalence	3.0
9	<i>E. coli</i> -produced PAT Protein Reference 10 % Equivalence	0.3
10	Broad Range™ Molecular Weight Markers	-

B.2(b)(iii)(iii) Heat susceptibility of the MON 94313 FT_T.1 protein

Temperature can have a profound effect on the structure and function of proteins. Heat treatment is widely used in the preparation of foods derived from soybean ([Hammond and Jez, 2011](#)). It is reasonable that such processing will have an effect on the functional activity and structure of FT_T.1 protein when consumed in different food products derived from MON 94313, thus reducing any potential safety concerns posed by the protein. Therefore, an assessment of the effect of heating was conducted as a surrogate for the conditions encountered during the preparation of foods from MON 94313.

The effect of heat treatment on the activity of the FT_T.1 protein was evaluated using purified protein. Heat treated samples and an unheated control sample of FT_T.1 protein were analyzed: 1) using a functional assay to assess the impact of temperature on the enzymatic activity of the FT_T.1 protein; and 2) using SDS-PAGE to assess the impact of temperature on protein integrity.

Aliquots of FT_T.1 protein were heated to 25, 37, 55, 75 and 95 °C for either 15 or 30 minutes, while a separate aliquot of FT_T.1 protein was maintained on ice for the duration of the heat treatments to serve as a temperature control. The effect of heat treatment on the activity of FT_T.1 was evaluated using a functional activity assay. The effect of heat treatment on the integrity of the FT_T.1 protein was evaluated using SDS-PAGE analysis of the heated and temperature control FT_T.1 protein samples.

The effects of heating on the functional activity of FT_T.1 protein are presented in Table 44 and Table 45. The control sample had an activity of $911 \text{ nmol} \times \text{minute}^{-1} \times \text{mg}^{-1}$ of FT_T.1 protein, thus demonstrating that protein activity was maintained during incubation on ice. Protein activity was retained when incubated for 15 and 30 minutes at temperatures of 25 and 37°C. Incubation for 15 minutes at a temperature of 55°C reduced the specific activity of the FT_T.1 protein to 34%. Incubation at a temperature of 55°C for 30 minutes and at temperatures of 75°C and above for either 15 or 30 minutes, reduced functional activity to below the LOD to 0% of the control FT_T.1 protein activity. These results suggest that temperature has a considerable effect on the activity of FT_T.1.

Analysis by SDS-PAGE stained with Brilliant Blue G-Colloidal demonstrated that heat treatment to temperatures of 25, 37, 55, 75 and 95 °C for 15 or 30 minutes did not result in observable changes in the FT_T.1 protein band intensity (Figure 61 and Figure 62, respectively). There was a slight visible appearance of higher and lower molecular weight species at heat treatments of 95 °C for 15 and 30 minutes, which may be due to slight aggregation and degradation of the protein when exposed to high temperatures.

These data demonstrate that the FT_T.1 protein remains largely intact but behaves with a predictable tendency toward protein denaturation and loss of functional activity at elevated temperatures. Therefore, it is reasonable to conclude that FT_T.1 protein would not be consumed as an active protein in food or feed products due to standard processing practices that include heat treatment.

For details, please refer to Appendix 19.

Table 44. Functional Activity of Heat Treated FT_T.1 Protein After 15 Minutes at Elevated Temperatures

Temperature	Specific Activity (nmol x minute ⁻¹ x mg ⁻¹) ¹	Relative Activity (% of control sample) ^{2,3}
0 °C (control)	911	100
25°C	984	108
37°C	1100	121
55°C	308	34
75°C	≤LOD ⁴	0
95°C	≤LOD ⁴	0

¹Mean specific activity determined from n=3.

²FT_T.1 protein activity of control sample was assigned 100% activity.

³Relative activity = [specific activity of sample/specific activity of control sample] x 100.

⁴23 nmol × minute⁻¹ × mg⁻¹ is the limit of detection (LOD) of the assay.

Table 45. Functional Activity of Heat Treated FT_T.1 Protein After 30 Minutes at Elevated Temperatures

Temperature	Specific Activity (nmol x minute ⁻¹ x mg ⁻¹) ¹	Relative Activity (% of control sample) ^{2,3}
0 °C (control)	911	100
25°C	804	88
37°C	1056	116
55°C	≤LOD ⁴	0
75°C	≤LOD ⁴	0
95°C	≤LOD ⁴	0

¹Mean specific activity determined from n=3.

²FT_T.1 protein activity of control sample was assigned 100% activity.

³Relative activity = [specific activity of sample/specific activity of control sample] x 100.

⁴23 nmol × minute⁻¹ × mg⁻¹ is the limit of detection (LOD) of the assay.

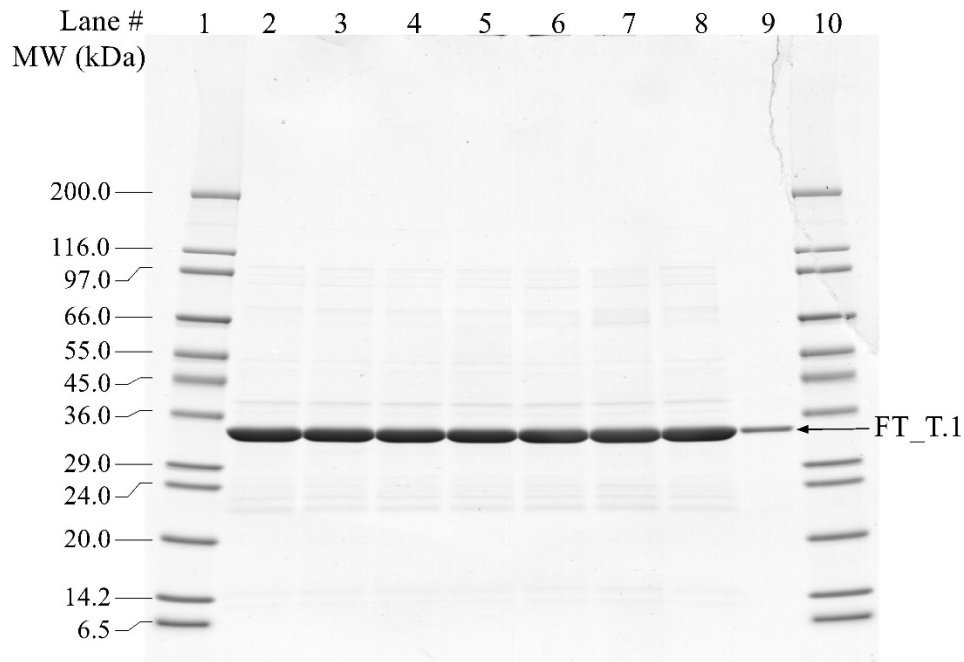


Figure 61. SDS-PAGE of *E. coli*-Produced FT_T.1 Protein Demonstrating the Effect After 15 Minutes at Elevated Temperatures on Protein Structural Stability

Heat treated samples of *E. coli*-produced FT_T.1 (3.0 µg total protein) separated on a Tris-glycine 4-20% polyacrylamide gel under denaturing and reducing conditions. The gel was stained with Brilliant Blue G-Colloidal. Approximate molecular weights (kDa) are shown on the left and correspond to molecular weight markers in lanes 1 and 10.

Lane	Description	Total Amount
1	SigmaMarker™ Molecular Weight Markers	-
2	<i>E. coli</i> -produced FT_T.1 Protein Control	3.0 µg
3	<i>E. coli</i> -produced FT_T.1 Protein 25 °C	3.0 µg
4	<i>E. coli</i> -produced FT_T.1 Protein 37 °C	3.0 µg
5	<i>E. coli</i> -produced FT_T.1 Protein 55 °C	3.0 µg
6	<i>E. coli</i> -produced FT_T.1 Protein 75 °C	3.0 µg
7	<i>E. coli</i> -produced FT_T.1 Protein 95 °C	3.0 µg
8	<i>E. coli</i> -produced FT_T.1 Protein Reference 100 % Equivalence	3.0 µg
9	<i>E. coli</i> -produced FT_T.1 Protein Reference 10 % Equivalence	0.3 µg
10	SigmaMarker™ Molecular Weight Markers	-

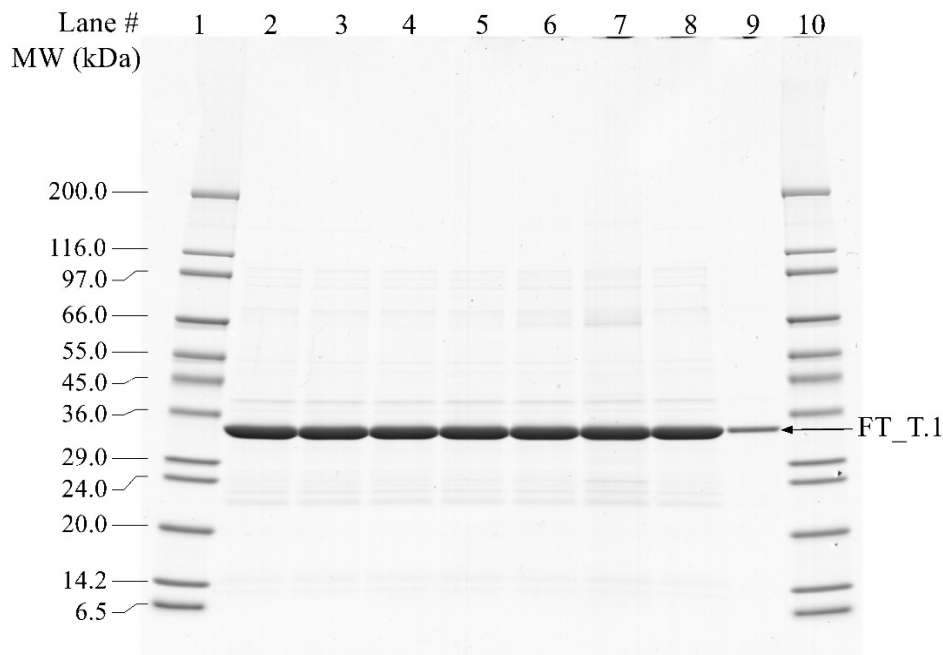


Figure 62. SDS-PAGE of *E. coli*-Produced FT_T.1 Protein Demonstrating the Effect After 30 Minutes at Elevated Temperatures on Protein Structural Stability

Heat treated samples of *E. coli*-produced FT_T.1 (3.0 µg total protein) separated on a Tris-glycine 4-20% polyacrylamide gel under denaturing and reducing conditions. The gel was stained with Brilliant Blue G-Colloidal. Approximate molecular weights (kDa) are shown on the left and correspond to molecular weight markers in lanes 1 and 10.

Lane	Description	Total Amount
1	SigmaMarker™ Molecular Weight Markers	-
2	<i>E. coli</i> -produced FT_T.1 Protein Control	3.0 µg
3	<i>E. coli</i> -produced FT_T.1 Protein 25 °C	3.0 µg
4	<i>E. coli</i> -produced FT_T.1 Protein 37 °C	3.0 µg
5	<i>E. coli</i> -produced FT_T.1 Protein 55 °C	3.0 µg
6	<i>E. coli</i> -produced FT_T.1 Protein 75 °C	3.0 µg
7	<i>E. coli</i> -produced FT_T.1 Protein 95 °C	3.0 µg
8	<i>E. coli</i> -produced FT_T.1 Protein Reference 100 % Equivalence	3.0 µg
9	<i>E. coli</i> -produced FT_T.1 Protein Reference 10 % Equivalence	0.3 µg
10	SigmaMarker™ Molecular Weight Markers	-

B.2(b)(iii)(iv) Heat susceptibility of the MON 94313 TDO protein

Temperature can have a profound effect on the structure and function of proteins. Heat treatment is widely used in the preparation of foods derived from soybean ([Hammond and Jez, 2011](#)). It is reasonable that such processing will have an effect on the functional activity and structure of TDO protein when consumed in different food products derived from MON 94313, thus reducing any potential safety concerns posed by the protein. Therefore, an assessment of the effect of heating was conducted as a surrogate for the conditions encountered during the preparation of foods from MON 94313.

The effect of heat treatment on the activity of the TDO protein was evaluated using purified protein. Heat treated samples and an unheated control sample of TDO protein were analyzed: 1) using a functional assay to assess the impact of temperature on the enzymatic activity of the TDO protein; and 2) using SDS-PAGE to assess the impact of temperature on protein integrity.

Aliquots of TDO protein were heated to 25, 37, 55, 75 and 95 °C for either 15 or 30 minutes, while a separate aliquot of TDO protein was maintained on ice for the duration of the heat treatments to serve as a temperature control. The effect of heat treatment on the activity of TDO was evaluated using a functional activity assay. The effect of heat treatment on the integrity of the TDO protein was evaluated using SDS-PAGE analysis of the heated and temperature control TDO protein samples.

The effects of heating on the functional activity of TDO protein are presented in Table 46 and Table 47. The control sample had an activity of $197 \text{ nmol} \times \text{minute}^{-1} \times \text{mg}^{-1}$ of TDO protein, thus demonstrating that protein activity was maintained during incubation on ice. Protein activity was retained when incubated for 15 and 30 minutes at a temperature of 25°C (104% of activity compared to the control). Incubation for 15 and 30 minutes at 37°C reduced functional activity to 82% and 42%, respectively. Incubation for 15 and 30 minutes at 55°C and above reduced functional activity to below the LOD to 0% of the control TDO protein activity. These results suggest that temperature has a considerable effect on the activity of TDO.

Analysis by SDS-PAGE stained with Brilliant Blue G-Colloidal are illustrated in Figure 63 and Figure 64, respectively. The control sample loaded on each gel Figure 63 and Figure 64, lane 2) showed equivalent ~37 kDa band intensity to the 100% reference standard (Figure 63 and Figure 64, lane 8), demonstrating that the TDO protein was stable on wet ice during the incubation period. No apparent decrease in band intensity of the ~37 kDa TDO protein was observed when heated at any of the temperatures ranging from 25 to 95°C for 15 minutes (Figure 63, lanes 3-7) or 30 minutes (Figure 64, lanes 3-7).

These data demonstrate that the TDO protein remains largely intact but behaves with a predictable tendency toward protein denaturation and loss of functional activity at elevated temperatures. Therefore, it is reasonable to conclude that TDO protein would not be consumed as an active protein in food or feed products due to standard processing practices that include heat treatment.

For details, please refer to Appendix 20.

Table 46. TDO Activity After 15 Minutes at Elevated Temperatures

Treatment	Specific Activity (nmol × minute ⁻¹ × mg ⁻¹) ¹	Relative Activity (% of control sample) ³
Control Treatment (wet ice)	197	100 ²
25 °C	204	104
37 °C	162	82
55 °C	≤LOD ⁴	0
75 °C	≤LOD ⁴	0
95 °C	≤LOD ⁴	0

¹ Mean specific activity determined from n=3.

² TDO protein activity of the control sample was assigned 100 % active.

³ Relative Activity = [specific activity of sample/specific activity of control sample] x 100

⁴ 22.8 nmol × minute⁻¹ × mg⁻¹ is the limit of detection (LOD) of the assay

Table 47. TDO Activity After 30 Minutes at Elevated Temperatures

Treatment	Specific Activity (nmol × minute ⁻¹ × mg ⁻¹) ¹	Relative Activity (% of control sample) ³
Control Treatment (wet ice)	197	100 ²
25 °C	205	104
37 °C	83	42
55 °C	≤LOD ⁴	0
75 °C	≤LOD ⁴	0
95 °C	≤LOD ⁴	0

¹ Mean specific activity determined from n=3.

² TDO protein activity of the control sample was assigned 100 % active.

³ Relative Activity = [specific activity of sample/specific activity of control sample] x 100

⁴ 22.8 nmol × minute⁻¹ × mg⁻¹ is the limit of detection (LOD) of the assay

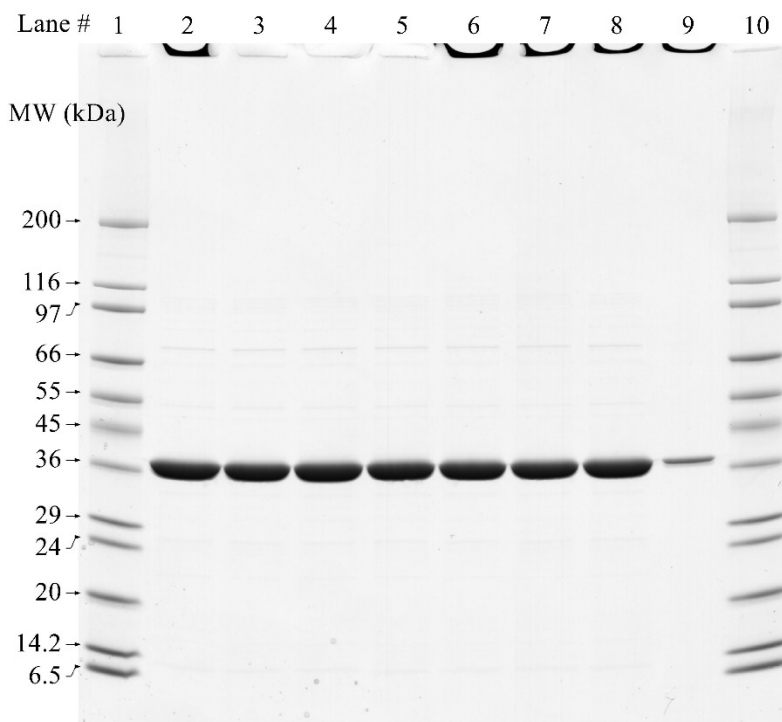


Figure 63. SDS-PAGE of *E. coli*-Produced TDO Protein Following Heat Treatment for 15 Minutes

Heated-treated samples of *E. coli*-produced TDO (3.0 µg total protein) separated on a Tris-glycine 4-20% polyacrylamide gel under denaturing and reducing conditions. The gel was stained with Brilliant Blue G-Colloidal. Approximate molecular weights (kDa) are shown on the right and correspond to molecular weight markers in lanes 1 and 10.

Lane	Description	Total Amount
1	SigmaMarker™ Molecular Weight Marker	-
2	<i>E. coli</i> -produced TDO Protein Control	3.0 µg
3	<i>E. coli</i> -produced TDO Protein 25 °C	3.0 µg
4	<i>E. coli</i> -produced TDO Protein 37 °C	3.0 µg
5	<i>E. coli</i> -produced TDO Protein 55 °C	3.0 µg
6	<i>E. coli</i> -produced TDO Protein 75 °C	3.0 µg
7	<i>E. coli</i> -produced TDO Protein 95 °C	3.0 µg
8	<i>E. coli</i> -produced TDO Protein Reference 100 % Equivalence	3.0 µg
9	<i>E. coli</i> -produced TDO Protein Reference 10 % Equivalence	0.3 µg
10	SigmaMarker™ Molecular Weight Marker	-

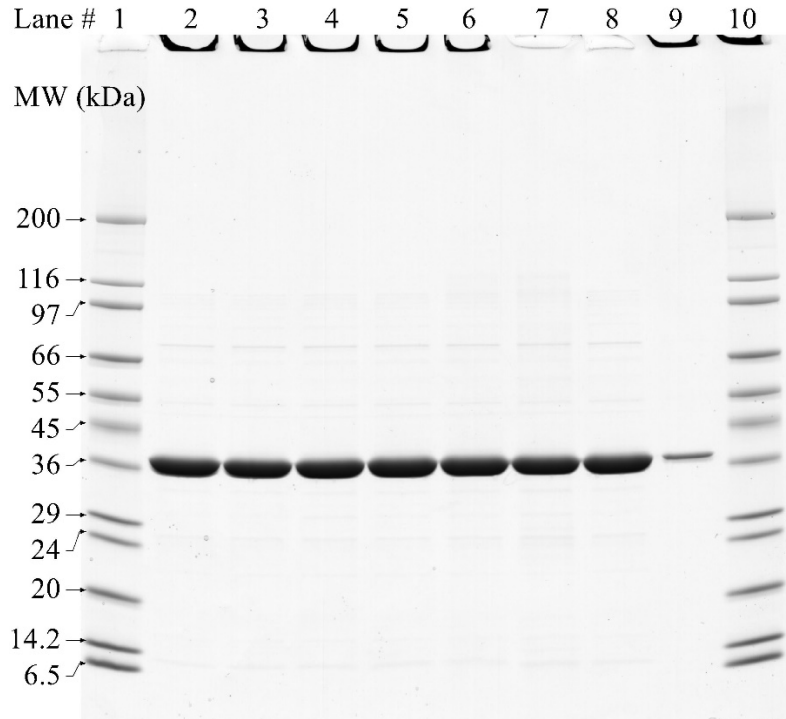


Figure 64. SDS-PAGE of *E. coli*-Produced TDO Protein Following Heat Treatment for 30 Minutes

Heat-treated samples of *E. coli*-produced TDO (3.0 µg total protein) separated on a Tris-glycine 4-20% polyacrylamide gel under denaturing and reducing conditions. The gel was stained with Brilliant Blue G-Colloidal. Approximate molecular weights (kDa) are shown on the right and correspond to molecular weight markers in lanes 1 and 10.

Lane	Description	Total Amount
1	SigmaMarker™ Molecular Weight Marker	-
2	<i>E. coli</i> -produced TDO Protein Control	3.0 µg
3	<i>E. coli</i> -produced TDO Protein 25 °C	3.0 µg
4	<i>E. coli</i> -produced TDO Protein 37 °C	3.0 µg
5	<i>E. coli</i> -produced TDO Protein 55 °C	3.0 µg
6	<i>E. coli</i> -produced TDO Protein 75 °C	3.0 µg
7	<i>E. coli</i> -produced TDO Protein 95 °C	3.0 µg
8	<i>E. coli</i> -produced TDO Protein Reference 100 % Equivalence	3.0 µg
9	<i>E. coli</i> -produced TDO Protein Reference 10 % Equivalence	0.3 µg
10	SigmaMarker™ Molecular Weight Marker	-

Degradation and Degradation and Heat Susceptibility of the MON 94313 DMO, PAT, FT_T.1 and TDO Proteins – Conclusions

The susceptibility of a protein to heat or its degradation in the presence of pepsin and pancreatin is a factor in the assessment of its potential toxicity. The degradation of MON 94313 DMO, PAT, FT_T.1 and TDO proteins were evaluated by incubation with solutions containing pepsin and pancreatin, and the results show that MON 94313 DMO, PAT, FT_T.1 and TDO proteins were readily degraded. Exposure to heat during food processing or cooking, and to digestive fluids is likely to have a profound effect on the structure and function of proteins.

The effect of heat treatment on the activity of MON 94313 DMO, PAT, FT_T.1 and TDO proteins was evaluated using functional assays to assess the impact of temperature on enzymatic activity, and using SDS-PAGE to assess the impact of temperature on protein integrity. The results show that MON 94313 DMO protein was completely deactivated by heating at 55 °C or higher for 15 min or more, PAT protein was substantially deactivated by heating at 55 °C and completely deactivated at 75°C or above for 15 min or more, FT_T.1 protein heated to 75°C for 15 min and 55°C for 30 min had activities below the limit of detection, and TDO heated to 55 °C for 15 min or more had an activity below the limit of detection. Therefore, it is anticipated that exposure to functionally active MON 94313 DMO, PAT, FT_T.1 or TDO protein from the consumption of MON 94313 or foods derived from MON 94313 is unlikely.

B.2(b)(iv) Specific serum screening where a new protein is derived from a source known to be allergenic or has sequence homology with a know allergen

Not relevant for this product.

B.2(b)(v) Information on whether the new protein(s) have a role in the elicitation of gluten-sensitive enteropathy, in cases where the introduced genetic material is obtained from wheat, rye, barley, oats, or related cereal grains

Not relevant for this product.

B.3 Other (non-protein) New Substances

Not applicable.

B.4 Novel Herbicide Metabolites in GM Herbicide-Tolerant Plants

The novel metabolites for dicamba and glufosinate have previously been assessed in applications A1063 and A481 respectively. Hence in the subsequent subsections of B.4, only novel herbicide metabolites of mesotrione and 2,4-D shall be addressed.

B.4.(a) Mesotrione Residue Study in MON 94313

A study was conducted in 2020 in the U.S. to determine residue levels of mesotrione and its metabolite 4-(methylsulphonyl)-2-nitrobenzoic acid (MNBA) in/on herbicide-tolerant (HT) soybean MON 94313 raw agricultural commodities (RACs) following two applications of a formulation of mesotrione.

PART 2: SPECIFIC DATA REQUIREMENTS FOR SAFETY ASSESSMENT

Combined maximum application rate in the U.S. is proposed to be 0.24 lb a.i./A (0.269 kg a.i./ha). The proposed maximum application rates and corresponding application growth stages of mesotrione to MON 94313 in the U.S. are summarized below. Any combination of application rates and timings may be used within the allowed limits for individual rates and timings as specified on the label.

Maximum Application Rates	
Combined maximum of all applications per year	0.24 lb a.i./A (0.269 kg a.i./ha)
Total of all preemergence applications	0.188 lb a.i./A (0.211 kg a.i./ha)
Total in-crop applications at R1 soybean growth stage	0.094 lb a.i./A (0.105 kg a.i./ha)

The purpose of this summary is to report the residue levels of mesotrione and its metabolite 4-(methylsulphonyl)-2-nitrobenzoic acid (MNBA) in MON 94313 soybean seed that resulted from applications of MON 57217, a formulation of mesotrione-based herbicide. Use of MON 94313 soybean in this study was required to generate data that may be used to support regulatory approval of MON 94313 soybean.

The field trials for the study were conducted in the U.S. at 22 sites in 13 states: Georgia, South Carolina, Arkansas, Louisiana, Mississippi, Iowa, Illinois, Kansas, Michigan, Missouri, Indiana, Nebraska, and Wisconsin. These states were typical of the major soybean producing regions of the U.S. and accounted for approximately 61% of the total soybean acreage in the U.S. in 2017 ([USDA-NASS, 2019](#)).

The target application timings and rates are summarized in the following table:

Treatment	Application Rates	
	Preemergence Application	Postemergence Application (R1)
Control	-	-
Treated	0.188 lb a.i./A (0.211 kg a.i./ha)	0.094 lb a.i./A (0.105 kg a.i./ha)

Actual application rates were within $\pm 5\%$ of the target rates for all locations with the exception of one trial site's postemergence application which was approximately -9% of the target rate.

At each sampling event, duplicate composite samples were taken from at least 12 different areas in each treated plot. Soybean seed samples were harvested from the treated plots at commercial maturity (= R8, BBCH 89: fully ripe, pods ripe, bean hard). Single composite samples of soybean seed were harvested from the control plot on the same day that the seed RAC samples were harvested from the treated plots.

PART 2: SPECIFIC DATA REQUIREMENTS FOR SAFETY ASSESSMENT

No residues were observed in MON 94313 seed, but mesotrione and MNBA were identified in other tissues. The residue of concern for tolerance setting is mesotrione parent in the U.S.

The analytical method, *Method for determination of Mesotrione and its Metabolites in Crop Matrices Using LC-MS/MS* with modifications, was used in this study, and measured the residues of mesotrione and MNBA in soybean seed ([U.S. EPA, 2015](#)). The residues of mesotrione and MNBA were quantitated via electro-spray ionization liquid chromatography tandem mass spectrometry (ESI LC-MS/MS) using stable isotopically labeled internal standards.

The limit of quantitation (LOQ) for each analyte was determined to be 0.010 ppm. The limit of detection (LOD) was determined to be 0.0012 ppm and 0.0016 ppm for mesotrione and MNBA, respectively.

For this study, one untreated control and two treated soybean seed samples from each site were analyzed.

Method performance was evaluated during method validation and by use of concurrent recovery samples by fortifying soybean seed at 0.010, 0.10 and 2.0 ppm. The fortification levels bracketed the measured residues.

All recoveries were corrected for any interferences in corresponding controls. The overall mean of the recoveries for each matrix at each fortification level was within the acceptable range of 70 to 120%, and the relative standard deviation values were below 20%. The method was considered valid for the analysis of mesotrione and MNBA residues in soybean seed.

The residues in samples collected from Treatment 2 are summarized in the following table:

Mesotrione and MNBA Residues in MON 94313 Soybean Seed

	Treatment 2		
Analyte	Median PHI (days) ¹	Median (ppm) ^{2,3}	Min. – Max. (ppm) ^{2,3}
Mesotrione	82	ND	ND
MNBA	82	[0.00103]	ND-[0.002]

¹PHI - Preharvest Interval - Interval between last application and sampling.

²Median of site averaged mesotrione and MNBA values and range of individual field sample values.

³This method has a limit of quantitation (LOQ) of 0.010 ppm (mg/kg) for both analytes. The limit of detection (LOD) was calculated as 0.0012 ppm and 0.0016 ppm for mesotrione and MNBA, respectively. Values below the limit of detection (LOD) are reported as ND (Not Detected). Residues between the LOD and the LOQ are reported in square brackets.

PART 2: SPECIFIC DATA REQUIREMENTS FOR SAFETY ASSESSMENT

The residue results indicate that the existing US EPA mesotrione MRL of 0.01 ppm in soybean seed (§ 180.571 Mesotrione; tolerances for residues) is sufficient to account for the use of mesotrione on MON 94313 tolerant soybean.

The safety of mesotrione, and its relevant metabolites have been assessed by US EPA. US EPA concluded that there is a reasonable certainty that no harm will result to the general population, or to infants and children from aggregate exposure to mesotrione residues or its metabolites ([U.S. EPA, 2015](#)).

For details, please also refer to Appendix 21.

B.4.(b) 2,4-D Residue Study in MON 94313

A study was conducted in 2021 in the U.S. to determine the magnitude of 2,4-dichlorophenoxyacetic acid (2,4-D) and its metabolite, 2,4-dichlorophenol (2,4-DCP) in/on herbicide-tolerant (HT) soybean MON 94313 raw agricultural commodities (RACs) following 3 applications of a formulation of 2,4-D herbicide.

Combined maximum application rate in the U.S. is proposed to be 2.85 lb a.e./A (3.19 kg a.e./ha). Currently proposed maximum application rates and corresponding application growth stages of 2,4-D to MON 94313 soybean in the U.S. are summarized below. Any combination of application rates and timings may be used within the allowed limits for individual rates and timings as specified on the label.

Maximum Application Rates	
Combined maximum of all applications per year	2.85 lb a.e./A (3.19 kg a.e./ha)
Total of all burndown, preplant, at-planting, and preemergence applications	0.95 lb a.e./A (1.064 kg a.e./ha)
Total in-crop applications from emergence up to V8 corn growth stage or 48 inches tall	1.9 lb a.e./A (2 x 0.95 lb a.e./A)* (2.13 kg a.e./ha) (2 x 1.064 kg a.e./ha)*
Maximum single in-crop application	0.95 lb a.e./A (1.064 kg a.e./ha)

*Two applications at 0.95 lb a.e./A (1.064 kg a.e./ha)

The purpose of this summary is to report the residue levels of 2,4-dichlorophenoxyacetic acid (2,4-D) and its major metabolite, 2,4-dichlorophenol (2,4-DCP) in MON 94313 soybean grain that resulted from applications of MON 301820, a water-soluble concentrate herbicide containing 3.5 lb a.e. of 2,4-D per gallon. Use of MON 94313 soybean in this study was required to generate data that may be used to support regulatory approval of MON 94313 soybean.

The field trials for the study were conducted in the U.S. at 18 sites in 12 states: Georgia, South Carolina, Arkansas, Louisiana, Mississippi, Iowa, Illinois, Kansas, Michigan, Missouri, Nebraska, and Wisconsin. These states were typical of the major soybean producing regions of the U.S. and accounted for approximately 50% of the total soybean acreage in the U.S. in 2017 ([USDA-NASS, 2019](#)).

The target application timings and rates are summarized in the following table:

	Application Rates		
Treatment	Peemergence Application	Early Postemergence Application (VC-V4)	Late Postemergence Application (R2)
Control	-	-	-
Treated	0.95 lb a.e./A (1.064 kg a.e./ha)	0.95 lb a.e./A (1.064 kg a.e./ha)	0.95 lb a.e./A (1.064 kg a.e./ha)

Actual application rates were within $\pm 5\%$ of the target rates for all locations. The average % of target rate across all applications and all sites was 100%.

Soybean seed samples were collected at full maturity (BBCH 89 - 99). Samples were harvested by hand from each plot, while generally avoiding the outer rows and ends of rows. Each sample was field composited from 12 or more different locations across the entire plot. In this manner, one sample from the untreated plot was collected first, followed by the two replicate samples from the treated plot.

Results and conclusions

The residue of concern for tolerance setting is 2,4-D parent in the U.S.

The analytical method, ME2172-01, *Method for Determination of 2,4-Dichlorophenoxyacetic Acid (2,4-D) and 2,4-Dichlorophenol (2,4-DCP) Residues in Crop Matrices Using LC-MS/MS* with modifications, was used in this study, and measured the residues of 2,4-D and 2,4-DCP in soybean seed. The residues of 2,4-D and 2,4-DCP were quantitated by high performance liquid chromatography/tandem mass spectrometry (LC-MS/MS) using stable isotopically labeled internal standards.

The limit of quantitation (LOQ) for each analyte was determined to be 0.010 ppm. The limit of detection (LOD) was determined to be 0.0020 ppm and 0.0018 ppm for 2,4-D and 2,4-DCP, respectively.

For this study, one untreated control and two treated soybean seed samples from each site were analyzed.

Method performance was evaluated by use of concurrent recovery samples by fortifying soybean seed at 0.010 and 0.100 ppm. The fortification levels bracketed the measured residues.

All recoveries were corrected for any interferences in corresponding controls. The overall mean of the recoveries for each matrix at each fortification level was within the acceptable range of 70 to 120%, and the relative standard deviation values were below 20%. The method was considered acceptable for the analysis of 2,4-D and 2,4-DCP residues in soybean seed.

The residues in samples collected from Treatment 2 are summarized in the following table:

2,4-D and 2,4-DCP Residues in MON 94313 Soybean Seed

	Treatment 2		
Analyte	Median PHI (days) ¹	Median (ppm) ^{2,3}	Min. – Max. (ppm) ^{2,3}
2,4-D	79	ND	ND-[0.0028]
2,4-DCP	79	[0.0076]	[0.0020]-0.0157

¹PHI - Preharvest Interval - Interval between last application and sampling.

²Median of site averaged 2,4-D and 2,4-DCP values and range of individual field sample values.

³This method has a limit of quantitation (LOQ) of 0.010 ppm (mg/kg) for both analytes. The limit of detection (LOD) was calculated as 0.0020 ppm and 0.0018 ppm for 2,4-D and 2,4-DCP, respectively. Values below the limit of detection (LOD) are reported as ND (Not Detected). Residues between the LOD and the LOQ are reported in square brackets

The residue results indicate that the existing US EPA 2,4-D MRL of 0.02 ppm in soybean seed (§ 180.142 2,4-D; tolerances for residues.) is sufficient to account for the use of 2,4-D on MON 94313 tolerant soybean.

The safety of 2,4-D, and its relevant metabolites have been assessed by US EPA. US EPA concluded that there is a reasonable certainty that no harm will result to the general population, or to infants and children from aggregate exposure to 2,4-D residues or its metabolites ([U.S. EPA, 2017](#)).

For details, please also refer to Appendix 22

B.5 Compositional Assessment

Safety assessments of biotechnology-derived crops follow the comparative safety assessment process ([Codex Alimentarius, 2009](#)) in which the composition of grain and/or other raw agricultural commodities of the biotechnology-derived crop are compared to the appropriate conventional control that has a history of safe use. For soy, assessments are performed based on the general principles outlined in the OECD consensus document for soy composition ([OECD, 2012](#)).

A review of compositional assessments conducted according to OECD guidelines, that encompassed a total of seven biotechnology-derived crop varieties, nine countries, and eleven growing seasons, concluded that incorporation of biotechnology-derived agronomic traits has had little impact on crop composition compared to other sources of variation. Most compositional variation is attributable to growing region, agronomic practices, and genetic background ([Harrigan et al., 2010](#)). Numerous scientific publications have further documented the extensive variability in the concentrations of crop components that reflect the influence of environmental and genetic factors as well as extensive conventional breeding efforts to improve nutrition, agronomics, and yield ([Harrigan et al., 2010](#); [Harrigan et al., 2009](#); [Ridley et al., 2011](#); [Zhou et al., 2011](#)).

Compositional equivalence between biotechnology-derived and conventional crops supports an “equal or increased assurance of the safety of foods derived from genetically modified plants” ([OECD, 2002b](#)). OECD consensus documents on compositional considerations for new crop varieties emphasize quantitative measurements of key nutrients and known anti-nutrients. These quantitative measurements effectively discern any compositional changes that could imply potential nutritional or safety (e.g., antinutritional) concerns. Levels of the components in grain and/or other raw agricultural commodities of the biotechnology-derived crop product are compared to: 1) corresponding levels in a conventional comparator, a genetically similar conventional line, grown concurrently under similar field conditions, and 2) natural ranges from data published in the scientific literature or in publicly-available databases (e.g. AFSI Crop Composition Database). This second comparison places any potential differences between the assessed crop and its comparator in the context of the well-documented variation in the concentrations of crop nutrients and anti-nutrients.

This section provides analyses of concentrations of key nutrients, anti-nutrients and isoflavones in grain and forage of MON 94313 compared to that of a conventional control soybean with a similar genetic background grown and harvested under similar conditions. The production of materials for compositional analyses used a sufficient variety of field trial sites, reflecting a range of environmental conditions under which MON 94313 is expected to be grown and robust field designs (randomized complete block design with four replicates). Samples were subjected to sensitive analytical methods that allow quantitative and accurate measurements of key components. The information provided in this section addresses relevant factors in Codex Plant Guidelines, Section 4, paragraphs 44 and 45 for compositional analyses ([Codex Alimentarius, 2009](#)).

B.5(a) Levels of key nutrients, toxicants and anti-nutrients in the food produced using gene technology compared with the levels in an appropriate comparator**Compositional Equivalence of MON 94313 Grain and Forage to Conventional Soybean**

Grain and forage samples were harvested from MON 94313 and the conventional control grown in the United States during the 2020 season. The field production was conducted at five sites. The field sites were planted in a randomized complete block design with four replicates at each site. MON 94313 and the conventional control were grown under normal agronomic field conditions for their respective growing regions. MON 94313 plots were treated with glufosinate, dicamba, 2,4-D and mesotrione herbicides.

The compositional analysis provided a comprehensive comparative assessment of the levels of key nutrients, anti-nutrients and isoflavones in grain and forage of MON 94313 and the conventional control.

The evaluation of MON 94313 followed considerations relevant to the compositional quality of soybean as defined by the OECD consensus document ([OECD, 2012](#)). Harvested grain samples were assessed for moisture and levels of nutrients including proximates (protein, total fat and ash), amino acids (18 components), fatty acids (22 components), carbohydrates by calculation, fiber (acid detergent fiber (ADF) and neutral detergent fiber (NDF)), minerals (calcium and phosphorus) and vitamins (vitamin E and vitamin K₁). Grain samples were also assessed for levels of other components including anti-nutrients (phytic acid, raffinose, soybean lectin, stachyose and trypsin inhibitor) and isoflavones (daidzein, genistein and glycitein). Harvested forage samples were assessed for moisture and levels of nutrients including proximates (protein, total fat and ash), carbohydrates by calculation, and fiber (ADF and NDF). In all, 66 different components were analyzed.

Of the 66 measured components, nine components (caprylic acid, capric acid, lauric acid, myristoleic acid, pentadecanoic acid, pentadecenoic acid, gamma linolenic acid, eicosatrienoic acid and arachidonic acid in grain) had more than 50% of the observations below the assay limit of quantitation (LOQ) and were excluded from statistical analysis. Moisture values for grain and forage were measured for conversion of components from fresh to dry weight but were not statistically analyzed. Therefore, 55 components were statistically analyzed (Table 48 to Table 54).

The statistical comparisons of MON 94313 and the conventional control were based on compositional data combined across all field sites. Statistically significant differences were identified at the 5% level ($\alpha = 0.05$). A statistically significant difference between MON 94313 and the conventional control does not necessarily imply biological relevance from a food and feed safety perspective. Therefore, any statistically significant differences observed between MON 94313 and the conventional control were evaluated further to determine whether the detected difference indicated a biologically relevant compositional change or supported a conclusion of compositional equivalence, as follows:

Step 1 – Determination of the Magnitude of Difference between Test (MON 94313) and Conventional Control Means

The difference in mean values between MON 94313 and the conventional control was determined for use in subsequent steps. For protein and amino acids only, the relative magnitude of the difference (percent change relative to the control) between MON 94313 and the conventional control was determined to allow an assessment of any observed difference in amino acids in relation to the difference in protein.

Step 2 – Assessment of the Difference in the Context of Natural Variation within the Conventional Control across Multiple Sites

The difference between MON 94313 and the conventional control was evaluated in the context of variation within the conventional control germplasm grown across multiple sites (i.e., variation due to environmental influence) by determining the range of replicate values for the conventional control (range value = maximum value minus the minimum value). A mean difference less than the variability seen due to natural environmental variation within the single, closely related germplasm is typically not a food or feed safety concern ([Venkatesh *et al.*, 2014](#)).

Step 3 – Assessment of the Difference in the Context of Natural Variation Due to Multiple Sources

The relative impact of MON 94313 on composition was also evaluated in the context of sources of natural variation such as environmental and germplasm influences. This assessment determined whether the component mean value of MON 94313 was within the natural variability defined by the literature values and/or the AFSI Crop Composition Database (AFSI CCDB)⁴ values (Table 55). This natural variability is important in assessing the biological relevance to food and feed safety of statistically significant differences in composition between MON 94313 and the conventional control.

These evaluations of natural variation are important as crop composition is known to be greatly influenced by environment and variety ([Harrigan *et al.*, 2010](#)). Although used in the comparative assessment process, detection of statistically significant differences between MON 94313 and the conventional control mean values does not imply a meaningful contribution by MON 94313 to compositional variability. Only if the impact of MON 94313 on levels of components is large relative to natural variation inherent to conventional soybean would the difference in composition be potentially meaningful from a food and feed safety and nutritional perspective. Differences between MON 94313 the conventional control that are within the observed natural variation for soybean are not meaningful, therefore the results support a conclusion of compositional equivalence.

Compositional Equivalence of MON 94313 Grain and Forage to that of Conventional Soybean

⁴ Effective May 1, 2020, the ILSI RF publishing the CCDB became an unaffiliated non-profit scientific organization, no longer part of the ILSI federation, and changed its name to Agriculture and Food Systems Institute (AFSI). There is no change to the current structure or function of the CCDB, only name change: AFSI CCDB. The CCDB working group and their website still the same <https://www.cropcomposition.org/>

There were no statistically significant differences ($p < 0.05$) for 48 of the 55 components analyzed. There were seven components (cystine, tryptophan, palmitic acid, linolenic acid, carbohydrates by calculation, vitamin K₁ and glycitein in grain) that showed a statistically significant difference ($p < 0.05$) between MON 94313 and the conventional control.

Since total amino acids measured in grain are predominantly derived from hydrolysis of protein, the relative magnitude of differences (percent change relative to the control) in cystine and tryptophan levels between MON 94313 and the conventional control were assessed relative to those in protein. The relative magnitude of the difference in mean protein values for MON 94313 and the conventional control was 0.93%, and the relative magnitudes of the differences for the amino acids that had statistically significant differences were similar to that for protein and ranged from 1.59% (tryptophan) to 5.77% (cystine) (Table 48). This range reflects small relative magnitudes of the differences between MON 94313 and the conventional control, as would be expected based on the relative magnitude of difference in protein (Table 48). Also, as shown in Table 48, the magnitude of differences for the two amino acids between MON 94313 and the conventional control were less than the corresponding conventional control range values. This indicates that MON 94313 does not impact levels of these components more than the natural variation within the conventional control grown at multiple locations. The mean levels of the two amino acids were within the natural variability of these components as published in the scientific literature on soybean composition and/or the AFSI CCDB (Table 55).

For palmitic acid and linolenic acid, the magnitudes of differences ranged from 0.17% Total FA (palmitic acid) to 0.40% Total FA (linolenic acid) (Table 49). As shown in Table 49, the magnitude of differences for the two fatty acids between MON 94313 and the conventional control were less than the corresponding conventional control range values. This indicates that MON 94313 does not impact levels of these components more than the natural variation within the conventional control grown at multiple locations. The mean levels of the two fatty acids were within the natural variability of these components as published in the scientific literature on soybean composition and/or the AFSI CCDB (Table 55).

For carbohydrates by calculation, the difference was 0.63% dw (Table 50). As shown in Table 50, the magnitude of difference for carbohydrates by calculation between MON 94313 and the conventional control was less than the corresponding conventional control range values. This indicates that MON 94313 does not impact levels of this component more than the natural variation within the conventional control grown at multiple locations. The mean level of carbohydrates by calculation was within the natural variability of this component as published in the scientific literature on soybean composition and/or the AFSI CCDB (Table 55). The data demonstrated that MON 94313 was not a major contributor to variation in carbohydrates by calculation or fiber levels in soybean and confirmed the compositional equivalence of MON 94313 to the conventional control in levels of these components.

For vitamin K₁, the difference was -0.046 µg/g dw (Table 52). As shown in Table 52, the magnitude of difference for vitamin K₁ between MON 94313 and the conventional control was less than the corresponding conventional control range values. This indicates that MON 94313 does not impact levels of this component more than the natural variation within the conventional control grown at multiple locations. The mean level of vitamin K₁ was within the natural variability of this component as published in the scientific literature on soybean composition

and/or the AFSI CCDB (Table 55). The data demonstrated that MON 94313 was not a major contributor to variation in vitamin levels in soybean and confirmed the compositional equivalence of MON 94313 to the conventional control in levels of these components.

For glycitein, the difference was 9.33µg/g dw (Table 53). As shown in Table 53, the magnitude of difference for glycitein between MON 94313 and the conventional control was less than the corresponding conventional control range values. This indicates that MON 94313 does not impact levels of this component more than the natural variation within the conventional control grown at multiple locations. The mean level of glycitein was within the natural variability of these components as published in the scientific literature on soybean composition and/or the AFSI CCDB (Table 55). The data demonstrated that MON 94313 was not a major contributor to variation in anti-nutrient or isoflavone levels in soybean and confirmed the compositional equivalence of MON 94313 to the conventional control in levels of these components.

For details, please refer to Appendix 23.

Conclusions

Compositional analysis was conducted on grain and forage of MON 94313 and the conventional control grown at five sites in the United States during the 2020 field season. Of the 55 components statistically assessed, 48 showed no statistically significant differences ($p < 0.05$) between MON 94313 and the conventional control. A total of seven components (cystine, tryptophan, palmitic acid, linolenic acid, carbohydrates by calculation, vitamin K₁ and glycitein for grain) showed a statistically significant difference ($p < 0.05$) between MON 94313 and the conventional control. For these components, the mean difference in component values between MON 94313 and the conventional control was less than the range of the conventional control values. The MON 94313 mean component values were within the range of values observed in the literature and/or the AFSI-CCDB.

These results support the overall conclusion that MON 94313 soybean was not a major contributor to variation in component levels in grain or forage and confirmed the compositional equivalence of MON 94313 to the conventional control in levels of these components. The statistically significant differences observed were not compositionally meaningful from a food and feed safety perspective.

Table 48. Summary of Soybean Grain Protein and Amino Acids for MON 94313 and the Conventional Control

Component (% dw) ¹	MON 94313 Mean (S.E.) ² Range	Control Mean (S.E.) Range	Control Range Value ³	Difference (Test minus Control)		
				Mean (S.E.)	p-Value	% Relative ⁴
Protein	37.75 (0.67) 33.96 - 39.51	38.11 (0.67) 34.26 - 40.05	5.79	-0.36 (0.22)	0.129	-0.93
Alanine	1.74 (0.024) 1.59 - 1.86	1.76 (0.024) 1.64 - 1.86	0.21	-0.015 (0.016)	0.358	-0.85
Arginine	2.55 (0.060) 2.16 - 2.78	2.59 (0.060) 2.29 - 2.82	0.53	-0.031 (0.031)	0.321	-1.22
Aspartic Acid	4.83 (0.10) 4.21 - 5.37	4.90 (0.10) 4.42 - 5.31	0.89	-0.065 (0.078)	0.413	-1.33
Cystine	0.59 (0.014) 0.51 - 0.68	0.63 (0.014) 0.55 - 0.71	0.16	-0.036 (0.011)	0.002	-5.77
Glutamic Acid	7.63 (0.17) 6.53 - 8.44	7.75 (0.17) 7.03 - 8.43	1.40	-0.12 (0.12)	0.322	-1.55

Table 48. Summary of Soybean Grain Protein and Amino Acids for MON 94313 and the Conventional Control (Continued)

Component (% dw) ¹	MON 94313 Mean (S.E.) ² Range	Control Mean (S.E.) Range	Control Range Value ³	Difference (Test minus Control)		
				Mean (S.E.)	p-Value	% Relative ⁴
Glycine	1.72 (0.026) 1.54 - 1.80	1.74 (0.026) 1.63 - 1.82	0.19	-0.014 (0.014)	0.312	-0.82
Histidine	1.11 (0.015) 0.98 - 1.16	1.12 (0.015) 1.05 - 1.19	0.14	-0.012 (0.011)	0.274	-1.10
Isoleucine	1.85 (0.032) 1.66 - 1.97	1.87 (0.032) 1.74 - 1.98	0.24	-0.02 (0.017)	0.256	-1.06
Leucine	2.99 (0.047) 2.68 - 3.14	3.02 (0.047) 2.80 - 3.18	0.39	-0.029 (0.025)	0.250	-0.97
Lysine	2.79 (0.044) 2.52 - 3.04	2.82 (0.044) 2.57 - 3.00	0.44	-0.036 (0.036)	0.318	-1.28
Methionine	0.64 (0.018) 0.47 - 0.73	0.68 (0.018) 0.53 - 0.75	0.22	-0.031 (0.016)	0.059	-4.62
Phenylalanine	1.95 (0.031) 1.72 - 2.06	1.97 (0.031) 1.82 - 2.08	0.26	-0.02 (0.020)	0.338	-1.00

Table 48. Summary of Soybean Grain Protein and Amino Acids for MON 94313 and the Conventional Control (Continued)

Component (% dw) ¹	MON 94313 Mean (S.E.) ² Range	Control Mean (S.E.) Range	Control Range Value ³	Difference (Test minus Control)		
				Mean (S.E.)	p-Value	% Relative ⁴
Proline	2.00 (0.041) 1.77 - 2.14	2.03 (0.041) 1.84 - 2.14	0.30	-0.027 (0.017)	0.120	-1.35
Serine	2.01 (0.029) 1.78 - 2.09	2.04 (0.029) 1.88 - 2.14	0.26	-0.025 (0.019)	0.201	-1.24
Threonine	1.62 (0.020) 1.49 - 1.68	1.63 (0.020) 1.53 - 1.70	0.17	-0.016 (0.013)	0.203	-0.99
Tryptophan	0.47 (0.0071) 0.43 - 0.48	0.47 (0.0071) 0.42 - 0.50	0.080	-0.0076 (0.0034)	0.031	-1.59
Tyrosine	1.17 (0.016) 1.00 - 1.26	1.18 (0.016) 1.08 - 1.27	0.19	-0.0064 (0.017)	0.711	-0.54
Valine	1.91 (0.032) 1.73 - 2.03	1.92 (0.032) 1.82 - 2.04	0.22	-0.02 (0.018)	0.285	-1.02

¹dw=dry weight² Mean (S.E.) = least-square mean (standard error)³Maximum value minus minimum value for the control soybean variety⁴The relative magnitude of the difference in mean values between MON 94313 and the control, expressed as a percent of the control.

Table 49. Summary of Soybean Grain Total Fat and Fatty Acids for MON 94313 and the Conventional Control

Component	MON 94313 Mean (S.E.) ¹ Range	Control Mean (S.E.) Range	Control Range Value ²	Difference (Test minus Control)	
				Mean (S.E.)	p-Value
Total Fat (% dw) ³	18.21 (0.53) 16.69 - 20.17	18.49 (0.53) 17.06 - 20.75	3.69	-0.28 (0.14)	0.056
14:0 Myristic (% Total FA) ⁴	0.10 (0.0021) 0.090 - 0.11	0.10 (0.0021) 0.093 - 0.11	0.014	-0.00015 (0.0011)	0.898
16:0 Palmitic (% Total FA)	12.16 (0.065) 11.88 - 12.38	11.99 (0.065) 11.73 - 12.27	0.54	0.17 (0.026)	<0.001
16:1 Palmitoleic (% Total FA)	0.10 (0.0021) 0.091 - 0.11	0.10 (0.0021) 0.094 - 0.11	0.018	0.00046 (0.0010)	0.678
17:0 Heptadecanoic (% Total FA)	0.12 (0.0030) 0.11 - 0.13	0.12 (0.0030) 0.11 - 0.13	0.021	0.00048 (0.0011)	0.682
17:1 Heptadecenoic (% Total FA)	0.075 (0.00083) 0.067 - 0.078	0.075 (0.00082) 0.070 - 0.080	0.0098	-0.00046 (0.0012)	0.701

Table 49. Summary of Soybean Grain Total Fat and Fatty Acids for MON 94313 and the Conventional Control (Continued)

Component	MON 94313 Mean (S.E.) ¹ Range	Control Mean (S.E.) Range	Difference (Test minus Control)		
			Control Range Value ²	Mean (S.E.)	p-Value
18:0 Stearic (% Total FA)	3.99 (0.13) 3.56 - 4.32	4.09 (0.13) 3.64 - 4.68	1.03	-0.091 (0.047)	0.123
18:1 Oleic (% Total FA)	19.11 (0.72) 16.35 - 20.40	19.77 (0.72) 16.86 - 22.45	5.58	-0.66 (0.30)	0.095
18:2 Linoleic (% Total FA)	54.55 (0.64) 52.69 - 57.04	54.36 (0.64) 51.82 - 56.87	5.06	0.19 (0.32)	0.578
18:3 Linolenic (% Total FA)	8.89 (0.33) 8.01 - 9.95	8.48 (0.33) 7.57 - 9.72	2.15	0.40 (0.085)	0.009
20:0 Arachidic (% Total FA)	0.31 (0.0091) 0.27 - 0.33	0.31 (0.0091) 0.28 - 0.36	0.078	-0.006 (0.0041)	0.219
20:1 Eicosenoic (% Total FA)	0.20 (0.0071) 0.17 - 0.22	0.20 (0.0071) 0.17 - 0.22	0.050	-0.0011 (0.0020)	0.625

Table 49. Summary of Soybean Grain Total Fat and Fatty Acids for MON 94313 and the Conventional Control (Continued)

Component	MON 94313 Mean (S.E.) ¹ Range	Control Mean (S.E.) Range	Difference (Test minus Control)		
			Control Range Value ²	Mean (S.E.)	p-Value
20:2 Eicosadienoic (% Total FA)	0.068 (0.0013) 0.062 - 0.074	0.067 (0.0013) 0.062 - 0.079	0.017	0.00060 (0.0011)	0.606
22:0 Behenic (% Total FA)	0.33 (0.0068) 0.31 - 0.35	0.33 (0.0068) 0.31 - 0.37	0.057	0.0010 (0.0041)	0.817

¹ Mean (S.E.) = least-square mean (standard error)

²Maximum value minus minimum value for the control soybean variety

³dw=dry weight

⁴FA=Fatty Acid

The following components with more than 50% of observations below the assay LOQ were excluded from statistical analysis: caprylic acid, capric acid, lauric acid, myristoleic acid, pentadecanoic acid, pentadecenoic acid, gamma linolenic acid, eicosatrienoic acid and arachidonic acid.

Table 50. Summary of Soybean Grain Carbohydrates by Calculation and Fiber for MON 94313 and the Conventional Control

Component (% dw) ¹	MON 94313 Mean (S.E.) ² Range	Control Mean (S.E.) Range	Control Range Value ³	Difference (Test minus Control)	
				Mean (S.E.)	p-Value
Carbohydrates by Calculation	39.36 (0.81) 36.84 - 43.34	38.72 (0.81) 36.66 - 43.13	6.46	0.63 (0.18)	0.002
ADF	17.57 (0.38) 14.80 - 20.16	16.89 (0.38) 14.49 - 20.10	5.61	0.69 (0.42)	0.177
NDF	17.03 (0.27) 15.35 - 18.73	17.26 (0.27) 15.84 - 20.28	4.44	-0.23 (0.29)	0.440

¹dw=dry weight

²Mean (S.E.) = least-square mean (standard error)

³Maximum value minus minimum value for the control soybean variety

Table 51. Summary of Soybean Grain Ash and Minerals for MON 94313 and the Conventional Control

Component (% dw) ¹	MON 94313 Mean (S.E.) ² Range	Control Mean (S.E.) Range	Control Range Value ³	Difference (Test minus Control)	
				Mean (S.E.)	p-Value
Ash	4.68 (0.066) 4.36 - 4.90	4.68 (0.066) 4.34 - 5.03	0.68	0.0046 (0.023)	0.844
Calcium	0.28 (0.012) 0.21 - 0.33	0.29 (0.012) 0.24 - 0.33	0.092	-0.0063 (0.0061)	0.359
Phosphorus	0.62 (0.019) 0.55 - 0.69	0.62 (0.019) 0.52 - 0.71	0.19	-0.0027 (0.0085)	0.752

¹dw=dry weight

²Mean (S.E.) = least-square mean (standard error)

³Maximum value minus minimum value for the control soybean variety

Table 52. Summary of Soybean Grain Vitamins for MON 94313 and the Conventional Control

Component	MON 94313 Mean (S.E.) ² Range	Control Mean (S.E.) Range	Control Range Value ³	Difference (Test minus Control)	
				Mean (S.E.)	p-Value
Vitamin E (mg/100g dw) ¹	1.89 (0.28) 1.26 - 2.95	2.06 (0.28) 1.19 - 3.21	2.02	-0.16 (0.066)	0.067
Vitamin K ₁ (µg/g dw)	0.56 (0.043) 0.43 - 0.72	0.61 (0.043) 0.41 - 0.77	0.36	-0.046 (0.017)	0.009

¹dw=dry weight; Common names of vitamins: E=α-Tocopherol; K₁=phylloquinone

²Mean (S.E.) = least-square mean (standard error)

³Maximum value minus minimum value for the control soybean variety

Table 53. Summary of Soybean Grain Anti-Nutrients and Isoflavones for MON 94313 and the Conventional Control

Component	MON 94313 Mean (S.E.) ¹ Range	Control Mean (S.E.) Range	Control Range Value ²	Difference (Test minus Control)	
				Mean (S.E.)	p-Value
Phytic Acid (% dw) ³	1.27 (0.058) 1.00 - 1.50	1.26 (0.058) 0.95 - 1.51	0.56	0.011 (0.024)	0.649
Raffinose (% dw)	1.06 (0.050) 0.84 - 1.32	1.07 (0.050) 0.89 - 1.39	0.50	-0.011 (0.032)	0.745
Soybean Lectin (mg/g dw)	2.06 (0.095) 1.50 - 2.73	1.97 (0.095) 1.56 - 2.59	1.03	0.086 (0.10)	0.395
Stachyose (% dw)	4.50 (0.046) 4.24 - 4.77	4.47 (0.046) 4.19 - 4.71	0.51	0.033 (0.032)	0.362
Trypsin Inhibitor (TIU/mg dw)	23.05 (1.36) 16.71 - 28.61	24.22 (1.36) 17.32 - 33.54	16.22	-1.17 (1.38)	0.444
Daidzein (µg/g dw)	1281.83 (169.21) 970.95 - 2132.67	1235.84 (169.21) 809.88 - 2116.44	1306.55	45.99 (46.05)	0.374

Table 53. Summary of Soybean Grain Anti-Nutrients and Isoflavones for MON 94313 and the Conventional Control (Continued)

Component	MON 94313 Mean (S.E.) ¹ Range	Control Mean (S.E.) Range	Difference (Test minus Control)		
			Control Range Value ²	Mean (S.E.)	p-Value
Genistein (µg/g dw)	987.54 (129.67) 763.63 - 1618.71	965.47 (129.67) 634.96 - 1640.92	1005.96	22.07 (31.16)	0.517
Glycitein (µg/g dw)	136.81 (5.78) 91.89 - 164.00	127.48 (5.78) 96.03 - 167.19	71.16	9.33 (4.10)	0.034

¹Mean (S.E.) = least-square mean (standard error)

²Maximum value minus minimum value for the control soybean variety

³dw=dry weight

Table 54. Summary of Soybean Forage Proximates, Carbohydrates by Calculation, Fiber and Minerals for MON 94313 and the Conventional Control

Component (% dw) ¹	MON 94313 Mean (S.E.) ² Range	Control Mean (S.E.) Range	Control Range Value ³	Difference (Test minus Control)	
				Mean (S.E.)	p-Value
Protein	20.73 (0.94) 17.61 - 23.80	20.50 (0.94) 15.10 - 23.31	8.21	0.23 (0.38)	0.572
Total Fat	7.87 (0.27) 5.72 - 9.87	7.69 (0.27) 5.49 - 9.31	3.82	0.17 (0.25)	0.493
Carbohydrates by Calculation	64.33 (0.95) 60.35 - 68.44	65.22 (0.95) 61.82 - 70.80	8.98	-0.89 (0.80)	0.329
ADF	35.25 (0.67) 27.99 - 41.38	34.34 (0.67) 31.38 - 43.30	11.92	0.91 (0.74)	0.236
NDF	38.86 (1.59) 32.94 - 46.09	40.49 (1.59) 30.37 - 52.77	22.40	-1.63 (2.02)	0.464
Ash	7.07 (0.39) 4.76 - 11.58	6.58 (0.39) 5.34 - 9.83	4.49	0.49 (0.49)	0.377

¹dw=dry weight²Mean (S.E.) = least-square mean (standard error)³Maximum value minus minimum value for the control soybean variety

B.5(b) Information on the range of natural variation for each constituent measure to allow for assessment of biological significance**Table 55. Literature and AFSI Database Ranges for Components in Soybean Grain and Forage**

Tissue Components¹	Literature Range²	AFSI Range³
Grain Nutrients		
Proximates		
protein (% dw)	34.78-43.35 ^a ; 32.29-42.66 ^b	29.51-46.60
total fat (% dw)	14.40-20.91 ^a ; 15.10-23.56 ^b	6.97-25.00
ash (% dw)	4.61-6.32 ^a ; 4.32-5.88 ^b	3.75-10.90
Amino Acids		
alanine (% dw)	1.62-1.89 ^a ; 1.43-1.93 ^b	1.15-2.35
arginine (% dw)	2.57-3.34 ^a ; 2.15-3.05 ^b	1.73-3.93
aspartic acid (% dw)	4.16-5.02 ^a ; 4.01-5.72 ^b	3.13-6.83
cystine (% dw)	0.52-0.69 ^a ; 0.41-0.71 ^b	0.32-0.93
glutamic acid (% dw)	6.52-8.19 ^a ; 5.49-8.72 ^b	4.35-10.90
glycine (% dw)	1.59-1.90 ^a ; 1.41-1.99 ^b	1.16-2.55
histidine (% dw)	0.96-1.13 ^a ; 0.86-1.24 ^b	0.20-1.59
isoleucine (% dw)	1.59-2.00 ^a ; 1.41-2.02 ^b	1.20-2.48
leucine (% dw)	2.79-3.42 ^a ; 2.39-3.32 ^b	2.04-4.13
lysine (% dw)	2.36-2.77 ^a ; 2.19-3.15 ^b	1.79-3.94
methionine (% dw)	0.45-0.63 ^a ; 0.39-0.65 ^b	0.29-1.15
phenylalanine (% dw)	1.82-2.29 ^a ; 1.62-2.44 ^b	1.40-2.73
proline (% dw)	1.83-2.23 ^a ; 1.63-2.25 ^b	1.32-2.95
serine (% dw)	1.95-2.42 ^a ; 1.51-2.30 ^b	0.86-2.80
threonine (% dw)	1.44-1.71 ^a ; 1.23-1.74 ^b	1.07-2.18
tryptophan (% dw)	0.30-0.48 ^a ; 0.41-0.56 ^b	0.254-0.746
tyrosine (% dw)	1.27-1.53 ^a ; 0.74-1.31 ^b	0.74-2.32
valine (% dw)	1.68-2.11 ^a ; 1.50-2.13 ^b	1.24-2.66
Fatty Acids		
myristic acid (% Total FA)	0.063-0.11 ^b	0.056-0.243
palmitic acid (% Total FA)	9.80-12.63 ^b	8.03-15.99
palmitoleic acid (% Total FA)	0.055-0.14 ^b	0.055-0.247
heptadecanoic acid (% Total FA)	0.076-0.13 ^b	0.075-0.166
heptadecenoic acid (% Total FA)	0.019-0.064 ^b	0.037-0.088
stearic acid (% Total FA)	3.21-5.63 ^b	2.68-6.74
oleic acid (% Total FA)	16.69-35.16 ^b	14.5-46.3
linoleic acid (% Total FA)	44.17-57.72 ^b	34.8-72.5
linolenic acid (% Total FA)	4.27-9.90 ^b	3.00-12.84
arachidic acid (% Total FA)	0.35-0.57 ^b	0.167-0.611
eicosenoic acid (% Total FA)	0.13-0.30 ^b	0.110-0.387
eicosadienoic acid (% Total FA)	0.016-0.071 ^b	0.032-0.341
behenic acid (% Total FA)	0.35-0.65 ^b	0.181-0.723

Information on the range of natural variation for each constituent measure to allow for assessment of biological significance

Table 55. Literature and AFSI Database Ranges for Components in Soybean Grain and Forage (Continued)

Tissue Components ¹	Literature Range ²	AFSI Range ³
Carbohydrates By Calculation		
carbohydrates by calculation (% dw)	32.75-40.98 ^a ; 29.88-43.48 ^b	25.2-55.8
Fiber		
acid detergent fiber (% dw)	9.22-26.26 ^a ; 11.81-19.45 ^b	4.60-35.30
neutral detergent fiber (% dw)	10.79-23.90 ^a ; 13.32-23.57 ^b	7.38-31.90
Minerals		
calcium (% dw)	0.24-0.41 ^c	0.12-0.49
phosphorus (% dw)	0.40-0.61 ^c	0.28-0.94
Vitamins		
vitamin E (mg/100g dw)	1.29-4.80 ^a ; 1.12-8.08 ^b	0.193-12.738
vitamin K ₁ (µg/g dw)	0.49-0.909 ^d	0.07-2.07
Grain Other		
Anti-Nutrients		
phytic acid (% dw)	0.41-1.92 ^a ; 0.81-2.66 ^b	0.2855-2.6775
raffinose (% dw)	0.26-0.84 ^a ; 0.43-1.85 ^b	0.1778-1.8542
soybean lectin (mg/g dw)	1.82-2.92 ^c	0.9630-6.7195
stachyose (% dw)	1.53-3.04 ^a ; 1.97-6.65 ^b	0.6183-6.8900
trypsin inhibitor (TIU/mg dw)	20.79-59.03 ^a ; 18.14-42.51 ^b	3.23-118.68
Isoflavones		
daidzein (µg/g dw)	224.03-1571.91 ^a ; 198.95-1458.24 ^b	60.04-3,061.20
genistein (µg/g dw)	338.24-1488.89 ^a ; 148.06-1095.57 ^b	35.71-2,837.20
glycitein (µg/g dw)	52.72-298.57 ^a ; 32.42-255.94 ^b	14.10-1,630.00
Forage Nutrients		
Proximates		
protein (% dw)	16.48-24.29 ^a ; 12.68-23.76 ^b	9.51-46.25
total fat (% dw)	2.65-9.87 ^a ; 2.96-7.88 ^b	0.5-20.0
ash (% dw)	5.28-9.24 ^a ; 4.77-8.54 ^b	2.866-36.600
Carbohydrates By Calculation		
carbohydrates by calculation (% dw)	62.25-72.30 ^a ; 60.61-77.26 ^b	27.8-80.6
Fiber		
acid detergent fiber (% dw)	23.86-50.89 ^a ; 25.49-47.33 ^b	12.845-64.100
neutral detergent fiber (% dw)	19.61-43.70 ^a ; 30.96-64.19 ^b	19.26-82.00

¹dw=dry weight; FA=Fatty Acid; mg/kg/ dw

²Literature range references: ^a(Lundry *et al.*, 2008); ^b(Berman *et al.*, 2009); ^c(Bellaloui *et al.*, 2011);

^d(Thompson *et al.*, 2016); ^e(Breeze *et al.*, 2015)

³AFSI range is from AFSI CCDB, 2020 (Accessed April 20, 2021).

C. INFORMATION RELATED TO THE NUTRITIONAL IMPACT OF THE FOOD PRODUCED USING GENE TECHNOLOGY

There are no nutritional impacts on the food and feed derived from MON 94313. This product is developed to confer herbicide tolerance. It is not a nutritionally altered product.

D. OTHER INFORMATION

The data and information presented in this submission demonstrate that the food and feed derived from MON 94313 are as safe and nutritious as those derived from commercially-available, conventional soybean for which there is an established history of safe consumption.

PART 3 STATUTORY DECLARATION – AUSTRALIA

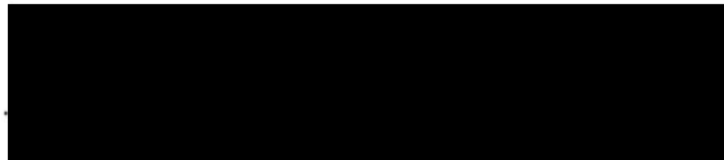
I, Nina McCormick, declare the following points in this application:

1. The information provided in this application fully sets out the matters required.
2. The information provided in this application is true to the best of my knowledge and belief.
3. No information has been withheld that might prejudice this application, to the best of my knowledge and belief.

Signature: _____



Declared before me



This Wednesday day of 19th April 2023.

PART 4 REFERENCES

- Adrian-Romero, M., G. Blunden, B.G. Carpenter and E. Tyihák. 1999. HPLC quantification of formaldehyde, as formaldemethone, in plants and plant-like organisms. *Chromatographia* 50:160-166.
- Alarcón, A., F.T. Davies, R.L. Autenrieth and D.A. Zuberer. 2008. Arbuscular mycorrhiza and petroleum-degrading microorganisms enhance phytoremediation of petroleum-contaminated soil. *International Journal of Phytoremediation* 10:251-263.
- An, S.-q. and G. Berg. 2018. *Stenotrophomonas maltophilia*. *Trends in Microbiology* 26:637-638.
- Anderson, J.E., J.-M. Michno, T.J.Y. Kono, A.O. Stec, B.W. Campbell, S.J. Curtin and R.M. Stupar. 2016. Genomic variation and DNA repair associated with soybean transgenesis: A comparison to cultivars and mutagenized plants. *BMC Biotechnology* 16:41.
- ASA. 2021. SoyStats 2021. International: World soybean production. American Soybean Association, St. Louis, Missouri. <http://soystats.com/international-world-soybean-production/>.
- Axelos, M., C. Bardet, T. Liboz, A. Le Van Thai, C. Curie and B. Lescure. 1989. The gene family encoding the *Arabidopsis thaliana* translation elongation factor EF-1 α : Molecular cloning characterization and expression. *Molecular and General Genetics* 219:106-112.
- Barker, R.F., K.B. Idler, D.V. Thompson and J.D. Kemp. 1983. Nucleotide sequence of the T-DNA region from the *Agrobacterium tumefaciens* octopine Ti plasmid pTi15955. *Plant Molecular Biology* 2:335-350.
- Bäumlein, H., W. Boerjan, I. Nagy, R. Bassüner, M. Van Montagu, D. Inzé and U. Wobus. 1991. A novel seed protein gene from *Vicia faba* is developmentally regulated in transgenic tobacco and *Arabidopsis* plants. *Molecular and General Genetics* 225:459-467.
- Bautista-Zapanta, J.-n., K. Suzuki and K. Yoshida. 2002. Characterization of four ribosomal RNA operons in the genome of *Agrobacterium tumefaciens* MAFF301001. *Nucleic Acids Research* S2:91-92.
- Beck, E., G. Ludwig, E.A. Auerswald, B. Reiss and H. Schaller. 1982. Nucleotide sequence and exact localization of the neomycin phosphotransferase gene from transposon Tn5. *Gene* 19:327-336.
- Behrens, M.R., N. Mutlu, S. Chakraborty, R. Dumitru, W.Z. Jiang, B.J. LaVallee, P.L. Herman, T.E. Clemente and D.P. Weeks. 2007. Dicamba resistance: Enlarging and preserving biotechnology-based weed management strategies. *Science* 316:1185-1188.
- Bellaloui, N., J.R. Smith, A.M. Gillen and J.D. Ray. 2011. Effects of maturity, genotypic background, and temperature on seed mineral composition in near-isogenic soybean lines in the early soybean production system. *Crop Science* 51:1161-1171.

- Berg, G. and J.L. Martinez. 2015. Friends or foes: Can we make a distinction between beneficial and harmful strains of the *Stenotrophomonas maltophilia* complex? *Frontiers in Microbiology* 6:241.
- Berman, K.H., G.G. Harrigan, S.G. Riordan, M.A. Nemeth, C. Hanson, M. Smith, R. Sorbet, E. Zhu and W.P. Ridley. 2009. Compositions of seed, forage, and processed fractions from insect-protected soybean MON 87701 are equivalent to those of conventional soybean. *Journal of Agricultural and Food Chemistry* 57:11360-11369.
- Bevan, M., W.M. Barnes and M.-D. Chilton. 1983. Structure and transcription of the nopaline synthase gene region of T-DNA. *Nucleic Acids Research* 11:369-385.
- Biron, D.G., C. Brun, T. Lefevre, C. Lebarbenchon, H.D. Loxdale, F. Chevenet, J.-P. Brizard and F. Thomas. 2006. The pitfalls of proteomics experiments without the correct use of bioinformatics tools. *Proteomics* 6:5577-5596.
- Bradshaw, R.A., W.W. Brickey and K.W. Walker. 1998. N-terminal processing: The methionine aminopeptidase and N^α-acetyl transferase families. *Trends in Biochemical Sciences* 23:263-267.
- Breeze, M.L., C. Meng, J.M. Harrison, C. George and J.D. Colyer. 2015. Relationship between composition of oilseed processed fractions and the whole oilseeds. *Journal of the American Oil Chemists' Society* 92:203-213.
- Brooke, J.S., G. Di Bonaventura, G. Berg and J.-L. Martinez. 2017. Editorial: A multidisciplinary look at *Stenotrophomonas maltophilia*: An emerging multi-drug-resistant global opportunistic pathogen. *Frontiers in Microbiology* 8:1511.
- Buchanan, B.B., W. Gruissem and R.L. Jones. 2000. Phenylpropanoid and phenylpropanoid-acetate pathway metabolites. Pages 1286-1289 in *Biochemistry and Molecular Biology of Plants*. American Society of Plant Biologists, Rockville, Maryland.
- Bugg, T.D.H. 2003. Dioxygenase enzymes: Catalytic mechanisms and chemical models. *Tetrahedron* 59:7075-7101.
- Caetano-Anollés, G., M. Wang, D. Caetano-Anollés and J.E. Mittenhal. 2009. The origin, evolution and structure of the protein world. *Biochemical Journal* 417:621-637.
- Chakraborty, S., M. Behrens, P.L. Herman, A.F. Arendsen, W.R. Hagen, D.L. Carlson, X.-Z. Wang and D.P. Weeks. 2005. A three-component dicamba *O*-demethylase from *Pseudomonas maltophilia*, strain DI-6: Purification and characterization. *Archives of Biochemistry and Biophysics* 437:20-28.
- Chaudhary, D.K., S.-W. Jeong and J. Kim. 2017. *Sphingobium naphthae* sp. nov., with the ability to degrade aliphatic hydrocarbons, isolated from oil-contaminated soil. *International Journal of Systematic and Evolutionary Microbiology* 67:2986-2993.
- Christ, B., R. Hochstrasser, L. Guyer, R. Francisco, S. Aubry, S. Hortensteiner and J.K. Weng. 2017. Non-specific activities of the major herbicide-resistance gene *BAR*. *Nature Plants* 3:937-945.

Clark, S.E. and G.K. Lamppa. 1992. Processing of the precursors for the light-harvesting chlorophyll-binding proteins of photosystem II and photosystem I during import and in an organelle-free assay. *Plant Physiology* 98:595-601.

Codex Alimentarius. 2009. Foods derived from modern biotechnology. Second Edition. Codex Alimentarius Commission, Joint FAO/WHO Food Standards Programme, Food and Agriculture Organization of the United Nations, Rome, Italy.

Coruzzi, G., R. Broglie, C. Edwards and N.-H. Chua. 1984. Tissue-specific and light-regulated expression of a pea nuclear gene encoding the small subunit of ribulose-1, 5-bisphosphate carboxylase. *EMBO Journal* 3:1671-1679.

Cross, T. 1989. Other genera. Pages 2586-2615 in *Bergey's Manual of Systematic Bacteriology*. Volume 4. S.T. Williams and M.E. Sharpe (eds.). Williams & Wilkins, Baltimore, Maryland.

D'Ordine, R.L., T.J. Rydel, M.J. Storek, E.J. Sturman, F. Moshiri, R.K. Bartlett, G.R. Brown, R.J. Eilers, C. Dart, Y. Qi, S. Flasiniski and S.J. Franklin. 2009. Dicamba monooxygenase: Structural insights into a dynamic Rieske oxygenase that catalyzes an exocyclic monooxygenation. *Journal of Molecular Biology* 392:481-497.

Dai, S., N. Georgelis, M. Bedair, Y.-J. Hong, Q. Qi, C.T. Larue, B. Sitoula, W. Huang, B. Krebel, M. Shepard, W. Su, K. Kretzmer, J. Dong, T. Slewinski, S. Berger, C. Ellis, A. Jerga and M. Varagona. 2022. Ectopic expression of a rice triketone dioxygenase gene confers mesotrione tolerance in soybean. *Pest Management Science* 78:2816-2827.

De Carolis, E. and V. De Luca. 1994. 2-Oxoglutarate-dependent dioxygenase and related enzymes: Biochemical characterization. *Phytochemistry* 36:1093-1107.

della-Cioppa, G., S.C. Bauer, B.K. Klein, D.M. Shah, R.T. Fraley and G.M. Kishore. 1986. Translocation of the precursor of 5-enolpyruvylshikimate-3-phosphate synthase into chloroplasts of higher plants *in vitro*. *Proceedings of the National Academy of Sciences of the United States of America* 83:6873-6877.

Depicker, A., S. Stachel, P. Dhaese, P. Zambryski and H.M. Goodman. 1982. Nopaline synthase: Transcript mapping and DNA sequence. *Journal of Molecular and Applied Genetics* 1:561-573.

Dong, H., C. Zhu, J. Chen, X. Ye and Y.-P. Huang. 2015. Antibacterial activity of *Stenotrophomonas maltophilia* endolysin P28 against both gram-positive and gram-negative bacteria. *Frontiers in Microbiology* 6:1299.

Dumitru, R., W.Z. Jiang, D.P. Weeks and M.A. Wilson. 2009. Crystal structure of dicamba monooxygenase: A Rieske nonheme oxygenase that catalyzes oxidative demethylation. *Journal of Molecular Biology* 392:498-510.

Enya, J., H. Shinohara, S. Yoshida, T. Tsukiboshi, H. Negishi, K. Suyama and S. Tsushima. 2007. Culturable leaf-associated bacteria on tomato plants and their potential as biological control agents. *Microbial Ecology* 53:524-536.

- FAO-WHO. 2011a. Summary report: Acceptable daily intakes, acute reference doses, short-term and long-term dietary intakes, recommended maximum residue limits and supervised trials median residue values recorded by the 2011 meeting. Food and Agriculture Organization of the United Nations, World Health Organization, Geneva, Switzerland.
- FAO-WHO. 2011b. Pesticide residues in food 2010: Joint FAO/WHO meeting on pesticide residues. FAO Plant Production and Protection Paper 200. Food and Agriculture Organization of the United Nations, World Health Organization, Rome, Italy.
- Ferraro, D.J., L. Gakhar and S. Ramaswamy. 2005. Rieske business: Structure-function of Rieske non-heme oxygenases. *Biochemical and Biophysical Research and Communications* 338:175-190.
- Fialho, A.M., L.M. Moreira, A.T. Granja, A.O. Popescu, K. Hoffmann and I. Sá-Correia. 2008. Occurrence, production, and applications of gellan: Current state and perspectives. *Applied Microbiology and Biotechnology* 79:889-900.
- Fling, M.E., J. Kopf and C. Richards. 1985. Nucleotide sequence of the transposon Tn7 gene encoding an aminoglycoside-modifying enzyme, 3''(9)-*O*-nucleotidyltransferase. *Nucleic Acids Research* 13:7095-7106.
- Fraley, R.T., S.G. Rogers, R.B. Horsch, P.R. Sanders, J.S. Flick, S.P. Adams, M.L. Bittner, L.A. Brand, C.L. Fink, J.S. Fry, G.R. Galluppi, S.B. Goldberg, N.L. Hoffmann and S.C. Woo. 1983. Expression of bacterial genes in plant cells. *Proceedings of the National Academy of Sciences of the United States of America* 80:4803-4807.
- Frottin, F., A. Martinez, P. Peynot, S. Mitra, R.C. Holz, C. Giglione and T. Meinnel. 2006. The proteomics of N-terminal methionine cleavage. *Molecular & Cellular Proteomics* 5:2336-2349.
- Giglione, C., A. Boularot and T. Meinnel. 2004. Protein N-terminal methionine excision. *Cellular and Molecular Life Sciences* 61:1455-1474.
- Giza, P.E. and R.C.C. Huang. 1989. A self-inducing runaway-replication plasmid expression system utilizing the Rop protein. *Gene* 78:73-84.
- Goodfellow, M. and S.T. Williams. 1983. Ecology of actinomycetes. *Annual Review of Microbiology* 37:189-216.
- Gribble, G.W. 2010. Occurrence. Pages 9-348 in *Naturally Occurring Organohalogen Compounds - A Comprehensive Update*. Volume 91. Springer-Verlag, New York, New York.
- Hammond, B.G. and J.M. Jez. 2011. Impact of food processing on the safety assessment for proteins introduced into biotechnology-derived soybean and corn crops. *Food and Chemical Toxicology* 49:711-721.
- Harayama, S., M. Kok and E.L. Neidle. 1992. Functional and evolutionary relationships among diverse oxygenases. *Annual Review of Microbiology* 46:565-601.

- Harrigan, G.G., D. Lundry, S. Drury, K. Berman, S.G. Riordan, M.A. Nemeth, W.P. Ridley and K.C. Glenn. 2010. Natural variation in crop composition and the impact of transgenesis. *Nature Biotechnology* 28:402-404.
- Harrigan, G.G., W.P. Ridley, K.D. Miller, R. Sorbet, S.G. Riordan, M.A. Nemeth, W. Reeves and T.A. Pester. 2009. The forage and grain of MON 87460, a drought-tolerant corn hybrid, are compositionally equivalent to that of conventional corn. *Journal of Agricultural and Food Chemistry* 57:9754-9763.
- Harrison, L.A., M.R. Bailey, M.W. Naylor, J.E. Ream, B.G. Hammond, D.L. Nida, B.L. Burnette, T.E. Nickson, T.A. Mitsky, M.L. Taylor, R.L. Fuchs and S.R. Padgett. 1996. The expressed protein in glyphosate-tolerant soybean, 5-enolpyruvylshikimate-3-phosphate synthase from *Agrobacterium* sp. strain CP4, is rapidly digested in vitro and is not toxic to acutely gavaged mice. *Journal of Nutrition* 126:728-740.
- Hausinger, R.P. 2004. Fe(II)/ α -Ketoglutarate-dependent hydroxylases and related enzymes. *Critical Reviews in Biochemistry and Molecular Biology* 39:21-68.
- Heller, D., E.J. Helmerhorst, A.C. Gower, W.L. Siqueira, B.J. Paster and F.G. Oppenheim. 2016. Microbial diversity in the early *in vivo*-formed dental biofilm. *Applied and Environmental Microbiology* 82:1881-1888.
- Hensley, K., E.J. Benaksas, R. Bolli, P. Comp, P. Grammas, L. Hamdheydari, S. Mou, Q.N. Pye, M.F. Stoddard, G. Wallis, K.S. Williamson, M. West, W.J. Wechter and R.A. Floyd. 2004. New perspectives on Vitamin E: γ -tocopherol and carboxyethylhydroxy chroman metabolites in biology and medicine. *Free Radical Biology & Medicine* 36:1-15.
- Herman, P.L., M. Behrens, S. Chakraborty, B.M. Chrastil, J. Barycki and D.P. Weeks. 2005. A three-component dicamba *O*-demethylase from *Pseudomonas maltophilia*, strain DI-6: Gene isolation, characterization, and heterologous expression. *Journal of Biological Chemistry* 280:24759-24767.
- Hérouet, C., D.J. Esdaile, B.A. Mallyon, E. Debruyne, A. Schulz, T. Currier, K. Hendrickx, R.-J. van der Klis and D. Rouan. 2005. Safety evaluation of the phosphinothricin acetyltransferase proteins encoded by the *pat* and *bar* sequences that confer tolerance to glufosinate-ammonium herbicide in transgenic plants. *Regulatory Toxicology and Pharmacology* 41:134-149.
- Herrmann, K.M. 1995. The shikimate pathway: Early steps in the biosynthesis of aromatic compounds. *The Plant Cell* 7:907-919.
- Hochuli, E., W. Bannwarth, H. Döbeli, R. Gentz and D. Stüber. 1988. Genetic approach to facilitate purification of recombinant proteins with a novel metal chelate adsorbent. *Nature Biotechnology* 6:1321-1325.
- Hunt, A.G. 1994. Messenger RNA 3' end formation in plants. *Annual Review of Plant Physiology and Plant Molecular Biology* 45:47-60.
- Illergård, K., D.H. Ardell and A. Elofsson. 2009. Structure is three to ten times more conserved than sequence - A study of structural response in protein cores. *Proteins* 77:499-508.

- ILSI-CERA. 2011. A review of the environmental safety of the PAT protein. International Life Sciences Institute, Center for Environmental Risk Assessment, Washington, D.C.
- Janas, K.M., M. Cvikrová, A. Pałagiewicz and J. Eder. 2000. Alterations in phenylpropanoid content in soybean roots during low temperature acclimation. *Plant Physiology and Biochemistry* 38:587-593.
- Jin, D., X. Kong, B. Cui, Z. Bai and H. Zhang. 2013. Biodegradation of di-n-butyl phthalate by a newly isolated *Halotolerant Spingobium* sp. *International Journal of Molecular Sciences* 14:24046-24054.
- Kämpfer, P. 2006. The family *Streptomycetaceae*, Part I: Taxonomy. Pages 538-604 in *The Prokaryotes. A Handbook on the Biology of Bacteria: Archaea, Bacteria: Firmicutes, Actinomycetes*. Volume 3. M.Dworkin, S. Falkow, E. Rosenberg, K.-H. Schleifer, and E. Stackebrandt (eds.). Springer+ Business Media, LLC., New York, New York.
- Khush, G.S. 1997. Origin, dispersal, cultivation and variation of rice. *Plant Molecular Biology* 35:25-34.
- Klee, H.J., Y.M. Muskopf and C.S. Gasser. 1987. Cloning of an *Arabidopsis thaliana* gene encoding 5-enolpyruvylshikimate-3-phosphate synthase: Sequence analysis and manipulation to obtain glyphosate-tolerant plants. *Molecular and General Genetics* 210:437-442.
- Kovalic, D., C. Garnaat, L. Guo, Y. Yan, J. Groat, A. Silvanovich, L. Ralston, M. Huang, Q. Tian, A. Christian, N. Cheikh, J. Hjelle, S. Padgett and G. Bannon. 2012. The use of next generation sequencing and junction sequence analysis bioinformatics to achieve molecular characterization of crops improved through modern biotechnology. *The Plant Genome* 5:149-163.
- Krause, E., H. Wenschuh and P.R. Jungblut. 1999. The dominance of arginine-containing peptides in MALDI-derived tryptic mass fingerprints of proteins. *Analytical Chemistry* 71:4160-4165.
- Krueger, J.P., R.G. Butz, Y.H. Atallah and D.J. Cork. 1989. Isolation and identification of microorganisms for the degradation of dicamba. *Journal of Agricultural and Food Chemistry* 37:534-538.
- Kutzner, H.J. 1981. The family streptomycetaceae. Pages 2028-2090 in *The Prokaryotes: A Handbook on Habitats, Isolation, and Identification of Bacteria*. Volume 2. M.P. Starr, H. Stolp, H.G. Trüper, A. Balows, and H.G. Schlegel (eds.). Springer-Verlag, Berlin, Germany.
- Larue, C.T., M. Goley, L. Shi, A.G. Evdokimov, O.C. Sparks, C. Ellis, A.M. Wollacott, T.J. Rydel, C.E. Halls, B. Van Scoyoc, X. Fu, J.R. Nageotte, A.M. Adio, M. Zheng, E.J. Sturman, G.S. Garvey and M.J. Varagona. 2019. Development of enzymes for robust aryloxyphenoxypropionate and synthetic auxin herbicide tolerance traits in maize and soybean crops. *Pest Management Science* 75:2086-2094.
- Lege, K.E., J.T. Cothren and C.W. Smith. 1995. Phenolic acid and condensed tannin concentrations of six cotton genotypes. *Environmental and Experimental Botany* 35:241-249.

- Lira, F., G. Berg and J.L. Martínez. 2017. Double-face meets the bacterial world: The opportunistic pathogen *Stenotrophomonas maltophilia*. *Frontiers in Microbiology* 8:2190.
- Liu, K.S. 2004. Soybeans as a powerhouse of nutrients and phytochemicals. Pages 1-22 in *Soybeans as Functional Foods and Ingredients*. AOCS Press, Champaign, Illinois.
- Locci, R. 1989. Streptomycetes and related genera. Pages 2451-2508 in *Bergey's Manual of Systematic Bacteriology*. Volume 4. S.T. Williams and M.E. Sharpe (eds.). Williams & Wilkins, Baltimore, Maryland.
- Lundry, D.R., W.P. Ridley, J.J. Meyer, S.G. Riordan, M.A. Nemeth, W.A. Trujillo, M.L. Breeze and R. Sorbet. 2008. Composition of grain, forage, and processed fractions from second-generation glyphosate-tolerant soybean, MON 89788, is equivalent to that of conventional soybean (*Glycine max* L.). *Journal of Agricultural and Food Chemistry* 56:4611-4622.
- Maeda, H., K. Murata, N. Sakuma, S. Takei, A. Yamazaki, M.R. Karim, M. Kawata, S. Hirose, M. Kawagishi-Kobayashi, Y. Taniguchi, S. Suzuki, K. Sekino, M. Ohshima, H. Kato, H. Yoshida and Y. Tozawa. 2019. A rice gene that confers broad-spectrum resistance to β -triketone herbicides. *Science* 365:393-396.
- Manderscheid, R. and A. Wild. 1986. Studies on the mechanism of inhibition by phosphinothricin of glutamine synthetase isolated from *Triticum aestivum* L. *Journal of Plant Physiology* 123:135-142.
- Mazodier, P., P. Cossart, E. Giraud and F. Gasser. 1985. Completion of the nucleotide sequence of the central region of Tn5 confirms the presence of three resistance genes. *Nucleic Acids Research* 13:195-205.
- Meier, U. 2001. Growth stages of mono- and dicotyledonous plants. BBCH Monograph. Second Edition. Federal Biological Research Centre for Agriculture and Forestry, Grossbeeren, Germany.
- Meinzel, T. and C. Giglione. 2008. Tools for analyzing and predicting N-terminal protein modifications. *Proteomics* 8:626-649.
- Messina, M.J. 1999. Legumes and soybeans: Overview of their nutritional profiles and health effects. *American Journal of Clinical Nutrition* 70:439S-450S.
- Mitchell, G., D.W. Bartlett, T.E.M. Fraser, T.R. Hawkes, D.C. Holt, J.K. Townson and R.A. Wichert. 2001. Mesotrione: A new selective herbicide for use in maize. *Pest Management Science* 57:120-128.
- Mukherjee, P. and P. Roy. 2016. Genomic potential of *Stenotrophomonas maltophilia* in bioremediation with an assessment of its multifaceted role in our environment. *Frontiers in Microbiology* 7:967.

- Müller, T.A., M.I. Zavodszky, M. Feig, L.A. Kuhn and R.P. Hausinger. 2006. Structural basis for the enantiospecificities of *R*- and *S*-specific phenoxypropionate/ α -ketoglutarate dioxygenases. *Protein Science* 15:1356-1368.
- Myouga, F., R. Motohashi, T. Kuromori, N. Nagata and K. Shinozaki. 2006. An *Arabidopsis* chloroplast-targeted Hsp101 homologue, APG6, has an essential role in chloroplast development as well as heat-stress response. *Plant journal* 48:249-260.
- Norris, S.R., S.E. Meyer and J. Callis. 1993. The intron of *Arabidopsis thaliana* polyubiquitin genes is conserved in location and is a quantitative determinant of chimeric gene expression. *Plant Molecular Biology* 21:895-906.
- OECD. 1999. Consensus document on general information concerning the genes and their enzymes that confer tolerance to phosphinothricin herbicide. ENV/JM/MONO(99)13. Series on Harmonization of Regulatory Oversight in Biotechnology No.11. Organisation for Economic Co-operation and Development, Paris, France.
- OECD. 2002a. Module II: Herbicide biochemistry, herbicide metabolism and the residues in glufosinate-ammonium (Phosphinothricin)-tolerant transgenic plants. ENV/JM/MONO(2002)14. Series on Harmonization of Regulatory Oversight in Biotechnology No. 25. Organisation for Economic Co-operation and Development, Paris, France.
- OECD. 2002b. Report of the OECD workshop on the toxicological and nutritional testing of novel foods. SG/ICGB(1998)1/FINAL. Organisation for Economic Co-operation and Development, Paris, France.
- OECD. 2012. Revised consensus document on compositional considerations for new varieties of soybean [*Glycine max* (L.) Merr.]: Key food and feed nutrients, anti-nutrients, toxicants and allergens. ENV/JM/MONO(2012)24. Series on the Safety of Novel Foods and Feeds No. 25. Organisation for Economic Co-operation and Development, Paris, France.
- OECD. 2016. Revised consensus document on compositional considerations for new varieties of rice (*Oryza sativa*): Key food and feed nutrients, anti-nutrients and other constituents. ENV/JM/MONO(2016)38. Organisation for Economic Co-operation and Development, Paris, France.
- Okuno, N.T., I.R. Freire, R.T.R.S. Segundo, C.R. Silva and V.A. Marin. 2018. Polymerase chain reaction assay for detection of *Stenotrophomonas maltophilia* in cheese samples based on the *smeT* gene. *Current Microbiology* 75:1555-1559.
- Palleroni, N.J. and J.F. Bradbury. 1993. *Stenotrophomonas*, a new bacterial genus for *Xanthomonas maltophilia* (Hugh 1980) Swings et al. 1983. *International Journal of Systematic Bacteriology* 43:606-609.
- Piper, K.R., S.B. von Bodman, I. Hwang and S.K. Farrand. 1999. Hierarchical gene regulatory systems arising from fortuitous gene associations: Controlling quorum sensing by the opine regulon in *Agrobacterium*. *Molecular Microbiology* 32:1077-1089.

- Pozo, C., B. Rodelas, M.-T.V. M., R. Vilchez and J. Gonzalez-Lopez. 2007. Removal of organic load from olive washing water by an aerated submerged biofilter and profiling of the bacterial community involved in the process. *Journal of Microbiology and Biotechnology* 17:784-791.
- Rademacher, T.W., R.B. Parekh and R.A. Dwek. 1988. Glycobiology. *Annual Review of Biochemistry* 57:785-838.
- Richins, R.D., H.B. Scholthof and R.J. Shepherd. 1987. Sequence of figwort mosaic virus DNA (caulimovirus group). *Nucleic Acids Research* 15:8451-8466.
- Ridley, W.P., G.G. Harrigan, M.L. Breeze, M.A. Nemeth, R.S. Sidhu and K.C. Glenn. 2011. Evaluation of compositional equivalence for multitrait biotechnology crops. *Journal of Agricultural and Food Chemistry* 59:5865-5876.
- Rijavec, T., A. Lapanje, M. Dermastia and M. Rupnik. 2007. Isolation of bacterial endophytes from germinated maize kernels. *Canadian Journal of Microbiology* 53:802-808.
- Rogers, S.G. 2000. Promoter for transgenic plants. Patent 6,018,100, U.S. Patent Office, Washington, D.C.
- Salomon, S. and H. Puchta. 1998. Capture of genomic and T-DNA sequences during double-strand break repair in somatic plant cells. *EMBO Journal* 17:6086-6095.
- Schafer, F.Q., E.E. Kelley and G.R. Buettner. 2003. Oxidative stress and antioxidant intervention. Pages 849-869 in *Critical Reviews of Oxidative Stress and Aging: Advances in Basic Science, Diagnostics and Intervention*. R.G. Cutler and H. Rodriguez (eds.). World Scientific, New Jersey.
- Schmelz, E.A., J. Engelberth, H.T. Alborn, P. O'Donnell, M. Sammons, H. Toshima and J.H. Tumlinson. 2003. Simultaneous analysis of phytohormones, phytotoxins, and volatile organic compounds in plants. *Proceedings of the National Academy of Sciences of the United States of America* 100:10552-10557.
- Silvanovich, A., M.A. Nemeth, P. Song, R. Herman, L. Tagliani and G.A. Bannon. 2006. The value of short amino acid sequence matches for prediction of protein allergenicity. *Toxicological Sciences* 90:252-258.
- Sutcliffe, J.G. 1979. Complete nucleotide sequence of the *Escherichia coli* plasmid pBR322. *Cold Spring Harbor Symposia on Quantitative Biology* 43:77-90.
- Takeuchi, M., K. Hamana and A. Hiraishi. 2001. Proposal of the genus *Sphingomanas sensu stricto* and three new genera, *Sphingobium*, *Novosphingobium* and *Sphingopyxis*, on the basis of phylogenetic and chemotaxonomic analyses. *International Journal of Systematic and Evolutionary Microbiology* 51:1405-1417.
- Tashkov, W. 1996. Determination of formaldehyde in foods, biological media and technological materials by headspace gas chromatography. *Chromatographia* 43:625-627.

- Thomas, K., M. Aalbers, G.A. Bannon, M. Bartels, R.J. Dearman, D.J. Esdaile, T.J. Fu, C.M. Glatt, N. Hadfield, C. Hatzos, S.L. Hefle, J.R. Heylings, R.E. Goodman, B. Henry, C. Herouet, M. Holsapple, G.S. Ladics, T.D. Landry, S.C. MacIntosh, E.A. Rice, L.S. Privalle, H.Y. Steiner, R. Teshima, R. van Ree, M. Woolhiser and J. Zawodny. 2004. A multi-laboratory evaluation of a common in vitro pepsin digestion assay protocol used in assessing the safety of novel proteins. *Regulatory Toxicology and Pharmacology* 39:87-98.
- Thomas, K., G. Bannon, S. Hefle, C. Herouet, M. Holsapple, G. Ladics, S. MacIntosh and L. Privalle. 2005. In silico methods for evaluating human allergenicity to novel proteins: International Bioinformatics Workshop Meeting Report, 23-24 February 2005. *Toxicological Sciences* 88:307-310.
- Thomas, P., S. Kumari, G.K. Swarna and T.K. Gowda. 2007. Papaya shoot tip associated endophytic bacteria isolated from in vitro cultures and host-endophyte interaction in vitro and in vivo. *Canadian Journal of Microbiology* 53:380-390.
- Thompson, C.J., N.R. Movva, R. Tizard, R. Cramer, J.E. Davies, M. Lauwereys and J. Botterman. 1987. Characterization of the herbicide-resistance gene *bar* from *Streptomyces hygroscopicus*. *EMBO Journal* 6:2519-2523.
- Thompson, M.M., A. Niemuth, J. Sabbatini, D. Levin, M.L. Breeze, X. Li, T. Perez, M. Taylor and G.G. Harrigan. 2016. Analysis of vitamin K₁ in soybean seed: Assessing levels in a lineage representing over 35 years of breeding. *Journal of the American Oil Chemists' Society* 93:587-594.
- To, J.P.C., I.W. Davis, M.S. Marengo, A. Shariff, C. Baublite, K. Decker, R.M. Galvão, Z. Gao, O. Haragutchi, J.W. Jung, H. Li, B. O'Brien, A. Sant and T.D. Elich. 2021. Expression elements derived from plant sequences provide effective gene expression regulation and new opportunities for plant biotechnology traits. *Frontiers in Plant Science* 12:712179.
- Todaro, M., N. Francesca, S. Reale, G. Moschetti, F. Vitale and L. Settanni. 2011. Effect of different salting technologies on the chemical and microbiological characteristics of PDO Pecorino Siciliano cheese. *European Food Research and Technology* 233:931-940.
- U.S. EPA. 1997. Phosphinothricin acetyltransferase and the genetic material necessary for its production in all plants; Exemption from the requirement of a tolerance on all raw agricultural commodities. *Federal Register* 62:17717-17720.
- U.S. EPA. 2009. Reregistration eligibility decision for dicamba and associated salts. U.S. Environmental Protection Agency, Washington, D.C.
- U.S. EPA. 2015. Mesotrione; Pesticide tolerances. *Federal Register* 80:30625-30630.
- U.S. EPA. 2017. 2,4-D; Pesticide tolerances. *Federal Register* 82:9523-9529.
- USDA-NASS. 2019. 2017 Census of Agriculture. U. S. Department of Agriculture, National Agriculture Statistics Service, Washington D.C.
- Varman, A.M., L. He, R. Follenfant, W. Wu, S. Wemmer, S.A. Wrobel, Y.J. Tang and S. Singh. 2016. Decoding how a soil bacterium extracts building blocks and metabolic energy from

ligninolysis provides road map for lignin valorization. Proceedings of the National Academy of Sciences of the United States of America 113:pE5802-pE5811.

Venkatesh, T.V., M.L. Breeze, K. Liu, G.G. Harrigan and A.H. Culler. 2014. Compositional analysis of grain and forage from MON 87427, an inducible male sterile and tissue selective glyphosate-tolerant maize product for hybrid seed production. Journal of Agricultural and Food Chemistry 62:1964-1973.

Wang, X.-Z., B. Li, P.L. Herman and D.P. Weeks. 1997. A three-component enzyme system catalyzes the O demethylation of the herbicide dicamba in *Pseudomonas maltophilia* DI-6. Applied and Environmental Microbiology 63:1623-1626.

Wehrmann, A., A.V. Vliet, C. Opsomer, J. Botterman and A. Schulz. 1996. The similarities of *bar* and *pat* gene products make them equally applicable for plant engineers. Nature Biotechnology 14:1274-1278.

Wild, A. and R. Manderscheid. 1984. The effect of phosphinothricin on the assimilation of ammonia in plants. Zeitschrift für Naturforschung C 39:500-504.

Wingfield, P.T. 2017. N-terminal methionine processing. Current Protocols in Protein Science 88:6.14.11-16.14.13.

Wohlleben, W., W. Arnold, I. Broer, D. Hillemann, E. Strauch and A. Pühler. 1988. Nucleotide sequence of the phosphinothricin *N*-acetyltransferase gene from *Streptomyces viridochromogenes* Tü494 and its expression in *Nicotiana tabacum*. Gene 70:25-37.

Ye, X., E. Williams, J. Shen, J. Esser, A. Nichols, M. Petersen and L. Gilbertson. 2008. Plant development inhibitory genes in binary vector backbone improve quality event efficiency in soybean transformation. Transgenic Research 17:827-838.

Ye, X., E.J. Williams, J. Shen, S. Johnson, B. Lowe, S. Radke, S. Strickland, J.A. Esser, M.W. Petersen and L.A. Gilbertson. 2011. Enhanced production of single copy backbone-free transgenic plants in multiple crop species using binary vectors with a pRi replication origin in *Agrobacterium tumefaciens*. Transgenic Research 20:773-786.

Zambryski, P., A. Depicker, K. Kruger and H.M. Goodman. 1982. Tumor induction by *Agrobacterium tumefaciens*: Analysis of the boundaries of T-DNA. Journal of Molecular and Applied Genetics 1:361-370.

Zastrow-Hayes, G.M., H. Lin, A.L. Sigmund, J.L. Hoffman, C.M. Alarcon, K.R. Hayes, T.A. Richmond, J.A. Jeddeloh, G.D. May and M.K. Beatty. 2015. Southern-by-sequencing: A robust screening approach for molecular characterization of genetically modified crops. The Plant Genome 8:1-15.

Zhou, J., G.G. Harrigan, K.H. Berman, E.G. Webb, T.H. Klusmeyer and M.A. Nemeth. 2011. Stability in the composition equivalence of grain from insect-protected maize and seed from glyphosate-tolerant soybean to conventional counterparts over multiple seasons, locations, and breeding germplasms. Journal of Agricultural and Food Chemistry 59:8822-8828.

Zipper, C., K. Nickel, W. Angst and H.-P.E. Kohler. 1996. Complete microbial degradation of both enantiomers of the chiral herbicide mecoprop [(RS)-2-(4-chloro-2-methylphenoxy)propionic acid] in an enantioselective manner by *Sphingomonas herbicidovorans* sp. nov. Applied and Environmental Microbiology 62:4318-4322.